



UvA-DARE (Digital Academic Repository)

Glycosylation defects in lipid metabolism

van den Boogert, M.A.W.

Publication date

2020

Document Version

Final published version

License

Other

[Link to publication](#)

Citation for published version (APA):

van den Boogert, M. A. W. (2020). *Glycosylation defects in lipid metabolism*. [Thesis, fully internal, Universiteit van Amsterdam].

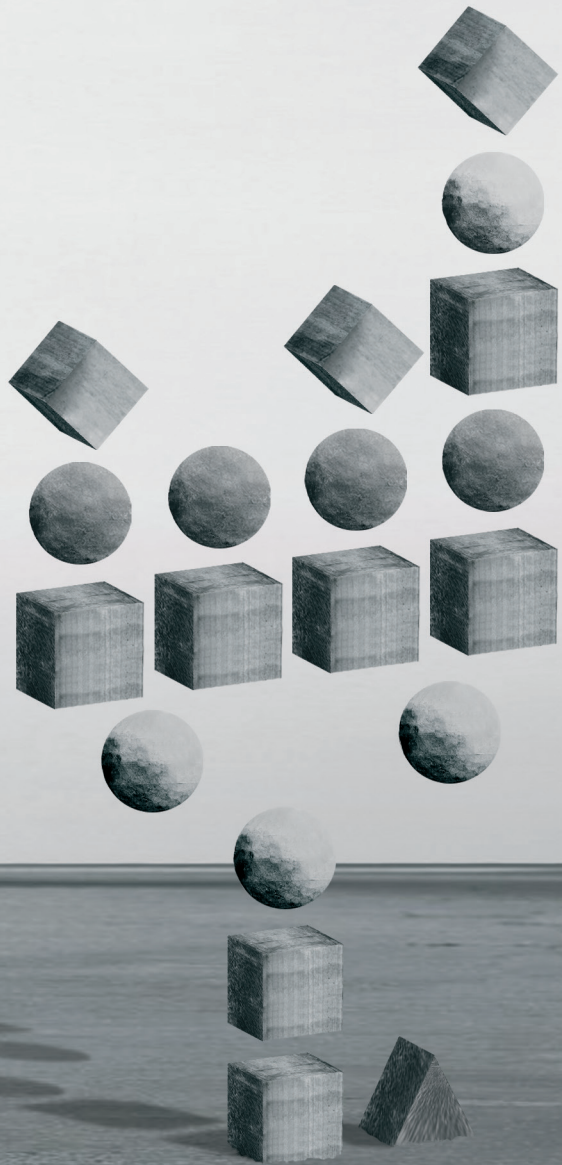
General rights

It is not permitted to download or to forward/distribute the text or part of it without the consent of the author(s) and/or copyright holder(s), other than for strictly personal, individual use, unless the work is under an open content license (like Creative Commons).

Disclaimer/Complaints regulations

If you believe that digital publication of certain material infringes any of your rights or (privacy) interests, please let the Library know, stating your reasons. In case of a legitimate complaint, the Library will make the material inaccessible and/or remove it from the website. Please Ask the Library: <https://uba.uva.nl/en/contact>, or a letter to: Library of the University of Amsterdam, Secretariat, Singel 425, 1012 WP Amsterdam, The Netherlands. You will be contacted as soon as possible.

GLYCOSYLATION DEFECTS IN LIPID METABOLISM



Marjolein A.W. van den Boogert

Glycosylation defects in lipid metabolism

Marjolein A.W. van den Boogert

Copyright 2020, Marjolein van den Boogert, Amsterdam, The Netherlands

No part of this thesis may be reproduced, stored in a retrieval system or transmitted in any form or by any means, without prior written permission of the author.

ISBN 978-94-6380-926-9

Author: Marjolein A.W. van den Boogert

Layout: proefschriftmaken.nl

Cover design: Ron Zijlmans (design inspired by Noémie Goudal's *Observatoires*)

Printed by: proefschriftmaken.nl

The research described in this thesis was supported by a grant of the AMC PhD Graduate School (AMC PhD Scholarship).

Financial support by the Dutch Heart Foundation for the publication of this thesis is gratefully acknowledged.

Financial support for printing this thesis was kindly provided by Stichting tot Steun Promovendi Vasculaire Geneeskunde, Servier Nederland Farma BV and Chipsoft.

Glycosylation defects in lipid metabolism

ACADEMISCH PROEFSCHRIFT

ter verkrijging van de graad van doctor

aan de universiteit van Amsterdam

op gezag van de Rector Magnificus

mw. prof. dr. ir. K.I.J. Maex

ten overstaan van een door het College voor Promoties ingestelde commissie,

in het openbaar te verdedigen in de Agnietenkapel

op woensdag 16 september 2020, te 13.00 uur

door

Marjolein Anita Willemijn van den Boogert

geboren te Amsterdam

Promotiecommissie:

Promotores:	prof. dr. E.S.G. Stroes	AMC - UvA
	prof. dr. D.J. Lefeber	Radboud Universiteit Nijmegen
Copromotores:	dr. A.G. Holleboom	AMC - UvA
	dr. ir. G.M. Dallinga-Thie	AMC - UvA
Overige leden:	prof. dr. N. Zelcer	AMC - UvA
	prof. dr. C.D.M. van Karnebeek	Radboud Universiteit Nijmegen
	dr. M. Langeveld	AMC - UvA
	dr. A.J.A. van de Sluis	Rijksuniversiteit Groningen
	prof. dr. A.K. Groen	AMC - UvA
	prof. dr. E. Lutgens	AMC - UvA

Faculteit der Geneeskunde

Extreme Value Theory by Leonard Tippett (paraphrased):

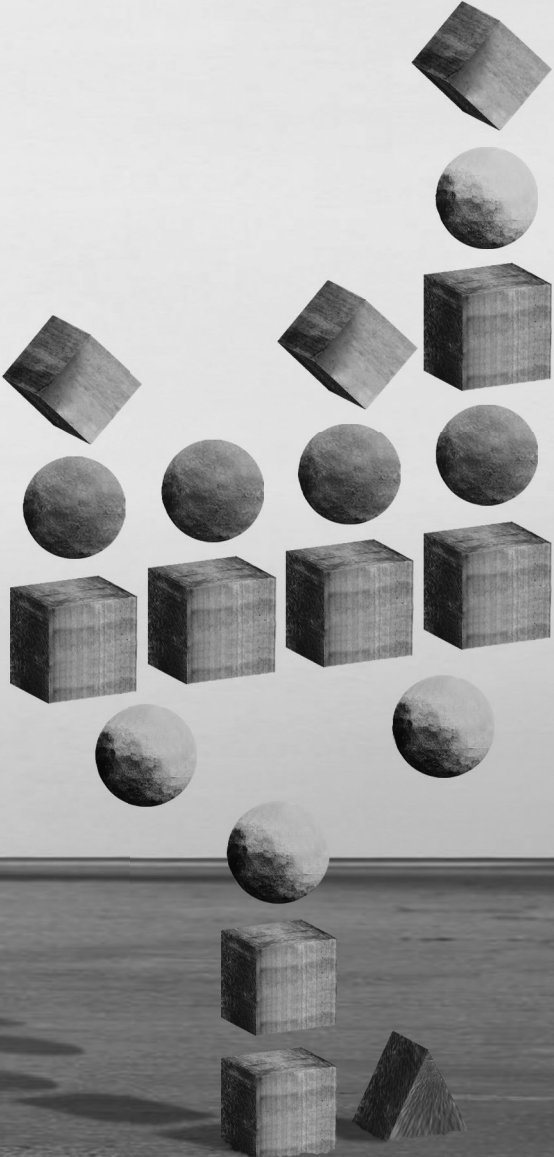
“Use the rare and extreme to study the common.”

Glycosylation defects in lipid metabolism		Page
General Introduction and thesis outline		9
Part I		16
<u>Lipid phenotypes in patients with congenital disorders of (de)glycosylation</u>		
Chapter 1	N-glycosylation defects in man lower LDL-cholesterol through increased LDL receptor expression. <i>Circulation (2019)</i>	19
Chapter 2	Reduced CETP glycosylation and activity in patients with homozygous B4GALT1 mutations. <i>Journal of Inherited Metabolic Disease (2019)</i>	59
Chapter 3	Deficiency of TMEM199 and CCDC115 results in fatty liver disease, hyperlipidemia and defective lipid droplet – lysosome interaction. <i>Cellular and Molecular Gastroenterology and Hepatology, manuscript in revision</i>	71
Chapter 4	Disordered glycosylation caused by NGLY1 deficiency links cholesterol homeostasis to disease mechanism. <i>Manuscript in preparation</i>	93
Part II		118
<u>Other roles for glycosylation in lipoprotein metabolism</u>		
Chapter 5	Common gene variants in <i>ASGR1</i> Gene Locus Associate with reduced cardiovascular risk in absence of pleiotropic effects. <i>Atherosclerosis (2020)</i>	121
Chapter 6	New insights into the role of glycosylation in lipoprotein metabolism. <i>Current Opinion in Lipidology (2017) Review</i>	139
Summary, general discussion and future perspective		151

Appendices	163
Nederlandse samenvatting	164
Authors and affiliations	168
List of publications	171
Portfolio	172
Dankwoord	174
Curriculum Vitae	178



GENERAL INTRODUCTION AND THESIS OUTLINE



“Glycosylation is everything”,

is something that I have been proclaiming ever since I started working on the studies displayed in this thesis. It was a joke to promote our research field with a catchphrase, but also an opening to start explaining what our research entails. Many fellow clinicians and scientists in the cardiovascular field did not seem to know what glycosylation was or why it could be important - at many conferences it was mistaken for another relevant process *glycation*.

But as I dove into the field of glycosylation and understood more about it and its interactions, I also started to believe in the truth of the phrase. The importance of the glycobiology field was underlined a few years ago by the European Science Foundation and similar institutes in the United States, founding a network of collaborative research groups and funding to create new resources and methods to make the study of glycans more accessible (e.g. Euroglycoforum and NIH Glycoscience).

So, what is protein glycosylation? It is one of the most prevalent intracellular post-translational processes and comprises of the covalent attachment of a mono- or oligosaccharide to proteins. It is sometimes referred to as the “third language of life” after nucleic acids and proteins¹. Glycans are on the outer surface of cells and on secreted proteins, and as such play a critical role in a wide variety of interactions between proteins, cells and organisms (e.g. between host and pathogen)². There are several distinct glycosylation pathways. They are defined by the first monosaccharide added to a protein or lipid, of which asparagine-linked or N-linked glycosylation is the most widely studied. The effect of a specific N-glycan on the function of the protein is in most cases impossible to predict and can range from irrelevant to very influential². Glycans can affect the function of proteins through their physical properties (by their relatively large size and potential negative charge)³, by being a target for glycan-binding proteins⁴, or by modulating the properties of the protein to which they are attached².

Cardiovascular disease (CVD), comprising stroke and ischemic heart disease, are still the leading cause of death worldwide (WHO fact sheet 2018⁵). Apart from well-known risk factors for CVD like physical inactivity, smoking, obesity and diabetes, hypercholesterolemia is another major driver of cardiovascular events, despite the well-established beneficial effects of widely used lipid lowering drugs like statins⁶⁻⁹. Even in subjects with low levels of low-density-lipoprotein (LDL-)cholesterol, (further) lipid lowering has been shown to be effective in reducing CVD risk¹⁰. Yet even in people with very low LDL-c levels, cardiovascular events still occur. New treatment strategies for the prevention of CVD targeting mechanisms distinct from existing therapies are still needed. A relatively novel terrain in the search for these new strategies, is the role of protein glycosylation.

Advances in research techniques like glycomics by mass spectrometry have greatly enhanced the insight into specific glycan structures^{11,12}. Consequently, better understanding of glycan functionality has led to increased interest in the therapeutic utilization of glycan interactions in a variety of diseases.

In cancers, tumor growth is usually accompanied by tumor evasion of the immune system. This

evasion is in some tumors established by aberrant sialylation - a form of glycosylation - through upregulation of certain sialyltransferases, which changes the way the immune system perceives the tumor. Identifying and targeting the aberrantly sialylated tumor cells is being explored as a new therapeutic option^{13,14}.

Furthermore, many pathogens rely on the binding to specific carbohydrate structures on host cells for their infection strategy¹⁵, and therapeutic mimicry of these carbohydrate receptors use this concept to prevent pathogen invasion¹⁶.

Targeting protein glycosylation in lipid metabolism has not been pursued yet, as knowledge of its role has been limited. However, many proteins involved in lipid synthesis, lipoprotein particle assembly, and clearance from plasma are N-glycosylated, suggesting opportunities in targeting these processes to affect plasma lipids. Additionally, several large genome-wide association studies have increased the importance of this area since certain genetic variants in genes involved in protein glycosylation are associated with plasma lipid phenotypes and coronary artery disease¹⁷⁻¹⁹.

The aim of this thesis was to gain mechanistic insights into the observed associations between genes involved in protein glycosylation and lipid metabolism. To this end, we studied the lipid phenotypes in patients with congenital disorders of glycosylation (CDGs).

CDGs are a group of rare inborn defects of glycan metabolism with autosomal recessive inheritance. Less than 2000 patients have been diagnosed with the most common type of CDG worldwide, which illustrates the rarity of CDGs. In recent years there has been a rapid expansion of identified CDG subtypes²⁰. Clinical phenotypes in different subsets of CDG show a broad spectrum of clinical features and severity, but most involve neuromuscular defects and psychomotor retardation²¹.

CDGs were formerly grouped according to the cellular localization of the affected protein (Figure 1). In type I CDG (CDG-I), the affected enzymes are located in the endoplasmic reticulum (ER); early in the N-glycan assembly²². In CDG-II the affected enzymes are located in the Golgi apparatus, causing problems later in the glycan tree building machinery. However, in recent years, many novel gene defects have been studied that cannot be grouped as easily, demonstrating mixed glycosylation disorders and more general disruption of Golgi homeostasis and trafficking of proteins.

Furthermore, only recently, a congenital disorder of *deg*lycosylation (CDDG) was discovered: N-glycanase 1 (NGLY1) deficiency²³. NGLY1 is an enzyme that is involved in removing glycans from glycoproteins destined for degradation and plays a key part in the ER associated degradation machinery for identifying and degrading misfolded proteins²⁴⁻²⁶. The spectrum of symptoms observed in these patients overlaps with that seen in CDG patients.

Thesis outline

Part I of this thesis focuses on studying the mechanisms behind the lipid phenotypes found in patients with CDG. Based on the observed link between plasma lipids and glycosylation and on case reports of dyslipidemia in CDG-I patients²⁷⁻³⁰, we obtained plasma of a large cohort of CDG-I patients with homozygous or compound heterozygous mutations in asparagine-linked glycosylation protein 6 (*ALG6*) and phosphomannomutase 2 (*PMM2*) - two glycosylation enzymes located in the ER and cytosol - and analyzed plasma lipids prospectively. As we found hypobetalipoproteinemia in all patients, we also included a set of family members who were heterozygous carriers of the mutation, to assess whether there was a gene-dose response. Next, we used *in vitro* cellular models mimicking, or patient-derived cells harboring, the enzyme deficiencies to study the mechanism behind the lipid phenotype (**Chapter 1**). In three CDG-II patients with mutations in UDP-Gal:N-acetylglucosamine β -1,4-galactosyltransferase I (*B4GALT1*) we found reduced non-high density lipoprotein cholesterol and total cholesterol-to-HDL-c ratio. (**Chapter 2**). Furthermore, we found hypercholesterolemia, in the range seen in patients with familial hypercholesterolemia, in patients with mutations in *TMEM199* and *CCDC115*, both encoding V-ATPase assembly factors. These are recently discovered disorders of Golgi homeostasis causing mixed glycosylation disorders and steatohepatitis, in addition to the hypercholesterolemia. We used *in vitro* cellular models and a *Tmem199* deficient murine model to study the underlying pathobiology (**Chapter 3**). Last, we studied plasma lipids in patients with NGLY1-CDDG and found hypocholesterolemia. In collaboration with a research group in the United States, we studied the lipid metabolism and its possible correlation to the neurological phenotype in these patients, using an *in vitro* cellular model and *ngly1*^{-/-} zebrafish (**Chapter 4**).

Part II looks at other roles for glycosylation processes in lipid metabolism. Recently, an association between CVD and the del12 variant in *ASGR1*, the major subunit of the asialoglycoprotein receptor (ASGPR). The presence of the variant was associated with reduced LDL-c levels and a lower risk of coronary artery disease³¹. We studied the possibly pleiotropic effects of the *ASGR1* variant, that may explain the observed association. And to further evaluate the disproportionality of the effect of *ASGR1* variants on lipids versus CAD risk, we selected three common variants located within 100 kB in and around the *ASGR1* gene that were significantly associated with LDL-c and found that this risk reduction was proportionally similar to the gene risk scores in *HMCGR*, *NPC1L1*, *PCSK9*, and *LDLR* (**Chapter 5**). And finally, we reviewed the influence of glycosylation in lipid pathways, also touching upon the potential of therapeutic targeting (**Chapter 6**).

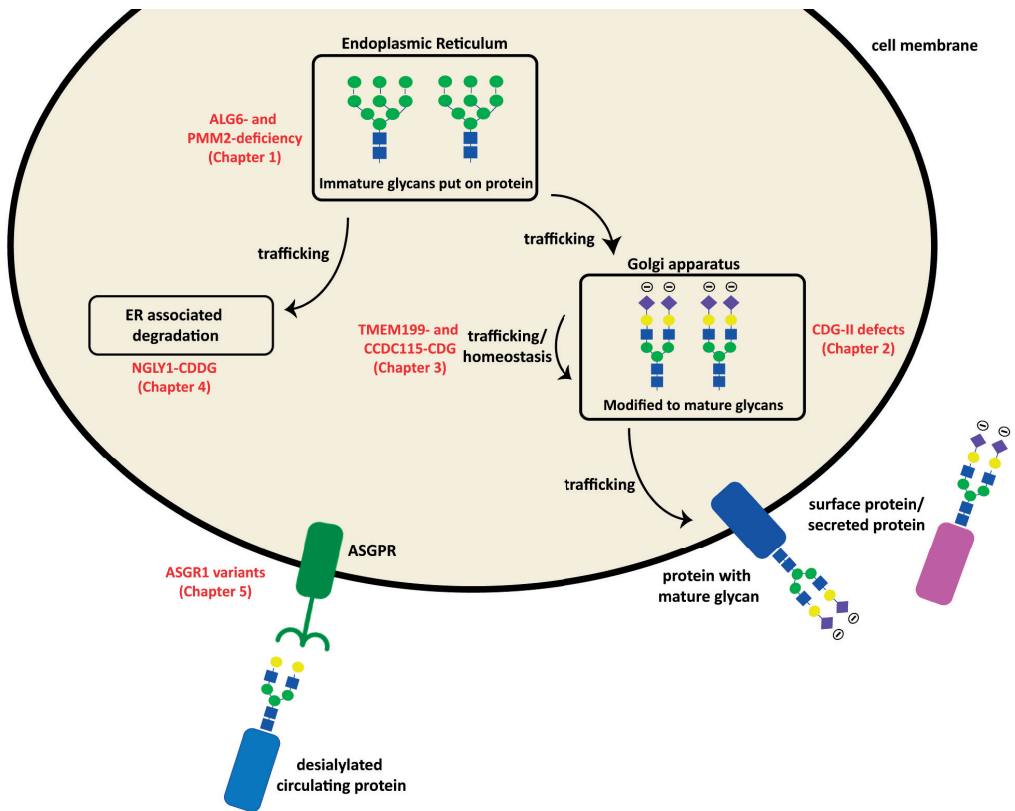


Figure 1. Cellular localization of CD(D)G defects and the ASGPR.

Glycan tree building starts in the endoplasmic reticulum, where the immature glycan is eventually put on a protein; defects in enzymes located this early in the glycosylation process, like in ALG6- and PMM2-CDG, cause CDG-I and are discussed in **Chapter 1**.

The immature glycoprotein is transported to the Golgi apparatus where the glycan is further modified; defects in enzymes located in this step of the glycosylation process, like B4GALT1-CDG, cause CDG-II and are discussed in **Chapter 2** of this thesis. Golgi homeostasis is disrupted in TMEM199- and CCDC115-CDG and these disorders are discussed in **Chapter 3**. The mature glycoprotein is finally transported to the cell membrane where it can fulfill its function as a surface protein or be secreted out of the cell.

When appropriate however, when the glycoprotein is misfolded or in overabundance, the glycoprotein can be transported from the ER to the degradative systems. As *deglycosylation* is a necessary step for the degradation process, defects in NGLY1, a deglycosylation enzyme, disrupts this process and NGLY1 deficiency is discussed in **Chapter 4**.

A separate process that involves glycosylation is also shown: the asialoglycoprotein receptor (ASGPR) is a mainly hepatic receptor that facilitates the uptake of circulating desialylated proteins. Variants in this receptor are discussed in **Chapter 5**.

References

1. Ohtsubo, K. & Marth, J.D. Glycosylation in cellular mechanisms of health and disease. *Cell* **126**, 855-867 (2006).
2. Varki, A. Essentials of glycobiology. 1 online resource (Cold Spring Harbor Laboratory Press,, Cold Spring Harbor (NY), 2015).
3. Wormald, M.R. & Dwek, R.A. Glycoproteins: glycan presentation and protein-fold stability. *Structure* **7**, R155-160 (1999).
4. Sperandio, M., Gleissner, C.A. & Ley, K. Glycosylation in immune cell trafficking. *Immunol Rev* **230**, 97-113 (2009).
5. <https://www.who.int/news-room/fact-sheets/detail/the-top-10-causes-of-death>
6. Baigent, C., *et al.* Efficacy and safety of cholesterol-lowering treatment: prospective meta-analysis of data from 90,056 participants in 14 randomised trials of statins. *Lancet* **366**, 1267-1278 (2005).
7. Stone, N.J., *et al.* 2013 ACC/AHA guideline on the treatment of blood cholesterol to reduce atherosclerotic cardiovascular risk in adults: a report of the American College of Cardiology/American Heart Association Task Force on Practice Guidelines. *J Am Coll Cardiol* **63**, 2889-2934 (2014).
8. Yusuf, S., *et al.* Blood-Pressure and Cholesterol Lowering in Persons without Cardiovascular Disease. *N Engl J Med* **374**, 2032-2043 (2016).
9. Authors/Task Force, M., *et al.* 2016 ESC/EAS Guidelines for the Management of Dyslipidaemias: The Task Force for the Management of Dyslipidaemias of the European Society of Cardiology (ESC) and European Atherosclerosis Society (EAS) Developed with the special contribution of the European Association for Cardiovascular Prevention & Rehabilitation (EACPR). *Atherosclerosis* **253**, 281-344 (2016).
10. Cholesterol Treatment Trialists, C., *et al.* Efficacy and safety of more intensive lowering of LDL cholesterol: a meta-analysis of data from 170,000 participants in 26 randomised trials. *Lancet* **376**, 1670-1681 (2010).
11. van Scherpenzeel, M., Steenbergen, G., Morava, E., Wevers, R.A. & Lefeber, D.J. High-resolution mass spectrometry glycoprofiling of intact transferrin for diagnosis and subtype identification in the congenital disorders of glycosylation. *Transl Res* **166**, 639-649 e631 (2015).
12. Reiding, K.R., Blank, D., Kuijper, D.M., Deelder, A.M. & Wuhler, M. High-throughput profiling of protein N-glycosylation by MALDI-TOF-MS employing linkage-specific sialic acid esterification. *Anal Chem* **86**, 5784-5793 (2014).
13. Bull, C., *et al.* Targeting aberrant sialylation in cancer cells using a fluorinated sialic acid analog impairs adhesion, migration, and in vivo tumor growth. *Mol Cancer Ther* **12**, 1935-1946 (2013).
14. Rodriguez, E., Schetters, S.T.T. & van Kooyk, Y. The tumour glyco-code as a novel immune checkpoint for immunotherapy. *Nat Rev Immunol* **18**, 204-211 (2018).
15. Moran, A.P., Gupta, A. & Joshi, L. Sweet-talk: role of host glycosylation in bacterial pathogenesis of the gastrointestinal tract. *Gut* **60**, 1412-1425 (2011).
16. Dalziel, M., Crispin, M., Scanlan, C.N., Zitzmann, N. & Dwek, R.A. Emerging principles for the therapeutic exploitation of glycosylation. *Science* **343**, 1235681 (2014).
17. Kathiresan, S., *et al.* Common variants at 30 loci contribute to polygenic dyslipidemia. *Nat Genet* **41**, 56-65 (2009).
18. Teslovich, T.M., *et al.* Biological, clinical and population relevance of 95 loci for blood lipids. *Nature* **466**, 707-713 (2010).
19. Willer, C.J., *et al.* Newly identified loci that influence lipid concentrations and risk of coronary artery disease. *Nat Genet* **40**, 161-169 (2008).

20. Freeze, H.H., Chong, J.X., Bamshad, M.J. & Ng, B.G. Solving glycosylation disorders: fundamental approaches reveal complicated pathways. *Am J Hum Genet* **94**, 161-175 (2014).
21. Jaeken, J. Congenital disorders of glycosylation. *Ann N Y Acad Sci* **1214**, 190-198 (2010).
22. Scott, K., Gadomski, T., Kozicz, T. & Morava, E. Congenital disorders of glycosylation: new defects and still counting. *J Inherit Metab Dis* **37**, 609-617 (2014).
23. Enns, G.M., *et al.* Mutations in NGLY1 cause an inherited disorder of the endoplasmic reticulum-associated degradation pathway. *Genet Med* **16**, 751-758 (2014).
24. Park, H., Suzuki, T. & Lennarz, W.J. Identification of proteins that interact with mammalian peptide:N-glycanase and implicate this hydrolase in the proteasome-dependent pathway for protein degradation. *Proc Natl Acad Sci U S A* **98**, 11163-11168 (2001).
25. Kamiya, Y., Satoh, T. & Kato, K. Molecular and structural basis for N-glycan-dependent determination of glycoprotein fates in cells. *Biochim Biophys Acta* **1820**, 1327-1337 (2012).
26. Kato, K. & Kamiya, Y. Structural views of glycoprotein-fate determination in cells. *Glycobiology* **17**, 1031-1044 (2007).
27. de Lonlay, P. & Seta, N. The clinical spectrum of phosphomannose isomerase deficiency, with an evaluation of mannose treatment for CDG-Ib. *Biochim Biophys Acta* **1792**, 841-843 (2009).
28. Jaeken, J., Eggermont, E. & Stibler, H. An apparent homozygous X-linked disorder with carbohydrate-deficient serum glycoproteins. *Lancet* **2**, 1398 (1987).
29. Ohno, K., *et al.* The carbohydrate deficient glycoprotein syndrome in three Japanese children. *Brain Dev* **14**, 30-35 (1992).
30. Pavone, L., *et al.* Olivopontocerebellar atrophy leading to recognition of carbohydrate-deficient glycoprotein syndrome type I. *J Neurol* **243**, 700-705 (1996).
31. Nioi, P., *et al.* Variant ASGR1 Associated with a Reduced Risk of Coronary Artery Disease. *N Engl J Med* **374**, 2131-2141 (2016).

PART I

Lipid phenotypes in patients with congenital disorders of (de)glycosylation





CHAPTER 1

N-glycosylation defects in man lower LDL-cholesterol through increased LDL receptor expression.

Marjolein A.W. van den Boogert, Lars E. Larsen, Lubna Ali, Sacha D. Kuil, Patrick L.W. Chong, Anke Loregger, Jeffrey Kroon, Johan G. Schnitzler, Alinda W.M. Schimmel, Jorge Peter, Johannes H.M. Levels, Gerry Steenbergen, Eva Morava, Geesje M. Dallinga-Thie, Ron A. Wevers, Jan Albert Kuivenhoven, Nicholas J. Hand, Noam Zelcer, Daniel J. Rader, Erik S.G. Stroes, Dirk J. Lefeber, Adriaan G. Holleboom

Circulation (2019)

Abstract

Background

The importance of protein glycosylation in regulating lipid metabolism is increasingly becoming apparent. We set out to further investigate this by studying patients with type I congenital disorders of glycosylation (CDG-I) with defective N-glycosylation.

Methods

We studied 29 patients of the two most prevalent types of CDG-I: ALG6- and PMM2-CDG, and 23 first- and second-degree relatives with a heterozygote mutation and measured plasma cholesterol levels. LDL metabolism was studied in three cell models – gene silencing in HepG2 cells; patient fibroblasts; patient hepatocyte-like cells derived from induced pluripotent stem cells – by measuring apolipoprotein B (apoB) production and secretion, LDL receptor (LDLR) expression and membrane abundance, and LDL particle uptake. Furthermore, SREBP2 protein expression and activation, as well as ER stress markers were studied.

Results

We report hypobetalipoproteinemia (LDL-cholesterol (LDL-c) and apoB below the 5th percentile) in a large cohort of CDG-I patients (mean age: 9 years), together with reduced LDL-c and apoB in clinically unaffected heterozygous relatives (mean age: 46 years), compared to two separate sets of age- and gender-matched controls. ALG6 and PMM2 deficiency led to markedly increased LDL uptake due to increased cell surface LDLR abundance. Mechanistically, this outcome was driven by increased SREBP2 protein expression accompanied by amplified target gene expression resulting in higher LDLR protein levels. ER stress was not found to be a major mediator.

Conclusion

Our study establishes N-glycosylation as an important regulator of LDL metabolism. Given that LDL-c was also reduced in a group of clinically unaffected heterozygotes, we propose that increasing LDLR-mediated cholesterol clearance by targeting N-glycosylation in the LDL pathway may represent a novel therapeutic strategy to reduce LDL-c and cardiovascular disease

Introduction

The importance of protein glycosylation in regulating lipid metabolism is increasingly becoming apparent¹. This intracellular process covalently attaches glycans to proteins and is an essential modification for protein function, referred to as the “third language of life” after nucleic acids and proteins². We and others previously reported a link between glycosylation and plasma lipids based on genome-wide association studies (GWAS). Single Nucleotide Polymorphisms (SNPs) in *GALNT2*, encoding ppGalNAc-transferase 2, a specific O-glycosylation enzyme, are associated with elevated plasma high-density lipoprotein cholesterol (HDL-c) and decreased triglycerides (TG)^{3,4}. We subsequently demonstrated that *GALNT2* could specifically initiate glycan synthesis on apolipoprotein C-III⁵, while others found that it also glycosylates angiopoietin-like protein 3 (ANGPTL3)⁶ and phospholipid transfer protein⁷. Collectively, these findings implicate a role for this glycosyltransferase in modifying proteins involved in lipid metabolism.

To further investigate this, we focused on lipid metabolism in patients with congenital disorders of glycosylation (CDGs). CDGs are a rare group of inborn defects of glycan metabolism with autosomal recessive inheritance and a rapid expansion of identified subtypes in recent years⁸. CDGs are associated with a broad spectrum of clinical features and severity, typically involving neuromuscular defects and psychomotor retardation⁹. Numerous gene defects resulting in abnormal glycosylation have been documented⁸. Defects are located in diverse biological pathways, ranging from glycosylation enzymes located in the endoplasmic reticulum (ER) or the Golgi apparatus, to a general disruption of Golgi trafficking and homeostasis. The nomenclature for CDGs is based on the mutated gene and can be grouped according to the cellular localization of the affected protein. In type I CDG (CDG-I), the affected enzymes are located in the ER; early in the asparagine-linked or N-glycan assembly¹⁰.

Based on the observed link between plasma lipids and glycosylation and on case reports of hypocholesterolemia in CDG-I patients¹¹⁻¹⁴, we studied plasma lipids in a large cohort of the two most prevalent CDG-I subtypes: ALG6-CDG, characterized by asparagine-linked glycosylation protein 6 deficiency and PMM2-CDG, characterized by phosphomannomutase 2 deficiency. ALG6 and PMM2 are enzymes located in the ER and cytosol, respectively, and both are required for the earliest steps of N-glycan assembly. Deficiency of these enzymes disrupts assembly of dolichol-linked glycans, or the transfer of these glycans onto proteins, resulting in unoccupied glycosylation sites and consequently potentially altered folding and protein function⁹.

In this study, we report analyses of plasma lipid levels in a cohort of ALG6- and PMM2-CDG patients and their clinically unaffected, heterozygous family members. We found that these patients have a new form of primary hypobetalipoproteinemia (HBL), defined by very low plasma levels of total cholesterol (TC), low-density lipoprotein cholesterol (LDL-c) and apolipoprotein B (apoB). Experiments in a human liver cell model, patient fibroblasts, and hepatocyte-like cells (HLCs) derived from induced pluripotent stem cells (iPSCs) demonstrate an increased LDL receptor (LDLR) abundance on the cell surface mediating the observed plasma lipid phenotype.

Methods

For detailed description of the performed experiments please refer to the supplemental information. The data, analytical methods, and study materials for purposes of reproducing results or replicating procedures can be made available on request to the corresponding author.

Subjects

First, we reviewed medical records of 17 patients with CDG-I (diagnosed by standard methods¹⁵) from the CDG database of the Radboud UMC in Nijmegen, The Netherlands, for plasma lipids to assess whether there was a lipid phenotype in these patients.

Then we collected plasma samples of 29 patients (15 ALG6-CDG and 14 PMM2-CDG patients, diagnosed with transferrin isoelectric focusing and genetic testing, confirming homozygosity or compound heterozygosity for *ALG6* or *PMM2* mutations), and a set of 30 healthy, age- and gender-matched (child) controls from the plasma biobank at the Amsterdam UMC, location AMC, The Netherlands. These were unaffected siblings of patients with dyslipidemia, without mutations in genes known to affect apoB and LDL-c (*APOB*, *LDLR* and *PCSK9*) or in *ALG6* or *PMM2*, from our lipid clinic with plasma stored in our blood bank.

In addition, we included 23 first- and second-degree family members of patients with CDG-I (10 carriers of PMM2-CDG mutations, 7 of ALG6-CDG, 2 of ALG12-CDG and 4 of MPI-CDG mutations; the latter two being two other subtypes of CDG-I^{16,17}). In line with the recessive mode of inheritance, heterozygous carriers were clinically unaffected: none had the characteristic neurological defects found in CDG-I patients. Heterozygosity for the mutations was assessed by DNA sequencing for the known mutations. Because the heterozygous carriers were mostly obligate heterozygous parents of the CDG-I patients and thus significantly older (mean age of heterozygous carriers 45,5 years versus 9 years in the CDG-I patients) we have included a separate set of 23 healthy, age- and gender-matched (adult) controls without mutations in genes known to affect apoB and LDL-c (*APOB*, *LDLR* and *PCSK9*) or in *ALG6* or *PMM2*. These adult controls were unaffected family members of patients with dyslipidemia from our clinic with plasma stored in our blood bank.

Furthermore, we assessed all available exomes of subjects in the biobank of our lipid clinic and found a heterozygous carrier of a relatively common pathogenic *PMM2* mutation. She was referred to our clinic for having a plasma HDL-c above the 95th percentile and expansion of her family was done. Upon further investigation, she also had low LDL-c levels and her family was included for segregation analysis of the *PMM2* mutation and low plasma LDL-c levels.

None of the subjects included in these studies used medication that could affect lipid metabolism.

Plasma lipids

We analyzed plasma lipids in venous blood samples collected after an overnight fast in EDTA-coated tubes. Plasma was isolated after centrifugation at 3000 RPM for 15 minutes at 4°C and stored at -80°C until further analyses. TC, LDL-c, HDL-c, TG, apoA-I and apoB were measured using commercially available assays (DiaSys and WAKO) on a Selectra analyzer (Sopachem, The Netherlands). Proprotein convertase subtilisin/kexin type 9 (*PCSK9*) plasma levels were measured with a commercially available ELISA (R&D systems).

Study approval

Written informed consent was obtained from all participants before enrolling in the study, according to a protocol approved by the Medical Ethical Committee of the Amsterdam University Medical Center, location AMC (protocol NL46676.018.13), in compliance with the Declaration of Helsinki.

Cell lines

RNA silencing was done in human hepatoma (HepG2) cells, to mimic the ALG6 and PMM2 deficiency. Patient fibroblasts from 6 CDG-I patients (3 ALG6- and 3 PMM2-CDG) were obtained from the Radboud UMC and two healthy control fibroblast cell lines were obtained from subjects in the biobank at our lipid clinic in Amsterdam. Compared to cell lines such as the HepG2 model, the use of patient fibroblasts with their inherent glycosylation defect represents an improvement in terms of clinical relevance; however, LDL metabolism mainly occurs in the liver. Therefore, we also studied patient-derived hepatocyte-like cells (HLCs). Easily accessible differentiated cells, like fibroblasts, can be reprogrammed to iPSCs and subsequently re-differentiated to HLCs¹⁸. This enables the study of liver metabolism in patients in a non-invasive way. Last, we used a HepG2 cell line stably expressing LDLR-green fluorescent protein (GFP) under a CMV promoter¹⁹.

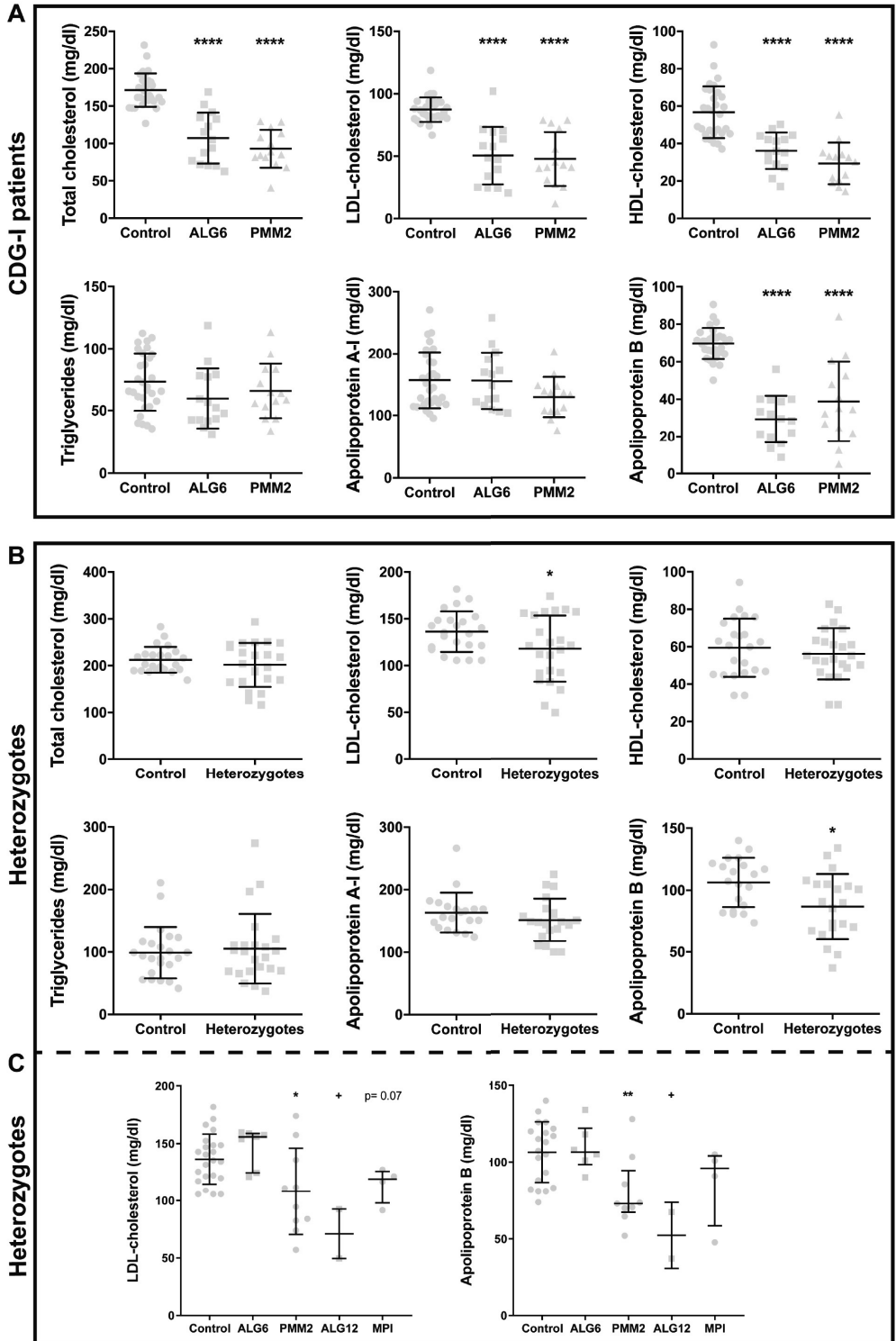
In vitro experiments

The HepG2 cell model was used for a wide quantitative polymerase chain reaction (qPCR) screen of expression levels of important players in plasma lipid and lipoprotein metabolism (see Table S1 for primer sequences), and apoB secretion assays with or without oleic acid stimulation, ER degradation inhibition (with MG-132 for 4 hours) or autophagy inhibition (with bafilomycin A (BafA) for 4 hours). In addition, HepG2s, fibroblasts and HLCs were used to assess cellular and surface LDLR protein expression levels with western blot and flow cytometry and LDL uptake with Dylight labeled LDL particles in combination with flow cytometry²⁰. In HLCs, apoB secretion was assessed by ³⁵S steady-state protein labelling and precipitation in methionine-free Hepatocyte Basal Medium as described by Ota et al.²¹ Cholesterol efflux assays were performed on the patient fibroblasts as described by Franssen et al.²² Cellular sterol regulatory element-binding protein 2 (SREBP2) protein levels and mRNA expression of SREBP2 targets were assessed in siALG6 treated HepG2s with western blot and qPCR. Furthermore, SREBP2 activation was assessed using cyclodextrin cholesterol (β -MCD, which inhibits SREBP2 by delivering cholesterol that directly binds to SREBP cleavage-activating protein (SCAP)) and 25-hydroxycholesterol (which is an oxysterol that is shown to bind INSIG to SCAP²³) for 4 hours. Intracellular cholesterol levels were measured quantitatively with filipin staining in combination with flow cytometry. Lipid droplets were isolated and assessed for lipid content using high-performance liquid chromatography. ER stress was assessed by measuring mRNA and protein levels of certain indicators of ER stress, such as CHOP. Tunicamycin (TM) and thapsigargin (TG), both known inducers of ER stress and the unfolded protein response, were used as positive controls. For the Myc-tagged INSIG1 overexpression experiments, the siRNA treated HepG2 cells were co-transfected with INSIG1-Myc and used for RNA and protein isolation after 48 hours. All *in vitro* cell experiments were performed at least twice with triplicate measurements per condition.

Statistical analyses

Data are compared between groups with a Students t-test and presented as means \pm standard deviation or, when appropriate, tested with a Mann-Whitney U test and presented as medians with interquartile ranges for nonparametric parameters. Categorical variables were tested with a Chi-square test. All statistical analyses were done using SPSS software (version 22.0, SPSS Inc., Chicago IL). Error bars indicate standard deviations. Probability values of < 0.05 were considered statistically significant.

Figure 1 CDG-I patients and mutation carriers exhibit an HBL phenotype. (A) Plasma samples from CDG-I patients (15 ALG6-CDG and 14 PMM2-CDG) were collected from the plasma biobank. Plasma TC, LDL-c, HDL-c, ApoA-I, ApoB and TG were measured in EDTA plasma after an overnight fast and compared to 30 age- and gender-matched controls. **(B)** Twenty-three first- or second-degree relatives of CDG-I patients proven to be heterozygous for known CDG-I mutations were included. Plasma TC, LDL-c, HDL-c, ApoA-I, ApoB and TG were analyzed after an overnight fast and compared to twenty-three age- and gender-matched controls. **(C)** Plasma LDL-c and apoB of the twenty-three heterozygotes per CDG-I gene (here the statistical comparisons for the ALG6, ALG12 and MPI heterozygotes are done with Mann-Whitney U tests due to the low number of subjects per group and for those the median with interquartile range is shown in the panel). All measurements are shown as a scatter plot with mean \pm SD and each data point depicts a single measure from an individual subject plasma sample. **** indicates $p < 0.0001$, ** $p < 0.01$, * $p < 0.05$ as calculated with Student's unpaired two-sided t-tests; + indicates $p < 0.01$ as calculated with Mann-Whitney U test.



Results

The medical records of 17 patients (mean age: 10 years, SD 9,7) with CDG-I (diagnosed by established methods¹⁵) were reviewed for plasma lipids. Analysis revealed a markedly decreased TC and LDL-c, with normal HDL-c and TG levels (Figure S1). On average, TC was 31% lower and LDL-c 61% lower in CDG-I patients, compared to reference values for children in the relevant age category, i.e. age of 0 to 14 years, as measured in our lipid clinic. Available data on liver and thyroid function, nutritional status and enteric absorption did not show signs of secondary causes of hypocholesterolemia, such as malabsorption or malnutrition, hyperthyroidism, renal or liver failure (Table S2).

To validate these findings, we retrieved plasma samples of 29 patients of the two most prevalent CDG-I subtypes (15 ALG6-CDG and 14 PMM2-CDG patients) from the plasma biobank at the Radboud UMC, and 30 healthy, age- and gender-matched controls. The ALG6- and PMM2-CDG patients had an average age of 9.3 ± 10.8 years and 8.6 ± 10.7 years respectively and were comparable to the also prospectively collected controls (10.2 ± 2.6 years; $p = 0.750$ and $p = 0.576$). As depicted in Figure 1A, homozygous or compound heterozygous carriers of *ALG6* or *PMM2* mutations had marked hypocholesterolemia: plasma TC and LDL-c were half of controls (TC: 107 ± 34 in ALG6 and 93 ± 25 in PMM2 versus 171 ± 22 mg/dl in controls and LDL-c: 51 ± 23 and 48 ± 22 versus 87 ± 10 mg/dl in controls, for all $p < 0.0001$). ApoB was 59% and 44% lower in ALG6- and PMM2-CDG patients, respectively (29 ± 13 and 39 ± 21 mg/dl versus 70 ± 8 in controls, both $p < 0.0001$). In fact, TC, LDL-c and apoB were below the 5th percentile for age and gender, thereby qualifying as hypobetalipoproteinemia²⁴. Additionally, HDL-c was lower in patients: 36% and 45% lower in patients compared to controls (36 ± 10 and 29 ± 11 mg/dl respectively versus 57 ± 14 mg/dl, $p < 0.0001$ for both). Plasma apoA-I and TG levels were comparable to controls. The discrepancy between HDL-c and apoA-I may indicate reduced maturation of HDL particles due to reduced efflux of cholesterol from ABCA1 to apoA-I (in support, see Figure S2) and/or reduced cholesterol esterification driven by LCAT, both of which could explain the reduced HDL-c. Importantly, potential secondary causes for the HBL phenotype in this validation cohort were not found (Table S3).

Heterozygous carriers of CDG-I mutations have decreased plasma LDL-c and apoB

To determine whether clinically unaffected, heterozygous carriers of CDG-I mutations had altered plasma lipids, these were analyzed in first- and second-degree family members of CDG-I patients. For this analysis 23 heterozygous carriers were available: 10 carriers of PMM2-CDG mutations, 7 of ALG6-CDG, 2 of ALG12-CDG and 4 of MPI-CDG mutations (the latter being two other subtypes of CDG-I^{16,17}). Their mean age was 45,5 years (SD 13,6). In congruence with the observation in the CDG-I patients, plasma LDL-c (118 ± 35 versus 136 ± 22 mg/dl in controls, $p = 0.038$) and apoB (84 ± 28 versus 106 ± 20 mg/dl, $p = 0.007$) in heterozygous carriers ($n = 23$) were significantly lower compared to age- and gender-matched controls (Figure 1B). No significant differences in HDL-c or apoA-I were observed between heterozygous carriers and controls. When assessed per CDG-I subtype, this difference remained significant for heterozygous carriers of *PMM2* mutations ($n = 10$) and *ALG12*

mutations (n = 2); a trend towards lower LDL-c was observed in carriers of *MPI* mutations (n = 4). (Figure 1C).

In a complementary approach, we screened for heterozygous carriers of CDG-I mutations among the subjects in a cohort of 150 subjects recruited from our outpatient clinic with available exome sequence data. This approach resulted in the identification of one family with four carriers of a previously described, pathogenic *PMM2* mutation: p.Pro113Leu²⁵. The heterozygotes (n = 4) tended to have lower TC (182 ± 25 mg/dl vs 227 ± 41 mg/dl, p = 0.115) and LDL-c (100 ± 25 mg/dl vs 131 ± 27 mg/dl, p = 0.137) than their unaffected family members (n = 4) (Table S4) and compared to a larger group of 12 age- and gender-matched unrelated controls, the heterozygote carriers of CDG-I mutations had significantly lower LDL-c (100 ± 25 mg/dl vs 132 ± 17 mg/dl, p = 0.012, Table S4).

Molecular explanations of hypobetalipoproteinemia in CDG-I

We subsequently set out to unravel the potential cellular mechanism(s) underlying the effect of CDG-I mutations on LDL metabolism. First, we used small-interference RNAs (siRNAs) to silence *ALG6* and *PMM2* expression in human hepatoma cells (HepG2), using non-targeting siRNAs as control.

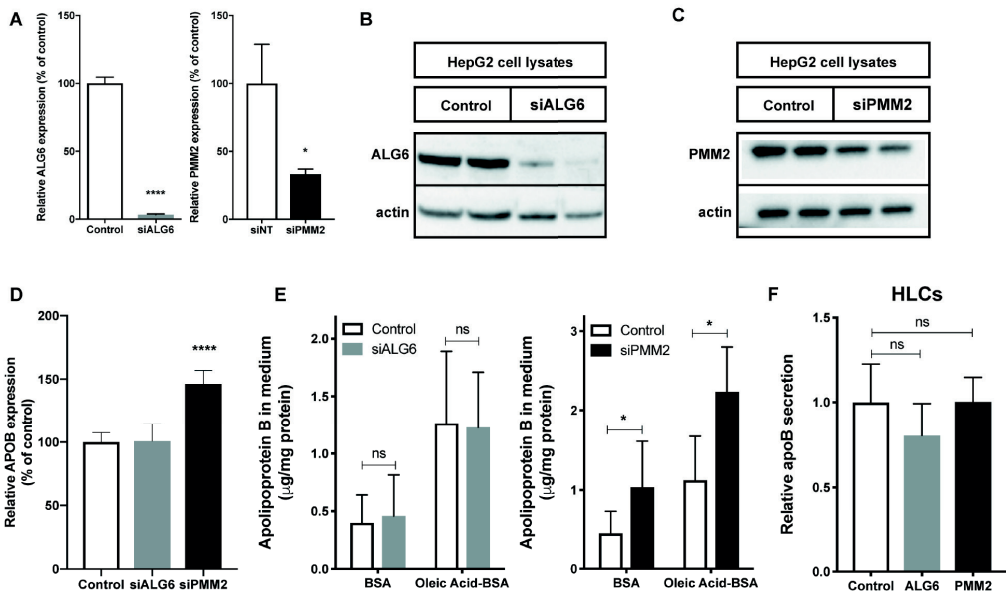


Figure 2 ApoB production and secretion is unaffected in siALG6 and siPMM2 treated HepG2 cells and CDG-I HLCs. siRNA knockdown of *ALG6* and *PMM2* in HepG2 cells. Panels show *ALG6* (left) and *PMM2* (right) mRNA expression levels (A), *ALG6* protein levels (B), *PMM2* protein levels (C), apoB mRNA expression (D), secretion of apoB into the medium (normalized for total protein) in normal and oleic acid stimulated conditions (E) for siALG6 treated cells (left) and siPMM2 treated cells (right). Relative 35S apoB secretion into the medium in patient-derived HLCs is shown in (G). All panels show representative western blots or means ± SD from three experiments with triplicate measurements per experiment. **** indicates p < 0.0001, * indicates p < 0.05 and ns indicates non-significant results as calculated with Student’s unpaired two-sided t-tests. BSA = bovine serum albumin; oleic acid-BSA = oleate complexed to BSA; HLCs = hepatocyte-like cells.

We achieved effective silencing of *ALG6* and *PMM2* (>95% on average for *ALG6* and 67% for *PMM2*; Figure 2A), which was accompanied by a corresponding decrease in ALG6 (Figure 2B) and PMM2 protein level (Figure 2C).

ApoB production and secretion is unaffected in siALG6 and siPMM2 treated HepG2 cells and patient-derived HLCs re-differentiated from iPSCs

Decreased apoB production can limit its secretion²⁶. Additionally, ER-associated degradation and autophagy of apoB are major rate limiting steps of its secretion, such that experimental inhibition of these degradation pathways generally increases apoB secretion²⁷. To address apoB production in siRNA treated cells, APOB mRNA expression was assessed with qPCR (Figure 2D); there was no difference in APOB expression in siALG6 treated cells compared to controls. A significant increase in APOB expression was observed in the siPMM2 treated cells. Secretion of apoB protein into the medium was measured with ELISA (Figure 2E). Basal and oleic-acid stimulated apoB secretion were not affected by siALG6. In siPMM2 cells, apoB secretion was significantly increased, analogous to the increased APOB mRNA expression.

Inhibiting degradation pathways with the proteasomal inhibitor MG-132 or with bafilomycin A (BafA), an inhibitor of autophagy, for four hours did not affect apoB secretion in siALG6 treated more than in control cells (Figure S3). Lastly, we also assessed apoB secretion by ³⁵S steady-state protein labelling in patient-derived HLCs and found no significant differences between the ALG6- or PMM2-CDG patient cells compared to controls (Figure 2F).

Cell surface LDLR expression is increased in siALG6 treated HepG2 cells, CDG-I fibroblasts and patient-derived HLCs re-differentiated from iPSCs

The presence of HBL in absence of steatosis and unaltered apoB secretion strongly suggest an increased clearance of apoB-containing lipoproteins from the circulation. Thus, we determined LDLR protein abundance after sterol depletion in whole cell lysates of siALG6 and siPMM2 treated HepG2 cells (Figure 3A) and specifically on the cell surface (Figure 3B). Indeed, we found both to be markedly increased in siALG6 treated cells; LDLR expression on the cell membrane was on average 145% of controls in siALG6 ($p = 0.005$) and this was accompanied by a 153% increase ($p < 0.0001$) in the uptake of fluorescently labeled LDL (Figure 3C). In siPMM2 cells, we observed almost tripled LDLR protein in whole cell lysates (Figure 3A), however siPMM2 did not seem to affect surface LDLR expression (Figure 3B) and was only accompanied by a slight, yet significant increase in LDL uptake (114% of controls, $p = 0.003$; Figure 3C).

To verify these findings, we studied patient-derived fibroblasts; an established model to study LDLR functionality in patients with familial hypercholesterolemia²⁸. Fibroblasts of 6 CDG-I patients were analyzed (3 ALG6 and 3 PMM2 patients, versus 2 healthy controls). Also in this model, there was markedly increased LDLR protein abundance, both in cell lysates (Figure 3E) and on the cell surface (Figure 3F), which was again accompanied by enhanced uptake of LDL (on average 159%, $p < 0.001$ in ALG6-CDG, and a 5-fold increase in PMM2-CDG, $p = 0.011$; Fig 3H), together with an increased LDLR mRNA expression in both siALG6 and siPMM2 treated HepG2 cells and in ALG6-CDG fibroblasts

– in PMM2-CDG fibroblasts this failed to reach significance ($p = 0.06$) (Fig 3D and H), arguing against a solely post-transcriptional effect on LDLR abundance.

Moreover, in both HepG2 cells and ALG6- and PMM2-CDG fibroblasts the LDLR protein migrated at approximately its expected molecular weight on SDS-PAGE gels (~160 kD) with no apparent difference compared to controls (Figure 3A and E). This also argues against a direct post-transcriptional effect on LDLR.

To further establish this, we used HepG2 cells that stably over-express an LDLR-GFP fusion protein. Indeed, when we silenced *ALG6* expression in these cells, the endogenous, untagged LDLR protein increased, as observed in our other cell models. However, the GFP-tagged LDLR was refractory to *ALG6* silencing, as its levels remained unchanged (Figure S4). This reinforces the notion that *ALG6* influences a pre-translational step in LDLR production.

We replicated these findings in patient-derived HLCs and again found increased LDLR protein levels in whole cell lysates of the patient HLCs compared to controls (Figure 3I): when normalized for cellular albumin – a marker of well-differentiated HLCs – there was a 2 to 3-fold increase in LDLR protein compared to controls. Cell surface LDLR on HNF4 α -positive HLCs was also significantly increased both in ALG6 and PMM2 patient HLCs (129% and 134% of controls respectively, $p < 0,01$ and $p < 0,001$; Figure 3J) which was also accompanied by increased ^{125}I LDL uptake (Figure 3K). Of note, the PMM2-CDG patient derived cells differentiated less efficiently compared to controls, however all cell lines reached >70% re-differentiation efficiency on average. Collectively, the results from three cell models convincingly show increased LDLR protein expression and function in CDG-I patients.

In our cohort, total and free PCSK9 plasma levels were comparable between the CDG-I patients and matched controls. In the carriers, total and free PCSK9 plasma levels were higher than in adult controls (Figure S5A). Furthermore, we found increased mRNA expression of *PCSK9* (Figure 4B) and comparable levels of secreted PCSK9 in siALG6 treated HepG2 cells compared to controls (Figure S5B).

No major role for ER stress in the LDLR upregulation in siALG6 and siPMM2 treated cells

Several studies have shown a role for ER stress in activating SREBP $^{29-31}$ and subsequent *LDLR* transcription 32 . To investigate this in our CDG-I cell models, we studied mRNA and protein expression levels of ER stress markers in siALG6 and siPMM2 treated HepG2 cells. mRNA levels for *ATF3*, *ATF4*, spliced *XBP1* and *CHOP* were not elevated in siPMM2 treated HepG2 cells and only *ATF3* was slightly increased in siALG6 cells (Figure 4A), however not nearly to the degree that was observed when the cells were treated with known ER stress inducers TG and TM. TG and TM did significantly increase mRNA levels of the ER stress markers (Figure 4A). Protein levels of ER stress marker CHOP, were also not increased in the siALG6 and siPMM2 treated cells compared to controls, whereas TG and TM did induce protein expression of CHOP, however this was not accompanied by a concomitant LDLR increase (Figure 4B).

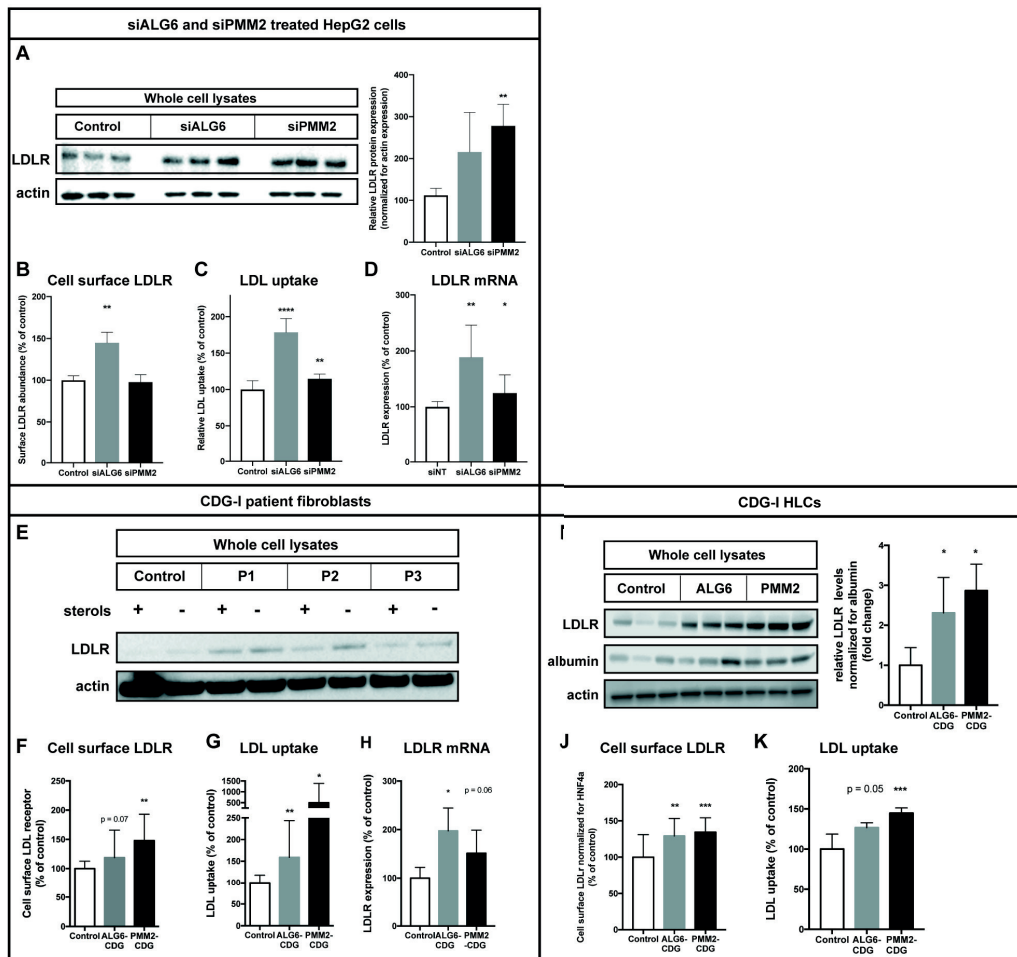


Figure 3 LDLR expression is increased in siALG6 and siPMM2 treated HepG2 cells, CDG-I patient fibroblasts and CDG-I patient HLCs. Panels show representative blots of analysis of LDLR protein expression in whole cell lysates before and after sterol depletion, cell surface LDLR abundance measured with FACS, Dy-light488-labeled LDL uptake and LDLR mRNA expression in siALG6 treated HepG2 cells (**A-D**) and in CDG-I patient fibroblasts (**E-H**). In patient-derived HLCs, panel (**I**) shows LDLR protein expression in whole cell lysates after sterol depletion and relative LDLR expression normalized for albumin, (**J**) shows cell surface LDLR measured with FACS, (**K**) shows ¹²⁵I LDL uptake for the different HLC lines. All panels show representative western blots or means \pm SD from three experiments with triplicate measurements per experiment. **** indicates $p < 0.0001$, *** $p < 0.001$, ** $p < 0.01$, * $p < 0.05$ as calculated with Student's unpaired two-sided t-tests. HLCs = hepatic-like cells re-differentiated from CDG-I patient iPSCs, GFP = green fluorescent protein, P1-3 are two ALG6- and 1 PMM2-CDG patients.

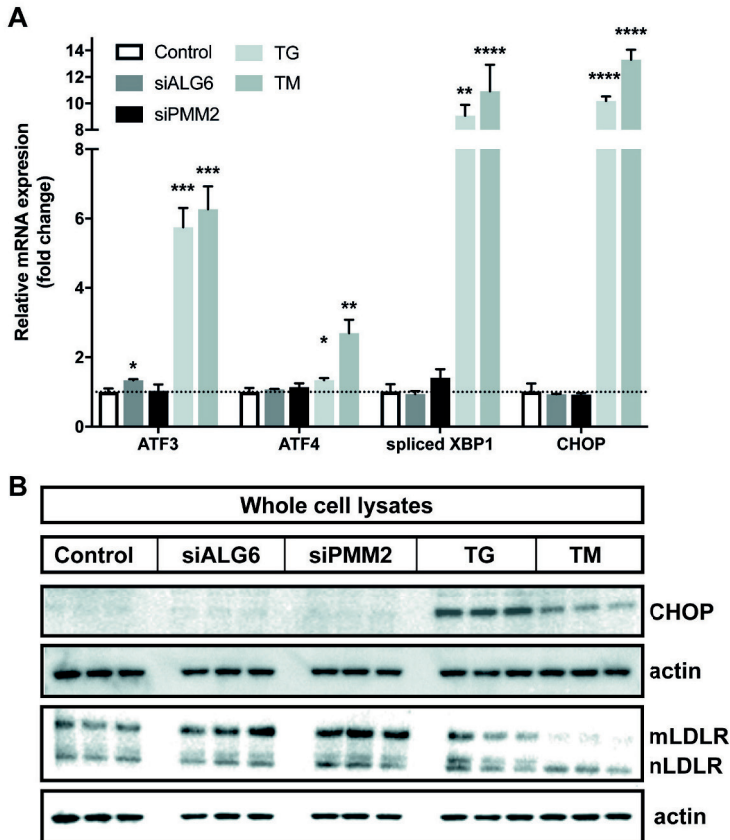


Figure 4 ER stress markers in siALG6 and siPMM2 HepG2 cells. (A) mRNA levels of ER stress markers ATF3, ATF4, spliced XBP1 and CHOP. **(B)** Representative blot of CHOP protein expression and LDLR in cells treated with siALG6, siPMM2, TG and TM. All panels show representative western blots or means \pm SD from at least two experiments with triplicate measurements per experiment. **** indicates $p < 0.0001$, *** $p < 0.001$, ** $p < 0.01$, * $p < 0.05$ as calculated with Student's unpaired two-sided t-tests. TG = thapsigargin, TM = tunicamycin.

In addition, mRNA expression of several other SREBP2 targets, such as *HMGCR*, *HMGCS* and *PCSK9*, was increased (Figure 5B), although not to the same extent as *LDLR* mRNA. To test whether sterol sensing in the ER was intact, we evaluated the ability of β -MCD and 25-hydroxycholesterol to inhibit the SREBP2 pathway. Despite higher basal LDLR levels in siALG6 treated HepG2 cells compared to control cells, a similar response upon SREBP2 inhibition was found (Figure 5C). Collectively, these results suggest that both SREBP2 activation and sterol sensing is intact in our CDG-I cell model.

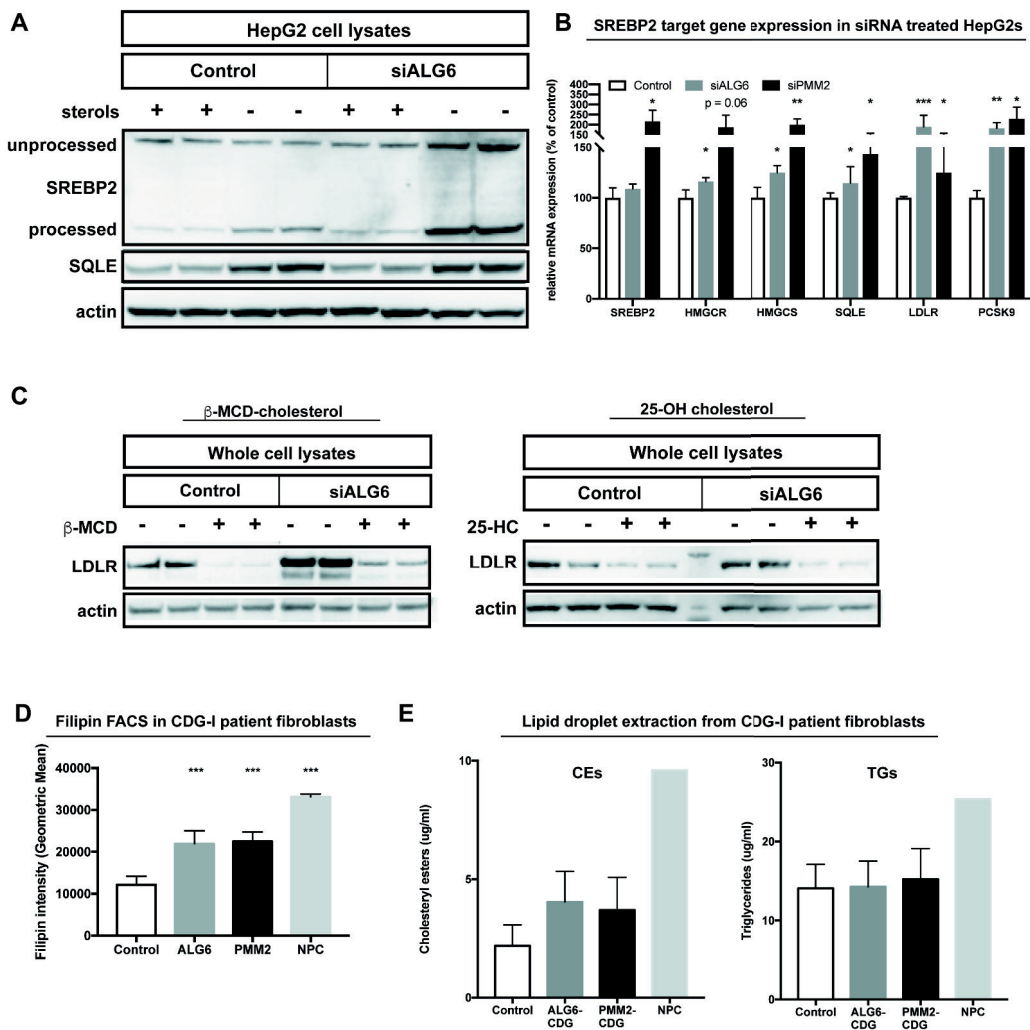


Figure 5 Increased SREBP2 levels with intact cholesterol sensing in cells with decreased ALG6 or PMM2 activity. Panels show unprocessed and processed SREBP2 and SREBP2-target SQLE protein expression in HepG2 cells before and after sterol depletion (**A**), mRNA expression of other SREBP2 targets (**B**), whole cell lysate LDLR protein levels before and after 4 hr β -MCD cholesterol or 25-hydroxycholesterol incubation (**C**), intracellular cholesterol levels measured with filipin staining in patient fibroblasts (**D**) and CE and TG content of lipid droplets in patient fibroblasts (**E**). All panels show representative western blots or means \pm SD from at least two experiments with triplicate measurements per experiment. *** indicates $p < 0.001$, ** $p < 0.01$, * $p < 0.05$ as calculated with Student's unpaired two-sided t-tests. NPC = Niemann Pick C patient, CEs = cholesteryl esters.

As SREBP2 activation and expression of cholesterologenic enzymes are elevated in CDG-I cells, we measured intracellular cholesterol levels in fibroblasts. As a positive control, we used fibroblasts of a patient with genetically proven Niemann-Pick C disease because of the known accumulation of free cholesterol in the cells of these patients (NPC in Figure 5D). Filipin staining of siALG6 treated HepG2s showed similar amounts of intracellular cholesterol compared to controls. In contrast, patient fibroblasts all showed significantly increased intracellular cholesterol (Figure 5D). Furthermore, lipid droplets in CDG-I fibroblasts showed a 2-fold increase in cholesteryl esters without affecting triglyceride content (Figure 5E), possibly suggesting higher esterification activity due to increased free cholesterol.

Combined, the increased LDLR and SREBP2 despite high intracellular cholesterol, and the intact sterol sensing without significant ER stress, led us to investigate whether the ER resident protein INSIG1 could link the disturbed N-glycan synthesis in the ER to increased levels of SREBP2 and LDLR. To this end, we overexpressed Myc-tagged INSIG1 in siALG6 HepG2 cells, which abolished the upregulation of LDLR (Figure S6).

Discussion

This study provides evidence for a novel molecular origin of low plasma LDL-c levels and describes a new primary HBL phenotype without hepatic steatosis or steatorrhea. This evidence was collected in a cohort of patients with biallelic mutations in *ALG6* or *PMM2*, the two most common forms of autosomal recessive CDG-I, who demonstrated HBL; their clinically unaffected, heterozygous relatives, who also had decreased LDL-c plasma levels; and *in vitro* studies with patient-derived cells demonstrating increased LDLR expression and LDL particle uptake. Furthermore, the HBL phenotype in the patients was not associated with signs of secondary causes of low plasma cholesterol.

Primary HBL comprises a group of rare genetic dyslipidemias characterized by plasma levels of TC, LDL-c and apoB below the 5th percentile³⁴. Physiologically, there are two potential explanations for profound reductions in plasma apoB-containing lipoproteins: 1) decreased production or secretion of apoB/VLDL particles, as observed in patients with *APOB* or *MTTP* mutations and 2) increased clearance of apoB-containing lipoproteins through increased LDLR, as is observed in patients with *PCSK9*³⁵ or *ANGPTL3* loss-of-function (LOF) mutations³⁶. In homozygous *APOB* or *MTP* deficient patients, decreased hepatic secretion of VLDL causes hepatic steatosis and in some cases fat malabsorption leading to severe steatorrhea. Heterozygosity for *APOB* mutations displays a milder clinical phenotype²⁴ as well as patients with HBL caused by LOF mutations in *PCSK9*^{35,37}, in whom increased cell surface LDLR expression leads to increased LDL clearance without hepatic steatosis.

The underlying mechanism we identify in the development of HBL in CDG-I patients involves a pathway that results in increased LDLR mRNA and higher LDLR membrane abundance via increased basal levels of processed SREBP2. To date, the mentioned LOF mutations in *PCSK9* are the only other known cause of HBL due to increased LDLR^{35,37} and increased LDL-c clearance, as is seen in CDG-I patients. The role of *PCSK9* in LDLR membrane abundance and LDL clearance is well established³⁸. Benjannet and colleagues³⁹ showed that impaired glycosylation of *PCSK9* did not significantly alter its secretion or function at least in Huh7 cells. And indeed, we did not find a role for *PCSK9* in the

HBL phenotype in CDG-I patients.

Our *in vitro* studies demonstrate that cell surface LDLR and LDL particle uptake were significantly increased when ALG6 or PMM2 activity is decreased, without affecting apoB secretion. In contrast, others reported increased apoB degradation upon inhibition of glycosylation with tunicamycin^{40,41} or site-specific mutagenesis of N-glycosylation sites in truncated apoB constructs⁴². The discrepancy with the latter study might lie in a difference in the apoB isoform that was studied (apoB37 versus apoB100) and in the different cell model (rat McArdle cells versus human HepG2 cells). We have no specific explanation for the discrepancy with the tunicamycin model in the former study. Taken together, our observations do not support a significant role for reduced production or increased degradation of apoB in the HBL phenotype in ALG6- and PMM2-CDG.

The main driver of LDLR transcription is decreased intracellular cholesterol through SREBP2 activation. SREBP2 is located in the ER and held in place by the association with SCAP and INSIG³³. When cells are depleted of sterols, a conformational change in SCAP allows SREBP2 to translocate to the Golgi apparatus to undergo sequential proteolytic activation by site-1-protease (S1P) and S2P. The cleaved product, nuclear SREBP2, is responsible for transcription of the ~30 genes involved in cholesterol synthesis, such as the rate-limiting enzymes HMGCR and SQLE, as well as those involved in cellular cholesterol uptake, such as LDLR and PCSK9. In our study, SREBP2 protein levels and expression of SREBP2 target proteins were significantly increased in cell models for CDG-I despite elevated intracellular cholesterol, and intact SREBP2 activation through sterol sensing was observed.

Several studies have shown a role for ER stress in activating SREBP2²⁹⁻³¹ and subsequent *PCSK9* and *LDLR* transcription³². Lebeau et al³² additionally showed that TM increased LDLR mRNA expression and reduced plasma LDL-c in mice. So, it could be hypothesized that ER stress caused by an accumulation of unfolded proteins due to deficient glycosylation plays a role in the SREBP2 activation in the CDG-I models. However, we did not find elevated ER stress markers in the siALG6 and siPMM2 treated HepG2 cells; we therefore concluded that ER stress does not underlie the increased LDLR function in our CDG-I cells.

Taken together, we observed increased LDLR and SREBP2 function despite high intracellular cholesterol, together with intact sterol sensing, yet in absence of significant ER stress. This led us to postulate that in CDG-I, the defective N-glycan assembly in the ER may affect INSIG1, the ER resident protein that controls proteolytic activation of SREBP2 via retention of SCAP.⁴³ In our hands and in those of others, endogenous INSIG1 protein levels are below detection limit. Thus, we overexpressed Myc-tagged INSIG1 in our siALG6 HepG2 model. In support of our postulated mechanism, overexpression of INSIG1 in siALG6 HepG2 cells abolished the upregulation of the LDL receptor which we so strongly observed in the three complimentary cell models of our study.

Four aspects merit closer consideration. First, CDG-I patients have a general glycosylation defect early in the glycan tree assembly machinery, causing empty glycosylation sites on a wide variety of glycoproteins. This evidently poses a challenge to the identification of the causal pathway

underlying the HBL in CDG-I. This is further compounded by biological and technical aspects related to N-glycosylation: the sequon (amino acid consensus motif) for N-glycosylation enzymes to initiate and attach N-glycans is identical for each individual N-glycosylated protein. In addition, no N-glycoproteomics technology is available at the moment that allows proper normalization to allow quantification of glycan site-occupancy at the proteome scale. Yet, all *in vitro* studies point to one distinct pathway; increased LDLR expression, without indications of disrupted apoB secretion or VLDL assembly.

Secondly, the HBL phenotype seems to be specific to CDG-I: we have studied plasma lipids in other CDG types: CDG-II, affecting editing of N-glycans in the Golgi apparatus, and Golgi trafficking defects, affecting ER- to Golgi-transport and the N- and O-glycosylation enzymes located within these compartments. These CDG patients have different, yet still global protein glycosylation defects, but importantly, they show completely different plasma lipid abnormalities than the HBL observed in CDG-I patients. CDG-II patients sequester all their plasma cholesterol in the HDL fraction⁴⁴. Patients with Golgi trafficking and mixed glycosylation defects, such as CCDC115- or TMEM199-deficiency, have marked hypercholesterolemia, in the range of familial hypercholesterolemia^{45,46}. These distinctions again suggest a specific influence of N-linked glycosylation on LDL pathways.

Thirdly, the observation that heterozygous carriers also display a hypolipidemic phenotype without other clinical features of the CDG-I syndrome, underscores the more general notion that the influence of genetic variation in protein glycosylation on metabolic pathways in the general population is understudied⁴⁷.

Finally, it is well established that low plasma LDL-c levels reduce atherosclerotic cardiovascular disease. Whether CDG-I patients are protected from atherosclerosis cannot yet be determined. The oldest patients known to date are in their forties; the prognosis and life expectancy of CDG-I patients is predominantly determined by their neuromuscular pathology⁴⁸. Promising in this respect is our finding that most heterozygous carriers also show the beneficial lipid phenotype of low LDL-c, but none of the clinical symptoms found in CDG-I patients.

Conclusion

We have shown that mutations in *ALG6* and *PMM2* can cause an HBL phenotype. Mechanistically, these changes can be explained by increased LDLR protein abundance with concomitant increased hepatic LDL clearance, driven by increased SREBP2 in absence of major ER stress. Our data thus establish a major impact of protein glycosylation on LDL metabolism. Heterozygous carriers of CDG-I mutations exhibit marked hypocholesterolemia in absence of adverse clinical symptoms observed in the homozygous patients. In this light, our findings warrant exploration of therapeutic targeting of N-linked glycosylation in the LDLR pathway to reduce LDL-c in patients at increased cardiovascular risk, especially because therapeutic targeting of protein glycosylation is already being ventured in virology, immunology and oncology^{49,50}.

References

1. van den Boogert MAW, Rader DJ, Holleboom AG. New insights into the role of glycosylation in lipoprotein metabolism. *Curr Opin Lipidol*. 2017;28:502–506.
2. Ohtsubo K, Marth JD. Glycosylation in cellular mechanisms of health and disease. *Cell*. 2006;126:855–867.
3. Kathiresan S, Willer CJ, Peloso GM, Demissie S, Musunuru K, Schadt EE, Kaplan L, Bennett D, Li Y, Tanaka T, Voight BF, Bonnycastle LL, Jackson AU, Crawford G, Surti A, Guiducci C, Burt NP, Parish S, Clarke R, Zelenika D, Kubalanza KA, Morken MA, Scott LJ, Stringham HM, Galan P, Swift AJ, Kuusisto J, Bergman RN, Sundvall J, Laakso M, Ferrucci L, Scheet P, Sanna S, Uda M, Yang Q, Lunetta KL, Dupuis J, de Bakker PIW, O'Donnell CJ, Chambers JC, Kooner JS, Hercberg S, Meneton P, Lakatta EG, Scuteri A, Schlessinger D, Tuomilehto J, Collins FS, Groop L, Altshuler D, Collins R, Lathrop GM, Melander O, Salomaa V, Peltonen L, Orho-Melander M, Ordovas JM, Boehnke M, Abecasis GR, Mohlke KL, Cupples LA. Common variants at 30 loci contribute to polygenic dyslipidemia. *Nat Genet*. 2009;41:56–65.
4. Willer CJ, Sanna S, Jackson AU, Scuteri A, Bonnycastle LL, Clarke R, Heath SC, Timpson NJ, Najjar SS, Stringham HM, Strait J, Duren WL, Maschio A, Busonero F, Mulas A, Albai G, Swift AJ, Morken MA, Narisu N, Bennett D, Parish S, Shen H, Galan P, Meneton P, Hercberg S, Zelenika D, Chen W-M, Li Y, Scott LJ, Scheet PA, Sundvall J, Watanabe RM, Nagaraja R, Ebrahim S, Lawlor DA, Ben-Shlomo Y, Davey-Smith G, Shuldiner AR, Collins R, Bergman RN, Uda M, Tuomilehto J, Cao A, Collins FS, Lakatta E, Lathrop GM, Boehnke M, Schlessinger D, Mohlke KL, Abecasis GR. Newly identified loci that influence lipid concentrations and risk of coronary artery disease. *Nat Genet*. 2008;40:161–169.
5. Holleboom AG, Karlsson H, Lin R-S, Beres TM, Sierts JA, Herman DS, Stroes ESG, Aerts JM, Kastelein JJP, Motazacker MM, Dallinga-Thie GM, Levels JHM, Zwinderman AH, Seidman JG, Seidman CE, Ljunggren S, Lefeber DJ, Morava E, Wevers RA, Fritz TA, Tabak LA, Lindahl M, Hovingh GK, Kuivenhoven JA. Heterozygosity for a loss-of-function mutation in GALNT2 improves plasma triglyceride clearance in man. *Cell Metab*. 2011;14:811–818.
6. Schjoldager KT-BG, Vester-Christensen MB, Bennett EP, Levery SB, Schwientek T, Yin W, Blixt O, Clausen H. O-glycosylation modulates proprotein convertase activation of angiotensin-like protein 3: possible role of polypeptide GalNAc-transferase-2 in regulation of concentrations of plasma lipids. *J Biol Chem*. 2010;285:36293–36303.
7. Khetarpal SA, Schjoldager KT, Christoffersen C, Raghavan A, Edmondson AC, Reutter HM, Ahmed B, Ouazzani R, Peloso GM, Vitali C, Zhao W, Somasundara AVH, Millar JS, Park Y, Fernando G, Livanov V, Choi S, Noé E, Patel P, Ho SP, Myocardial Infarction Exome Sequencing Study, Kirchgessner TG, Wandall HH, Hansen L, Bennett EP, Vakhrushev SY, Saleheen D, Kathiresan S, Brown CD, Abou Jamra R, LeGuern E, Clausen H, Rader DJ. Loss of Function of GALNT2 Lowers High-Density Lipoproteins in Humans, Nonhuman Primates, and Rodents. *Cell Metab*. 2016;24:234–245.
8. Freeze HH, Chong JX, Bamshad MJ, Ng BG. Solving glycosylation disorders: fundamental approaches reveal complicated pathways. *Am J Hum Genet*. 2014;94:161–175.
9. Jaeken J. Congenital disorders of glycosylation. *Ann N Y Acad Sci*. 2010;1214:190–198.
10. Scott K, Gadomski T, Kozicz T, Morava E. Congenital disorders of glycosylation: new defects and still counting. *J Inherit Metab Dis*. 2014;37:609–617.
11. de Lonlay P, Seta N. The clinical spectrum of phosphomannose isomerase deficiency, with an evaluation of mannose treatment for CDG-Ib. *Biochim Biophys Acta*. 2009;1792:841–843.
12. Jaeken J, Eggermont E, Stibler H. An apparent homozygous X-linked disorder with carbohydrate-deficient serum glycoproteins. *Lancet*. 1987;2:1398.
13. Ohno K, Yuasa I, Akaboshi S, Itoh M, Yoshida K, Ehara H, Ochiai Y, Takeshita K. The carbohydrate

- deficient glycoprotein syndrome in three Japanese children. *Brain Dev.* 1992;14:30–35.
14. Pavone L, Fiumara A, Barone R, Rizzo R, Buttitta P, Dobyns WB, Jaeken J. Olivopontocerebellar atrophy leading to recognition of carbohydrate-deficient glycoprotein syndrome type I. *J Neurol.* 1996;243:700–705.
 15. Lefeber DJ, Morava E, Jaeken J. How to find and diagnose a CDG due to defective N-glycosylation. *J Inherit Metab Dis.* 2011;34:849–852.
 16. Chantret I, Dupré T, Delenda C, Bucher S, Dancourt J, Barnier A, Charollais A, Heron D, Bader-Meunier B, Danos O, Seta N, Durand G, Oriol R, Codogno P, Moore SEH. Congenital disorders of glycosylation type Ig is defined by a deficiency in dolichyl-P-mannose:Man7GlcNAc2-PP-dolichyl mannosyltransferase. *J Biol Chem.* 2002;277:25815–25822.
 17. Freeze HH, Aebi M. Molecular basis of carbohydrate-deficient glycoprotein syndromes type I with normal phosphomannomutase activity. *Biochim Biophys Acta.* 1999;1455:167–178.
 18. Cayo MA, Cai J, DeLaForest A, Noto FK, Nagaoka M, Clark BS, Collery RF, Si-Tayeb K, Duncan SA. JD induced pluripotent stem cell-derived hepatocytes faithfully recapitulate the pathophysiology of familial hypercholesterolemia. *Hepatology.* 2012;56:2163–2171.
 19. Zelcer N, Hong C, Boyadjian R, Tontonoz P. LXR regulates cholesterol uptake through Idol-dependent ubiquitination of the LDL receptor. *Science.* 2009;325:100–104.
 20. Sorrentino V, Fouchier SW, Motazacker MM, Nelson JK, Defesche JC, Dallinga-Thie GM, Kastelein JJP, Kees Hovingh G, Zelcer N. Identification of a loss-of-function inducible degrader of the low-density lipoprotein receptor variant in individuals with low circulating low-density lipoprotein. *Eur Heart J.* 2013;34:1292–1297.
 21. Ota T, Gayet C, Ginsberg HN. Inhibition of apolipoprotein B100 secretion by lipid-induced hepatic endoplasmic reticulum stress in rodents. *J Clin Invest.* 2008;118:316–332.
 22. Franssen R, Schimmel AWM, van Leuven SI, Wolfkamp SCS, Stroes ESG, Dallinga-Thie GM. In Vivo Inflammation Does Not Impair ABCA1-Mediated Cholesterol Efflux Capacity of HDL. *Cholesterol.* 2012;2012:610741.
 23. Adams CM, Reitz J, De Brabander JK, Feramisco JD, Li L, Brown MS, Goldstein JL. Cholesterol and 25-hydroxycholesterol inhibit activation of SREBPs by different mechanisms, both involving SCAP and Insigs. *J Biol Chem.* 2004;279:52772–52780.
 24. Schonfeld G, Lin X, Yue P. Familial hypobetalipoproteinemia: genetics and metabolism. *Cellular and Molecular Life Sciences.* 2005;62:1372–1378.
 25. Böhles H, Sewell AA, Gebhardt B, Reinecke-Lüthge A, Klöppel G, Marquardt T. Hyperinsulinaemic hypoglycaemia--leading symptom in a patient with congenital disorder of glycosylation Ia (phosphomannomutase deficiency). *J Inherit Metab Dis.* 2001;24:858–862.
 26. Rutledge AC, Qiu W, Zhang R, Kohen-Avramoglu R, Nemat-Gorgani N, Adeli K. Mechanisms targeting apolipoprotein B100 to proteasomal degradation: evidence that degradation is initiated by BiP binding at the N terminus and the formation of a p97 complex at the C terminus. *Arterioscler Thromb Vasc Biol.* 2009;29:579–585.
 27. Fisher EA, Zhou M, Mitchell DM, Wu X, Omura S, Wang H, Goldberg AL, Ginsberg HN. The degradation of apolipoprotein B100 is mediated by the ubiquitin-proteasome pathway and involves heat shock protein 70. *J Biol Chem.* 1997;272:20427–20434.
 28. Goldstein JL, Brown MS. Binding and degradation of low density lipoproteins by cultured human fibroblasts. Comparison of cells from a normal subject and from a patient with homozygous familial hypercholesterolemia. *J Biol Chem.* 1974;249:5153–5162.
 29. Pai JT, Brown MS, Goldstein JL. Purification and cDNA cloning of a second apoptosis-related cysteine

- protease that cleaves and activates sterol regulatory element binding proteins. *Proc Natl Acad Sci USA*. 1996;93:5437–5442.
30. Lee JN, Ye J. Proteolytic activation of sterol regulatory element-binding protein induced by cellular stress through depletion of Insig-1. *J Biol Chem*. 2004;279:45257–45265.
 31. Werstuck GH, Lentz SR, Dayal S, Hossain GS, Sood SK, Shi YY, Zhou J, Maeda N, Krisans SK, Malinow MR, Austin RC. Homocysteine-induced endoplasmic reticulum stress causes dysregulation of the cholesterol and triglyceride biosynthetic pathways. *J Clin Invest*. 2001;107:1263–1273.
 32. Lebeau P, Al-Hashimi A, Sood S, Lhoták Š, Yu P, Gyulay G, Pare G, Chen SRW, Trigatti B, Prat A, Seidah NG, Austin RC. Endoplasmic Reticulum Stress and Ca²⁺ Depletion Differentially Modulate the Sterol Regulatory Protein PCSK9 to Control Lipid Metabolism. *J Biol Chem*. 2017;292:1510–1523.
 33. Brown MS, Goldstein JL. The SREBP pathway: regulation of cholesterol metabolism by proteolysis of a membrane-bound transcription factor. *Cell*. 1997;89:331–340.
 34. Contois JH, McNamara JR, Lammi-Keefe CJ, Wilson PW, Massov T, Schaefer EJ. Reference intervals for plasma apolipoprotein B determined with a standardized commercial immunoturbidimetric assay: results from the Framingham Offspring Study. *Clin Chem*. 1996;42:515–523.
 35. Cohen J, Pertsemlidis A, Kotowski IK, Graham R, Garcia CK, Hobbs HH. Low LDL cholesterol in individuals of African descent resulting from frequent nonsense mutations in PCSK9. *Nat Genet*. 2005;37:161–165.
 36. Musunuru K, Pirruccello JP, Do R, Peloso GM, Guiducci C, Sougnez C, Garimella KV, Fisher S, Abreu J, Barry AJ, Fennell T, Banks E, Ambrogio L, Cibulskis K, Kernysky A, Gonzalez E, Rudzicz N, Engert JC, DePristo MA, Daly MJ, Cohen JC, Hobbs HH, Altshuler D, Schonfeld G, Gabriel SB, Yue P, Kathiresan S. Exome sequencing, ANGPTL3 mutations, and familial combined hypolipidemia. *N Engl J Med*. 2010;363:2220–2227.
 37. Cariou B, Ouguerram K, Zaïr Y, Guerois R, Langhi C, Kourimate S, Benoit I, Le May C, Gayet C, Belabbas K, Dufernez F, Chétiveaux M, Tarugi P, Krempf M, Benlian P, Costet P. PCSK9 dominant negative mutant results in increased LDL catabolic rate and familial hypobetalipoproteinemia. *Arterioscler Thromb Vasc Biol*. 2009;29:2191–2197.
 38. Seidah NG, Awan Z, Chrétien M, Mbikay M. PCSK9: a key modulator of cardiovascular health. *Circ Res*. 2014;114:1022–1036.
 39. Benjannet S, Rhainds D, Hamelin J, Nassoury N, Seidah NG. The proprotein convertase (PC) PCSK9 is inactivated by furin and/or PC5/6A: functional consequences of natural mutations and post-translational modifications. *J Biol Chem*. 2006;281:30561–30572.
 40. Bonen DK, Nassir F, Hausman AM, Davidson NO. Inhibition of N-linked glycosylation results in retention of intracellular apo[a] in hepatoma cells, although nonglycosylated and immature forms of apolipoprotein[a] are competent to associate with apolipoprotein B-100 in vitro. *J Lipid Res*. 1998;39:1629–1640.
 41. Liao W, Chan L. Tunicamycin induces ubiquitination and degradation of apolipoprotein B in HepG2 cells. 2001;353:493–501.
 42. Vukmirica J, Nishimaki-Mogami T, Tran K, Shan J, McLeod RS, Yuan J, Yao Z. The N-linked oligosaccharides at the amino terminus of human apoB are important for the assembly and secretion of VLDL. *J Lipid Res*. 2002;43:1496–1507.
 43. Yabe D, Xia Z-P, Adams CM, Rawson RB. Three mutations in sterol-sensing domain of SCAP block interaction with insig and render SREBP cleavage insensitive to sterols. *Proc Natl Acad Sci USA*. 2002;99:16672–16677.
 44. van den Boogert MAW, Kuil SD, Hovingh GK, Motazacker MM, Levels JHM, Dallinga-Thie GM,

- Kuivenhoven JA, Wevers R, Stroes ESG, Lefeber DJ, Holleboom AG. Genetic defects in protein glycosylation as a cause of dyslipidemia. Poster presented at American Heart Association Scientific Sessions in the Best of Basic Science Session; 2013; Dallas, Texas, USA.
45. Jansen JC, Cirak S, van Scherpenzeel M, Timal S, Reunert J, Rust S, Pérez B, Vicogne D, Krawitz P, Wada Y, Ashikov A, Pérez-Cerdá C, Medrano C, Arnoldy A, Hoischen A, Huijben K, Steenbergen G, Quelhas D, Diogo L, Rymen D, Jaeken J, Guffon N, Cheillan D, van den Heuvel LP, Maeda Y, Kaiser O, Schara U, Gerner P, van den Boogert MAW, Holleboom AG, Nassogne M-C, Sokal E, Salomon J, van den Bogaart G, Drenth JPH, Huynen MA, Veltman JA, Wevers RA, Morava E, Matthijs G, Foulquier F, Marquardt T, Lefeber DJ. CCDC115 Deficiency Causes a Disorder of Golgi Homeostasis with Abnormal Protein Glycosylation. *Am J Hum Genet.* 2016;98:310–321.
 46. Jansen JC, Timal S, van Scherpenzeel M, Michelakakis H, Vicogne D, Ashikov A, Moraitou M, Hoischen A, Huijben K, Steenbergen G, van den Boogert MAW, Porta F, Calvo PL, Mavrikou M, Cenacchi G, van den Bogaart G, Salomon J, Holleboom AG, Rodenburg RJ, Drenth JPH, Huynen MA, Wevers RA, Morava E, Foulquier F, Veltman JA, Lefeber DJ. TMEM199 Deficiency Is a Disorder of Golgi Homeostasis Characterized by Elevated Aminotransferases, Alkaline Phosphatase, and Cholesterol and Abnormal Glycosylation. *Am J Hum Genet.* 2016;98:322–330.
 47. Steentoft C, Vakhrushev SY, Joshi HJ, Kong Y, Vester-Christensen MB, Schjoldager KT-BG, Lavrsen K, Dabelsteen S, Pedersen NB, Marcos-Silva L, Gupta R, Bennett EP, Mandel U, Brunak S, Wandall HH, Lavery SB, Clausen H. Precision mapping of the human O-GalNAc glycoproteome through SimpleCell technology. *EMBO J.* 2013;32:1478–1488.
 48. Jaeken J, Matthijs G, Carchon H, Van Schaftingen E 2001 Defects of N-glycan synthesis. In: Scriver C, Beaudet A, Sly WS, Valle D (eds) *The Metabolic and Molecular Bases of Inherited Disease*, 8th edition. McGraw-Hill, New York, pp 1601–1622
 49. Dalziel M, Crispin M, Scanlan CN, Zitzmann N, Dwek RA. Emerging principles for the therapeutic exploitation of glycosylation. *Science.* 2014;343:1235681–1235681.
 50. Landhuis E. Glycobiology: Sweet success. *Nature.* 2017;547:127–129

Supplemental Methods

Cell culture

HepG2 cells and fibroblasts were cultured in 75 cm² flasks (Falcon) in *complete medium* (DMEM supplemented with 4.5 g glucose, 10% fetal bovine serum and 1% penicillin/streptomycin; Gibco). All cells were maintained in a 37°C humidified incubator with 5% CO₂ atmosphere and split when needed at ~80-100% confluency.

For siRNA experiments in HepG2 cells and LDL uptake assays in patient fibroblasts, cells were plated in 12 wells plates in a 300.000 and 400.000 cells/well density, respectively. For FACS analysis of LDL receptor and filipin staining, cells were plated in 24 wells.

ALG6 and PMM2 knockdown with siRNAs

Transfection medium was prepared according to the manufacturers' protocol. In short, siRNA targeting ALG6 (Life Technologies), PMM2 (FlexiTube GeneSolution, Qiagen), non-targeting siRNA (Life Technologies) were added to Opti-MEM I medium (Invitrogen) without supplements, especially no antibiotics, in a 250 nM concentration. RNAi MAX transfection vehicle (Invitrogen) was added to Opti-MEM I (Gibco) separately first and all solutions were incubated for 5 minutes at room temperature. RNAi max solution was added to the siRNA solution in a 1:1 proportion and left to incubate for 20 minutes at room temperature. Lastly, warm (37°C) *antibiotics-free medium* (DMEM with 4.5 g glucose and 10% fetal bovine serum) was added to a final siRNA concentration of 25 nM and the appropriate transfection medium (siPMM2, siALG6, non-targeting siRNA (Life Technologies) or transfection vehicle only) was added to each well.

The ALG6 and PMM2 protein level was analyzed using western blot with specific antibodies (Abcam). Furthermore, PMM2 activity was measured 48 hours after transfection as described before.¹ To this end, cells of 5 siPMM2 treated wells and 5 vehicle only treated wells were pooled separately after trypsinization and washed with 4 ml 0.9% NaCl and centrifuged (690 g, 8 min) three times before the cell pellet was stored at -80°C. The remaining siPMM2 treated well and vehicle only treated well was used for RNA isolation.

iPSC/HLC culture and differentiation

Patient derived fibroblasts were reprogrammed with Cytotune® reprogramming kit 2.0 by the iPSC core at University of Pennsylvania. First ten cell passages were cultivated on immortalized mouse embryonic fibroblasts as feeder cells in DMEM-F12 supplemented with 20% knock-out replacement serum (Life Tech), 4ng/ml FGF, and incubated at 37°C with 5% O₂/5% CO₂. Cells were passaged when they reached sustainable colony size with accutase® (Innovative Cell Technology) according to manufacturer's protocol. When the iPSCs reached appropriate confluency, they were transferred to Geltrex® (Gibco) and cultivated in StemMACS iPSBrew. Passages were performed with StemMACS non-enzymatic passaging solution according to manufacturer's instructions. After a minimum of four passages in iPSBrew, iPSCs were seeded 1x10⁴ cells per well in a 12-well plate coated with Geltrex®. Induction of differentiation to definitive endoderm (day 1-5) was achieved with StemDiff definitive endoderm kit according to manufacturer's protocol. Further maturation of endoderm to

mature induced hepatocytes (hepatocyte-like cells) was performed according the protocol of Jun Cai et al. (Stembook 2012).

Quantative polymerase chain reaction (qPCR) for expression patterns

mRNA was isolated with Trizol and reversed transcribed with iScript (SensiFAST, Bioline) for qPCR measurement with SYBR green (SensiFAST, Bioline) according to. The manufacturers procedure. The primer sequences used are specified in Supplemental Table S4.

ApoB secretion

Twenty-four hours after transfection the medium was changed to lipoprotein-deficient (LPDS) medium (DMEM supplemented with 4.5 g glucose, 10% lipoprotein-deficient serum and 1% penicillin/streptomycin; Life Technologies). After another 24 hours, either 0.3 mM oleic acid-BSA (OA; Sigma) in LPDS medium or fatty acid free BSA (Sigma) in LPDS medium was added to the wells. After 6 hours, the media were collected for apoB measurement and cells were lysed with Trizol for RNA isolation for expression analysis or RIPA buffer with protease inhibitors (Roche) for protein levels. ApoB levels in the medium were measured with a specific enzyme-linked immunosorbent assay (ELISA, as described in ²) and normalized for total cell protein measured with BCA protein assay (Pierce, ThermoScientific). Where indicated, cells were treated with 25 μ M MG-132 (BIOMOL International), or bafilomycin A (Sigma) for 4 hours or cell lysates were treated with N-glycosidase F (as described ³; Roche). ³⁵S apoB secretion was performed on the patient-derived HLCs at the University of Pennsylvania as described⁴.

LDL uptake assay

The LDL uptake assay was performed as described⁵ on both the siRNA treated HepG2 cells and the patient fibroblasts. In short, the cells were incubated for 24 hours in LPDS medium to induce LDLR expression. Cells were washed once with PBS and incubated with serum-deficient medium containing 5 μ g apoB-LDL/ml of Dylight-488 (Thermo Scientific) labeled LDL isolated by ultracentrifugation from Lp(a) deficient plasma from (30 minutes for HepG2 cells; 1 hour for patient fibroblasts) at 37°C. Next, the cells were washed twice with PBS containing 0.2% BSA prior to lysis with 300 μ l RIPA buffer supplemented with protease inhibitors. After centrifugation 30 μ l of the cleared lysates were transferred to a black 384 wells plate and fluorescence was measured on a Typhoon scanner (Amersham) with filters set to the Dylight label. Measured intensities were normalized for protein content using the BCA Protein Assay Reagent.

¹²⁵I LDL uptake assays were performed on patient-derived HLCs at the University of Pennsylvania as described earlier⁶.

Western Blotting

Total ALG6, PMM2, LDL receptor, PCSK9, SREBP2, ER stress proteins and Myc expression was assessed in cell lysates with Western Blot using an 8% or 4-12% Bis-Tris SDS-page gel (Life Technologies) and specific antibodies and normalized for β -actin: anti-ALG6 (Abcam, ab80873, rabbit); anti-PMM2 (Abcam, ab229996, rabbit); anti-LDLR (Abcam, ab52818, rabbit); anti- β -actin

(Abcam, ab8226, mouse); anti-SREBP2 (BD Pharmingen, 557037, mouse); anti-ERK1/2 (Cell signaling, 4695S, rabbit); anti-pERK (Cell signaling, 9101S, rabbit); ER Stress antibody sampler kit (Cell Signalling, 9956) and anti-Myc (Cell signaling, 2276).

LDL receptor protein expression on the membrane

Fluorescence-activated cell sorting (FACS) to assess the specific membrane protein expression of LDL receptor was performed as described earlier⁷.

Intracellular cholesterol content

Intracellular cholesterol content was assessed in different ways. Regular filipin staining of fixated cells was performed and quantified with FACS. In short, cells of all patients were plated in 24 wells plates in complete medium (4 wells per patient, triplet for filipin and one for background). The next day, trypsin was used to detach the cells. PBS was added and the cells were spun down for 5 minutes at 1200 RPM. The supernatant was removed and the cells were fixated in 1 ml 4% formalin with sucrose for 1 hour at room temperature. Then 2 ml PBS was added and the cells were spun down again. To permeabilize the cells, 1 ml of 0,05% Triton-X100 in PBS was added for 5 minutes. Again 2 ml PBS was added and the cells were spun down. The cells were incubated in 200 µl filipin in PBS for 2 hours in the dark at room temperature, before measuring absorbance with FACS.

Lastly, lipid droplets were isolated from cells. For this purpose, 5 million cells were kept apart while splitting flasks, spun down and resuspended in 150 µl PBS. This suspension was stored at -80C until lipid droplet extraction. Lipid droplet extraction on fibroblasts is performed according to manufacturer's instructions (#MET-5011: Cell Biolabs Inc, San Diego, CA). In short, fibroblasts were washed for three times with PBS and subsequently Reagent A was added. After a 10-min incubation on ice, Reagent B was added, incubated on ice for another 10 min. Subsequently the cells were homogenized by passing them through a 27-gauge needle. The homogenate was centrifuged at 100 x g for 5 secs and 600 µL Reagent B was added in a dropwise fashion. Density gradient ultracentrifugation was performed for 3 hours at 20,000 x g at 4°C using an Ultracentrifuge (Beckman, Uithoorn, The Netherlands). The top layer, containing the floating lipid droplets, were collected and used for lipid extraction. Lipids were isolated as previously described by performing a Butanol-Methanol extraction⁸. Neutral lipids were separated from polar lipids by dissolving the nitrogen-dried lipid extract in heptane:methanol [98:2]. After vortexing, 300 µl Methanol:H₂O + 1% NH₃ (of 23% NH₃ stock) was added and the upper phase, containing the neutral lipids, was collected and dried at 35°C under a continuous flow of nitrogen gas. The neutral lipid extractions were analyzed using a LC-4000 Series UHPLC system (Jasco, Tokyo, Japan). A volume of 5 µl sample was injected with a Jasco AS-4250 UHPLC autosampler (Jasco, Tokyo, Japan) on a Spherosorb 5.0 µM Sillica column (4.6 mm x 100mm) (Waters, Dublin, Ireland) which was temperature-regulated at 45 C. A linear gradient was applied on the mobile phase by mixing phase A in 9 min from 0% - 50% with phase B at a continuous flow of 1.6 ml/min. Phase A consisted of a Heptane/Ethylacetate (98.8/0.2 %) whereas phase B of a Acetone/Ethylacetate (2:1) mixture (Merck Chemicals, Amsterdam, The Netherlands). Finally, the relative peak areas of the cholesterol and triglycerides were calculated using Chromnav v 2.0 software (Jasco, Tokyo, Japan).

ER stress assessment in HepG2

ER stress was assessed as previously described. HepG2 cells were incubated with 0.5 µg/mL Tunicamycin (Sigma-Aldrich, T7765) or with 10nM Thapsigargin (Sigma-Aldrich, T9033) for 8 hours. Cells were subsequently harvested for ER stress quantification by RT-PCR and western blotting, (primers and antibodies were supplied by Cell Signalling ER-stress marker kit; 9956).

Myc-tagged Insig1 overexpression in HepG2

HepG2 cells were reverse transfected with 25 nM of non-targeting, ALG6 or PMM2 siRNA as described earlier. The next day, cells were co-transfected with INSIG1-Myc using JetPrime™ (Polyplus). 48 hrs later, total RNA was isolated and gene expression was determined by qPCR. Total cell lysates were used for protein quantification as indicated in the figure. The INSIG1-Myc expression plasmid was a kind gift from Dr. Robert Gemmill⁹.

ABCA1-mediated cholesterol efflux assays in fibroblasts

ABCA1-mediated cholesterol efflux to HDL and apoA1 in patient fibroblasts was performed as described by Franssen et al.¹⁰

Supplemental References

1. van Schaftingen E, Jaeken J. Phosphomannomutase deficiency is a cause of carbohydrate-deficient glycoprotein syndrome type I. *FEBS Lett.* 1995;377:318–320.
2. Kulozik P, Jones A, Mattijssen F, Rose AJ, Reimann A, Strzoda D, Kleinsorg S, Raupp C, Kleinschmidt J, Müller-Decker K, Wahli W, Sticht C, Gretz N, Loeffelholz von C, Stockmann M, Pfeiffer A, Stöhr S, Dallinga-Thie GM, Nawroth PP, Berriel Diaz M, Herzig S. Hepatic deficiency in transcriptional cofactor TBL1 promotes liver steatosis and hypertriglyceridemia. *Cell Metab.* 2011;13:389–400.
3. Reiding KR, Blank D, Kuijper DM, Deelder AM, Wuhrer M. High-throughput profiling of protein N-glycosylation by MALDI-TOF-MS employing linkage-specific sialic acid esterification. *Anal Chem.* 2014;86:5784–5793.
4. Conlon DM, Thomas T, Fedotova T, Hernandez-Ono A, Di Paolo G, Chan RB, Ruggles K, Gibeley S, Liu J, Ginsberg HN. Inhibition of apolipoprotein B synthesis stimulates endoplasmic reticulum autophagy that prevents steatosis. *J Clin Invest.* 2016;126:3852–3867.
5. Zelcer N, Hong C, Boyadjian R, Tontonoz P. LXR regulates cholesterol uptake through Idol-dependent ubiquitination of the LDL receptor. *Science.* 2009;325:100–104.
6. Patel KM, Strong A, Tohyama J, Jin X, Morales CR, Billheimer J, Millar J, Kruth H, Rader DJ. Macrophage sortilin promotes LDL uptake, foam cell formation, and atherosclerosis. *Circ Res.* 2015;116:789–796.
7. Lambert G, Petrides F, Chatelais M, Blom DJ, Choque B, Tabet F, Wong G, Rye K-A, Hooper AJ, Burnett JR, Barter PJ, Marais AD. Elevated plasma PCSK9 level is equally detrimental for patients with nonfamilial hypercholesterolemia and heterozygous familial hypercholesterolemia, irrespective of low-density lipoprotein receptor defects. *J Am Coll Cardiol.* 2014;63:2365–2373.
8. Löfgren L, Ståhlman M, Forsberg G-B, Saarinen S, Nilsson R, Hansson GI. The BUME method: a novel automated chloroform-free 96-well total lipid extraction method for blood plasma. *J Lipid Res.* 2012;53:1690–1700.
9. Lee JP, Brauweiler A, Rudolph M, Hooper JE, Drabkin HA, Gemmill RM. The TRC8 ubiquitin ligase is sterol regulated and interacts with lipid and protein biosynthetic pathways. *Mol Cancer Res.* 2010;8:93–106.
10. Franssen R, Schimmel AWM, van Leuven SI, Wolfkamp SCS, Stroes ESG, Dallinga-Thie GM. In Vivo Inflammation Does Not Impair ABCA1-Mediated Cholesterol Efflux Capacity of HDL. *Cholesterol.* 2012;2012:610741.

Supplemental Material.**Table S1 Primer sequences used for qPCR.**

ALG6	F	TCA AAG GAA AGG GGT TTG TG
ALG6	R	CAG GGT TTG TTC CCT TTC TG
APOB	F	GAC GAC TTT TCT AAA TGG AAC TTC TAC
APOB	R	CTC AGT TTT GAA TAT GGT GAG TTT TT
ATF6	F	CCT GTC CTA CAA AGT ACC ATG AG
ATF6	R	CCT TTA ATC TCG CCT CTA ACC C
CHOP	R	GATTCTTCCTCTTCATTTCCAGGAG
CHOP	F	TTGCCTTTCTCCTTCGGGAC
HMGCR	F	CCA ACT ACT TCG TGT TCA TGA CTT T
HMGCR	R	GCT GCC AAA TTG GAC GAC
HMGCS1	F	GCGTCCCCTCCAAATGATG
HMGCS1	R	GGCTTGGAATATGCTCAGTTGC
IRE1	F	GAAGCA TGT GCT CAA ACA CC
IRE1	R	TCT GTC GCT CAC GTC CTG
LDLR	F	AAGGACACAGCACACAACCA
LDLR	R	CCCAGAGCTTGGTGAGACAT
MTTP	F	ATA CCT GCA GCC TGA CAA CC
MTTP	R	GCC AGG AAG TTT CTG ACA GC
PCSK9	F	CTCAACTGCCAAGGGAAGGG
PCSK9	R	GCTGGCTTTTCCGAATAAACTCC
PMM2	F	AAG AAG CTG CAG CCA AGA AG
PMM2	R	AGC TGA TCT GGC CTC CTA TG
SREBP2	F	GGCTCATCTTTGACCTTTGC
SREBP2	R	AGGCTGGCTTCTCTCCCTAC

Table S2 No signs of secondary causes of hypocholesterolemia in analyzed patients with CDG-I (retrospective cohort).

No.	CDG-I type	Gender	Neurological status	Liver status	Thyroid function	Malabsorption, malnutrition
1	PMM2-CDG	F	Severe mental retardation, cerebellar ataxia	Very mild elevation of transaminases (<1.5 x ULN), no cholestasis (35 y)	hypothalamic hypothyroidism, substitution (19 y)	Growth retardation (6 months), overweight (39 y)
2	PMM2-CDG	M	Severe mental retardation, cerebellar hypoplasia, tetraparesis, epilepsy	N/A	N/A	Feeding difficulties, weight and length below 3rd percentile, (16 y)
3	PMM2-CDG	M	Mild psychomotor retardation, cerebellar hypoplasia, cerebellar ataxia, mild hypotonia	No LFT abnormalities. Ultrasound: no pathological findings (10 y)	Euthyroid	Obesity (+2SD) at 7 and 9 years
4	PMM2-CDG	M	Severe psychomotor retardation	Mild elevation of transaminases (<2 x ULN), no cholestasis (5 y)	TSH: 6.52, TBG: 201, fT4 9.2 (1 y)	Adipose (6y weight +2 SD and 11 y)
5	PMM2-CDG	F	Hypotonia	No LFT abnormalities. (1 y)	N/A	Weight -3.5 SD, length -3 SD (6 months)
6	PMM2-CDG	F	Psychomotor retardation, strabismus, epilepsy, deafness	No LFT abnormalities (10y). Ultrasound: no pathological findings (12 y)	Euthyroid	Obesity (+2SD) at 7 and 9 years
7	PMM2-CDG	M	Psychomotor retardation, hypotonia	ALAT: 826 U/L, (5 months). Slightly enlarged liver neonatal period.	N/A	N/A

8	PMM2-CDG	F	Mild motor retardation, cerebellar hypoplasia, apraxia	No LFT abnormalities. Abdominal ultrasound: no pathological findings (34 and 39 y)	Euthyroid (31 y)	Length -2SD, weight 0SD (9 y), length -2.5SD, weight -0.5SD (15 y), length -1.5SD, weight: 0SD (19 y), length -1.5SD, weight +0.5SD (20 y)
9	PMM2-CDG	F	Cerebellar hypoplasia with apraxia, hypotonia and ataxia	No LFT abnormalities. (2 y)	Euthyroid (2 y)	Weight -1SD, length 0SD, head circumference -1SD (1 y), length +1SD, weight -0.5SD, head circumference -0.5SD (2 y) length -0.5SD, weight 0SD (5 y), no feeding difficulties
10	PMM2-CDG	F	Psychomotor retardation, hypotonia	Elevated transaminases, no cholestasis (2.5 x ULN) (5 y)	Euthyroid (8 months)	Feeding difficulties, tube feeding
11	ALG6-CDG	M	Severe psychomotor retardation with epilepsy, myasthenia, ataxia, behavioral disorders	No LFT abnormalities. (7 y)	Euthyroid (11 y)	Length and weight conform age (17 y)
12	ALG6-CDG	M	Psychomotor retardation, epilepsy, hypotonia	No LFT abnormalities. (1 month)	Euthyroid (1 month)	No feeding difficulties. Intermittant protein losing enteropathy
13	DOLK-CDG	M	N/A	No LFT abnormalities. (10 y)	Euthyroid (10 y)	N/A
14	DOLK-CDG	M	N/A	No LFT abn. (6 months)	Euthyroid (6 months)	N/A

15	SRD5A3- CDG	F	Mental retardation, dystonic movements, axial hypotonia, hypertonia of extremities	Elevated transaminases, no cholestasis (2.5 x ULN) (5 y)	N/A	N/A
16	SRD5A3- CDG	M	Psychomotor retardation, hypotonia	Mild elevation of transaminases ($<2 \times$ ULN), no cholestasis. Abdominal ultrasound and liver biopsy: no pathological findings. (1 y)	N/A	Birth weight: 3300 (<-2 SD weight for length)
17	SRD5A3- CDG	F	Psychomotor retardation, severe hypotonia	Mild elevation of transaminases ($<2 \times$ ULN), no cholestasis (3 y)	Euthyroid (5 y)	Length -1SD, weight -1SD (1 y), length +1SD, weight +0.5SD (2 y), length 0SD, weight +1SD (4 y), length 0SD, weight +1SD (6 y)

Related to Figure S1 and Figure 1. Available medical records of the CDG-I patients in the retrospective cohort were analyzed for possible secondary causes of hypocholesterolemia. LFT = liver function tests, ULN = upper limit of normal, N/A = information was not available in the medical records.

Table S3 Demographics of CDG-I patients (prospective cohort).

Pt No.	Sex	Age	Mutation	TIEF	Neurological findings	Liver status	Liver US	Thyroid function	Malabsorption, nutrition
PM M2# 01	F	25	P113L/R141H	asialo 9,4%; disialo 36,7%; tetrasialo 40,6%	Severe mental retardation, cerebellar ataxia	AF 64 U/L, ASAT 17 U/L, ALAT 27 U/L, LD 218 U/L	N/A	TSH 0.15, T4 59 (euthyroid with supplementation)	Normal
PM M2# 02	M	9	R123Q/R162W	asialo 4,2%; disialo 14%; tetrasialo 59%	Mild psychomotor retardation, cerebellar hypoplasia, cerebellar ataxia, mild hypotonia	AF 272 U/L, ASAT 25 U/L, ALAT 25 U/L, LD 523 U/L, GGT 14 U/L (11 y)	no pathological findings (10 y)	TSH 3.4, thyroxine 91, free thyroxine 12.41 (14 y)	N/A
PM M2# 03	M	2	F119L/R141H	asialo 12,7%; disialo 31,2%; tetrasialo 35,4%	Severe psychomotor retardation	AF 201 U/L, ASAT 105 U/L, ALAT 137 U/L, LD 487 U/L, GGT 19 U/L (5 y)	N/A	TSH: 6.25mE/L (), T4 49 nmol/L (), ft4: 9.2pmol/L (1 y)	Feeding difficulties, stable weight <p10, length <p10, (1 y) albumin 36
PM M2# 04	F	6	R141H/F119L	asialo 4,6%; disialo 23,1%; tetrasialo 46,3%	Psychomotor retardation, strabismus, epilepsy, deafness	AF 206 U/L, ASAT 43 U/L, ALAT 42 U/L, LD 446 U/L, GGT 84 U/L (10 y)	no pathological findings (12 y)	TSH: 1.51, thyroxine 48 (), free thyroxine 9	Feeding difficulties, tube feeding
PM	M	21	N/A	asialo	Psychomotor	N/A	N/A	N/A	N/A

M2# 05				14,4%; disialo 29,7%; tetrasialo 33,7%	or retardation		A		
PM M2# 06	F	18	T18S/R141 H	asialo 1,4%; disialo 10,2%; tetrasialo 58,1%	Normal intelligence, mild motor retardation, strabism, tremor	Normal	N/ A	Normal	N/A
PM M2# 07	F	0	L35X/D188 G	asialo 15,9%; disialo 45,8%; tetrasialo 28,3%	Cerebellar hypoplasia with ataxia	N/A	N/ A	N/A	N/A
PM M2# 08	M	0	p.F119L p.R123Q	asialo 26,2%; disialo 38,7%; tetrasialo 15,4%	Dysmorphia , cardiologica l problems, lipodystrop hy, inverted nipples, hypogonadi sm	N/A	N/ A	N/A	N/A
PM M2# 09	F	30	K51R (152A>G)/ K51R	asialo 1,7%; disialo 16,1%; tetrasialo 62,8%	Normal intelligence, nystagmus, ataxia	Normal	N/ A	TSH 1,85; T4 94 nmol/l	normal
PM M2# 11	F	0	c.357C>A (p.F119L)/ c.422G>A (p.R141H)	asialo 18,4%;disi alo 35,4%; tetrasialo 28,3%	fatty pads, inverted nipples,	N/A	N/ A	N/A	N/A
PM M2# 12	M	0	c.24delC/p .V129M	asialo 21,2%; disialo 23,4%	Psychomot or retardation	N/A	N/ A	N/A	N/A

PM M2# 13	F	1	F119L/E15 1G	asialo 9,5%; disialo 25,7%; tetrasialo 45,3%	General hypotonia, strabism, intention tremor	N/A	N/ A	TSH 2.04	N/A
PM M2# 14	F	0	F119L/R14 1H	asialo 16,6%; mono 14,1%; disialo 32,3%; trisialo 14,0%; tetrasialo 16,8%	General hypotonia, normal psychologic al developme nt, retinitis pigmentosa , inverted nipples	ASAT 196 U/L, ALAT 178 U/L, AF 552 U/L, GGT 7 U/L	N/ A	N/A	normal (SD 0 for height and weight)
PM M2# 15	F	2	P113L/R14 1H	asialo 14,3%; disialo 32,4%; tetrasialo 29,6%	truncal hypotonia with periodic dystonia,	elevated transamin ases, normal GGT	N/ A	N/A	N/A
ALG 6#0 1	F	4	A333V/A3 33V	asialo 10,0%; disialo 32,5%; tetrasialo 34,8%	Severe psychomot or retardation, seizures, strabismus, hypotonia	Normal transamin ases	N/ A	N/A	N/A
ALG 6#0 2	M	2	A333V/A3 33V	asialo 9,8%; disialo 33,7%; tetrasialo 30,7%	Psychomot or retardation	Normal, transamin ases normal, albumin normal	N/ A	Normal	N/A
ALG 6#0 3	M	1	A333V/A3 33V	asialo 7,9%; disialo 37,8%	Severe psychomot or retardation	AF 191 U/L, ASAT 28 U/L, ALAT 30 U/L, LD 288 U/L,	N/ A	TSH 3,66 FT4 15,1 T3 1,5	adipose

						GT 7 U/L, albumin 36 g/L			
ALG 6#0 4	M	27	del299/IVS 3+5 g>a	asialo 3,7%; disialo 26,1%; tetrasialo 45,1%	Severe psychomot or retardation, mood disorders, epilepsy	Normal	N/ A	Normal	normal
ALG 6#0 5	M	1	A333V/A3 33V	asialo 16,8%; disialo 42,7%; tetrasialo 22,5%	Motor retardation, epilepsy	AF 678 U/L, ASAT 50 U/L, ALAT normal, LD normal, GGT normal, albumin normal	N/ A	N/A	normal
ALG 6#0 6	M	6	A333V/A3 33V	asialo 1,9%; disialo 27,7%; tetrasialo 52,8%	Hypotonia, ataxia, intractable seizures, mood disorders, severe psychomot or retardation, strabismus, nystagmus	Normal	N/ A	Normal	N/A
ALG 6#0 7	F	8	A333V/A3 33V	asialo 3,1%; disialo 34,4%; tetrasialo 43,1%	Hypotonia, intractable seizures, mood disorders, severe psychomot or	Normal	N/ A	Normal	overweigh t

					retardation, strabismus				
ALG 6#0 8	M		A333V; del 57-86	asialo 4,7%; disialo 32,1%; tetrasialo 41,7%	Psychomot or retardation, ataxia, dysmorphia	Normal	N/ A	N/A	overweigh t
ALG 6#0 9	F	4	A333V/A3 33V	asialo10,0 %; disialo 32,5%; tetrasialo 34,8%	Hypotonia, mild developme ntal delay, dysmorphia , epilepsy	N/A	N/ A	N/A	N/A
ALG 6#1 0		37	N/A	N/A	Psychomot or retardation	N/A	N/ A	N/A	N/A
ALG 6#1 1	F	1	IVS 3+5 g>a and dellso299	asialo 5,5%; disialo 36,9%; tetrasialo3 5,9%	Psychomot or retardation	N/A	N/ A	N/A	N/A
ALG 6#1 2	M		c.257+5G> A in intron 4, in exon 5 and c.911C.T in exon 11, homoz.	asialo 1,9%; disialo 21,7%; tetrasialo 50,9%	Psychomot or retardation	N/A	N/ A	N/A	N/A
ALG 6#1 3	F	8	del c.896- 898 (del I299)	asialo 2,5%; disialo 25,2%; tetrasialo 49,7%	Psychomot or retardation	N/A	N/ A	N/A	N/A

Related to Figure 1. Available medical records of the CDG-I patients in the prospective cohort were analyzed for possible secondary causes of hypocholesterolemia. TIEF = transferrin isoelectric focusing (showing the percentages of the asialo-, disialo- and tetrasialotransferrin isoform bands), LFT = liver function tests, N/A = information was not available in the medical records

	Heterozygotes (n = 4)		Family controls (n = 4)		p	Matched controls (n = 12)		p
Sex (% male)	50%		25%		0,456	50%		1
Age	44	(13,6)	60	(28,5)	0,356	44	(12,2)	0,991
BMI	26	(2,6)	24	(3,2)	0,273	24	(3,5)	0,299
TC (mg/dl)	182	(25)	227	(41)	0,115	197	(19)	0,247
LDL-c (mg/dl)	100	(25)	131	(27)	0,137	132	(17)	0,012

Table S4 Demographics and plasma lipids in a family with four subjects with a well-established *PMM2* mutation (P113L). Related to Figure 1. Plasma lipids in *PMM2* mutation carriers were compared to four family controls (without the *PMM2* mutation) and to 12 age- and gender-matched controls. P values were calculated with Student's unpaired two-sided t-test.

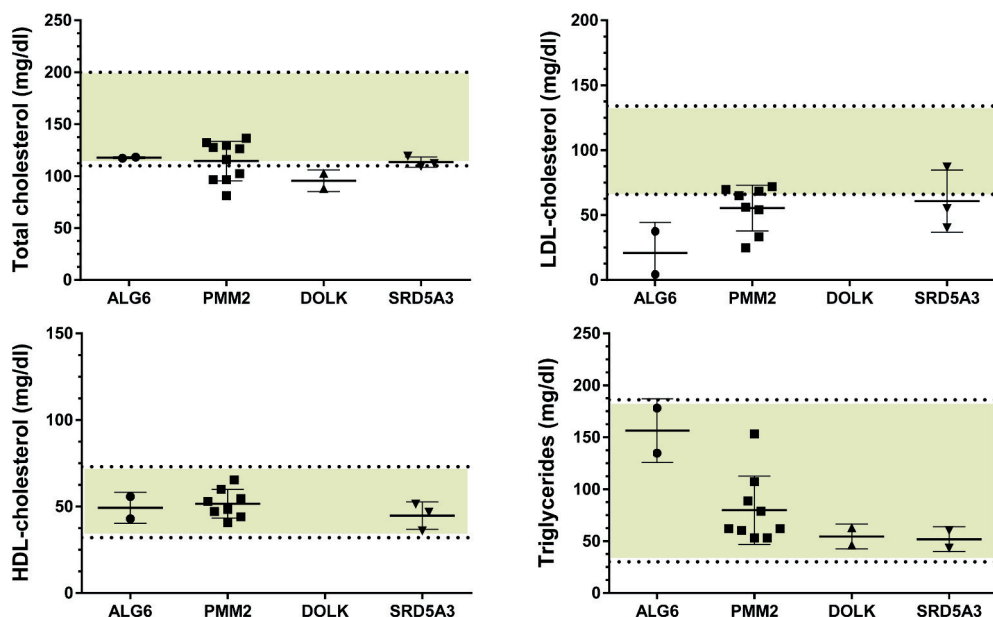
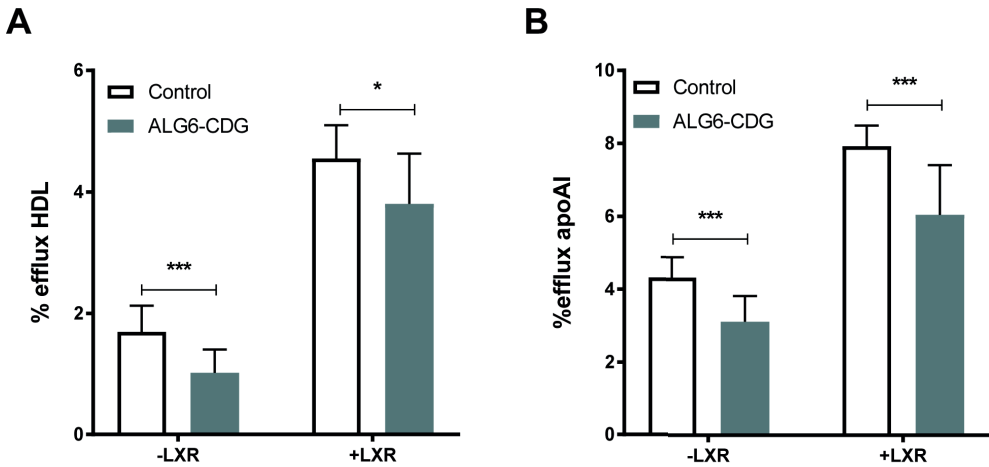
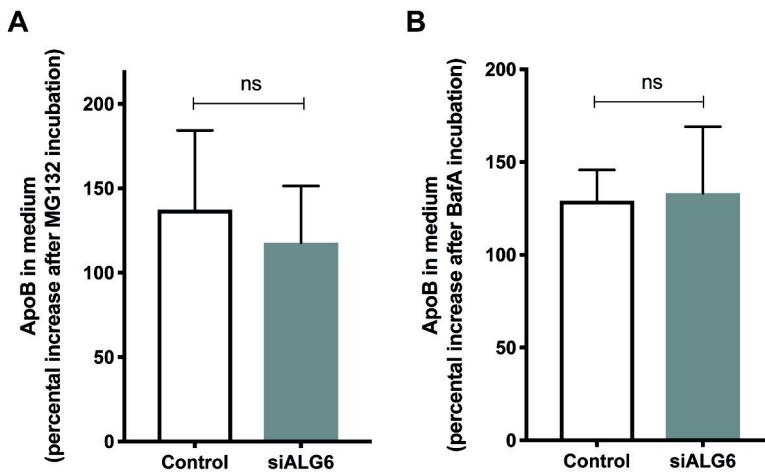


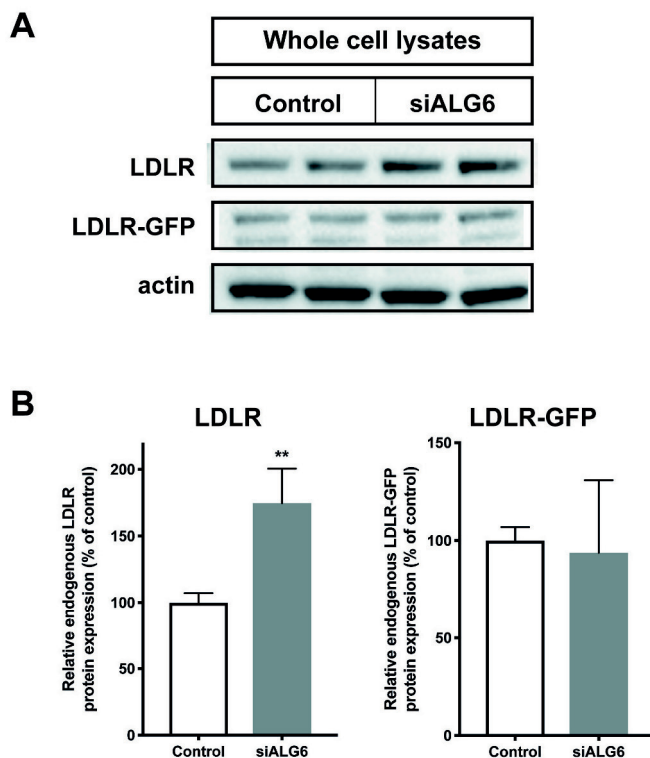
Figure S1 Retrospective analysis of plasma lipids in cohort of CDG-I patients. Related to figure 1. Panels show TC, LDL-c, HDL-c and TGs in patients with CDG-I in a retrospective analysis of medical records. Colored area between dotted lines depicts reference values for children in the age of 0 to 14 years old as measured in our lipid clinic.



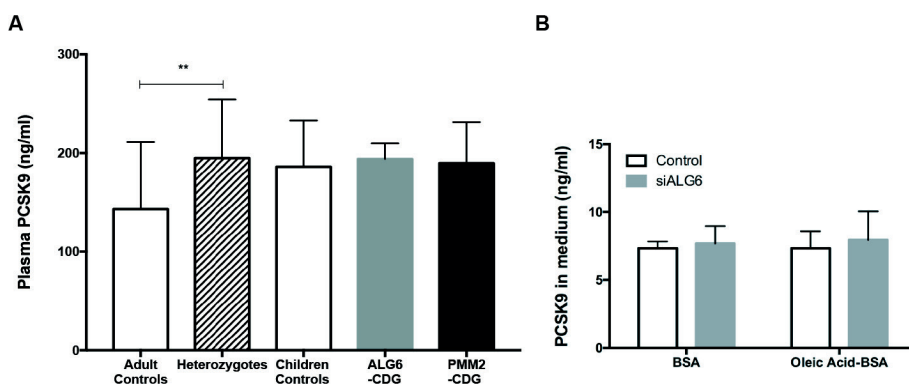
Supplemental Figure S2. ABCA1-mediated cholesterol efflux is decreased in ALG6-CDG fibroblasts. Panel (A) shows ABCA1-mediated cholesterol efflux with or without LXR and panel (B) shows apoA1 cholesterol efflux. *** indicates $p < 0.001$ and * $p < 0.05$. LXR = Liver X receptor.



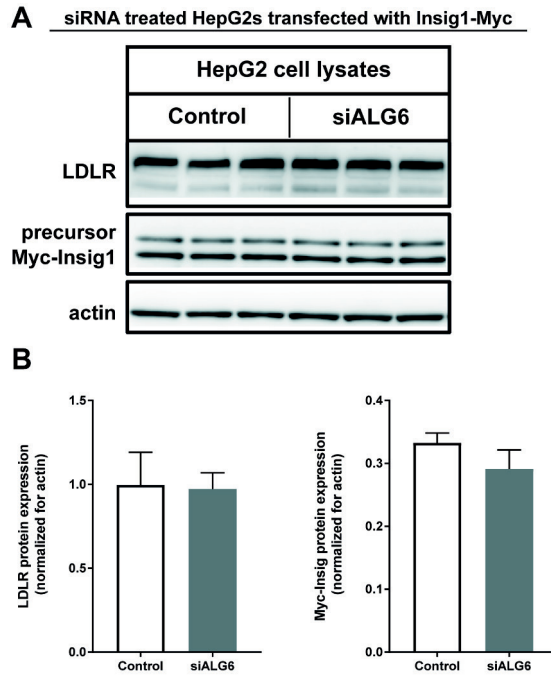
Supplemental Figure S3. ApoB secretion into the medium of siALG6 treated HepG2s after MG132 (left) or BafA incubation (right). ns = not significant.



Supplemental Figure S4. siALG6 treatment of HepG2s expressing LDLR-GFP under a strong CMV promoter affects only endogenous LDLR and not LDLR-GFP. (A) shows a representative western blot of LDLR protein and LDLR-GFP protein in siALG6 treated HepG2s expressing LDLR-GFP under a strong CMV promoter and (B) shows the quantification of the bands of the western blot. ** indicates $p < 0.01$.



Supplemental Figure S5. PCSK9 is not decreased in CDG-I patients, heterozygotes, nor is its secretion reduced in the siALG6 HepG2 cell model. Related to figure 3. Panels show plasma PCSK9 levels in patients and heterozygotes (A) and PCSK9 levels in the medium of HepG2 cells (B). Panel B shows means \pm SD from at least two experiments with triplicate measurements per experiment. ** indicates $p < 0,01$ as calculated with Student's unpaired two-sided t-test.



Supplemental Figure S6. Overexpressing Myc-INSIG1 in HepG2s treated with siALG6 abolished the upregulation of LDLR protein. Panel (A) shows a western blot of LDLR and Myc-INSIG1 protein expression and panel (B) shows the quantification of the bands of the western blot shown in (A).



CHAPTER 2

Reduced CETP glycosylation and activity in patients with homozygous B4GALT1 mutations.

M.A.W. van den Boogert, C.L. Crunelle, L. Ali, L.E. Larsen, S.D. Kuil, J.H.M. Levels, A.W.M. Schimmel, V. Konstantopoulou, M. Guerin, J.A. Kuivenhoven, G.M. Dallinga-Thie, E.S.G. Stroes, D.J. Lefeber, A.G. Holleboom

Journal of Inherited Metabolic Disease (2019)

Abstract

Objective

The importance of protein glycosylation in regulating lipid metabolism is becoming increasingly apparent. We set out to further investigate this by studying the effects of defective glycosylation on plasma lipids in patients with B4GALT1-CDG, caused by a mutation in *B4GALT1* with defective N-linked glycosylation.

Approach

We studied plasma lipids, cholesteryl ester transfer protein (CETP) glyco-isoforms with isoelectric focusing followed by a western blot and CETP activity in three known B4GALT1-CDG patients and compared them to eleven age- and gender-matched, healthy controls.

Results

B4GALT1-CDG patients have significantly lower non-high density lipoprotein cholesterol (HDL-c) and total cholesterol to HDL-c ratio compared to controls and larger HDL particles. Plasma CETP was hypoglycosylated and less active in B4GALT1-CDG patients compared to matched controls.

Conclusions

Our study provides insight into the role of protein glycosylation in human lipoprotein homeostasis. The hypogalactosylated, hypo-active CETP found in patients with B4GALT1-CDG indicates a role of protein galactosylation in regulating plasma HDL and LDL.

Introduction

Identification of novel patients and novel congenital disorders of glycosylation (CDG) is expanding rapidly¹. These inborn defects of glycan metabolism have a wide variety of clinical features and severity with generally neurological involvement^{2,3}.

Glycosylation is a crucial intracellular post-translational process that covalently attaches a glycan to proteins or lipids. The importance of protein glycosylation in regulating human lipoprotein homeostasis is increasingly being recognized^{4,5}. We found that ppGalNAc-transferase 2, a specific O-glycosylation enzyme, could specifically initiate glycan synthesis on apolipoprotein C-III (apoC-III)⁶ and others found that it also glycosylates phospholipid transfer protein⁷ and angiopoietin like protein 3^{7,8}, supporting an intricate role for this transferase in glycosylation of proteins and enzymes involved in lipid remodeling. Recently, we found hypobetalipoproteinemia in patients with type I congenital disorder of glycosylation (ALG6- and PMM2-CDG) due to increased LDL-receptor⁴. To increase insight into the role of glycosylation in lipid metabolism, we set out to study lipid pathways in patients with other types of CDG.

CDG-II are caused by mutations in genes coding for N-glycosylation enzymes located in the Golgi apparatus. Here, the high-mannose glycan structures produced in the ER are further modified and deficiencies in these enzymes result in unfinished, immature glycan structures⁹. One of these enzymes is UDP-Gal:N-acetylglucosamine β -1,4-galactosyltransferase I (B4GALT1). B4GALT1 is responsible for the galactosylation of N-linked glycans. There are three reported patients with B4GALT1-CDG¹⁰⁻¹² and a new patient reported here. All patients have an identical, homozygous insertion mutation (1031-1032insC) causing a premature translation stop with loss of the C-terminal 50 amino acids of B4GALT1. The patients have a mild clinical presentation compared to other CDG with dysmorphism, transient hypotonia and decreased blood coagulation factors and increased serum transaminases (highest aspartate aminotransferase (AST) measures between 200 and 300 IU/l; upper limit of normal is 40 IU/l)^{10,13}.

Here, we report specific plasma lipid abnormalities in B4GALT1-CDG patients. Notably, these were clearly distinct from the hypobetalipoproteinemia found in CDG-I patients. Plasma cholesterol was sequestered mostly in the HDL fraction, and glycosylation and activity of cholesteryl ester transfer protein (CETP) were reduced. CETP is a highly glycosylated protein that transfers cholesteryl esters from HDL particles to other lipoproteins. CETP deficiency leads to increased levels of HDL-c and decreased levels of LDL-c. The lipid phenotype found in the B4GALT1-CDG patients are similar to that found in patients with CETP deficiency, which prompted us to explore of CETP glycosylation and function in these patients.

Methods

Patients

Plasma of patient B1 was obtained from the blood plasma bank at Radboud University Medical Center in Nijmegen, the Netherlands. From B2 and B3, venous blood plasma samples were collected

after an overnight fast from patients and their parents at the Medical University of Vienna, Austria. Plasma samples of eleven age- and gender-matched, healthy, unaffected children from our own plasma databank were used as controls (unaffected siblings of children with familial hypercholesterolemia, proven to carry no mutations in known lipid genes). Plasma from a patient with CETP deficiency due to a mutation in *CETP* – also from our plasma biobank – was used as a positive control. The study was performed in accordance with the Declaration of Helsinki of the World Medical Association and informed consent was obtained from the parents. Due to the nature of the study, no ethical approval was requested from the local ethics committee.

Plasma lipid measurements

We analyzed plasma lipids in venous blood samples collected after an overnight fast in EDTA coated tubes. Plasma was isolated after centrifugation at 3000 RPM for 15 minutes at 4 °C and stored at -80 °C until further analyses. Total cholesterol (TC), LDL-c, HDL-c, TG, apolipoprotein A-I (apoA-I) and apoB were measured using commercially available assays (DiaSys) on a Selectra analyzer (Sopachem, the Netherlands). TC-to-HDL-c ratios were calculated from these results. Fast protein liquid chromatography (FPLC) profiling for cholesterol distribution across lipoprotein fractions was carried out as described¹⁴.

Deglycosylation treatment

Venous blood plasma samples (30 l) were treated with 15 l neuraminidase (Roche, 5U dissolved in 500 l 0.1M Tris/HCl, pH 7.0) for 3-4 hours at 37 °C to remove the terminal sialic acids from the glycans.

Isoelectric focusing of transferrin and CETP glyco-isoforms

Isoelectric focusing (IEF) of transferrin was performed and quantified as described¹⁵. IEF followed by a western blot of plasma CETP was performed similar to the transferrin IEF protocol. In short, plasma samples were diluted 1:1 in a physiological NaCl solution and run in the same system as for transferrin IEF with slight adjustments to the running protocol. Blotting occurred at 60 °C in the same system using nitrocellulose membranes. The membrane was subsequently blocked in a 5 % enhanced chemiluminescence (ECL) solution. After washing, the membrane was incubated for at least 3 hours at room temperature (or at 4 °C when overnight) with the first antibody TP1 in phosphate buffered saline supplemented with Tween 20 (PBST) with 1.5 % bovine serum albumin (BSA). After a second wash, the secondary antibody (goat anti-mouse) in PBST with 1.5 % BSA was added for at least 1.5 hours at room temperature. Imaging was performed after ECL reaction. Quantification of the different isoforms was performed as described for transferrin IEF¹⁵.

Endogenous plasma CETP Activity

Determination of endogenous cholesteryl ester (CE) transfer from HDL to apoB-containing lipoproteins was assayed using the method of Guérin et al.^{16,17} that estimates net physiological CE transfer between lipoprotein donor and acceptor particles in plasma. Radiolabeled HDL particles were obtained from the $d > 1.063$ g/ml plasma fraction by ultracentrifugation at 100000 rpm for

3h30 at 15 °C with a Beckman TL100 centrifuge. Then, the $d > 1.063$ g/ml fraction was labelled with [^3H]-cholesterol (4 $\mu\text{Ci/ml}$) at 37°C overnight. The radiolabeled [^3H]-HDL were then isolated from the $d > 1.063$ g/ml plasma fraction by centrifugation at 100000 rpm for 5.5 hours at 15 °C after adjustment of the density at 1.21 g/ml by addition of dry solid KBr. CETP-mediated cholesteryl ester transfer was determined after incubation of whole plasma from individual subjects at 37°C and 0°C for 3h in the presence of radiolabeled ^3H -HDL (25 μg HDL-CE) and iodoacetate (final concentration 1.5 mmol/l) for inhibition of lecithine-cholesterol-acyltransferase (LCAT). After incubation, apolipoprotein B-containing lipoproteins were precipitated using the dextran sulphate-magnesium procedure. The radioactive content of the supernatant was quantified by liquid scintillation spectrometry with a Trilux 1450 (Perkin Elmer). Endogenous plasma CETP activity (expressed as percentage) was calculated as the amount of the label recovered in the supernatant after incubation and divided by the label present in the supernatant before incubation. The CETP-dependent CE transfer was calculated from the difference between the radioactivity transferred at 37 °C and 0 °C.

Statistical analysis

Data were compared between groups with a two-tailed Students t-test and presented as means \pm standard deviation or, for nonparametric parameters, tested with a Mann-Whitney U test and presented as medians with interquartile ranges. Categorical variables were tested with a Chi-square test. All statistical analyses were done using SPSS software (version 22.0, SPSS Inc., Chicago IL). Error bars indicate standard deviations. Probability values < 0.05 were considered statistically significant.

	Controls (n = 11)	B1	B2	B3	B4GALT1-CDG patients pooled (n = 3)	p
Age (y)	8 \pm 1	4	14	3	7 \pm 6	0.664
Gender, n male (%)	7 (64%)	M	F	M	2 (67%)	
TC (mg/dl)	173 \pm 27	128	113	103	115 \pm 13	0.004
LDL-c (mg/dl)	88 \pm 14	67	41	32	47 \pm 19	0.001
HDL-c (mg/dl)	57 \pm 13	58	51	43	51 \pm 8	0.459
TG (mg/dl)	74 \pm 26	124	54	139	106 \pm 45	0.136
ApoA1 (mg/dl)	171 \pm 57	149	162	130	147 \pm 16	0.493
ApoB (mg/dl)	69 \pm 12	45	28	31	35 \pm 9	< 0.001
LDL-c/HDL-c ratio	1.63 \pm 0.38	1.15	0.8	0.74	0.90 \pm 0.04	0.005
TC/HDL-c ratio	3.12 \pm 0.56	2.20	2.20	2.40	2.27 \pm 0.11	0.025

Table 1. Characteristics and plasma lipids of the B4GALT1-CDG patients and controls. Characteristics and plasma lipids for the B4GALT1-CDG patients and their age- and gender-matched controls. B1, B2 and B3 are B4GALT1-CDG patients and; TC = total cholesterol, TG = triglycerides.

Results

Patients

Patient B1 and B2 with a homozygous insertion in exon 5 (c.1031-1032insC) of *B4GALT1* were previously identified and described¹⁰. Patient B3 is a sibling of patient B2 and has the same homozygous mutation. She was born to consanguineous parents and the pregnancy proceeded normally. In the 13th week ultrasound examination showed an increased neck fold measurement (5.6 mm, reference 1.6-2.4 mm). Chorion biopsy was performed. Intrauterine MRI showed a hypoplastic cerebellum, a small liver sinus, splenomegaly, hydrocolpus and subcutaneous edema. The delivery was uncomplicated and the Apgar score was 8/9/10. At two months of age, pulmonary artery banding was performed successfully for a large ventricle septal defect with left-to-right shunt, pulmonary hypertension and heart failure. Because of the known coagulopathy, coagulation factors were supplied. Later she needed a drain for pericardial effusion. Over the course of childhood, she had some developmental disability, especially in language development; this is in contrast to her older sister, who has a normal IQ. She has dysmorphic features with low-set ears, saddle nose, thin lips and fat pads. Serum transaminases are mildly elevated.

Lipids

Table 1 shows clinical characteristics and serum lipids of the patients and eleven age- and gender-matched controls. Patients have significantly lower plasma TC (115 ± 13 versus 173 ± 27 mg/dl, $p = 0.004$), LDL-c (47 ± 19 versus 88 ± 14 mg/dl, $p = 0.001$), apoB (35 ± 9 versus 69 ± 12 mg/dl, $p < 0.001$) and TC-to-HDL-c ratio (2.27 ± 0.11 versus 3.12 ± 0.56 , $p = 0.025$). HDL-c, apoA1 and TG were comparable between patients and controls. FPLC cholesterol profiles of 2 *B4GALT1*-CDG patients and of the controls confirm the lower cholesterol content in the LDL fraction in patients and also the distribution of most cholesterol into a larger, buoyant HDL fraction, attested by a shifted HDL peak size fraction. Of note, these profiles were found to be similar to the FPLC profile of a CETP deficient patient (Figure 1A).

Patients have hypoglycosylated CETP

CETP was analyzed on IEF followed by western blot to detect possible charge changes in CETP glyco-isoforms. CETP has four predicted glycosylation sites, suggesting eight possible bands on IEF. Figure 1B shows a representative normal pattern of isoforms in healthy controls (lane 1 and 5) and a profound loss of negative charges in patient B2 and B3 (lane 3 and 4), with bands ranging from asialo- to pentasialo-CETP, similar to the glyco-isoform pattern seen in controls treated with neuraminidase (lane 2).

CETP activity

To study whether the hypoglycosylated plasma CETP is also less active and thus could explain the observed lipoprotein abnormalities, endogenous CETP activity was measured. Indeed, *B4GALT1*-CDG patients had a 26% reduction in CETP activity compared to controls ($20 \pm 3\%$ versus $27 \pm 5\%$, $p = 0.019$, Figure 1C).

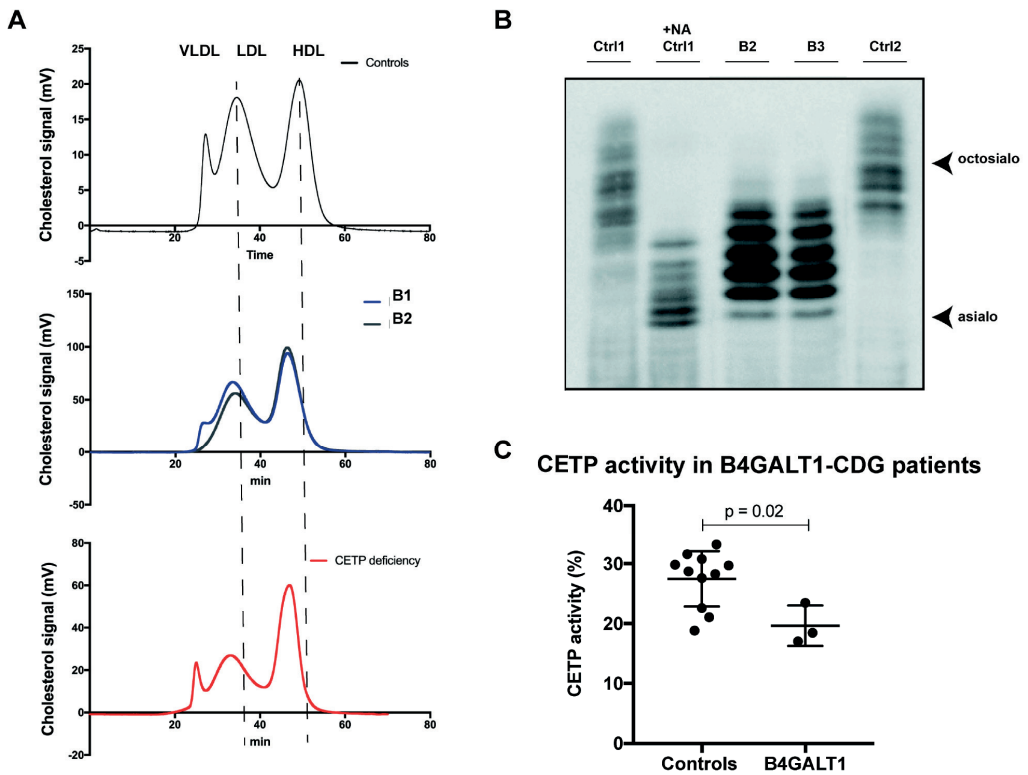


Figure 1. Hypoglycosylated hypo-active CETP in B4GALT1-CDG patients. (A) Pooled FPLC trace of child controls (*top panel*), representative traces of patients B1 and B2 (*middle panel*) and a CETP deficient patient (*bottom panel*). The vertical line illustrates the clear HDL peak shift to the left in B4GALT1 and CETP patients, indicating the HDL size increment. **(B)** Representative blot of CETP isoelectric focusing of a control (Ctrl1), a control treated with neuraminidase (Ctrl + NA), patient B2, patient B3 and a different control (Ctrl2). **(C)** CETP activity in B4GALT1 patients versus age- and gender-matched controls.

Discussion

In the present study, we demonstrate that patients with B4GALT1-CDG have increased cholesterol content in larger HDL particles, with lower cholesterol residing in the LDL fraction. IEF of CETP showed a marked loss of the more negatively charged CETP glyco-isoforms in the B4GALT1-CDG patients compared to healthy controls. There was not a complete loss of negatively charged CETP, as one would see after a long enough incubation with neuraminidase, similar to the transferrin IEF profile of B4GALT1-CDG patients. The hypoglycosylation of CETP was accompanied by a significant reduction of CETP lipid transfer activity compared to controls. The latter finding implies that glycosylation of CETP is essential for its activity, i.e. shuttling cholesteryl esters from the HDL fraction to the LDL fraction in exchange for triglycerides.

This notion may bear relevance to the clinical application of CETP inhibitors. These experimental drugs effectively lowered LDL and raised HDL in multiple phase 3 clinical trials. In most phase 3 trials, these effects failed to translate into cardiovascular benefit, leading to discontinuation of the drug development. Yet, in the recently published REVEAL study, anacetrapib added to intensive statin therapy resulted in significantly less major coronary events than statin therapy alone (10.8% versus 11.8% with a rate ratio of 0.91)¹⁸.

The relative paucity of cardiovascular benefit with CETP inhibition may be related to concomitant use of statins. ApoB, reflecting the total number of atherogenic lipid particles, has a stronger link with atherosclerotic cardiovascular disease than LDL-c¹⁹. When used in combination with statins, CETP inhibitors reduce apoB to a smaller extent than LDL: delta apoB / delta LDLc ratio ~ 15%. When used without statins, CETP inhibition reduces apoB proportionately to LDL: delta apoB / delta LDL-c is ~ 100%. The mechanism behind this discrepancy in apoB lowering and LDL lowering when CETP inhibitors are used on top of statin is unknown, but the discrepancy was supported by a recent mendelian randomization study with genetic *CETP* and *HMGCR* variants, the latter gene being the target of statins²⁰. Supporting a sole CETP effect in the B4GALT1 deficient patients, who did not use statins, we see a comparable proportionate reduction of LDL and apoB, ratio 92%.

Besides a reduction in CETP activity, other factors may have contributed to the observed HDL-c increase in our patients. First, B4GALT1-CDG patients have a global glycosylation defect and consequently other proteins known to regulate HDL-c levels may also contribute to the observed lipid changes. Recently, two different mutations in the genes encoding scavenger receptor class B type 1 (SR-B1), P376L²¹ and T175A²², have been described. Both cause impaired N-glycosylation of SR-B1 with subsequent reduced molecular weight and SR-B1 protein expression, causing high plasma HDL-c and reduced selective uptake of cholesteryl esters from HDL. Indeed, FPLC profiles of these mutation carriers show large buoyant HDL particles as well. These studies describe variants in SR-B1 leading to complete loss of glycans on the protein; it remains unstudied whether hypogalactosylation, as seen in B4GALT1-CDG patients, also affects SR-B1 function. In addition, endothelial lipase deficiency also leads to increased HDL-c concentrations with larger HDL particles²³. However, endothelial lipase activity has been shown to increase after (complete) removal of N-glycosylation sites²⁴, which would lead to decreased HDL-c and is therefore less likely to play a role in the lipid phenotype of the patients of our study. This discrepancy might be explained by the fact that in B4GALT1-CDG patients there is not a complete loss of glycans, but increased immature glycans due to hypogalactosylation.

Interestingly, the lipid phenotypes found in CDG patients are very specific to the particular glycosylation defect. CDG-I subtypes are hallmarked by hypobetalipoproteinemia⁴. In contrast, patients with *TMEM199*²⁵ and *CCDC115*²⁶ deficiency - resulting in a combined N- and O-linked glycosylation defect - exhibit very high levels of plasma non-HDL in combination with fatty liver disease. So even though all these patients have a generalized glycosylation defect due to mutations in factors involved in protein glycosylation, they show different and specific lipid abnormalities.

These differences again indicate the intricate influences of protein glycosylation on lipid pathways.

In conclusion, our study provides further specific insight into the role of protein glycosylation in human lipoprotein homeostasis. The hypogalactosylated, hypo-active CETP found in patients with B4GALT1-CDG indicates a distinct role of protein galactosylation in regulating plasma HDL-c and LDL-c.

References

1. Freeze, H.H., Chong, J.X., Bamshad, M.J. & Ng, B.G. Solving glycosylation disorders: fundamental approaches reveal complicated pathways. *Am J Hum Genet* **94**, 161-175 (2014).
2. Jaeken, J. Congenital disorders of glycosylation. *Ann N Y Acad Sci* **1214**, 190-198 (2010).
3. Funke, S., *et al.* Perinatal and early infantile symptoms in congenital disorders of glycosylation. *Am J Med Genet A* **161A**, 578-584 (2013).
4. van den Boogert, M.A.W., *et al.* N-Glycosylation Defects in Humans Lower Low-Density Lipoprotein Cholesterol Through Increased Low-Density Lipoprotein Receptor Expression. *Circulation* **140**, 280-292 (2019).
5. van den Boogert, M.A.W., Rader, D.J. & Holleboom, A.G. New insights into the role of glycosylation in lipoprotein metabolism. *Curr Opin Lipidol* **28**, 502-506 (2017).
6. Holleboom, A.G., *et al.* Heterozygosity for a loss-of-function mutation in GALNT2 improves plasma triglyceride clearance in man. *Cell Metab* **14**, 811-818 (2011).
7. Khetarpal, S.A., *et al.* Loss of Function of GALNT2 Lowers High-Density Lipoproteins in Humans, Nonhuman Primates, and Rodents. *Cell Metab* **24**, 234-245 (2016).
8. Schjoldager, K.T., *et al.* O-glycosylation modulates proprotein convertase activation of angiopoietin-like protein 3: possible role of polypeptide GalNAc-transferase-2 in regulation of concentrations of plasma lipids. *J Biol Chem* **285**, 36293-36303 (2010).
9. Aebi, M. & Hennet, T. Congenital disorders of glycosylation: genetic model systems lead the way. *Trends Cell Biol* **11**, 136-141 (2001).
10. Guillard, M., *et al.* B4GALT1-congenital disorders of glycosylation presents as a non-neurologic glycosylation disorder with hepatointestinal involvement. *J Pediatr* **159**, 1041-1043 e1042 (2011).
11. Guillard, M., *et al.* Plasma N-glycan profiling by mass spectrometry for congenital disorders of glycosylation type II. *Clin Chem* **57**, 593-602 (2011).
12. Medrano, C., *et al.* Clinical and molecular diagnosis of non-phosphomannomutase 2 N-linked congenital disorders of glycosylation in Spain. *Clin Genet* **95**, 615-626 (2019).
13. Hansske, B., *et al.* Deficiency of UDP-galactose:N-acetylglucosamine beta-1,4-galactosyltransferase I causes the congenital disorder of glycosylation type II. *J Clin Invest* **109**, 725-733 (2002).
14. Levels, J.H., Lemaire, L.C., van den Ende, A.E., van Deventer, S.J. & van Lanschot, J.J. Lipid composition and lipopolysaccharide binding capacity of lipoproteins in plasma and lymph of patients with systemic inflammatory response syndrome and multiple organ failure. *Crit Care Med* **31**, 1647-1653 (2003).
15. de Jong, G., van Noort, W.L. & van Eijk, H.G. Optimized separation and quantitation of serum and cerebrospinal fluid transferrin subfractions defined by differences in iron saturation or glycan composition. *Adv Exp Med Biol* **356**, 51-59 (1994).
16. Villard, E.F., *et al.* Endogenous CETP activity as a predictor of cardiovascular risk: determination of the optimal range. *Atherosclerosis* **227**, 165-171 (2013).
17. Guerin, M., Dolphin, P.J. & Chapman, M.J. A new in vitro method for the simultaneous evaluation of cholesteryl ester exchange and mass transfer between HDL and apoB-containing lipoprotein subspecies. Identification of preferential cholesteryl ester acceptors in human plasma. *Arterioscler Thromb* **14**, 199-206 (1994).
18. Group, H.T.R.C., *et al.* Effects of Anacetrapib in Patients with Atherosclerotic Vascular Disease. *N Engl J Med* **377**, 1217-1227 (2017).
19. Sniderman, A.D., *et al.* Apolipoproteins versus lipids as indices of coronary risk and as targets for statin treatment. *Lancet* **361**, 777-780 (2003).

20. Ference, B.A., *et al.* Association of Genetic Variants Related to CETP Inhibitors and Statins With Lipoprotein Levels and Cardiovascular Risk. *JAMA* **318**, 947-956 (2017).
21. Zanoni, P., *et al.* Rare variant in scavenger receptor BI raises HDL cholesterol and increases risk of coronary heart disease. *Science* **351**, 1166-1171 (2016).
22. Chadwick, A.C. & Sahoo, D. Functional characterization of newly-discovered mutations in human SR-BI. *PLoS One* **7**, e45660 (2012).
23. Ma, K., *et al.* Endothelial lipase is a major genetic determinant for high-density lipoprotein concentration, structure, and metabolism. *Proc Natl Acad Sci U S A* **100**, 2748-2753 (2003).
24. Skropeta, D., *et al.* N-Glycosylation regulates endothelial lipase-mediated phospholipid hydrolysis in apoE- and apoA-I-containing high density lipoproteins. *J Lipid Res* **48**, 2047-2057 (2007).
25. Jansen, J.C., *et al.* TMEM199 Deficiency Is a Disorder of Golgi Homeostasis Characterized by Elevated Aminotransferases, Alkaline Phosphatase, and Cholesterol and Abnormal Glycosylation. *Am J Hum Genet* **98**, 322-330 (2016).
26. Jansen, J.C., *et al.* CCDC115 Deficiency Causes a Disorder of Golgi Homeostasis with Abnormal Protein Glycosylation. *Am J Hum Genet* **98**, 310-321 (2016).



CHAPTER 3

Deficiency of V-ATPase assembly factors TMEM199 and CCDC115 results in fatty liver disease, hyperlipidemia and defective lipid droplet - lysosome interaction.

M.A.W. van den Boogert, L.E. Larsen, J.C. Jansen, D. Conlan, P.L.E. Chong, J.H.M. Levels, T. Raabe, M. He, N.J. Hand, J.P.H. Drenth, D.J. Rader, E.S.G. Stroes, J.W. Jonker, D.J. Lefeber, A.G. Holleboom

Cellular and Molecular Gastroenterology and Hepatology, manuscript in revision

Abstract

Background

Recently, novel inborn errors of metabolism were identified due to mutations in V-ATPase assembly factors *TMEM199* and *CCDC115*. Patients are characterized by generalized glycosylation defects, hypercholesterolemia and fatty liver disease. Here, we set out to characterize the lipid and liver phenotype in plasma, cell models and a mouse model.

Methods and results

Patients with *TMEM199* and *CCDC115* mutations displayed hyperlipidemia, due to lipoproteins in the very-low density lipoprotein range. HepG2 hepatoma cells, in which the expression of *TMEM199* and *CCDC115* was silenced, and iPSC-derived hepatocyte-like cells derived from patients with *TMEM199* mutations showed markedly increased secretion of apolipoprotein B compared to controls.

A mouse model for *TMEM199* deficiency with a CRISPR/Cas9-mediated knock-in of the human A7E mutation had marked hepatic steatosis on chow diet. Plasma N-glycans were hypogalactosylated, consistent with the clinical phenotype, but no clear plasma lipid abnormalities were observed in the mouse model.

In the si*TMEM199* and si*CCDC115* HepG2 hepatocyte model, increased numbers and sizes of lipid droplets were observed, including abnormally large lipid droplets that colocalized with lysosomes.

Conclusion

Our data suggest that the hypercholesterolemia in *TMEM199* and *CCDC115* deficiency is due to increased secretion of apoB-containing particles. This may in turn be secondary to the hepatic steatosis observed in these patients and in the mouse model. Importantly, the observed lipid accumulation in lysosomes could underly the hepatic steatosis seen in patients and would stress the importance of lipophagy in fatty liver disease. As this field remains understudied and its mechanism largely untargeted, exploration of this field may offer a new therapeutic axis to reduce lipotoxicity in fatty liver disease.

Introduction

The multi-subunit vacuolar-type H⁺-ATPase (V-ATPase) is responsible for acidification of intracellular organelles, thereby controlling several pH-sensitive intracellular processes such as protein glycosylation and autophagy¹. By sequencing human homologues of yeast V-ATPase assembly factors in families with formerly unsolved N- and mucin-type O-glycosylation abnormalities, two novel inborn errors of metabolism were identified with defects in two of these assembly factors, TMEM199 and CCDC115^{2,3}. Interestingly, the affected patients displayed fatty liver disease and marked hypercholesterolemia without mutations in any of the genes previously known to cause familial hypercholesterolemia.

Four of the patients described had mutations in *TMEM199*, the human homologue of yeast V-ATPase assembly factor Vma12p. They presented with hepatic steatosis, elevated transaminases, mild fibrosis and hypercholesterolemia. Their serum glycosylation pattern was similar to that seen in other mixed glycosylation defects, specifically N-glycans lacking galactose and sialic acids and abnormal mucin-type O-glycosylation of apolipoprotein C-III².

In three other unrelated families, we found mutations in another V-ATPase assembly factor, *CCDC115*, the human homologue of yeast Vma22p. Affected individuals showed marked hypercholesterolemia and a storage disease-like phenotype with hepatosplenomegaly, and steatohepatitis with fibrosis. In two patients, this led to liver failure requiring transplantation. Serum glycosylation analyses revealed abnormal N- and O-glycosylation, which was confirmed in patient fibroblasts and could be rescued by lentiviral transfection with wild-type *CCDC115*³.

Notably, overlapping liver and lipid phenotypes have been described in patients with mutations in other assembly factors of the V-ATPase as well, i.e. *ATP6AP1*⁴, *ATP6AP2*⁵, and *VMA21*⁶. The phenotypes in those patients range from mild steatohepatitis with mildly elevated liver transaminases to early cirrhosis and liver failure. In addition, they had similar defects in N- and O-glycosylation, associated with impaired Golgi homeostasis. Together this suggests that V-ATPase misassembly is the common pathogenic process in these syndromes.

Here, we aimed to further characterize the hypercholesterolemia in TMEM199 and CCDC115 deficiency is likely due to increased secretion of apolipoprotein B (apoB). In addition, we confirmed the observed fatty liver phenotype in a murine model of TMEM199 deficiency. Together, our results from two hepatocyte models point towards defective lipid droplet – lysosome interaction as an underlying mechanism for the lipotoxic hepatic phenotype in these V-ATPase assembly defects. These findings likely bear relevance for the understudied process of lipophagy in non-alcoholic fatty liver disease (NAFLD), the rapidly increasing common form of fatty liver disease associated with obesity and diabetes mellitus type 2.

Methods

Subjects

We collected plasma samples of 6 patients, 3 with homozygosity/compound heterozygosity for *TMEM199* mutations, and 3 with homozygosity/compound heterozygosity for *CCDC115* mutations, whose clinical characteristics were reported earlier^{2,3}. In addition, we included 12 healthy, age- and gender-matched controls from the plasma biobank at the Amsterdam UMC, location AMC, The

Netherlands. These were unaffected family members of patients with dyslipidemia, without mutations in genes known to affect apoB and LDL-cholesterol (LDL-c) (*APOB*, *LDLR* and *PCSK9*) or in *TMEM199* or *CCDC115*, from our lipid clinic with plasma stored in our blood bank.

Plasma lipids

We analyzed plasma lipids in venous blood samples collected after an overnight fast in EDTA-coated tubes. Plasma was isolated after centrifugation at 3000 RPM for 15 minutes at 4°C and stored at -80°C until further analyses.

Total cholesterol (TC), LDL-c, high-density lipoprotein cholesterol (HDL-c), triglycerides (TG), apolipoprotein A-I (apoA-I) and apoB were measured using commercially available assays (DiaSys and WAKO) on a Selectra analyzer (Sopachem, The Netherlands).

TC and TG content in the main lipoprotein classes (VLDL, LDL and HDL) was determined using fast protein liquid chromatography (FPLC) as described⁷. The main system consisted of a PU-980 ternary pump with an LG-980-02 linear degasser and an UV-975 UV/VIS detector (Jasco, Tokyo, Japan). After injection of 30 µl plasma (1:1 diluted with TBS) the lipoproteins were separated using a Superose 6 Increase 10/30 column (GE Healthcare Hoevelaken, The Netherlands). As eluent TBS pH 7.4 was used at a flow rate of 0.31 ml/min. A second pump (PU-2080i Plus, Jasco, Tokyo Japan) was used for either in-line cholesterol PAP or Triglyceride enzymatic substrate reagent (Sopachem, Ochten, The Netherlands) addition at a flowrate of 0.1 ml/min facilitating TC or TG detection. Commercially available lipid plasma standards (low, medium and high) were used for generation of TC or TG calibration curves for the quantitative analysis (SKZL, Nijmegen, the Netherlands) of the separated lipoprotein fractions. All calculations performed on the chromatograms were carried out with ChromNav chromatographic software, version 1.0 (Jasco, Tokyo, Japan).

Cell lines

HepG2 human hepatoma cells were cultured in 75 cm² flasks (Falcon) in complete medium (DMEM supplemented with 4.5 g glucose, 10% fetal bovine serum and 1% penicillin/streptomycin; Gibco). All cells were maintained in a 37°C humidified incubator supplemented with 5% CO₂ atmosphere and split when needed at ~80-100% confluency.

For siRNA experiments in HepG2 cells were plated in 12 wells plates at a density of 300.000 cells per well, respectively. RNA silencing was done in HepG2 hepatoma liver cells, to mimic the *TMEM199* and *CCDC115* deficiency.

Furthermore, we studied patient-derived hepatocyte-like cells (HLCs). Easily accessible differentiated cells, in this case fibroblasts of two patients with *TMEM199* mutations, two patients with *CCDC115* mutations and two age- and gender-matched controls, all obtained by biopsy at Radboud UMC, were reprogrammed to iPSCs and subsequently re-differentiated to HLCs (as described earlier)^{8,9}. In short, patient derived fibroblasts were reprogrammed with Cytotune® reprogramming kit 2.0 by the iPSC core at University of Pennsylvania. First ten cell passages were cultivated on immortalized mouse embryonic fibroblasts as feeder cells in DMEM-F12 supplemented with 20% knock-out replacement serum (Life Tech), 4ng/ml FGF, and incubated at

37°C with 5% O₂/5% CO₂. Cells were passaged when they reached sustainable colony size with accutase® (Innovative Cell Technology) according to manufacturer's protocol. When the iPSCs reached appropriate confluency, they were transferred to Geltrex® (Gibco) and cultivated in StemMACS iPSBrew. Passages were performed with StemMACS non-enzymatic passaging solution according to manufacturer's instructions. After a minimum of four passages in iPSBrew, iPSCs were seeded 1x10⁴ cells per well in a 12-well plate coated with Geltrex®. Induction of differentiation to definitive endoderm (day 1-5) was achieved with StemDiff definitive endoderm kit according to manufacturer's protocol. Further maturation of endoderm to mature induced hepatocytes (hepatocyte-like cells) was performed according the protocol of Jun Cai et al.¹⁰

In vitro experiments

The HepG2 cell model was used for a wide quantitative polymerase chain reaction (qPCR) screen of expression levels of important players in plasma lipid and lipoprotein metabolism (see Table S1 for primer sequences). mRNA was isolated with Trizol and reversed transcribed with iScript (SensiFAST, Bioline) for qPCR measurement with SYBR green (SensiFAST, Bioline) according to the manufacturer's procedure.

ApoB secretion assays with or without oleic acid stimulation were also performed in the HepG2 cell model. Twenty-four hours after transfection the medium was changed to lipoprotein-deficient (LPDS) medium (DMEM supplemented with 4.5 g glucose, 10% lipoprotein-deficient serum and 1% penicillin/streptomycin; Life Technologies). After another 24 hours, either 0.3 mM oleic acid-BSA (OA; Sigma) in LPDS medium or fatty acid free BSA (Sigma) in LPDS medium was added to the wells. After 4 hours, the media were collected for apoB measurement and cells were lysed with Trizol for RNA isolation for expression analysis or RIPA buffer with protease inhibitors (Roche) for protein levels. ApoB levels in the medium were measured with a specific enzyme-linked immunosorbent assay (ELISA, as described by Kulozik et al¹¹) and normalized for total cell protein measured with BCA protein assay (Pierce, ThermoScientific)).

In HLCs, apoB secretion was assessed by ³⁵S steady-state protein labelling and precipitation in methionine-free Hepatocyte Basal Medium as described^{12,13}.

Lipid droplet and lysosome Fluorescent imaging of HepG2 and Huh7 cells

For fluorescent microscopy, cells were grown on a coverslip till 50% confluency. Cells were incubated with 0,5 µM LysoTracker Red DND-99 (life technologies; L7528) in full medium for 45 minutes prior to fixation, for lysosomal staining. Cells were fixed with 4% PFA in PBS for 10 minutes at room temperature. For neutral lipid enclosed in cytosolic lipid droplets (LDs), cells were incubated with HCS LipidTOX™ Green neutral lipid stain (life technologies; H34475) according to manufactures protocol. Upon imaging, cells were mounted with Vectaschield DAPI stain (Vector laboratories; H-1000-10) according to manufacturer's protocol for nuclear staining. Cells were imaged at room temperature on a Zeiss Observer Z1 brightfield microscope equipped with ApoTome 2 and a 63x (W) objective lens (APO DIC III numerical aperture 1.2) and acquired using Zeiss software Zen 2010. Laser lines used in this study were 405, 488 and 568 nm. Red/green/blue (RGB) and greyscale images

were further processed with Zeiss software Zen 2010

In addition, HepG2s, fibroblasts and HLCs were used to assess cellular and surface LDLR protein expression levels with western blot and flow cytometry and LDL uptake with Dylight labeled LDL particles in combination with flow cytometry¹⁴.

Mouse model

As a *TMEM199* full knock-out proved to be embryonic lethal, C57BL/6J mouse embryos were gene-edited using a CRISPR/Cas9 homology-directed repair knock-in method with homologous Alanine-7-Glutamine (Ala7Glu) human-variant ssDNA oligos and inhibition of non-homologous end-joining using SCR7 (Xcess Bio, Chicago, IL).

Mouse plasma was used for plasma N-glycan profiling with MALDI-TOF mass spectrometry of permethylated glycans, as described earlier¹⁵.

As aforementioned, FPLC profiling for cholesterol distribution across lipoprotein fractions was carried out as described⁷. FPLC fraction TG and cholesterol contents were measured by enzymatic assays and normalized to protein as measured by BCA assay¹⁶.

RNA was isolated from liver tissue with Trizol according to the manufacturer's protocol. Subsequently, qPCR was performed for the listed target lipid panel (Table 1).

Liver samples were homogenized in commercial RIPA buffer for western blot analysis and normalized with BCA assay. The protein samples were run on a 14% TRIS-Bis gel and transferred to a PVDF membrane. These membranes were blocked with 5% skimmed milk in TBS-Tween 20 buffer and incubated with primary rabbit-anti-TMEM199 (ab121907) overnight at 4°C in 1% skimmed milk in TBS-Tween 20. Secondary HRP-conjugated donkey-anti-rabbit antibody was incubated for 1 hour at room temperature.

Western blots for apoB, PCSK9, and apoA1 were run by using 7 µl of undiluted plasma on a 4% Tris-Acetate gel. The proteins were in turn transferred to PVDF and blocked with 5% BSA in TBS-Tween 20. Overnight incubation at 4 °C was done with primary rabbit anti-apoB (ab20737), PCSK9 (ERP7627), and apoA1 (EP1368Y). Incubation with the secondary antibody was performed as mentioned above.

For the assessment of potential atherosclerotic injury in the heterozygous *TMEM199*-Ala7Glu mice, we isolated the aortic branch and descendant aorta of both control and *TMEM199*-Ala7Glu mice post mortem, and inspected the epithelium macroscopically under 4x magnification.

Statistical analyses

Data are compared between groups with a Students t-test and presented as means ± standard deviation or, when appropriate, tested with a Mann-Whitney U test and presented as medians with interquartile ranges for nonparametric parameters. Categorical variables were tested with a Chi-square test. All statistical analyses were done using SPSS software (version 22.0, SPSS Inc., Chicago IL). Error bars indicate standard deviations. Probability values of < 0.05 were considered statistically significant.

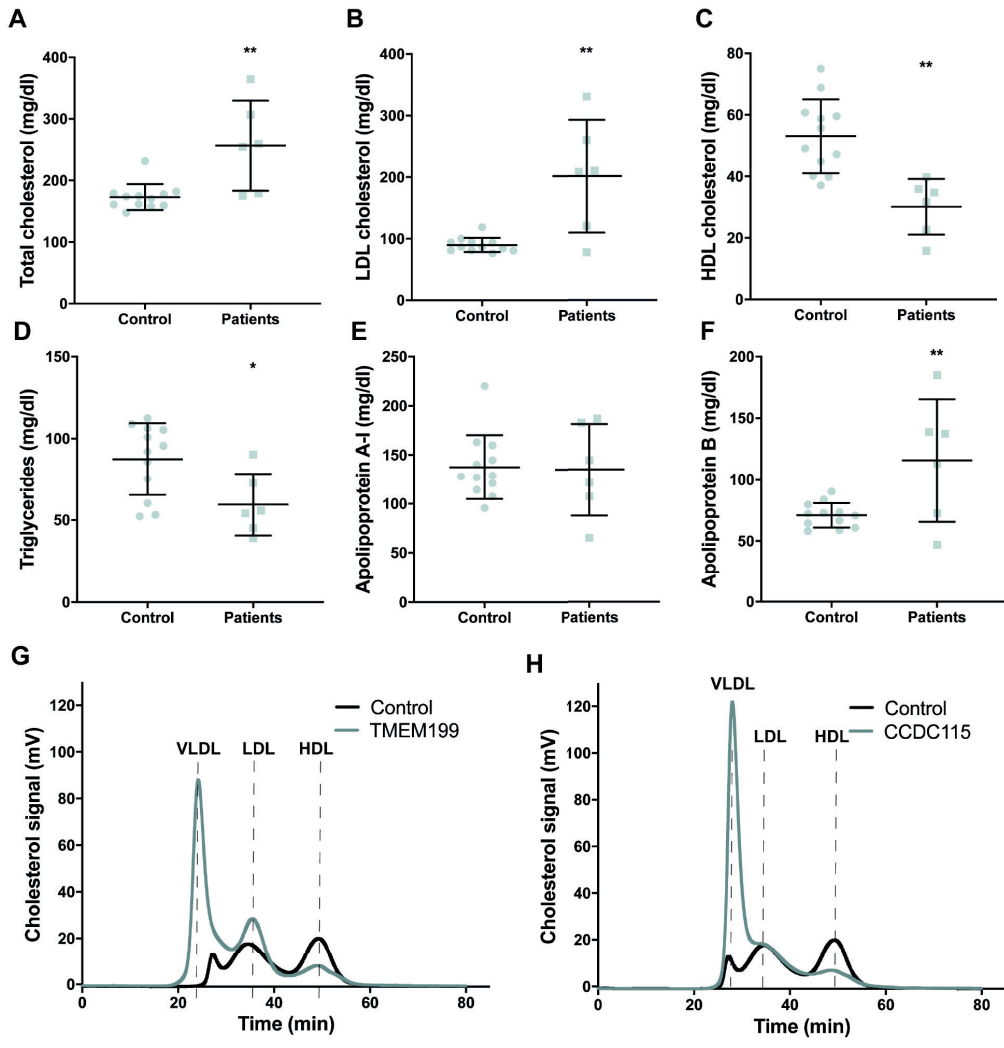


Figure 1. TMEM199- and CCDC115-CDG patients have hypercholesterolemia. Plasma samples from patients (3 TMEM199- and 3 CCDC115-CDG) were collected. **(A)** Plasma TC, **(B)** LDL-c, **(C)** HDL-c, **(D)** TG, **(E)** apoA-I and **(F)** apoB were measured in EDTA plasma after an overnight fast and compared to 12 age- and gender-matched controls. Representative traces of fast protein liquid chromatography (FPLC) of **(G)** TMEM199- and **(H)** CCDC115-CDG patients. All measurements are shown as a scatter plot with mean ± SD and each data point depicts a single measure from an individual subject plasma sample. ** indicates $p < 0.01$, * $p < 0.05$ as calculated with Student's unpaired two-sided t-tests.

Results

Patients with TMEM199 and CCDC115 mutations have hypercholesterolemia and increased apoB secretion

Plasma lipids were measured in three patients with *TMEM199* mutations, three with *CCDC115* mutations and in 12 age- and gender-matched controls. The results are given in Figure 1. *TMEM199*- and *CCDC115*-CDG patients had an average age of 6.6 ± 4 years, controls were 10 ± 2 years; $p = 0.073$. There was an approximate 1.5-fold increase in TC in the patients (257 ± 73 mg/dl) compared to controls (173 ± 21 mg/dl; $p = 0.0018$; Figure 1A). LDL-c was increased more than two-fold in patients (202 ± 92 mg/dl) compared to controls (90 ± 12 mg/dl; $p = 0.0006$; Figure 1B). ApoB was also significantly higher in patients (116 ± 50 mg/dl) compared to controls (71 ± 10 mg/dl; $p = 0.007$; Figure 1F). Interestingly, FPLC analysis of plasma cholesterol showed an altered cholesterol distribution in patients with *TMEM199* and *CCDC115* mutations, a considerable increase of the cholesterol content in large VLDL particles in combination with decreased HDL cholesterol content (Figure 1G and 1H).

Both HDL-c and TG were significantly lower in patients (30 ± 9 and 60 ± 19 mg/dl, respectively Figure 1C and 1D) compared to controls (53 ± 12 mg/dl and 87 ± 22 mg/dl; $p = 0.0008$ and $p = 0.018$, respectively). ApoA1 was comparable between patients and controls (135 ± 46 versus 138 ± 33 mg/dl; $p = 0.894$; Figure 1E).

Cellular models of TMEM199 and CCDC115 deficiency recapitulate increased apoB secretion.

In order to substantiate our *in vivo* findings, we studied apoB secretion in a HepG2 cell model. We used small-interfering RNAs (siRNAs) to silence *TMEM199* and *CCDC115* expression in human hepatoma cells (HepG2), using non-targeting siRNAs as control. We achieved effective silencing of *TMEM199* and *CCDC115* (90% on average for *TMEM199* and 93% for *CCDC115*; Figure 2A). First, mRNA expression of key lipid players was assessed with qPCR (Figure 2B). Compared to controls, there was no significant difference in APOB expression in si*TMEM199*, nor si*CCDC115* treated cells. There was, however, increased expression of cholesterol synthesis genes: *HMGCS* and *HMGCR* expression were significantly increased in both si*TMEM199* and si*CCDC115* cells (Figure 2B). In addition, si*TMEM199* and si*CCDC115* treated cells displayed significantly increased mRNA expression of *LDLR*.

Since increased apoB secretion can result in clinical hypercholesterolemia, *in vitro* apoB secretion was measured with ELISA under oleate stimulation and was significantly increased in both si*TMEM199* and si*CCDC115* treated cells compared to controls (a 75% and 28% increase respectively; $p < 0.0001$ and $p = 0.01$; Figure 2C). We also assessed apoB secretion by ^{35}S steady-state protein labelling in *TMEM199*-deficient patient-derived HLCs and found significantly increased apoB secretion (a 42% increase; $p = 0.008$; Figure S1).

Characterization of TMEM199 Ala7Glu mice indicates a functional knockout and hepatic steatosis.

To investigate the lipid and liver phenotype we observed in patients, we set out to generate a murine model. Full CRISPR-KO of *Tmem199* turned out to be lethal as there were no viable pups recovered. Next, we generated mice expressing a patient's mutation in *Tmem199*. Homozygous

TMEM199-Ala7Glu mice did not show any abnormalities in litter size nor were there dysmorphic features observed in these litters. Further juvenile development progressed comparable to control littermates (wild-type or heterozygous for the TMEM199-Ala7Glu allele) with normal weight gain.

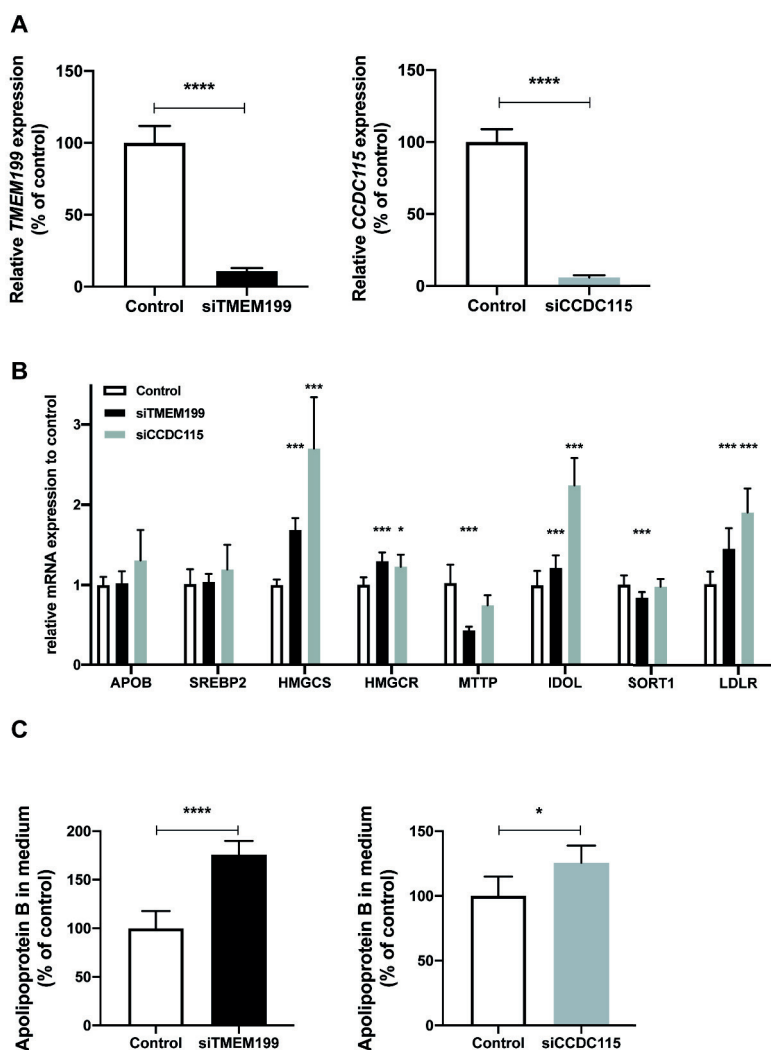


Figure 2. ApoB secretion in siTMEM199 and siCCDC115 treated HepG2 cells. siRNA knockdown of *TMEM199* and *CCDC115* in HepG2 cells. Panels show: **(A)** *TMEM199* (left) and *CCDC115* (right) mRNA expression levels, **(B)** mRNA expression of important lipid players in cholesterol synthesis, secretion and uptake, and **(C)** secretion of apoB into the medium (normalized for total protein) in oleic acid stimulated conditions for siTMEM199 treated cells (left) and siCCDC115 treated cells (right). All panels show representative western blots or means \pm SD from three experiments with triplicate measurements per experiment. **** indicates $p < 0.0001$, *** $p < 0.001$, * $p < 0.05$ and ns indicates non-significant results as calculated with Student's unpaired two-sided t-tests.

Similarly, the mice had apparently normal neurological development and no apparent neuromotor disabilities, as observed in patients (data not shown).

For characterization, 8-week old mice ($n = 5$ per group) on chow diet were sacrificed and hepatic *Tmem199* mRNA and protein expression were assessed. Relative *Tmem199* mRNA expression showed a reduction of 52% (0.48 ± 0.24 in TMEM199-Ala7Glu mice versus 1.00 ± 0.59 in controls; $p = 0.059$; Figure 3A, left panel). Using western blot analysis, virtually no TMEM199 protein could be detected in mouse livers homozygous for the TMEM199-Ala7Glu mutation (Figure 3A, right panel).

mRNA expression of lipid genes in homozygous TMEM199-Ala7Glu mouse livers revealed a significant reduction in *MTTP* (a 91% reduction; $p < 0.001$), *PCSK9* (67,5%; $p = 0.01$), and *MXL1PL* (*ChREBP*) expression (60%; $p = 0.01$). The expression of other genes involved in lipid metabolism were not different from control mice (Figure 3B).

Heparin treated plasma was pooled per genotype and analyzed with FPLC for distribution of lipoproteins. Fractions tended to have higher TG in the VLDL-containing fractions (AUC was 4.956 in TMEM199-Ala7Glu mutant mice versus 4.012 in controls; NS) in the mutant mice. Consistent with what we observed in the patients' cholesterol content was lower in the HDL-containing fractions, however this was not significant (AUC was 13.50 in mutants versus 15.85 in controls; ns Figure 3C). Further analysis with western blot showed that the ratio of apolipoprotein B100/48 was not different and PCSK9 in plasma was not affected, whereas apolipoprotein A1 was reduced (Figure 3D), in correlation with the reduced HDL-cholesterol found on FPLC.

In line with the hepatic phenotype seen in patients with TMEM199 deficiency, the livers of mice homozygous for TMEM199-Ala7Glu clearly showed macroscopic steatosis and increased hepatic triglycerides (80% higher than in controls, $p < 0.01$; Figure 3E). The mice showed no atherosclerotic lesions in the aortic root at 20 weeks (data not shown). Lastly, we analyzed mouse plasma N-glycan profiles by MALDI-TOF mass spectrometry and found that mice bearing the TMEM199-Ala7Glu mutation had a 1.5- to 2-fold decrease in complex fucosylated glycans and an increased amount of hyposialylated and hypogalactosylated glycans compared to controls (1% in TMEM199-Ala7Glu mice versus 0% in controls; Figure 3F and Table S2). This is consistent with the N-glycan profiles found in TMEM199 deficient patients.¹⁷

Silencing of TMEM199 and CCDC115 induces lipid accumulation in lysosomal vesicles.

To study the possible mechanism for hepatic steatosis we used the HepG2 cell model treated with siTMEM199 and siCCDC115. After 24hr OA stimulation (200 nmol), lipid accumulation was observed (Figure 4A). Although both siTMEM199 and siCCDC115 resulted in lipid accumulation, different accumulation patterns were observed. TMEM199 silencing resulted in a more microvesicular lipid accumulation with a significantly increased number of lipid-laden vesicles. Contrastingly, siCCDC115 treated cells had macrovesicular lipid accumulation. Both siTMEM199 and siCCDC115 treated cells had lipid accumulation in lysosomal vesicles, as detected by co-staining with lysotracker red DND-99 (Figure 4A). This was validated by quantification of LD mean area and number of LDs per cell. We found a significantly increased mean area in the siCCDC115 ($11.97 \pm 4.58 \mu\text{m}^2$, $p = 0.0022$) and

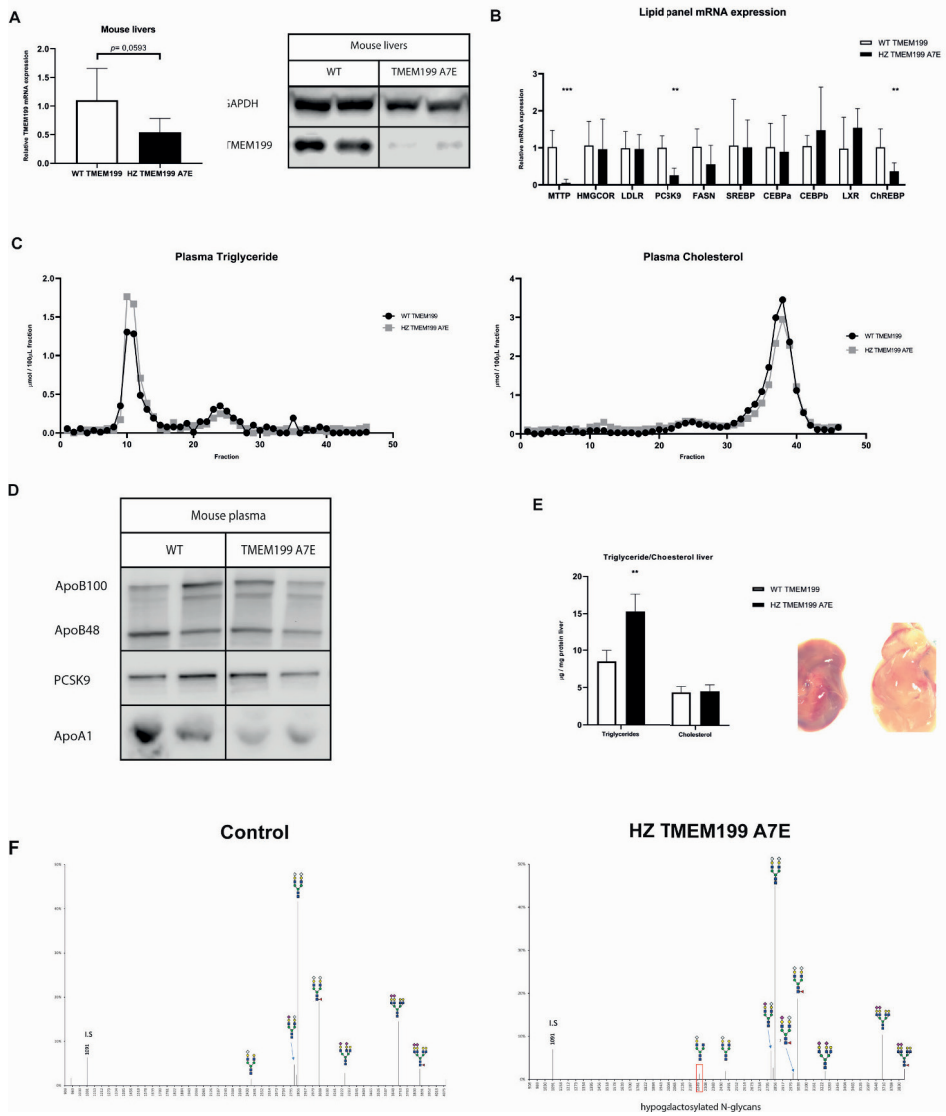
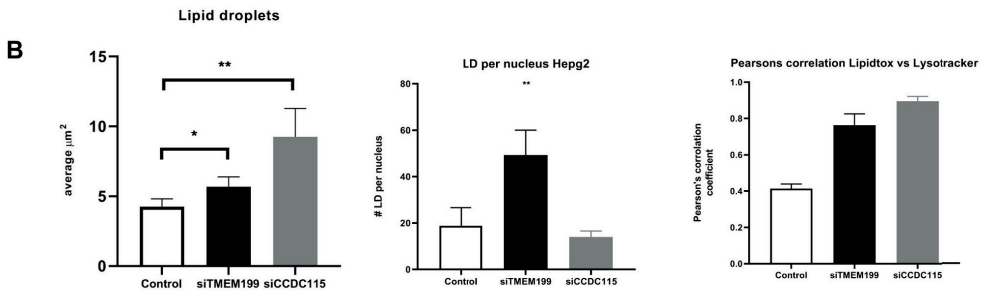
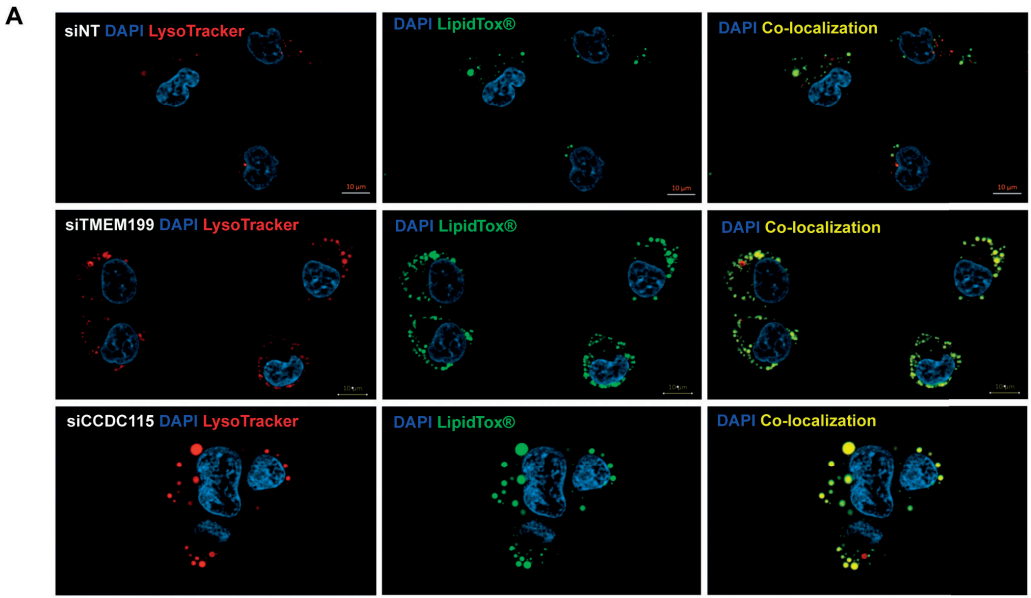


Figure 3. TMEM199 Ala7Glu mouse model on chow diet. Liver and plasma of 8-week-old mice were collected in liquid nitrogen or heparin coated tubes, respectively, following a 4 hour fast. **(A)** qPCR and Western blot for hepatic *TMEM199* mRNA (left) and protein expression (right). **(B)** *TMEM199*-Ala7Glu mice have macroscopic hepatic steatosis (left) and increased hepatic triglycerides (right) qPCR for lipid markers in mouse livers. **(C)** Plasma of control and heterozygous *TMEM199*-Ala7Glu were pooled for FPLC analysis (N = 5, per group; litter mates) and fractions were analyzed for triglyceride and cholesterol content. **(D)** mRNA expression panel for selected genes involved in the regulation, assembly, and uptake of apoB lipoproteins. **(E)** ApoB100/48, PCSK9, and apoA1 were analyzed from 7 μL whole plasma on western blot. **(F)** Representative MALDI-TOF spectra of N-glycans derived from mouse plasma. All panels show representative western blots from three experiments with triplicate measurements per experiment. *** represents $p < 0.001$ ** $p < 0.01$, * $p < 0.05$ as calculated with unpaired Mann-Whitney test.

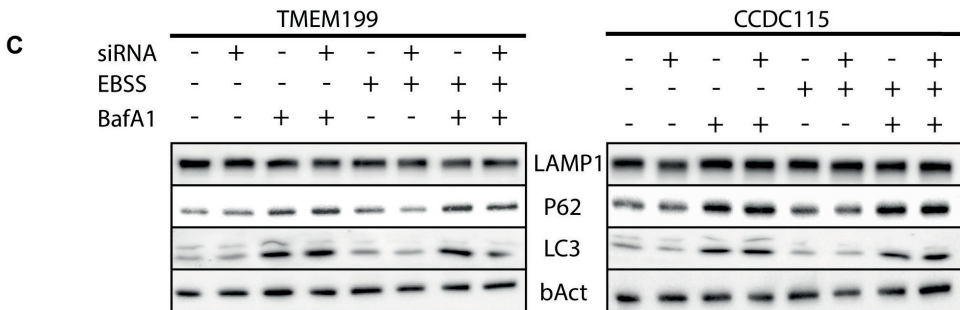
siTMEM199 ($6.46 \pm 0.84 \mu\text{m}^2$, $p < 0.01$ compared to control ($3.54 \pm 0.47 \mu\text{m}^2$) treated cells. We also found a significantly higher number of LDs in the siTMEM199 (49.31 ± 10.70 , $p < 0.01$, but not in the siCCDC115 (13.75 ± 2.56 , ns) treated cells when compared to controls (18.80 ± 7.80). When we addressed the colocalization of lipid droplets and lysosomes by applying Pearson's correlation coefficient for LipidTox[®] and LysoTracker red DND-99, we found significant colocalization in both treated cells (siTMEM199: $r = 0.76 \pm 0.06$, $p < 0.0001$; siCCDC115: $r = 0.89 \pm 0.02$, $p < 0.0001$; control: $r = 0.41 \pm 0.02$).

Lysosomes and lysosomal degradation are integrated with autophagy, which led us to investigate autophagy parameters. Autophagic markers (LC3 and P62) were not altered upon silencing of *TMEM199* or *CCDC115*, which suggests a dissociation between the lipid accumulation in lysosomes and autophagy-driven lipolysis (Figure 4C).

Figure 4. Lipid droplet accumulation and autophagy analysis of siTMEM199 and siCCDC15 HepG2 cells. HepG2 cells were treated with siRNAs for non-targeted (NT), TMEM199 (*left*), and CCDC115 (*right*). **(A)** After 24 hours siRNA treatment cells were incubated with 200 μmol bovine serum albumin (BSA) conjugated oleic acid (OA) in full medium for 24 hours. After incubation with OA cellular neutral lipids and lysosomes were labeled with LipidTox[®] and LysoTracker red DND-99, respectively. **(B)** Quantification of lipid droplet size, number of lipids per nucleus, and Pearson's correlation coefficient for LipidTox[®] green and LysoTracker Red DND-99. **(C)** After 48 hours of siRNA treatment cells were starved (autophagy induction; EBSS), treated with Bafilomycin A1 (autophagy inhibition; BafA1), or both. Panels represent whole cell lysate protein levels of lysosomal (LAMP1) and autophagy markers (P62; LC3B). All panels show representative western blots from three experiments with triplicate measurements per experiment.



HepG2 cells



Discussion

Here, we report on the plasma and hepatic lipid disorders in two recently found inborn errors of metabolism involving mutations in two V-ATPase assembly factors: *TMEM199* and *CCDC115*. Patients are hypercholesterolemic, with most cholesterol attributable to the VLDL fraction, while HDL cholesterol content is decreased. Consistent with this, we observed hypersecretion of apoB in our loss of function cellular models, providing a likely explanation for the clinical finding. Similarly, the steatohepatitis observed in the patients is phenocopied in cellular models by lipid droplet accumulation and defective lipid droplet – lysosome interaction, as well as by the observation of hepatic steatosis in our hypomorphic mouse model of *TMEM199* deficiency.

In comparison to earlier reports on hyperlipidemia in other V-ATPase assembly defects⁴⁻⁶, our study provides an in-depth characterization of the abnormal plasma lipids of these two V-ATPase assembly defects, including apolipoproteins and FPLC profiles. The latter revealed that in both *TMEM199* deficiency and *CCDC115* deficiency, elevated plasma cholesterol mostly sequesters in the VLDL fraction. Yet, these were likely not triglyceride-rich lipoproteins, since plasma triglycerides in patients were lower than in controls, suggesting a reduced ability of the liver to lipidate (V)LDL with triglycerides before secretion. Compared to *VMA21* deficiency (25% increase in LDL-c) and *ATP6AP2* deficiency (on average 20% increase in LDL-c), the hyperlipidemia in *TMEM199* and *CCDC115* deficiency clearly was more pronounced (124% increase in LDL-c).

In contrast to these elevations in (V)LDL-c, HDL-c was reduced in the patients and in the *TMEM199* mouse model. However, plasma levels of apoA1 were not reduced, which may point towards reduced lipidation of HDL particles via ATP-binding cassette protein A1 (ABCA1) or lecithin:cholesterol acyl transferase (LCAT). Indeed, the function of the latter can be affected when intracellular lipid pathways are disturbed, as occurs in acid sphingomyelinase deficiency (Niemann Pick disease type B)¹⁸.

The increased LDL and decreased HDL can be considered as a pro-atherogenic lipid profile. Atherogenesis can be of clinical relevance for *TMEM199* deficiency, a disease that has no severe neurocognitive defects or liver failure as main causes of morbidity and life expectancy. Yet, no premature atherosclerosis was reported in any of the *TMEM199* or *CCDC115* deficient patients. The strength of this observation has its limits, since these inborn disease phenotypes are rare and most patients were too young to develop clinically overt atherosclerotic cardiovascular disease. While we did not note any indications of atherogenesis in the *TMEM199*-Ala7Glu mouse model, this should be interpreted with caution, because, as this was not the primary aim of this study, we did not formally test for this using standard approaches (backcrossing to an atherogenic background, e.g. LDL-receptor *-/-* or apolipoprotein E *-/-*, dietary stress or aging).

In search of a potential explanation of the observed hypercholesterolemia in the *TMEM199* and *CCDC115* deficient patients, we next studied apoB secretion in two complementary cell models: HepG2 cells in which these factors had been silenced, and iPSC-derived hepatocytes harboring the patients' *TMEM199* mutations. Strikingly, these cell models indicated increased secretion of apolipoprotein B, a novel finding for the V-ATPase assembly defects, not studied before in the other

three V-ATPase assembly defects (ATP6AP1, ATP6AP2 or VMA21).

A potential explanation for the high apoB secretion and hypercholesterolemia can be derived from the related V-ATPase assembly defect VMA21 deficiency⁶. It was demonstrated that VMA21 deficiency resulted in increased sterol response element-binding protein-1 (SREBP1) activation and cleavage in a response to cholesterol sequestration in lysosomes. This would result in increased de novo lipogenesis that is often paired with elevated apoB secretion. In turn, we found a potential explanation for the reduced plasma triglycerides in plasma in our study: the evidently reduced expression of *MTTP*. This gene encodes the hepatic enzyme that transfers triglycerides to newly synthesized apoB-lipoproteins, thereby lipidating and maturing them into VLDL particles before their secretion into the plasma compartment. While it would be desirable to characterize the VLDL fraction in more depth by fractionation and by nuclear magnetic resonance spectroscopy, yet this was not feasible due to the very scarce availability of plasma of these rare, often pediatric patients.

To study the plasma lipids and liver defects in a physiological context, we used CRISPR-Cas9-mediated genome editing to generate a knock-in mouse model that carries the Ala7Glu mutation in *TMEM199*, a mutation found in one of the three patients. Compared to other V-ATPase assembly defects, i.e. ATP6AP1, ATP6AP2 and VMA21 deficiency, this is a unique model, because no mouse models of these defects have been generated and characterized to date. Here, we show that this mutation results in loss of TMEM199 protein in our mouse model.

In addition, plasma of these mice indicated glycosylation defects comparable to patients with TMEM199 deficiency showing hypogalactosylation of N-glycans. This may be secondary to disruption of the glycosylation enzymes in the Golgi apparatus, as zebrafish with defects in *atp6ap2* have been shown to have dilated Golgi¹⁹. Furthermore, we observed hepatic steatosis in the livers of these mice, similar to the clinical steatohepatitis in patients. On chow diet, these mice did not show any significant increase in VLDL-bound cholesterol or apoB, potentially due to the higher turnover of apoB-containing particles in murine plasma²⁰, yet the mice did illustrate a minor increase in TG content of VLDL-particles. Interestingly, these mice did display a reduction in HDL particles on FPLC and on western blot, in line with the HDL observation in the patients.

The increased number of lipid droplets described in liver biopsies of the patients with TMEM199 and CCDC115 deficiency combined with reports of disturbed autophagic flux in two other V-ATPase assembly defects^{5,6} led us to study lipid droplets and lysosomes in our HepG2 models of TMEM199 and CCDC115 deficiency. Lipid droplets are organelles with a core of neutral lipids – triglycerides and cholesterol esters – surrounded by a phospholipid monolayer²¹. Lipid droplets are catabolized via cytoplasmic lipases²² or via an autophagic route (lipophagy)²³. Indeed, the HepG2 model had increased number and size of lipid droplets. Interestingly, our colocalization studies in both the TMEM199 and CCDC115 hepatocyte model showed disturbed interaction between lipid droplets and lysosomes. This is compatible with a disturbed autophagic flux of lipid droplets. In turn, this indicates the hypothesis that the disturbed V-ATPase assembly in TMEM199 and CCDC115 deficiency results in steatohepatitis by defective lipid droplet turnover due reduced organellar acidification in the lipid-droplet – autophagosome – lysosome axis.

These findings may have implications in non-alcoholic fatty liver disease (NAFLD), the increasingly prevalent form of hepatic steatosis and steatohepatitis, strongly associated with obesity and features of the metabolic syndrome, predominantly insulin resistance and diabetes mellitus type 2^{24,25}. Central to the development of NAFLD is hepatic lipid accumulation. This accumulation overwhelms the liver's capacity for storage and mitochondrial oxidation of fatty acids, leading to lipotoxicity, a crucial step in the transition of simple steatosis to NASH²⁶. The lysosomal autophagy of lipid droplets and the potential cross-talk between lysosome and autophagic regulators²⁷ may be a central factor in protecting the liver from lipotoxicity. We postulate that deciphering regulators of lipophagy by studying V-ATPase assembly defects may help future targeting and drug development for both for the common form of non-alcoholic fatty liver disease and for these rare inborn errors of metabolism.

Conclusion

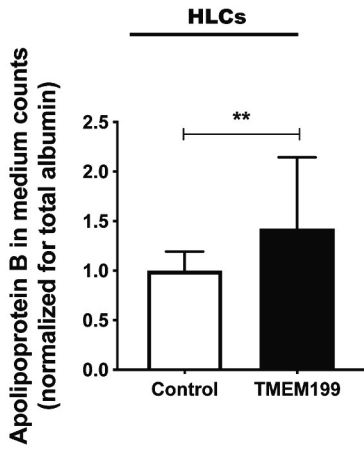
The hypercholesterolemia in TMEM199 and CCDC115 deficiency is likely due to increased secretion of apoB-containing particles. This may in turn be secondary to the hepatic steatosis observed in these patients and in the mouse model. Importantly, the hepatic steatosis may be caused by aberrant turnover of lipid droplets upon fusion with lysosomes. This can illustrate the importance of lipophagy in fatty liver disease, an understudied and largely untargeted mechanism that can potentially reduce lipotoxicity in fatty liver disease. Future studies aimed at the regulation of lipophagy may have therapeutic potential both for the common form of NAFLD and for these rare inborn errors of metabolism.

References

1. Hartley PD, Zhu G, L'Hernault SW. The spe-5 Gene Encodes a Vacuolar (H⁺)-ATPase Beta Subunit that is Required for Spermatogenesis. *Int C elegans Meet.* 2001.
2. Jansen JC, Timal S, Van Scherpenzeel M, et al. TMEM199 Deficiency is a Disorder of Golgi Homeostasis Characterized by Elevated Aminotransferases, Alkaline Phosphatase, and Cholesterol and Abnormal Glycosylation. *Am J Hum Genet.* 2016.
3. Jansen JC, Cirak S, Van Scherpenzeel M, et al. CCDC115 Deficiency Causes a Disorder of Golgi Homeostasis with Abnormal Protein Glycosylation. *Am J Hum Genet.* 2016.
4. Jansen EJR, Timal S, Ryan M, et al. ATP6AP1 deficiency causes an immunodeficiency with hepatopathy, cognitive impairment and abnormal protein glycosylation. *Nat Commun.* 2016.
5. Peanne R, Serio MC, Rujano MA, et al. Mutations in ATP6AP2 are associated to congenital disorders of glycosylation with autophagic defects. *Glycobiology.* 2017.
6. Cannata Serio M, Graham LA, Ashikov A, et al. sMutations in the V-ATPase assembly factor VMA21 cause a congenital disorder of glycosylation with autophagic liver disease. *Hepatology.* 2020.
7. Fedoseienko A, Wijers M, Wolters JC, et al. The COMMD family regulates plasma LDL levels and attenuates atherosclerosis through stabilizing the CCC complex in endosomal LDLR trafficking. *Circ Res.* 2018.
8. van den Boogert MAW, Larsen LE, Ali L, et al. N-Glycosylation Defects in Man Lower LDL-Cholesterol Through Increased LDL Receptor Expression. *Circulation.* 2019.
9. Cayo MA, Cai J, Delaforest A, et al. JD induced pluripotent stem cell-derived hepatocytes faithfully recapitulate the pathophysiology of familial hypercholesterolemia. *Hepatology.* 2012;56.
10. Cai J. Protocol for directed differentiation of human pluripotent stem cells toward a hepatocyte fate. *StemBook.* 2014.
11. Kulozik P, Jones A, Mattijssen F, et al. Hepatic deficiency in transcriptional cofactor TBL1 promotes liver steatosis and hypertriglyceridemia. *Cell Metab.* 2011.
12. Ota T, Gayet C, Ginsberg HN. Inhibition of apolipoprotein B100 secretion by lipid-induced hepatic endoplasmic reticulum stress in rodents. *J Clin Invest.* 2008.
13. Van Den Boogert MAW, Larsen LE, Ali L, et al. N-Glycosylation Defects in Humans Lower Low-Density Lipoprotein Cholesterol Through Increased Low-Density Lipoprotein Receptor Expression. *Circulation.* 2019.
14. Sorrentino V, Fouchier SW, Motazacker MM, et al. Identification of a loss-of-function inducible degrader of the low-density lipoprotein receptor variant in individuals with low circulating low-density lipoprotein. *Eur Heart J.* 2013.
15. Morelle W, Michalski JC. Analysis of protein glycosylation by mass spectrometry. *Nat Protoc.* 2007.
16. Bi X, Zhu X, Gao C, et al. Myeloid cell-specific ATP-binding cassette transporter A1 deletion has minimal impact on atherogenesis in atherogenic diet-fed low-density lipoprotein receptor knockout mice. *Arterioscler Thromb Vasc Biol.* 2014;34.
17. Jansen JC, Timal S, Van Scherpenzeel M, et al. TMEM199 Deficiency is a Disorder of Golgi Homeostasis Characterized by Elevated Aminotransferases, Alkaline Phosphatase, and Cholesterol and Abnormal Glycosylation. *Am J Hum Genet.* 2016;98.
18. Ching YL, Lesimple A, Larsen Å, Mamer O, Genest J. ESI-MS quantitation of increased sphingomyelin in Niemann-Pick disease type B HDL. *J Lipid Res.* 2005.
19. EauClaire SF, Cui S, Ma L, et al. Mutations in vacuolar H⁺-ATPase subunits lead to biliary developmental defects in zebrafish. *Dev Biol.* 2012.
20. Gordon SM, Li H, Zhu X, Shah AS, Lu LJ, Davidson WS. A comparison of the mouse and human

- lipoproteome: suitability of the mouse model for studies of human lipoproteins. *J Proteome Res.* 2015;14.
21. Olzmann JA, Carvalho P. Dynamics and functions of lipid droplets. *Nat Rev Mol Cell Biol.* 2019.
 22. Greenberg AS, Coleman RA, Kraemer FB, et al. The role of lipid droplets in metabolic disease in rodents and humans. *J Clin Invest.* 2011.
 23. Singh R, Kaushik S, Wang Y, et al. Autophagy regulates lipid metabolism. *Nature.* 2009.
 24. Hardy T, Oakley F, Anstee QM, Day CP. Nonalcoholic Fatty Liver Disease: Pathogenesis and Disease Spectrum. *Annu Rev Pathol Mech Dis.* 2016.
 25. Diehl AM, Day C. Cause, pathogenesis, and treatment of nonalcoholic steatohepatitis. *N Engl J Med.* 2017.
 26. Koliaki C, Szendroedi J, Kaul K, et al. Adaptation of Hepatic Mitochondrial Function in Humans with Non-Alcoholic Fatty Liver Is Lost in Steatohepatitis. *Cell Metab.* 2015.
 27. Zoncu R, Bar-Peled L, Efeyan A, Wang S, Sancak Y, Sabatini DM. mTORC1 senses lysosomal amino acids through an inside-out mechanism that requires the vacuolar H⁺-ATPase. *Science (80-).* 2011.

Supplemental Material.

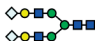
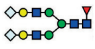
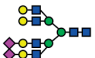
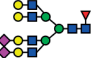
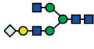


Supplemental Figure S1. ApoB secretion in TMEM199 deficient hepatocyte-like cells. Panel shows relative ³⁵S apoB secretion in medium of patient-derived hepatocyte-like cells.

Table S1 Primer sequences used for qPCR.

Human qPCR primers		
APOB	Forward	GAC GAC TTT TCT AAA TGG AAC TTC TAC
	Reverse	CTC AGT TTT GAA TAT GGT GAG TTT TT
SREB2	Reverse	GGCTCATCTTTGACCTTGC
	Forward	AGGCTGGCTTCTCTCCCTAC
HMGCS1	Forward	GCGTCCCACTCCAATGATG
	Reverse	GGCTTGGAAATAGCTCAGTTGC
HMGCR	Forward	CCA ACT ACT TCG TGT TCA TGA CTT T
	Reverse	GCT GCC AAA TTG GAC GAC
MTTP	Forward	ATA CCT GCA GCC TGA CAA CC
	Reverse	GCC AGG AAG TTT CTG ACA GC
IDOL	Forward	CGAGGACTGCCTCAACCA
	Reverse	TGCAGTCCAAAATAGTCAACTTCT
SORT1	Forward	GGC ATC ATT GTG GCC ATT
	Reverse	CAT TGA CCT TCG TCT GTG GA
LDLR	Forward	AAGGACACAGCACACAACCA
	Reverse	CCCAGAGCTTGGTGAGACAT
Mouse qPCR primers		
HMGCR	Forward	TGGTGGGACCAACCTTCTAC
	Reverse	GCCATCACACGTGCCACATAC
LDLr	Forward	GATGGCTATACCTACCCTCAA
	Reverse	TGCTCATGCCACATCGTC
PCSK9	Forward	GAAGACCGTCCCTGAT
	Reverse	GCACCCTGGATGCTGGTA
FASN	Forward	GCTGCTGTTGGAAGTCAGC
	Reverse	AGTGTTTCGTTCTCGGAGTG
SREBF1	Forward	GCAGACTCACTGCTGCTGAC
	Reverse	AGGTACTGTGGCCAAGATGG
CEBPA	Forward	AAG CAG GAT CAG TCC ATC CC
	Reverse	AGA CGC GCA CAT TCA CAT TG
LXR	Reverse	CAT CCT CTT CTC CCA GCA AG
	Forward	CAT TAC CAA GGC ACT GTC CA
CHREBP	Forward	GGCCTGGCTGGAACAGTA
	Reverse	CGAAGGGAATTCAGGACAGT

Table S2 Quantified N-glycan MALDI-TOF profiles derived from mouse plasma.

					
Wild type	42%	19%	15%	4%	0%
TMEM199 Ala7Glu	45%	19%	10%	2%	1%



CHAPTER 4

Disordered glycosylation caused by NGLY1 deficiency links cholesterol homeostasis to disease mechanism.

Julien Philippe, Marjolein A.W. van den Boogert, I-Chun Tsai, Adriaan G. Holleboom, Nicholas Katsanis

Manuscript in preparation

Abstract

Fewer than 100 individuals worldwide have been diagnosed with N-glycanase 1 (NGLY1) deficiency resulting from inherited loss of function mutations in the *NGLY1* gene. Previous clinical investigations associate NGLY1 deficiency with developmental delay, intellectual disability, alacrims, abnormal liver function, complex hyperkinetic movement disorder, and progressive neurodegeneration. These clinical features manifest with variable expressivity, though little is known regarding the underlying pathomechanism. Attempts at generating NGLY1 deficient animal models have faced challenges including sterility and embryonic lethality. Here, we develop a zebrafish model that recapitulates key clinical phenotypes of NGLY1 deficiency as a preamble to studies in pathomechanism and drug discovery. For this purpose, we used CRISPR/Cas9 to generate a stable *ngly1*^{-/-} zebrafish mutant. Phenotypic evaluation of F3 homozygous null zebrafish larvae showed several pathologies consistent with reports from human patients, including a reduction in the area of the cerebellar granule neurons and decreased liver size. Using live video tracking, we also observed decreased locomotor activity of larvae, reminiscent of those seen in patients for peripheral neuropathy, ataxia, and hypotonia. To better understand the underlying pathomechanism of the disorder, RNA sequencing of F3 larvae revealed several dysregulated pathways including an upregulation of cholesterol biosynthesis. Further analysis in mouse embryos as well as in patient fibroblasts and patient plasma supported hypocholesterolemia as a novel pathomechanism. Finally, injecting mevalonate (MVA), a precursor of cholesterol, into F3 embryos partially rescued the development of the granule cell layer and can potentially serve as therapeutic option in patients.

Introduction

In an initial cohort of 8 patients, N-glycanase 1 (NGLY1) deficiency resulting from inherited loss of function mutations in the gene *NGLY1*, presented clinically with developmental delay, hypotonia and movement disorders, with most patients also displaying alacrima, abnormal liver function, microcephaly, and diminished reflexes¹. Since then, almost 100 individuals worldwide have been diagnosed with a congenital disorder of deglycosylation (CDDG). Despite the anticipation that mutations in additional deglycosylation enzymes could contribute to this disease classification, so far *NGLY1* mutations remain the only known cause of CDDG in humans, and is designated as NGLY1-CDDG. In contrast, congenital disorders of glycosylation (CDG) have been associated with mutations in >130 genes². Notably, the spectrum of symptoms and disease severity overlap between CDDG and CDG.

One hypothesis for the lack of contributors to CDDG is that loss of function in deglycosylases is severely detrimental or even lethal. Attempts at generating knock-out animal models supports the presumption of lethality. Mouse models in a C57BL/6 background succumb to embryonic lethality³, which has shifted *in vivo* research toward viable *C. elegans*⁴ and semi-lethal and sterile *D. melanogaster*⁵ models. However, therapeutic screening on worms and flies lacks resolution of affected tissues, especially the liver and central nervous system⁶. To capture hepatic and neurodevelopmental phenotypes in a vertebrate model, we used CRISPR/Cas9 to generate a stable *ngly1*^{-/-} zebrafish. Phenotypic evaluation of F3 homozygous null zebrafish larvae showed several pathologies consistent with reports from human patients, including a reduction in the area of the cerebellar granule neurons and decreased liver size. Using live video tracking, we also observed decreased locomotor activity of larvae analogous to the peripheral neuropathy, ataxia, and hypotonia that patients experience.

Known pathomechanisms for NGLY1 deficiency center on its involvement in post-translational modifications (PTMs). In humans, PTMs account for a significant part of biological complexity with about 1 million sites in the proteome⁷. Glycosylation is one of the most common PTMs with almost 50% of the human proteome being glycosylated⁸. The specific N-linked glycosylation subtype is annotated for >590 human genes⁹ and is highly conserved in eukaryotes¹⁰. These genes play a vital role in biological functions ranging from antigen recognition¹¹ and cell-cell interaction¹² to receptor-ligand interactions¹³ and apoptosis¹⁴. In the endoplasmic reticulum (ER), N-glycosylation comprises the addition of N-linked glycans to asparagine residues within nascent polypeptides. The N-glycan-dependent ER quality control system monitors glycoprotein folding through repeated Calnexin/Calreticulin (CNX/CRT) cycles^{15,16}, and initiates the ER-associated degradation (ERAD) process upon detecting misfolding. During ERAD, these misfolded glycoproteins are ejected from the ER into the cytoplasm where NGLY1 is involved in their deglycosylation and non-lysosomal degradation through the proteasome¹⁷.

While the role of NGLY1 in ERAD is likely to impinge upon the processing of many proteins, only a few mechanisms are currently linked to NGLY1 deficiency. One known pathomechanism discovered in cell lines involves the transcription factor Nrf1¹⁸. NGLY1 initiates Nrf1 activation through ERAD, and thus Nrf1 activation has been used as a reporter assay to study NGLY1 deficiency. As a

transcription factor, Nrf1 also drives transcription of proteasome subunits downstream of its activation. As a consequence, loss of NGLY1 results in a reduced proteasome subunit production and hypersensitivity to proteasome inhibition. This pathomechanism has been used to justify therapeutic development of NGLY1 and proteasome inhibitor combinations in certain cancers where NGLY1 is elevated, rather than deficient. A second pathological axis involves the cytoplasmic glycosidases that act on free N-glycans downstream of NGLY1, such as ENGASE¹⁹ and the α -mannosidase MAN2C1²⁰. In rodents, *Engase*-deficient mice are viable and behave normally³, while *Man2c1*-deficient mice revealed major histopathological changes in the liver, the small intestine, the kidney, and in the central nervous system (CNS) with mainly neuronal and glial degeneration²¹. Strikingly, double knockout *Ngly1*^{-/-};*Engase*^{-/-} mice have mild defects and are short-lived, but viable. These mice suggest that glycoprotein processing in the cytoplasm plays a key role in the pathomechanism, but which protein targets account for the detrimental effects of MAN2C1 loss or ENGASE function, and how double knockout *Ngly1*^{-/-};*Engase*^{-/-} mice escape severe symptomology, remains unknown.

To better understand potential NGLY1 deficiency pathomechanisms, we take an agnostic, discovery-based approach using RNA sequencing of F3 *ngly1*^{-/-} larval zebrafish brain tissue. This approach revealed several dysregulated pathways including a previously unreported upregulation of cholesterol biosynthesis. We noted that the rate-limiting enzyme in synthesis of cholesterol, 3-Hydroxy-3-Methylglutaryl-CoA Reductase (HMGCR), is N-glycosylated and processed through ERAD²², and showed that it is downregulated at the protein level in our zebrafish mutant model and patient fibroblasts. We hypothesized that diminished HMGCR would lead to hypocholesterolemia in NGLY1 deficiency. Further analysis in mouse embryos as well as in patient fibroblasts and patient plasma supported a hypocholesterolemia hypothesis. Finally, we returned to our zebrafish mutants and microinjected mevalonate, a precursor of cholesterol and byproduct of the enzymatic reaction of HMGCR, into the yolk at the one-cell stage and observed a partial rescue of the cerebellar phenotype.

Results

Generation of ngly1^{-/-} zebrafish model

A tractable animal model that recapitulates the genetic, developmental and glycosylation deficiencies in NGLY1 deficient patients is essential for a thorough anatomical and biochemical evaluation of the disease mechanisms and experimental treatments. Given the advantages of the genetic and experimental attributes of zebrafish, we created an NGLY1 deficiency model in zebrafish using CRISPR/Cas9 gene editing in embryos. A guide RNA targeting exon 2 of *ngly1* induced efficient (~71%) Cas9-mediated genome editing in F0 (Suppl. Fig. 1A & 1C). Breeding the fish to F1, we collected DNA for sequencing by fin-clipping and confirmed several deletions ranging from 2bp to 16bp. We focused on a mutant bearing a 2bp deletion because we obtained the highest number of founder fish for this genetic event, which improved our chances of quickly generating a homozygous model. The 2bp deletion in exon 2 disrupts the reading frame and as a consequence truncates the peptide within the PUG (Peptide:N-glycanase/UBA or UBX-containing proteins) domain (suppl. Fig.

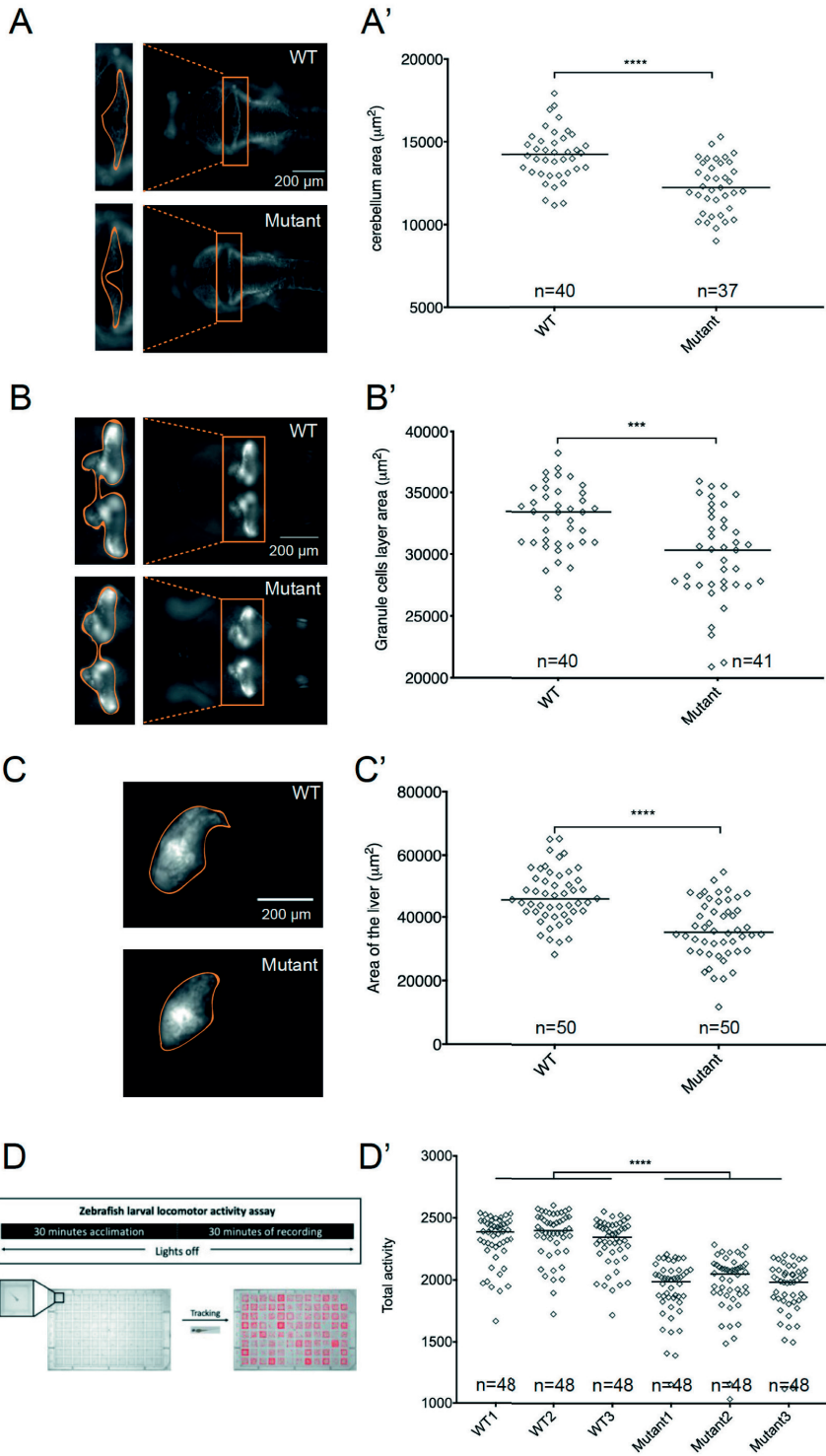


Figure 1. *ngly1*^{-/-} zebrafish larvae show several defects affecting the cerebellum, the liver, and mobility. **(A)** 3 dpf larvae of wild type and *ngly1*^{-/-} mutant were stained acetylated- α -tubulin and imaged dorsally with an AxioZoom.V16 microscope. Box and zoomed images indicate the cerebellar area region of interest (ROI) outlined in orange with ImageJ. **(A')** Quantification of the ROI area (μm^2). The area of the cerebellum is significantly reduced by 14% in *ngly1*^{-/-} mutant when compared to wild type. ****: $p < 0.0001$ (t test). **(B)** 3 dpf larvae were imaged alive dorsally on the VAST. The *ngly1*^{-/-} mutant was crossed to Tg(*neurod*:EGFP) to visualize the distribution of granule cells. Box and zoomed images indicate the granule cell layer area ROI outlined in orange with ImageJ. **(B')** Quantification of the ROI (μm^2). The area of the granule cell layer is significantly reduced by 10% in *ngly1*^{-/-} mutant when compared to wild type. ***: $p < 0.001$ (t test). **(C)** 4 dpf larvae were imaged alive laterally on the VAST. The *ngly1*^{-/-} mutant was crossed to 2CLIP reporter fish to visualize the structure of the liver. The area of the liver was outlined in orange with ImageJ. **(C')** Quantification of the liver area (μm^2). The area of the liver is significantly reduced by 12% in *ngly1*^{-/-} mutant when compared to wild type. ****: $p < 0.0001$ (t test). **(D)** Assay scheme for our behavioral assay. Individual zebrafish are placed in 96-well plate at 3dpf. The activity of zebrafish larvae was monitored by the DanioVision. **(D')** Quantification of the total locomotor activity of WT and *ngly1*^{-/-} mutant larvae across 3 different clutches. The data was analyzed with the EthoVision XT 14. ****: $p < 0.0001$ (Kruskal-Wallis test).

1B). Despite multiple in-frame ATG start codons after the mutation site, we were unable to perform Western blot analysis to assess protein production due to a lack of antibody against zebrafish Ngly1. As an alternative, we took advantage of the chemical reaction catalyzed by Ngly1 to cleave the bond between Asparagine (Asn) and the GlcNAc chain to functionally assess our *ngly1*^{-/-} zebrafish mutant. If the 2bp deletion causes the loss of Ngly1 protein, we reasoned that the byproduct of Ngly1, N-Acetylglucosaminyl-asparagine, will accumulate in the *ngly1*^{-/-} zebrafish mutant (Suppl. Fig. 2A). By carrying out mass spectrometry on tissues from juvenile fish, we were able to find a significant accumulation of N-Acetylglucosaminyl-asparagine, with a concomitant decline in N-acetylglucosamine in the liver, brain and eyes of *ngly1*^{-/-} mutants compared to wild type (suppl. Fig. 2B). This result is consistent with the clinical findings of NGLY1-deficient patients because a structurally similar metabolite is also present in the urine of patients²³. Taken together, we used CRISPR/Cas9 to introduce a 2bp deletion in zebrafish *ngly1*, leading to the loss of Ngly1.

*Phenotypic characterization of *ngly1*^{-/-} zebrafish model*

We then asked if our *ngly1*^{-/-} mutant recapitulates the clinical features seen in NGLY1 deficiency patients. To test this, we in-crossed *ngly1*^{+/-} F1 to obtain *ngly1*^{-/-} mutants. However, we did not observe any obvious morphological difference, including size, appearance and life span, in *ngly1*^{-/-} F2 mutants from the first in-cross of *ngly1*^{+/-}. To avoid potential compensation from maternal wild type *ngly1* RNA, we took advantage of adult *ngly1*^{-/-} mutants being viable and fertile and we assessed phenotypic defects at early developmental stages in F3 larvae.

In NGLY1-deficient patients, MRI imaging typically reveals a cerebellar atrophy²⁴. N-glycosylation is also known to be critical for neuronal adhesion and defects in this process especially impact the developing cerebellum²⁵. Therefore, we examined the cerebellum (Figure 1A) by performing an acetylated tubulin immunostaining of 3dpf larvae. In addition, we outcrossed our *ngly1*^{-/-} mutant to a transgenic fish where GFP is driven by the *neuroD* promoter so that we are able to examine the

cerebellar granule cells (Figure 1B). Both the cerebellar and granule cells layer areas were significantly decreased in the *ngly1*^{-/-} mutants (Figure 1A' and 1B'). Similar to several published morphants²⁶⁻²⁹, our *ngly1*^{-/-} mutant fish display fewer neuronal axons across the midline in the cerebellum, suggesting defective cerebellum integrity.

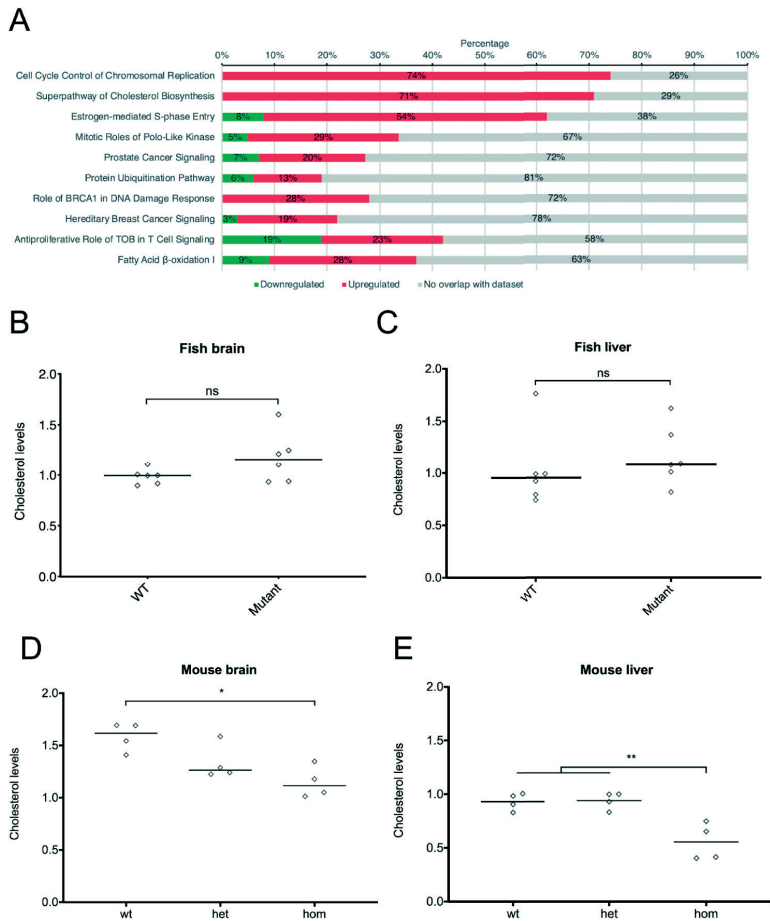


Figure 2. Loss of *ngly1/Ngly1* leads to a dysregulation of cholesterol. (A) IPA Pathway analysis of differentially expressed genes between WT and *ngly1*^{-/-} mutant zebrafish, based on RNA-Seq from pooled brain tissues (50 heads/sample; n = 4). The top ten dysregulated pathways are plotted. Downregulated pathways are green and upregulated pathways are red. The percentage indicates the percentage of genes in a specific pathway which are dysregulated (either down/up or a combination of both). **(B)** Total cholesterol measured in the brain of juvenile zebrafish. There is no statistical difference in cholesterol amount between WT and *ngly1*^{-/-} mutant (ANOVA, ns: non-significant, n = 6). **(C)** Total cholesterol measured in the liver of juvenile zebrafish. There is no statistical difference in cholesterol amount between WT and *ngly1*^{-/-} mutant (ANOVA, ns: non-significant, n = 6). **(D)** Total cholesterol measured in mouse brains. Homozygous mice display statistically significant hypocholesterolemia (ANOVA, *: p < 0.05, n = 4). **(E)** Total cholesterol measured in mouse livers. Homozygous mice display statistically significant hypocholesterolemia (ANOVA, **: p < 0.01, n = 4). ‘Het’ stands for heterozygous and ‘Hom’ stands for homozygous.

NGLY1-deficient patients also exhibit elevated liver transaminases (AST and ALT) in early childhood, and various other liver anomalies later on in development such as steatosis, liver dysmorphology, fibrosis, and hepatocellular carcinoma²⁴. Therefore, we asked whether liver morphology is affected by ablation of *ngly1*. To look at the liver, we outcrossed our *ngly1*^{-/-} mutant to the transgenic fish 2CLIP, where dsRed expression is driven by the liver-specific *fabp10* promoter. Lateral live imaging of 4dpf larvae revealed significantly decreased liver area with a rounder shape in the *ngly1*^{-/-} mutant fish (Figure 1C and C').

Finally, because NGLY1-deficient patients also exhibit hypotonic features²⁴, we used live video-tracking at 3dpf to assess fish mobility (Figure 1D). Wild-type (WT) and *ngly1*^{-/-} mutant fish are placed in a 96-well plate and their activities are recorded for 30 minutes in the dark after acclimatization. Total activity was measured by summing up the changed pixels between all the images. The total activity of the *ngly1*^{-/-} mutant fish was significantly decreased, recapitulating the hypotonia in NGLY1-deficient patients (Figure 1D'). Taken together, we have generated a zebrafish model of NGLY1 deficiency that recapitulates some of the clinical features seen in patients.

Cholesterol is dysregulated in zebrafish and mouse mutants

Given the multiplicity of neurodevelopmental phenotypes we observed, we proceeded with RNA sequencing of F3 larvae heads to better understand the molecular pathomechanisms of NGLY1 deficiency in neural tissue. For both WT and *ngly1*^{-/-} mutant zebrafish at 3dpf, we collected 4 samples comprising 50 pooled heads each. We expected that the genotype of the fish should represent the highest variance among our samples, and used principle component analysis as a quality control measure to assess this. As expected, the first principal component clearly distinguishes WT from *ngly1*^{-/-} mutant with a high variance (76.9%), while the variance captured by additional components drops off precipitously thereafter (Suppl. Fig. 4A). Next, we compared differentially expressed genes between *ngly1*^{-/-} mutants and WT fish using an FDR-corrected p-value (also called q-value) less than or equal to 0.2 to control for multiple testing and log₂ fold changes (FC) to interpret differential gene expression. With these parameters, about 46% of the transcripts are downregulated (log₂ FC<0) while 54% are upregulated (log₂ FC>0) (Suppl. Table 1). Subsequently, we generated a volcano plot to assess which of these transcripts accounted for larger effect sizes, and we identified several transcripts of large effect linked to the immune system (Suppl. Fig. 4B), which is in agreement with the literature^{30,31}. To better resolve dysregulated biological processes, we then used the Qiagen Ingenuity platform to perform pathway analysis (Figure 2A). Intriguingly, two of the top ten pathways were linked to an upregulation of lipid metabolism: cholesterol biosynthesis and fatty acid β-oxidation I. Since cholesterol is central to several neurodevelopmental disorders^{32,33} and is implicated in several neurodegenerative diseases³⁴⁻³⁶, we decided to pursue follow-up studies within this pathway. In zebrafish, the identified cholesterol pathway is composed of 31 orthologous genes. Three of these genes, lanosterol synthase (*lss*), squalene monooxygenase (*sqlea*), and mevalonate kinase (*mvk*), have the most upregulated transcripts in the superpathway for cholesterol biosynthesis from our RNA-seq data, and we

performed qPCR to validate them (Suppl. Fig. 4C). We found that the expression level of *lss*, *mvk* and *sqlea* are increased in *ngly1*^{-/-} mutant when compared to WT (1.7, 1.4 and 1.7 log fold increase respectively; Suppl. Tab. 2), consistent with the RNA-seq data. All three are key enzymes in the cholesterol synthesis downstream of the rate-limiting enzyme for the pathway, 3-Hydroxy-3-Methylglutaryl-CoA Reductase (HMGCR)³⁷. We were curious how HMGCR might be regulated in this system, and qPCR for HMGCR expression revealed decreased expression (0.48 log fold change). Collectively, these data support a dysregulation of cholesterol biosynthesis in our *ngly1*-deficient zebrafish. We next asked whether the total cholesterol level is affected in the *ngly1*^{-/-} mutant fish. Since cholesterol is mainly synthesized in the liver and in the brain, we examined cholesterol levels in juvenile *ngly1*^{-/-} mutant fish after dissecting those two organs. Despite the RNA-seq and qPCR results suggesting the dysregulation of cholesterol synthesis, we did not observe detectable significant differences of cholesterol levels in either the brain or the liver (Fig. 2B and 2C).

We considered that bulk collection of zebrafish brain and liver likely included surrounding tissues that may have confounded the signal for our cholesterol assays. Therefore, as an alternative approach, we assessed the cholesterol levels from the NGLY1^{R539X} knockout mouse. This mutation corresponds to the NGLY1^{R542X} mutation reported in a patient and results in a premature stop codon and homozygous embryonic lethality (suppl. Fig. 3A). In our hands, most of *Ngly1*^{-/-} embryos at E16.5 were underdeveloped with anemia and edema, which is consistent to previous reported findings³. To collect brain and liver tissue for western blot analysis, we timed matings and harvested the tissue from embryos before lethality at E15.5. We genotyped the embryos and confirmed a significant decrease of NGLY1 abundance between WT and *Ngly1*^{-/-} mutant in brain tissue (suppl. Fig. 3B & 3C). Both mouse brains and livers showed a significant decrease of cholesterol amount between WT and *Ngly1*^{-/-} mutant tissues (Fig. 2D and 2E), suggesting hypocholesterolemia in *Ngly1*^{-/-} embryos.

Collectively, we found that the transcriptional profile of cholesterol-related genes are affected by the ablation of *ngly1* in viable zebrafish models, and decreased cholesterol levels are observed in brain and liver tissues of embryonic lethal mouse models of *Ngly1*-deficiency.

NGLY1-deficient patients have hypocholesterolemia and patient fibroblasts show reduced intracellular cholesterol

To validate these findings, we analyzed plasma of 8 NGLY1-CDDG patients and compared them to 30 healthy age- and gender-matched controls. Patients had an average age of 9.3 ± 6.6 years and were comparable to controls: 10.2 ± 2.6 years; $p = 0.483$). As depicted in Figure 3A patients with NGLY1 deficiency have marked hypocholesterolemia with about 25% lower plasma levels of total cholesterol (128 ± 34 mg/dl in patients versus 171 ± 22 mg/dl in controls; $p = 0.0001$), LDL-cholesterol (69 ± 26 versus 87 ± 10 mg/dl; $p = 0.0024$) and HDL-cholesterol (42 ± 9 versus 57 ± 14 mg/dl; $p = 0.0062$) in patients compared to controls. This was accompanied by a 40% decrease in apolipoprotein A1 and B (92 ± 17 versus 157 ± 45 mg/dl and 43 ± 14 versus 70 ± 8 mg/dl respectively; $p = 0.0003$ and $p < 0.0001$). Plasma levels of triglycerides were not affected in NGLY1 deficiency and were comparable to controls (89 ± 47 versus 73 ± 23 mg/dl; $p = 0.1727$).

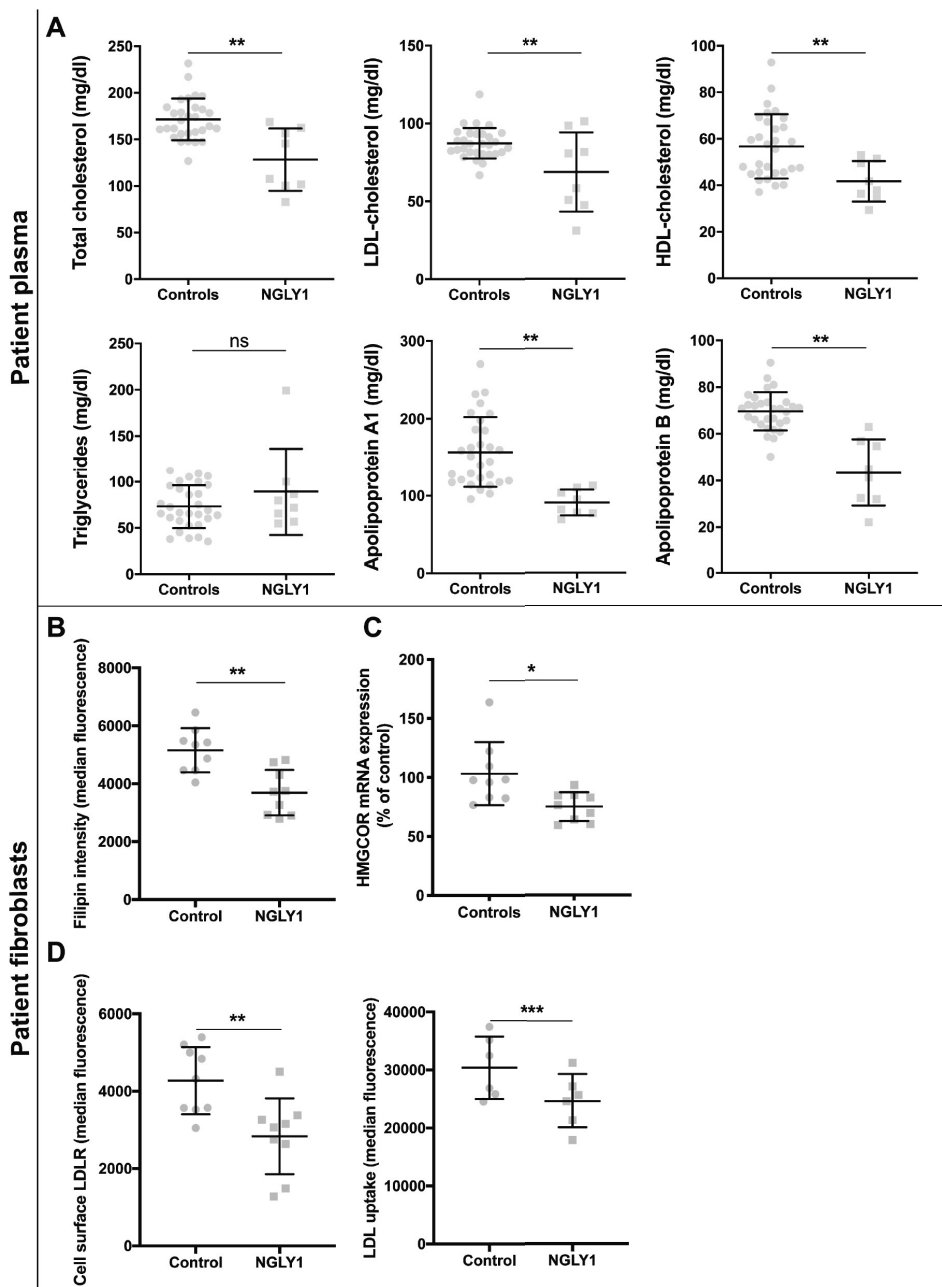


Figure 3. Cholesterol dysregulation in human in vitro models of NGLY1 deficiency. Total cholesterol, LDL-cholesterol, and HDL-cholesterol, triglycerides, apolipoprotein B and apolipoprotein A1 measured in plasma collected from human patients with NGLY1 deficiency (**A**). Human patient fibroblasts were used to measure total intracellular cholesterol (**B**), HMGCR mRNA expression (**C**), LDL receptor on the surface (left) and Dylight labeled LDL particle uptake (**D**). Statistical difference between controls and patient fibroblasts, determined by t-test (**: $p < 0.01$; ***: $p < 0.001$).

Next we assessed cellular cholesterol content with filipin staining and found a significant decrease in fibroblasts of NGLY1-deficient patients (Figure 1B; $p = 0.001$). To further substantiate this we measured mRNA expression levels of *HMGCR* in patient fibroblasts and in concordance with the zebrafish model found a significant downregulation of *HMGCR* (Figure 1C; $p = 0.010$). As decreased LDL-c levels are commonly caused by upregulation of LDL receptor, we tested this in patient fibroblasts as well. However, we found significantly decreased abundance of surface LDL receptor and concordantly diminished LDL particle uptake (Figure 3D).

*Mevalonate supplementation and HMGCR overexpression partially rescue the cerebellar granule cells' phenotype in the zebrafish *ngly1*^{-/-} mutant*

Based on evidence for conserved dysregulation of cholesterol biosynthesis among zebrafish, mice, and humans, we returned to our zebrafish model and reconsidered the role of this pathway in generating phenotypes relevant to NGLY1 deficiency in humans. Since we observed transcriptional repression of the rate-limiting enzyme for the pathway, we hypothesized that *HMGCR* expression would also be diminished at the protein level, and that the transcriptional upregulation of downstream enzymes, reflected a compensatory response in zebrafish.

We performed Western blot from heads of wild type or *ngly1*^{-/-} mutant and observed a significant decrease of *Hmgcr* abundance between WT and *ngly1*^{-/-} mutant (Fig. 4 A and A'). Both the abundance of glycosylated and un/deglycosylated *Hmgcr* are reduced in *ngly1*^{-/-} mutants, so this result suggests the downregulation of cholesterol synthesis.

If downregulation of cholesterol processing through *HMGCR* is involved in the *Ngly1* pathomechanism, we speculated that supplementing zebrafish larvae with the metabolite of *HMGCR* activity, mevalonate (MVA), may rescue some phenotypic features. In the brain, cholesterol is primarily supplied by de novo synthesis³⁸, and neurons, including granule neurons, are known to consume large quantities of cholesterol with a high turnover rate³⁹. Therefore, we focused on our *ngly1*^{-/-} NeuroD-GFP zebrafish model and injected MVA into the yolk immediately following fertilization. While *ngly1*^{-/-} mutants exhibit a decreased area of the cerebellar granule neurons, this phenotypic defect can be ameliorated by mevalonate supplementation (Figure 4 B and B', $P \leq 0.0001$). As another approach to test the downregulation of cholesterol in *Ngly1* deficiency, we overexpressed human *HMGCR* in *ngly1*^{-/-} mutants. Similar to the results of MVA treatment, *HMGCR* overexpression ameliorate significantly the defect of cerebellar granule neurons in the *ngly1*^{-/-} mutant (Figure 4C and C'; $P \leq 0.0001$). Taken together, our results revealed a reduction of *Hmgcr* abundance in *ngly1*^{-/-} mutant, suggesting the downregulation of cholesterol synthesis. More importantly, the cerebellum defect can be ameliorated by augmentation of MVA and *HMGCR* expression, opening a new therapeutic avenue for NGLY1 deficiency.

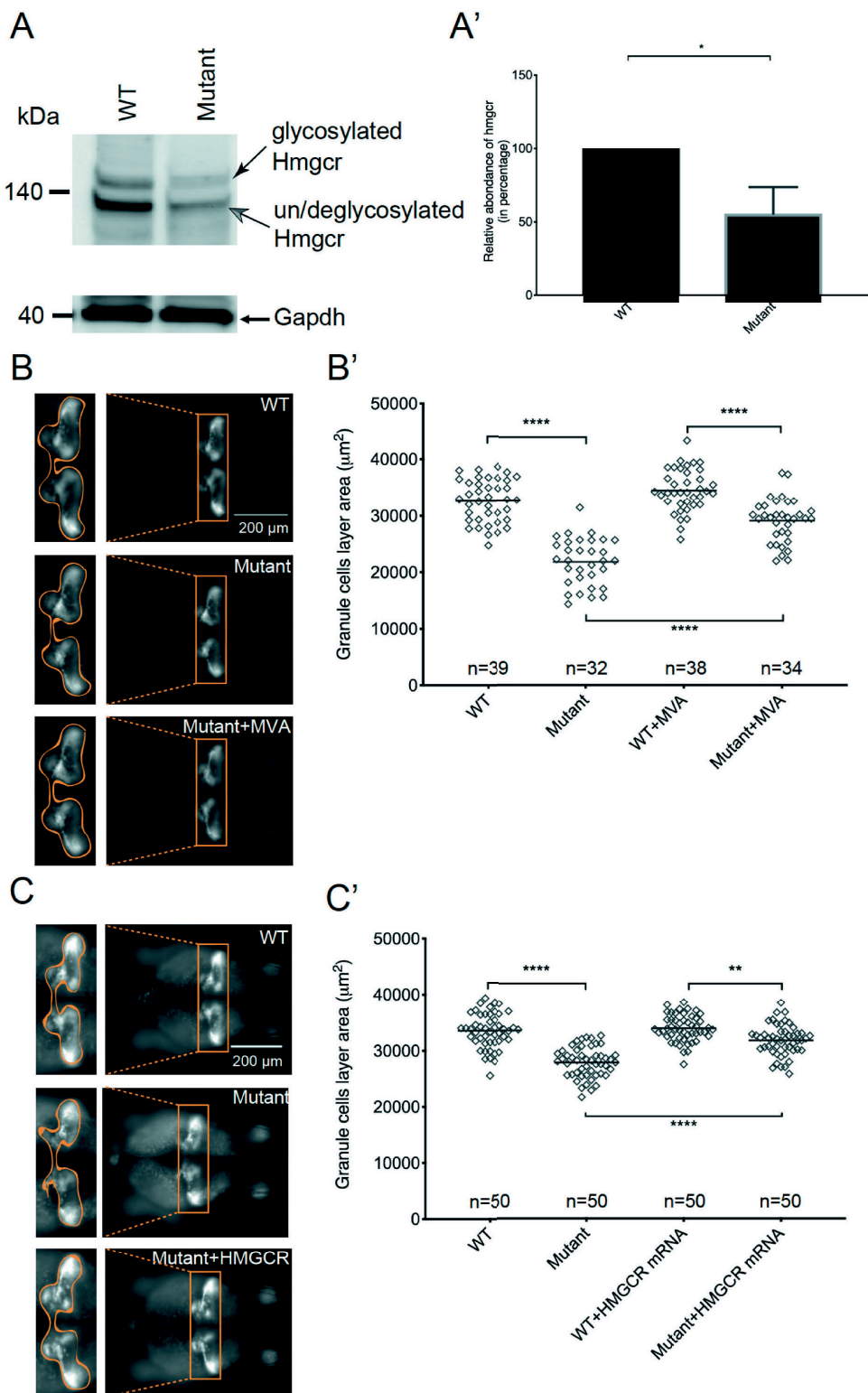


Figure 4. Mevalonate pathway, in particular Hmgcr, is critical in *ngly1* deficiency. (A) Western blot analysis for Hmgcr and Gapdh (loading control) in lysate from pooled heads of 5 dpf zebrafish. The glycosylated form of Hmgcr is indicated with a black arrow and the un/deglycosylated form of Hmgcr is indicated with a gray arrow. **(A')** Quantification of the immunoblot from 3 biological replicates reveals a decrease in abundance of Hmgcr relative to Gapdh in the *ngly1*^{-/-} mutant fish. (t test, *: $p < 0.05$) **(B)** Dorsal views of representative 3 dpf larvae imaged alive on the VAST. The larvae are on a Tg(neurod:EGFP) background to visualize the granule cell layer of the cerebellum. Box and zoomed images indicate the area of the granule cell layer outlined in orange with ImageJ. **(B')** Quantification of the granule cell layer area (μm^2). Mevalonate partially rescues the granule cells layer area of the cerebellum. (ANOVA, ****: $p < 0.0001$) **(C)** Dorsal views of representative 3 dpf larvae imaged alive on the VAST. The larvae are on a Tg(neurod:EGFP) background to visualize the granule cell layer of the cerebellum. Box and zoomed images indicate the area of the granule cell layer outlined in orange with ImageJ. **(C')** Quantification of the granule cell layer area (μm^2). HMGCR overexpression partially rescues the granule cells layer area of the cerebellum. (ANOVA, **: $p < 0.01$, ****: $p < 0.0001$)

Discussion

The only known congenital disorder of deglycosylation, NGLY1 deficiency, shares several phenotypic attributes with congenital disorders of glycosylation, including developmental delay, ataxia/hypotonia, hepatic dysfunction, and neurodevelopmental deficits including cerebellar hypoplasia². These severe phenotypes implicate (de)glycosylation as a critical cellular process during development, but the embryonic lethality of *Ngly1* deficiency in mice has limited the discovery of specific pathomechanisms explaining the phenotypes in particular organs. While the embryonic lethality in mice has been circumvented by a double knockout mutant harboring both an *Ngly1* deletion and an *Engase* deletion, these mice had negligible developmental phenotypes with no explanation for the detrimental effects of ENGASE³. In our work, we produce a viable, stable homozygous model for *ngly1* deficiency in zebrafish. We show that this model recapitulates several of the anatomical phenotypes that were not observed in double knockout mice and cannot be resolved in other invertebrate models, such as worms or flies that do not have close approximations for organs like the liver.

High rates of cholesterol synthesis are essential for early CNS development and while cholesterol biosynthesis is a well conserved⁴⁰ and extensively studied pathway⁴¹ that has been pharmacologically targeted for decades, including to treat both hepatic⁴² and neurodegenerative⁴³ diseases, it has not been a central pathomechanism linked to NGLY1-CDDG before. Hypocholesterolemia due to increased LDL particle clearance has recently been observed in patients with ALG6- and PMM2-CDG⁴⁴. However, we found no indication of increased plasma LDL clearance as an explanation for the hypocholesterolemia in NGLY1-CDDG, since in patient fibroblasts, LDL receptor abundance and LDL uptake was decreased compared to controls. However, there was a significant downregulation of the rate-limiting enzyme in cholesterol synthesis, HMGCR, in both the zebrafish model and in the patient fibroblasts.

In our work, we provide the framework for linking the downregulation of HMGCR, both transcriptionally and at protein level, as a driver of the low cholesterol levels and the neurological phenotype in *ngly1* deficiency. This framework builds on previous observations that HMGCR is both

N-glycosylated and processed through ERAD²², where *ngly1* is known to function as the initial cytosolic enzyme in the process. We overexpressed HMGCR itself and also bypassed it with mevalonate. These experiments provided partial rescue of the neurodevelopmental phenotypes in the zebrafish model. While we administered these therapies through microinjection immediately after fertilization, we are hopeful that neuroplasticity will enable us to delay therapeutic administration with similar phenotypic rescue. We also look forward to the potential for combination therapy with mevalonate supplementation and other therapeutics currently under consideration, such as GlcNAc supplementation⁴⁵ or proton pump inhibition of ENGASE⁴⁶.

An open question remains why our model is viable and fertile in the homozygous state, though we hypothesize that a compensatory transcriptional response downstream of HMGCR in the cholesterol synthesis pathway may account for some or most of our zebrafish's resiliency. Further analysis of downstream contributors to the regulation of cholesterol biosynthesis under *ngly1* deficient conditions remains an area of interest for future work.

Materials and methods

Zebrafish & Embryo Maintenance

Zebrafish studies were approved by Institutional Animal Care & Use Committee at Duke University (protocol # A154-18-06). All embryos were collected from natural matings of zebrafish adults from WT ZDR (Aquatica Biotech), TgBAC(*neurod:EGFP*)^{nl1} [18305245], or Tg(*fabp10:dsRed;ela3l:GFP*)^{gz12} [18367159] also referred as 2CLIP (2-Color Liver Insulin acinar Pancreas). Embryos were maintained in egg water until 4 days post-fertilization (dpf) at 28.5°C.

Mouse models of Ngly1^{-/-}

Mouse studies were approved by Institutional Animal Care & Use Committee at Duke University (protocol # A165-18-07). We used knockin mice generated using CRISPR/cas9 by The Jackson Laboratory (C57BL/6J-*Ngly1*^{em10Lutzy/J}Stock No: 028221). The *Ngly1*^{R539X} allele has a 1 bp replacement in the mouse N-glycanase 1 gene that encodes a nonsense mutation, resulting in a premature stop codon. This mutation corresponds to the R542X mutation identified in the patient population [24651605]. Mice heterozygous for the *Ngly1*^{R539X} allele are viable and fertile while homozygous mice are lethal.

CRISPR/Cas9 genome editing of ngly1 in zebrafish

We designed two guide (g) RNAs targeting *ngly1* (GRCz10: ENSDARG00000003205) using CHOPCHOP [27185894]: sgRNA1 (TCCTTTTACAGGCAGAAGCT) targets exon 2 and sgRNA2 (AAGGGTCACAGTGATCCAG) targets exon 7. The guides were synthesized in vitro with the GeneArt precision gRNA synthesis kit (Thermo Fisher) according to the manufacturer's instructions. In total, 100 pg of *ngly1* gRNA and 100 pg of Cas9 protein (PNA Bio) was co-injected into the cell of one-cell stage embryos. To determine targeting efficiency in F0 mutants, we harvested single embryos at 2 dpf, extracted genomic DNA and PCR amplified a region flanking the gRNA target site. To estimate the percent mosaicism, PCR products were Sanger sequenced on an ABI3730 and we used TIDE [25300484], a decomposition algorithm which reconstructs the spectrum of indels from the

sequence traces and accurately quantifies editing efficacy. To determine the genotype of F1/F2 mutants, we fin-clipped adult zebrafish, extracted genomic DNA and PCR amplified a region flanking the gRNA target site and Sanger sequenced on an ABI3730.

Rescue with overexpression and drug treatment

Rescue with mevalonate was performed as previously described [14960282] by injecting 1 nL of (R)-(-)-Mevalonolactone (68519, Sigma-Aldrich) at 500 mM into the yolk of embryos at the 1-cell stage. For overexpression, a wild-type (WT) human *HMGCR* ORF (GenBank NM_001130996.1) construct was obtained commercially (IOH21876, OriGene Technologies), subcloned into the pCS2+ vector, and sequence confirmed. WT construct was linearized with NotI, and mRNA was transcribed using the mMachine SP6 transcription kit (AM1340, Thermo Fisher). Rescue was performed by injecting 50 pg of *HMGCR* mRNA into the yolk of embryos at the 1-cell stage.

Automated zebrafish imaging

Larvae were positioned and imaged live with the Vertebrate Automated Screening Technology (VAST) platform (Union Biometrica). Larvae were anesthetized with 0.2 mg/mL Tricaine prior to being loaded into the sample reservoir. Dorsal and lateral images were acquired at a >70% minimum similarity from the pattern-recognition algorithm. Once recognized inside the 600 µm capillary of the VAST module on the microscope stage, larvae were positioned dorsally to capture a fluorescent image of the cerebellum (*neurod:EGFP*), or laterally on the left side to capture a fluorescent image of the liver (2CLIP). NIH ImageJ software was used to measure the cerebellum area and the liver size.

Whole-mount immunostaining

Embryos were fixed in Dent's solution and stained with primary antibody anti-acetylated tubulin (T7451, Sigma-Aldrich, 1:1000); and secondary detection was accomplished with Alexa Fluor goat anti-mouse IgG (A21207, Invitrogen; 1:1000) in blocking solution. Fluorescent signals were imaged on dorsally positioned larvae on a Nikon AZ100 microscope using NIS Elements AR software. Images were acquired manually on dorsally positioned larvae with an AxioZoom.V16 microscope using Zen Pro 2012 software (Zeiss). NIH ImageJ software was used to measure the area of the cerebellum.

Behavioral assays

At 3 dpf, larvae are moved to 96-well plate and maintained at a temperature of 28.5°C. The movement of the larvae was recorded using the DanioVision (Noldus B.V.) and the data was analyzed with the EthoVision XT 14 (Noldus B.V.). The acclimatization time is 30 minutes and spontaneous swimming behavior of zebrafish larvae was assessed for 30 minutes in the dark.

Tissue collection

Zebrafish larvae (3 or 5 dpf; n = 50) were decapitated to collect heads and zebrafish juveniles (2-3 months) were dissected to isolate the brain, the liver and the eyes. E15.5 mice were dissected to isolate the brain and liver. All tissues were flash frozen with dry ice. Zebrafish larvae heads were

collected at 3dpf for RNA-seq, and at 5dpf for western blot analysis and cholesterol assays. E15.5 mouse brains were processed for western blot analysis and cholesterol assay, while the livers were processed for cholesterol assay.

RNA-seq

RNA was extracted from zebrafish heads using a RNeasy micro kit (74004, Qiagen) and submitted to the Duke Center for Genomic and Computational Biology for library preparation and sequencing, as well as data analysis. Libraries were prepared from mRNA using Kapa Stranded mRNA-seq and sequenced on an Illumina NextSeq 500. RNA-seq data was processed using the TrimGalore toolkit which employs Cutadapt to trim low-quality bases and Illumina sequencing adapters from the 3' end of the reads. Only reads that were 20 nt or longer after trimming were kept for further analysis. Reads were mapped to the GRCz10v87 version of the zebrafish genome and transcriptome using the STAR RNA-seq alignment tool. Reads were kept for subsequent analysis if they mapped to a single genomic location. Gene counts were compiled using the HTSeq tool. Only genes that had at least 10 reads in any given library were used in subsequent analysis. Normalization and differential expression were carried out using the DESeq2 Bioconductor package with the R statistical programming environment. The false discovery rate was calculated to control for multiple hypothesis testing. Gene set enrichment analysis was performed to identify differentially regulated pathways and gene ontology terms for each of the comparisons performed. The list of differentially expressed genes, containing gene identifiers and corresponding expression values, was uploaded into the IPA software (Qiagen). The core analysis function included in the software was used to interpret the differentially expressed data, mainly dysregulated canonical pathways.

Real-time quantitative reverse transcription polymerase chain reaction analyses

Total RNA was isolated following the standard TRIzol (Invitrogen) protocol. cDNA was synthesized from 1 µg of total RNA using the QuantiTect kit (Qiagen). qRT-PCR was performed with Power SYBR Green PCR Master Mix (Applied Biosystems) on a 7900HT (Applied Biosystems). Real-time data were collected and analyzed with a Sequence Detection System software package version 2.3 (Applied Biosystems). Real-time qPCR data were analyzed and generated using Microsoft Excel.

Western blot analysis

To collect tissue, zebrafish larvae (5 dpf; n = 50) were decapitated and E15.5 mice were dissected to isolate the brain. Tissues were homogenized with RIPA buffer (50 mM NaCl, 1% NP40, 50 mM Tris-HCl pH 7.5, 0.1% SDS, 0.5% Na deoxycholate, 1 mM Na₃VO₄, and 1 mM NaF). Total protein concentration was determined by using the BCA Protein Assay Kit (Thermo Fisher Scientific) and 50 µg lysate per condition was subjected to 4–15% SDS-PAGE (Bio-Rad) and transferred to a PVDF membrane. Immunoblots were blocked in 5% BSA in PBS containing 0.1% Tween20 and probed with HMGR antibody (#ab214018, Abcam; 1:1000) for zebrafish tissue or Ngly1 antibody (HPA036825, Atlas Antibodies; 1:100) for mouse tissue. Blots were developed using an enhanced chemiluminescence system, Super Signal West Pico Chemiluminescent Substrate (Thermo Fisher Scientific), visualized on a ChemiDoc (Bio-Rad) and quantified by Quantity One (Bio-Rad).

Cholesterol assay

Tissues were weighted and chloroform: isopropanol: NP-40 (7:11:0.1) was added in relation to the weight (200 μ L / 10 mg) and homogenized with a pestle grinder system. The extract was transferred into a centrifuge tube and spun for 10 min at 15,000g. The organic phase was transferred into a new tube and air-dried at 50 °C to remove the chloroform. The tube was then placed under vacuum for 30 min to remove trace of organic solvent. Cholesterol levels were measured with Total Cholesterol and Cholesteryl Ester Quantification Colorimetric / Fluorometric assay kit (K603, Biovision) according to the manufacturer's protocols. The pellet was weighed to obtain the relative cholesterol content.

Human subjects

We retrieved plasma samples of 8 NGLY1-CDDG patients, courtesy of the NIH Undiagnosed Disease Program in Bethesda, Maryland, USA, and 30 healthy age- and gender-matched controls from the plasma biobank at the Amsterdam UMC, location AMC, the Netherlands. These controls were unaffected siblings of patients with dyslipidemia, without mutations in genes known to affect apoB and LDL-cholesterol (*APOB*, *LDLR* and *PCSK9*) or in *NGLY1*, from our lipid clinic with plasma stored in our blood bank.

Plasma lipids

We analyzed plasma lipids in venous blood samples collected after an overnight fast in EDTA-coated tubes. Plasma was isolated after centrifugation at 3000 RPM for 15 minutes at 4°C and stored at -80°C until further analyses.

Total cholesterol, LDL-cholesterol, HDL-cholesterol, triglycerides, apolipoprotein A-I and apolipoprotein B were measured using commercially available assays (DiaSys and WAKO) on a Selectra analyzer (Sopachem, The Netherlands).

Human cell lines and in vitro experiments

Patient fibroblasts from 3 NGLY1-CDDG patients were obtained from the NIH Undiagnosed Disease Program and two healthy control fibroblast cell lines were obtained from subjects in the biobank at our lipid clinic in Amsterdam.

Intracellular cholesterol levels were measured quantitatively with filipin staining in combination with flow cytometry as described earlier⁴⁴.

A wide qPCR screen of expression levels of important players in plasma lipid and lipoprotein metabolism was performed. Surface LDL receptor protein abundance was assessed with flow cytometry and LDL uptake with Dylight labeled LDL particles in combination with flow cytometry.⁴⁷

Statistical analysis

Data were analyzed and graphed using GraphPad Prism 8 software. Normality test was performed for each dataset and depending on the output, we used either a parametric test (unpaired t test or

Tukey multiple comparison testing following one-way analysis of variance) or a nonparametric test (Mann-Whitney test or Dunn's multiple comparison testing following Kruskal-Wallis test). P-values less than 0.05, 0.01, 0.001 and 0.0001 are summarized with *, **, *** or ****, respectively. P-values >0.05 are indicated by 'ns' (non-significant).

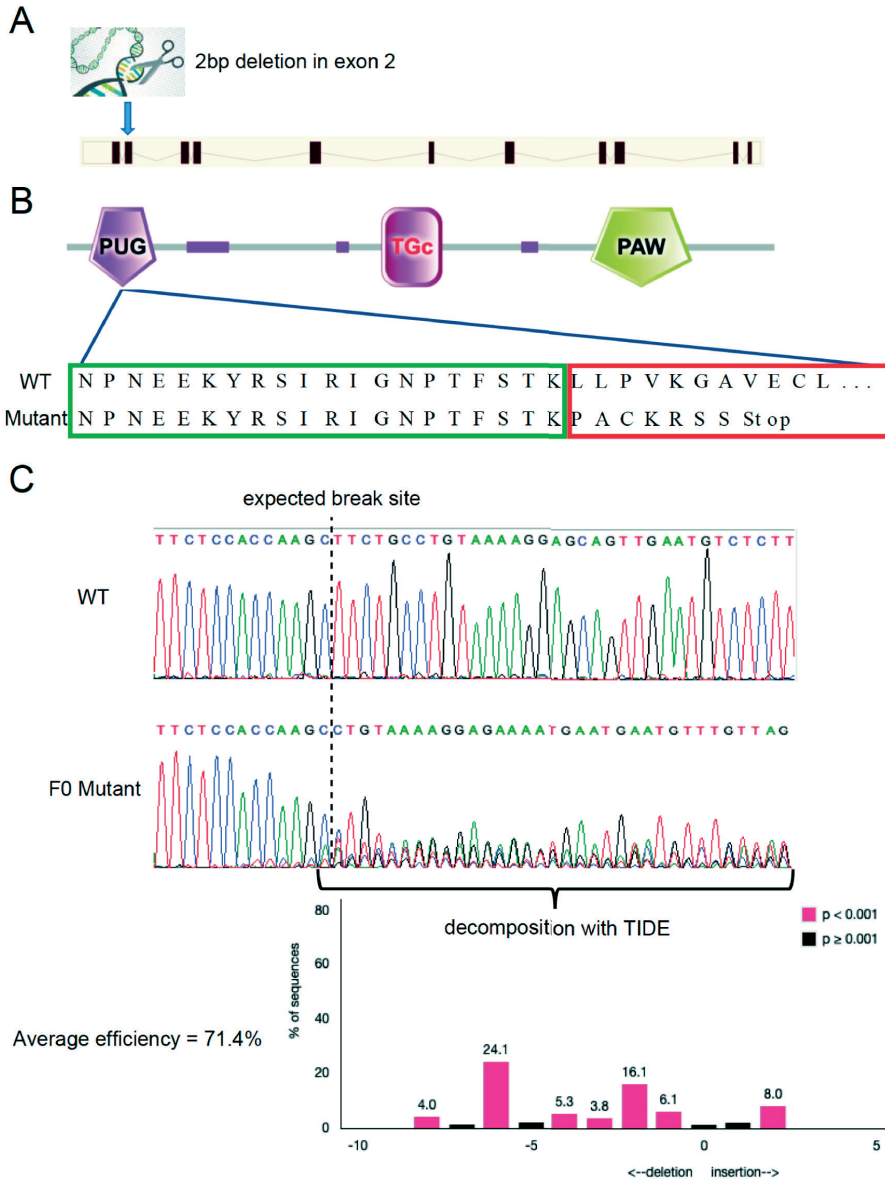
References

1. Enns, G.M., *et al.* Mutations in NGLY1 cause an inherited disorder of the endoplasmic reticulum-associated degradation pathway. *Genet Med* **16**, 751-758 (2014).
2. Chang, I.J., He, M. & Lam, C.T. Congenital disorders of glycosylation. *Ann Transl Med* **6**, 477 (2018).
3. Fujihira, H., *et al.* Lethality of mice bearing a knockout of the Ngly1-gene is partially rescued by the additional deletion of the Engase gene. *PLoS Genet* **13**, e1006696 (2017).
4. Habibi-Babadi, N., Su, A., de Carvalho, C.E. & Colavita, A. The N-glycanase png-1 acts to limit axon branching during organ formation in *Caenorhabditis elegans*. *J Neurosci* **30**, 1766-1776 (2010).
5. Funakoshi, Y., *et al.* Evidence for an essential deglycosylation-independent activity of PNGase in *Drosophila melanogaster*. *PLoS One* **5**, e10545 (2010).
6. Tickotsky-Moskovitz, N. New perspectives on the mutated NGLY1 enigma. *Med Hypotheses* **85**, 584-585 (2015).
7. Devabhaktuni, A., *et al.* TagGraph reveals vast protein modification landscapes from large tandem mass spectrometry datasets. *Nat Biotechnol* **37**, 469-479 (2019).
8. Akmal, M.A., Rasool, N. & Khan, Y.D. Prediction of N-linked glycosylation sites using position relative features and statistical moments. *PLoS One* **12**, e0181966 (2017).
9. (2019). UniProt: a worldwide hub of protein knowledge. *Nucleic Acids Res.* **47**, D506–D515.
10. Zielinska, D.F., Gnad, F., Schropp, K., Wisniewski, J.R. & Mann, M. Mapping N-glycosylation sites across seven evolutionarily distant species reveals a divergent substrate proteome despite a common core machinery. *Mol Cell* **46**, 542-548 (2012).
11. Ryan, S.O. & Cobb, B.A. Roles for major histocompatibility complex glycosylation in immune function. *Semin Immunopathol* **34**, 425-441 (2012).
12. Gu, J. & Taniguchi, N. Potential of N-glycan in cell adhesion and migration as either a positive or negative regulator. *Cell Adh Migr* **2**, 243-245 (2008).
13. Arshad, N., Ballal, S. & Visweswariah, S.S. Site-specific N-linked glycosylation of receptor guanylyl cyclase C regulates ligand binding, ligand-mediated activation and interaction with vesicular integral membrane protein 36, VIP36. *J Biol Chem* **288**, 3907-3917 (2013).
14. Zhang, D., *et al.* The role of epithelial cell adhesion molecule N-glycosylation on apoptosis in breast cancer cells. *Tumour Biol* **39**, 1010428317695973 (2017).
15. Lamriben, L., Graham, J.B., Adams, B.M. & Hebert, D.N. N-Glycan-based ER Molecular Chaperone and Protein Quality Control System: The Calnexin Binding Cycle. *Traffic* **17**, 308-326 (2016).
16. Caramelo, J.J. & Parodi, A.J. Getting in and out from calnexin/calreticulin cycles. *J Biol Chem* **283**, 10221-10225 (2008).
17. Suzuki, T., Huang, C. & Fujihira, H. The cytoplasmic peptide:N-glycanase (NGLY1) - Structure, expression and cellular functions. *Gene* **577**, 1-7 (2016).
18. Tomlin, F.M., *et al.* Inhibition of NGLY1 Inactivates the Transcription Factor Nrf1 and Potentiates Proteasome Inhibitor Cytotoxicity. *ACS Cent Sci* **3**, 1143-1155 (2017).
19. Suzuki, T., *et al.* Endo-beta-N-acetylglucosaminidase, an enzyme involved in processing of free oligosaccharides in the cytosol. *Proc Natl Acad Sci U S A* **99**, 9691-9696 (2002).
20. Suzuki, T., *et al.* Man2C1, an alpha-mannosidase, is involved in the trimming of free oligosaccharides in the cytosol. *Biochem J* **400**, 33-41 (2006).
21. Paciotti, S., *et al.* Accumulation of free oligosaccharides and tissue damage in cytosolic alpha-mannosidase (Man2c1)-deficient mice. *J Biol Chem* **289**, 9611-9622 (2014).
22. Leichner, G.S., Avner, R., Harats, D. & Roitelman, J. Dislocation of HMG-CoA reductase and Insig-1, two polytopic endoplasmic reticulum proteins, en route to proteasomal degradation. *Mol Biol Cell*

- 20, 3330-3341 (2009).
23. Hall, P.L., *et al.* Urine oligosaccharide screening by MALDI-TOF for the identification of NGLY1 deficiency. *Mol Genet Metab* **124**, 82-86 (2018).
 24. Lam, C., *et al.* Prospective phenotyping of NGLY1-CDDG, the first congenital disorder of deglycosylation. *Genet Med* **19**, 160-168 (2017).
 25. Medina-Cano, D., *et al.* High N-glycan multiplicity is critical for neuronal adhesion and sensitizes the developing cerebellum to N-glycosylation defect. *Elife* **7**(2018).
 26. Anttonen, A.K., *et al.* ZNHIT3 is defective in PEHO syndrome, a severe encephalopathy with cerebellar granule neuron loss. *Brain* **140**, 1267-1279 (2017).
 27. Reijnders, M.R.F., *et al.* RAC1 Missense Mutations in Developmental Disorders with Diverse Phenotypes. *Am J Hum Genet* **101**, 466-477 (2017).
 28. Muto, V., *et al.* Biallelic SQSTM1 mutations in early-onset, variably progressive neurodegeneration. *Neurology* **91**, e319-e330 (2018).
 29. Spataro, R., *et al.* Mutations in ATP13A2 (PARK9) are associated with an amyotrophic lateral sclerosis-like phenotype, implicating this locus in further phenotypic expansion. *Hum Genomics* **13**, 19 (2019).
 30. Kario, E., Tirosh, B., Ploegh, H.L. & Navon, A. N-linked glycosylation does not impair proteasomal degradation but affects class I major histocompatibility complex presentation. *J Biol Chem* **283**, 244-254 (2008).
 31. Yang, K., Huang, R., Fujihira, H., Suzuki, T. & Yan, N. N-glycanase NGLY1 regulates mitochondrial homeostasis and inflammation through NRF1. *J Exp Med* **215**, 2600-2616 (2018).
 32. Carstea, E.D., *et al.* Niemann-Pick C1 disease gene: homology to mediators of cholesterol homeostasis. *Science* **277**, 228-231 (1997).
 33. Cunniff, C., Kratz, L.E., Moser, A., Natowicz, M.R. & Kelley, R.I. Clinical and biochemical spectrum of patients with RSH/Smith-Lemli-Opitz syndrome and abnormal cholesterol metabolism. *Am J Med Genet* **68**, 263-269 (1997).
 34. Di Paolo, G. & Kim, T.W. Linking lipids to Alzheimer's disease: cholesterol and beyond. *Nat Rev Neurosci* **12**, 284-296 (2011).
 35. Rozani, V., *et al.* Higher serum cholesterol and decreased Parkinson's disease risk: A statin-free cohort study. *Mov Disord* **33**, 1298-1305 (2018).
 36. Leoni, V. & Caccia, C. The impairment of cholesterol metabolism in Huntington disease. *Biochim Biophys Acta* **1851**, 1095-1105 (2015).
 37. Cerqueira, N.M., *et al.* Cholesterol Biosynthesis: A Mechanistic Overview. *Biochemistry* **55**, 5483-5506 (2016).
 38. Jeske, D.J. & Dietschy, J.M. Regulation of rates of cholesterol synthesis in vivo in the liver and carcass of the rat measured using [3H]water. *J Lipid Res* **21**, 364-376 (1980).
 39. Martin, M.G., Pfrieger, F. & Dotti, C.G. Cholesterol in brain disease: sometimes determinant and frequently implicated. *EMBO Rep* **15**, 1036-1052 (2014).
 40. Zhang, T., *et al.* Evolution of the cholesterol biosynthesis pathway in animals. *Mol Biol Evol* (2019).
 41. Endo, A. A historical perspective on the discovery of statins. *Proc Jpn Acad Ser B Phys Biol Sci* **86**, 484-493 (2010).
 42. Arvind, A., Osganian, S.A., Cohen, D.E. & Corey, K.E. Lipid and Lipoprotein Metabolism in Liver Disease. in *Endotext* (eds Feingold, K.R., *et al.*) (South Dartmouth (MA), 2000).
 43. Anchisi, L., Dessi, S., Pani, A. & Mandas, A. Cholesterol homeostasis: a key to prevent or slow down neurodegeneration. *Front Physiol* **3**, 486 (2012).
 44. van den Boogert, M.A.W., *et al.* N-Glycosylation Defects in Humans Lower Low-Density Lipoprotein

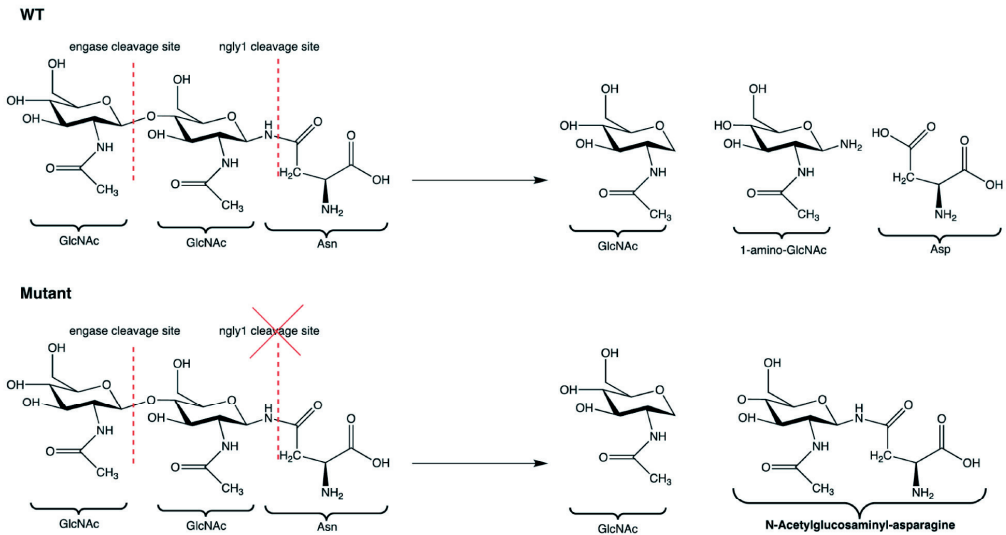
- Cholesterol Through Increased Low-Density Lipoprotein Receptor Expression. *Circulation* **140**, 280-292 (2019).
45. Owings, K.G., Lowry, J.B., Bi, Y., Might, M. & Chow, C.Y. Transcriptome and functional analysis in a *Drosophila* model of NGLY1 deficiency provides insight into therapeutic approaches. *Hum Mol Genet* **27**, 1055-1066 (2018).
 46. Bi, Y., Might, M., Vankayalapati, H. & Kuberan, B. Repurposing of Proton Pump Inhibitors as first identified small molecule inhibitors of endo-beta-N-acetylglucosaminidase (ENGase) for the treatment of NGLY1 deficiency, a rare genetic disease. *Bioorg Med Chem Lett* **27**, 2962-2966 (2017).
 47. Sorrentino, V., *et al.* Identification of a loss-of-function inducible degrader of the low-density lipoprotein receptor variant in individuals with low circulating low-density lipoprotein. *Eur Heart J* **34**, 1292-1297 (2013).

Supplementary material.

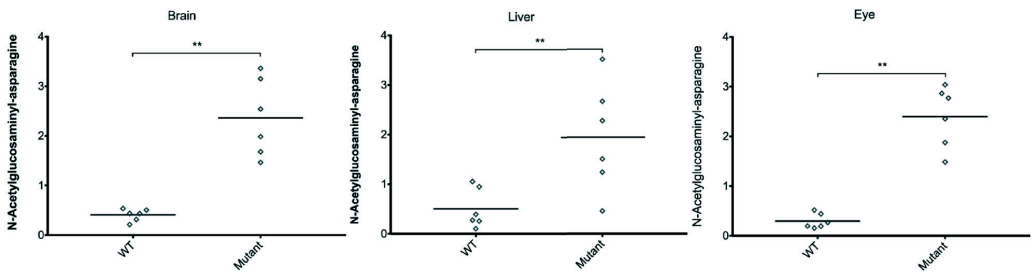


Supplementary Figure 1. Generation and molecular characterization of *ngly1*^{-/-} zebrafish stable mutant. (A) Schematic showing the generation of the *ngly1*^{-/-} mutant fish with CRISPR/Cas9 system. The 2bp deletion lies in exon 2 of *ngly1*. (B) Schematic showing *ngly1* structure and protein domains. The mutation lies in the PUG domain and is predicted to disrupt the reading frame leading to a null allele. (C) Schematic displaying the CRISPR efficiency assessed by TIDE. We sequenced PCR product from WT and F0 mutants, and the efficiency was determined to be 71%.

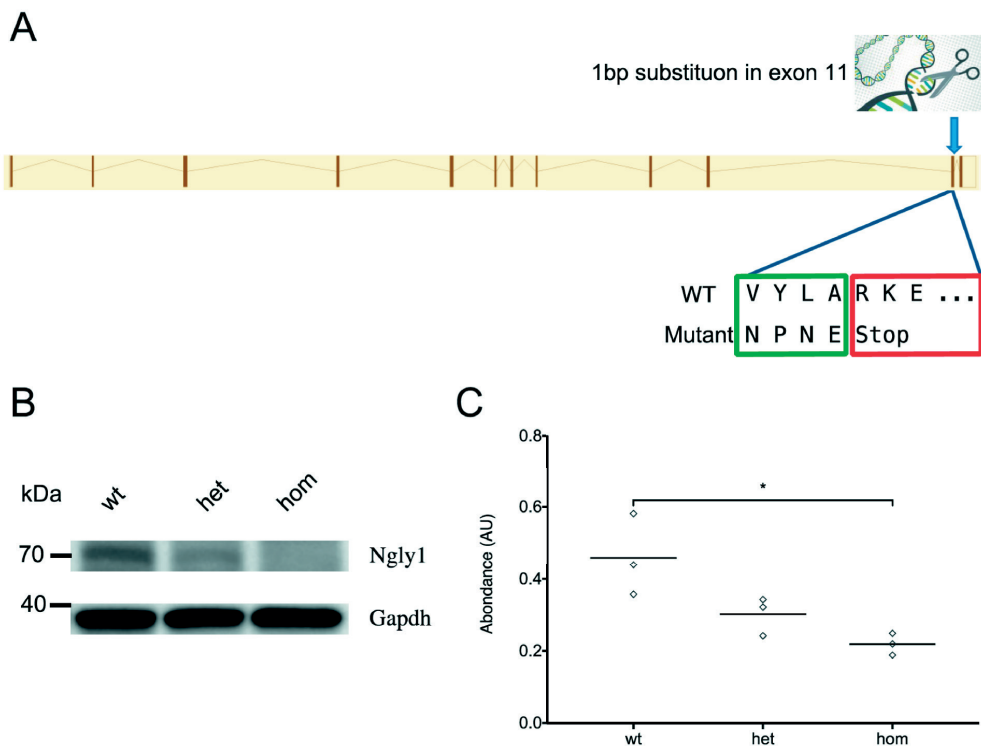
A



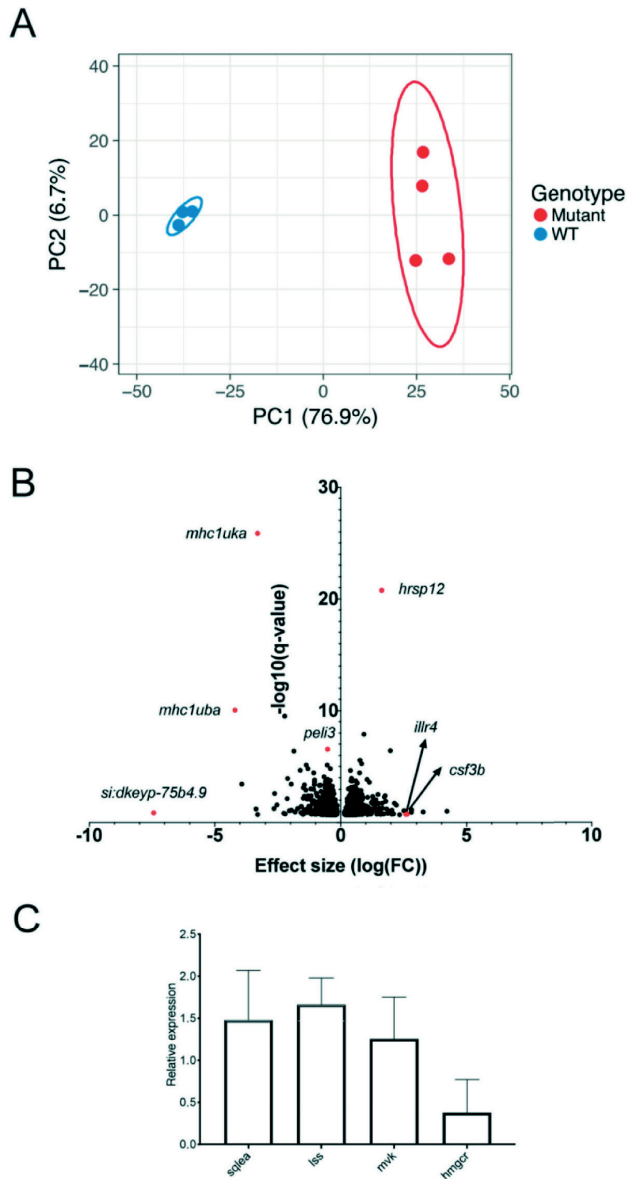
B



Supplementary Figure 2. Biochemical characterization of *ngly1*^{-/-} zebrafish stable mutants. (A) Enzymatic reaction catalyzed by *ngly1* and *engase*. The absence of *ngly1* should lead to accumulation of N-Acetylglucosaminyl-asparagine in the *ngly1*^{-/-} mutant. **(B)** Quantification of N-Acetylglucosaminyl-asparagine in different tissues of juvenile fish by mass spectroscopy. N-Acetylglucosaminyl-asparagine is accumulating significantly in *Ngly1*-KO tissues (liver, brain and eyes) in comparison to their WT counterpart. (Mann-Whitney test, **: $p < 0.01$, $n = 6$)



Supplementary Figure 3. Molecular characterization of a *Ngly1*^{-/-} mouse mutant. (A) Schematic showing the generation of the knock-in mouse with CRISPR/Cas9 system. The 1bp substitution in exon 11 of *Ngly1* leads to a premature stop codon. **(B)** Western blot analysis for the level of NGLY1 and GAPDH (loading control) using brain lysates from E15.5 mice. **(C)** Quantification of the immunoblot from 3 biological replicates revealed a significant decrease in abundance of NGLY1 relative to GAPDH in the homozygous mouse. (ANOVA, *: $p < 0.05$, $n = 3$). AU, arbitrary units.



Supplementary Figure 4. Transcriptional analysis of *ngly1*^{-/-} zebrafish stable mutants. (A) Principle Component (PC) analysis of RNA-seq data generated from control and *ngly1*^{-/-} zebrafish heads (pooled from 50 individuals, n = 4). Wild type and *ngly1*^{-/-} mutant are separated into two distinct groups by genotype on PC1, which explains 76% of the variance in the dataset. Wild type fish are shown with blue circles, *ngly1*^{-/-} mutants are shown in red circles. **(B)** Volcano plot obtained from DESeq2 analysis of WT and *ngly1*^{-/-} mutant fish. Red dots highlight transcripts previously linked to the immune system. **(C)** Key enzymes of the cholesterol synthesis pathway are dysregulated by qPCR. The error bar is the standard error of the mean.

PART II

Other roles for glycosylation in lipoprotein metabolism





CHAPTER 5

Common gene variants in *ASGR1* gene locus associate with reduced cardiovascular risk in absence of pleiotropic effects.

Lubna Ali, Arjen J. Cupido, Maaïke Rijkers, G. Kees Hovingh, Adriaan G. Holleboom,
Geesje M. Dallinga-Thie, Erik S. G. Stroes, Marjolein A.W. van den Boogert

Atherosclerosis (2020)

Introduction

Atherogenesis and eventually atherosclerotic plaque rupture occurs as a result of the intricate interplay between lipids and multiple other pathways, comprising inflammation and coagulation[1, 2]. The cornerstone of the treatment in cardiovascular risk reduction is intensive low-density lipoprotein cholesterol (LDLc) lowering by statins. Despite intensive statin treatment, patients with established cardiovascular disease (CVD) are often left with residual risk. This underscores the need for novel effective lipid lowering therapies. Human genetic studies in carriers of rare variants or in Mendelian randomization studies have led to potent alternative treatments. Proprotein convertase subtilisin/kexin type 9 (PCSK9) inhibitors lower LDL-c and atherosclerotic CVD risk and have been approved for the treatment of patients not on target lipid levels. Furthermore, angiopoietin-like protein 3 (ANGPTL3) inhibitors have been shown to lower triglycerides (TG) and increase high-density lipoprotein cholesterol (HDLc) and are being evaluated in clinical outcome trials.

It has been suggested that for every 1 mmol/l LDLc reduction causes a 21% relative risk reduction[8]. However, numerous studies have emphasized that genetic, and thus life-long, lower LDLc levels conveys substantially larger coronary artery disease (CAD) risk reductions compared to that reported in short-term LDLc intervention studies[9, 10]. In addition, there is a large consistency in the normalized LDLc long term exposure due to different variants in genes involved in cholesterol homeostasis, which is illustrated by the fact that a 10 mg/dl LDLc lowering using a gene risk score (GRS) in *PCSK9* equals the observed effect of a GRS in 3-hydroxy-3-methylglutaryl-CoA-reductase (*HMGCR*) if equally normalized to 10 mg/dl[11].

Nioi et al described a genetic variant in asialoglycoprotein receptor 1 (*ASGR1*), the major subunit of the asialoglycoprotein receptor (ASGPR), which conveyed a reduction in plasma LDLc levels of 12.5 mg/dl, corresponding to a 15.3 mg/dl reduction in non-high density lipoprotein cholesterol (non-HDLc) with a concomitant 34% decrease in CAD-risk compared to controls[12]. The disproportionality of the large cardiovascular benefit compared to the very modest LDLc reduction has led to speculations concerning additional non-lipid, anti-atherogenic effects of the *ASGR1* variant.

ASGPR is a highly conserved transmembrane receptor consisting of two subunits, *ASGR1* and *ASGR2*[13]. ASGPR is mainly expressed in the liver on the basolateral membrane of hepatocytes [14], where it facilitates the uptake of circulating glycoproteins such as alkaline phosphatase (ALP) and vitamin B12 [15]. Nioi et al.[12] observed an increase in alkaline phosphatase in carriers of the *ASGR1*del12 variant, suggesting that this variant results in decreased ASGPR function and subsequently decreased clearance of circulating desialylated glycoproteins. In our study, we used alkaline phosphatase and vitamin B12 as a readout for circulating glycoproteins and ASGPR function. More specifically, ASGPR binds the terminal N-acetyl-galactosamine or galactose units that become available upon cleavage of terminal sialic acid residues through sialidase activity. (Patho)physiological conditions such as infection and aging can induce desialylation and lead to the formation of an acetyl-galactosamine terminus with a greatly enhanced affinity for ASGPR binding

[16, 17]. Blood platelets are coated with sialylated glycoproteins, such as P-selectin (CD62P) and glycoprotein-Ib-alpha (GPIb α), which are known platelet activation markers [18]. Following desialylation, these platelets have been deemed to undergo rapid hepatic clearance via the ASGPR-mediated pathway [19, 20]. Hepatic platelet clearance by ASGPR has been shown to stimulate thrombopoietin secretion leading to novel platelet synthesis [21]. Reduced ASGPR function may disrupt this cycle, leading to a lower rate of platelet removal and consequently a reduced synthesis of new platelets. Conceptually, one could hypothesize that the observed magnitude of clinical benefit of the previously described *ASGR1del12* variant is in part mediated by an effect on thrombocyte count and function.

In the present study, we evaluated whether the potential pleiotropic effects of the *ASGR1del12* variant are explained by platelet number and function. We evaluated this in heterozygous carriers of the *ASGR1del12* variant and compared the results with wildtype controls. Additionally, we set out to validate the association of common genetic variants in the *ASGR1* gene locus with changes in plasma lipids as well as cardiovascular outcome in the UK-Biobank and the CARDIoGRAMplusC4D, using Mendelian randomization (MR).

Material and Methods

Participants for in vitro analyses

The Nijmegen Biomedical Study (Radboud University Medical Center, Nijmegen, The Netherlands) is a population-based cohort study comprising 5645 individuals randomly selected from the Nijmegen registry of municipality with a mean age of 56 years [22]. The minor allele frequency (MAF) of the *ASGR1del12* variant (c.283+33_284-36del; NM_0016771) has been analyzed previously and is 0.005[12], meaning that 28 subjects were heterozygous carrier of the *ASGR1del12* mutation. For the in vitro study twelve heterozygote carriers of the *ASGR1del12* variant and ten wild-type controls were willing to participate. This study was approved by the local Institutional Review Board of the Radboud University Medical Center. The study was conducted in accordance with the Declaration of Helsinki and written informed consent was obtained from all individuals.

After an overnight fast, the subjects visited the metabolic ward for blood withdrawal and assessment of anthropometric measurements. Blood samples were obtained in EDTA-containing tubes (BD, Franklin lakes, NJ, USA). Plasma was obtained after centrifugation at 3,000 rpm for 20 min at 4 °C and stored at -80°C for further analysis. Plasma levels of total cholesterol (TC), high-density lipoprotein cholesterol (HDLc), triglycerides (TG), apolipoprotein B (apoB), vitamin B12 and alkaline phosphate were analyzed using commercially available assays (Roche) on a Roche bioanalyzer. Plasma LDLc was calculated using the Friedewald equation [23]. Platelet counts, alkaline phosphatase and vitamin B12 were measured in the core clinical chemistry facility of the AMC.

Platelet analyses

Platelets were isolated from blood collected in citrate tubes (BD, Franklin lakes, NJ, USA). Platelet rich plasma (PRP) was obtained after centrifugation for 20 min at 120 g. 10% citrate buffer (85mM trisodium citrate, 71mM citric acid, 11mM glucose) and 5.9 nM prostaglandin E1 (PGE1) was added

to the platelet rich plasma, and a platelet pellet was obtained upon centrifugation for 8 min at 2,000g.

For platelet activation markers non-washed platelets were diluted in 2×10^6 cells/mL in storage buffer (SB: 10mM HEPES, 140mM NaCl, 3mM KCl, 0.5mM MgCl₂, 10mM glucose and 0.5mM NaHCO₃, pH 7.4) and incubated with PE-conjugated mouse anti-human CD62P (1:400, clone AK-4, BD, BD Bioscience) and FITC-conjugated mouse anti-human CD42b (GPIb α ; 1:100, clone SZ2, Beckman Coulter, Marseille, France). For lectin staining, washed platelets were resuspended in SB in a concentration of 2×10^6 platelets/mL and incubated without or with 50mU neuramidase from *Vibrio Cholerae* (Merck, KGaA, Darmstadt, Germany) or 1000mU neuramidase from *Clostridium perfringens* (Merck) for 10 min at 37°C. Cells were stained using the following lectins: 1 μ g/mL FITC-conjugated Succinyl Triticum vulgare lectin from wheat germ (s-WGA; Ey Laboratories, San Mateo, CA, USA), 2 μ g/mL FITC-conjugated Erythrina cristagalli lectin from coral tree (ECL; Ey Laboratories, San Mateo, CA, USA) and 2 μ g/mL Alexa647-conjugated Wheat Germ Agglutinin (WGA; Life Technologies, Eugene, OR, USA). Platelets were incubated with the antibody or lectins for 20 min at room temperature or 37°C followed by analysis on a flow cytometer (FACS Canto II with HTS, Becton Dickinson). Flow cytometer data were analyzed using FlowJo software, version 10.0.7. Data are represented as either percentage of positive platelets (based on isotype control) or mean fluorescent intensity (MFI). All analyses were performed in duplicate [24].

Platelet aggregation analysis

Platelets were resuspended in 5 mL 360 mM citric acid, 103 mM NaCl, 5mM KCl, 5mM EDTA, 56 mM glucose, pH 6.5 containing 0.1% PGE1. Subsequently cells were stained with 20 μ M Calcein green-AM (Thermo Fisher Scientific, Burlington, ONT, Canada) or with 10 μ L Calcein violet-AM (Biolegend, San Diego, CA) as described [24]. Calcein-green stained platelets and calcein-violet stained platelets were mixed 1:1. Platelet aggregation was induced with 5 μ M proteinase-activated receptor 1 activating peptide (PAR1-AP) (Peptides international, Louisville, KY, USA), 20 μ M adenosine diphosphate (ADP) (Hart Biologicals, Hartlepool, UK) or 10 μ g/mL Collagen (Chronolog Corp, Havertown, PA, USA) for 5, 10, 30 and 60 min, respectively. The reaction was stopped by adding 2% paraformaldehyde and aggregation was analyzed using flow cytometry (FACS Canto II with HTS, Becton Dickinson). Events positive for both calcein green and calcein violet were considered to be aggregates [25]. Flow cytometer data were analyzed using FlowJo software, version 10.0.7.

Genetic risk score in large population cohorts

To validate the results by Nioi et al[12], we performed a two-sample Mendelian randomization study. We used summary data on genetic variants and their association with plasma lipids and alkaline phosphatase levels in the UK Biobank dataset including 343,621 participants (<https://www.naellab.is/uk-biobank>). The association of common variants in the *ASGR1* locus, as identified in the UK biobank, with CVD was assessed using summary data from the CARDIoGRAMplus4D meta-analysis, including 60,801 CAD cases and 123,504 control subjects [26]. Five hundred two European samples available from the 1000 Genomes phase 3 dataset were used to assess the between-variant correlation for all genetic variants included in the gene scores [27].

Common variants in and 100kb on both sides of the *ASGR1* locus that are associated with LDLc at a threshold of $p < 5.0 \times 10^{-8}$, have a minor allele frequency > 0.01 and are in low linkage disequilibrium (LD) with each other ($R^2 < 0.3$) were used for the *ASGR1* GRS. To compare the results of the *ASGR1* gene score, we constructed gene scores for *HMGCR* (the proxy of statins), Nieman Pick Disease Like Intracellular Cholesterol Transporter (*NPC1L1*, the proxy of ezetimibe), *PCSK9* (the proxy for PCSK9 inhibitors) and low-density lipoprotein receptor (*LDLR*) using variants that have been described in detail before [28, 29]. Six variants were included in the *HMGCR* score, five in the *NPC1L1* score, seven in the *PCSK9* score, and three in the *LDLR* score. Effect sizes of the included variants and the correlation matrices between the genetic variants are included in the supplementary appendix. The association of these gene scores with CVD risk was determined using the CARDioGRAMplusC4D dataset. The primary outcome was coronary artery disease as defined by CARDIOGRAMplusC4D. The secondary outcome was myocardial infarction (MI).

Statistical Analysis

All data are expressed as mean \pm standard deviation. All experiments represent a minimum of three replications unless otherwise stated. Student's T-test statistics or non-parametric Mann-Whitney U tests were performed to compare the groups as indicated in each separate experiment. All statistical analyses were performed using GraphPad Prism Software, version 8. A value of $p < 0.05$ was considered statistically significant.

The two sample MR study was performed using the inverse-variance weighted method, while taking the remaining correlation between the variants included in the gene scores into account [30]. Results were scaled to 10mg/dl reduction in LDLc to allow comparison between the gene score effects. Results were visualized using the R package 'meta'. All analyses were conducted using R version 3.6.1 (the R Foundation for Statistical Computing).

Results

In vitro platelet studies

The baseline characteristics of the subjects are shown in Table 1. There were no major differences in plasma lipids between the two groups. Plasma alkaline phosphatase levels – used as a readout for circulating desialylated glycoproteins and thus an indirect measure of ASGPR function – were significantly higher in heterozygous *ASGR1del12* carriers as compared to controls (89.4 ± 2.2 versus 64.1 ± 1.6 U/l; $p < 0.05$), whereas plasma vitamin B12 levels were comparable. There was no significant difference in platelet count in the *ASGR1del12* carriers compared to platelet count in control subjects.

The expression of activation marker CD62P on the platelet membrane from *ASGR1del12* carriers showed a numerical, but not statistically significant lower abundance on platelets from *ASGR1del12* carriers ($p = 0.18$; Figure 1A). The expression of GPIb α was similar in both groups (ns; Figure 1B).

Table 1 Biochemical characteristics of the study population

	Controls (n=10)	ASGR1del12 (n=12)	p-value
Sex (% female)	40%	75%	
Age	67 ± 15	60 ± 12.4	0.593
BMI	26 ± 6.0	28 ± 5.5	0.285
SBP (mmHg)	132.3 ± 14.9	135.7 ± 24.02	0.702
DBP (mmHg)	83.2 ± 10.16	82.45 ± 11.07	0.874
CRP (mg/L)	2.6 ± 3.16	2.93 ± 2.76	0.830
TC (mmol/L)	5.0 ± 0.9	5.0 ± 0.8	0.967
HDLc (mmol/L)	1.8 ± 0.4	1.6 ± 0.4	0.492
LDLc (mmol/L)	2.7 ± 0.7	2.9 ± 0.6	0.395
apoB (mg/dL)	86.9 ± 23.9	81.8 ± 20.2	0.640
TG (mmol/L)	0.9 ± 0.5	1.2 ± 0.5	0.237
Vitamin B12 (pmol/L)	336 ± 127	340 ± 93	0.990
Alkaline phosphatase (U/L)	64.1 ± 14.6	89.4 ± 31.7	0.038
Thrombocytes 10 ⁹ cells/L	249 ± 62	285 ± 65	0.202

Data are expressed as mean ± SD. SBP = systolic blood pressure; DBP = diastolic blood pressure; CRP = C-reactive protein; TC = total cholesterol; HDL = high density lipoprotein; LDL = low density lipoprotein; TG = triglycerides. Statistical analysis was performed using a Student's T-test. Data are presented as mean ± SD.

Next, the glycosylation of surface proteins on platelets was analyzed using lectins to detect either galactose (ECL), sialic acid and *N*-Acetylglucosamine (GlcNAc) (WGA) or GlcNAc residues (s-WGA) (Figures 1C, p = 0.707; 1D p = 0.0013; 1E p = 0.07; respectively). To this end, isolated platelets were treated with neuraminidase to induce cleavage of sialic acid residues. We used two different neuraminidases, one derived from *Vibrio Chlorae* and one from *Clostridium Perfringens* because neuraminidases differ in cleavage efficiency. We observed a relatively small difference in sialic acid expression.

To study platelet function, aggregation assays were performed by incubating the platelets with PAR1-activating peptide, collagen or PMA. Upon platelet stimulation using PAR1-activating peptide, collagen or PMA (Figures 2A- 2C, Figure S1) we did not observe any difference in platelet aggregation between platelets from carriers of the *ASGR1del12* variant as compared to platelets from controls.

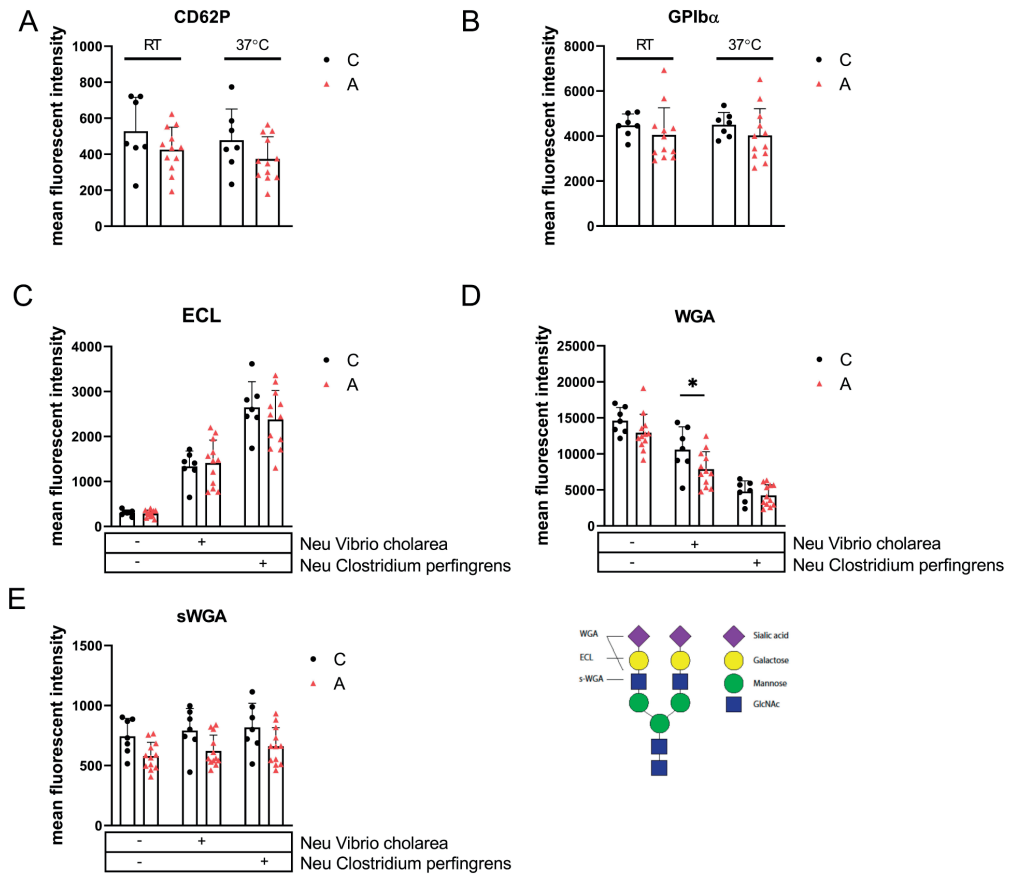


Figure 1 Expression of surface platelet activation markers and glycosylation of surface proteins. A. Expression of platelet CD62P B. Expression of GPIb α Panel C-E: presents the glycosylation pattern of platelet surface markers after incubation of the platelets of the control subjects and the *ASGR1del12* mutation carriers with or without different neuraminidases to induce sialic acid cleavage. Bottom right panel illustrates the glycan tree with lectin binding sites C. Analysis of FITC-conjugated *Erythrina cristagalli* lectin (ECL) binding to exposed galactose residues on platelets D. Analysis of Alexa647-conjugated Wheat Germ agglutinin (WGA) binding to sialic acid - and GlcNAc residues. E. Analysis of FITC-conjugated *Succinyl Triticum vulgare* lectin binding to exposed galactose and GlcNAc residues. Data are presented as MFI \pm SD. Data were tested for significance using Student T-test statistics. * $p < 0.05$

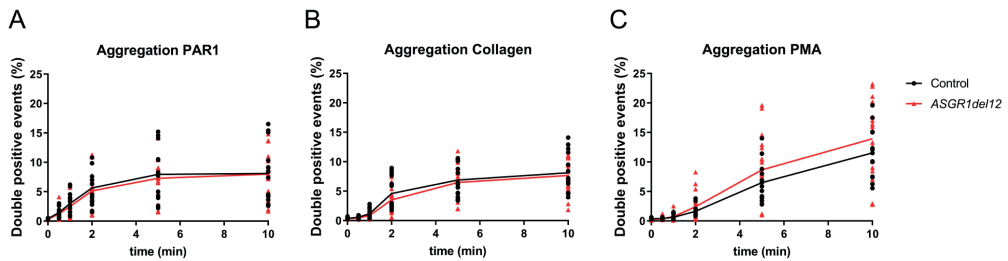


Figure 2 Functional analysis of platelets. Platelets isolated from blood of control subjects (black) or *ASGR1del12* mutation carriers (red) were incubated in the presence of different agonists to test the capacity of platelets to aggregate. A. incubation with PAR-1-activating peptide. B. incubation with collagen. C. Incubation with PMA. Data are presented as mean \pm SD.

Mendelian Randomization Study

We identified a total of 21 variants with a MAF > 0.01 that were associated with plasma LDLc levels at genome-wide significance ($p < 5.0 \times 10^{-8}$) and for which outcome data were available (Figure 3). Three variants were selected based on LD. These variants were rs55714927, located in *ASGR1*; rs58574748 and rs12449427, both located in the intergenic region downstream from the *ASGR1* gene (Table S1, S2). All variants in our score are also associated with plasma apoB levels, in concordant direction with their effects on LDLc (Table S3). The variants are not associated with HDLc and triglycerides at genome-wide significance level. Interestingly, the three variants were also strongly associated with plasma alkaline phosphatase levels, suggesting that the variants included in our genetic score indeed affect *ASGR1* function (Table S3).

The estimates of the genetic scores on CAD and MI are depicted in Figures 4A and 4B. Scaled per 10 mg/dl LDLc reduction, the *ASGR1* gene score lowered the risk on CAD with 26% (OR 0.74, 95% CI 0.57 – 0.96). This is proportionally similar to the results for the gene scores using variants in *HMGCR*, *NPC1L1*, *PCSK9*, *LDLR*. The estimates of the *ASGR1* gene score for myocardial infarction (OR 0.71, 95% CI 0.53 – 0.95) (Figure 4, Tables S4-S7)) were also similar to the estimates for the other gene scores included in the analysis. We found no evidence for pleiotropy, as our Q statistic for the *ASGR1* gene score was not significant (CAD: Q statistic = 2.543 ($p = 0.280$), MI: Q statistic 5.962 ($p = 0.051$)).

Discussion

In this study, we did not find evidence of a pleiotropic effect on CAD of carriership of an *ASGR1* variant over and above its effect on plasma LDLc levels. Only a small difference in the presence of sialic acid and GlcNAc residues on the surface of platelets derived from heterozygous *ASGR1del12* mutation carriers was observed, which did not affect their aggregation capacity. The estimated impact of the *ASGR1* gene score on CAD and MI per 10 mg/dl LDLc reduction revealed that the *ASGR1* gene score lowered the risk on CAD with 26 percent and was comparable to the effects of gene scores in *HMGCR*, *NPC1L1*, *PCSK9* and *LDLR*.

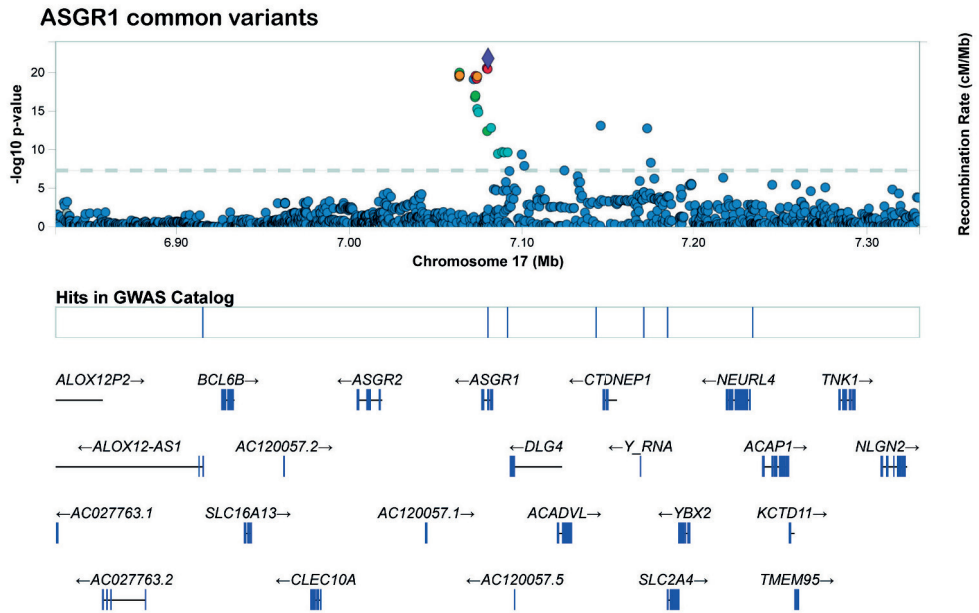
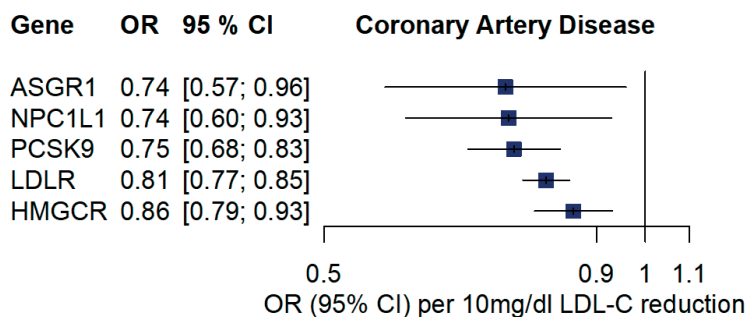


Figure 3. Detailed ASGR1 gene locus map showing the LD blocks of the variants in the region. A MAF>0.01 was chosen to select the common variants associated with LDLc. Locuszoom (<https://www.locuszoom.org>) was used to generate the figure. The chromosomal region expands towards ± 500 kb on both side of the ASGR1 gene.

We substantiated that subjects with the *ASGR1del12* mutation have increased levels of circulating plasma alkaline phosphatase, supporting the notion that the function of ASGR1 is compromised. ASGR1 has been suggested to be involved in the clearance of desialylated platelets as has been shown in *Asgr1*^{-/-} mice [31]. Inline, in genetically modified pigs with a deficiency in ASGR1 protein, a reduced hepatic uptake of human platelets was observed [32], lending support to the concept that ASGR1 may play a role in platelet homeostasis in vivo. In heterozygote carriers of the *ASGR1del12* variant we could not demonstrate significant differences in either platelet number or platelet aggregation. We did observe a significant reduction in sialic acid residues on platelet surface proteins. Collectively, these data do not support a role for ASGR1 in human platelet homeostasis in healthy individuals. However, we cannot completely rule out that in conditions of increased cardiovascular damage with a pro-inflammatory and pro-coagulant state ASGR1 function may play a role in modulating platelet function in carriers of variants in ASGR1 [33].

A



B

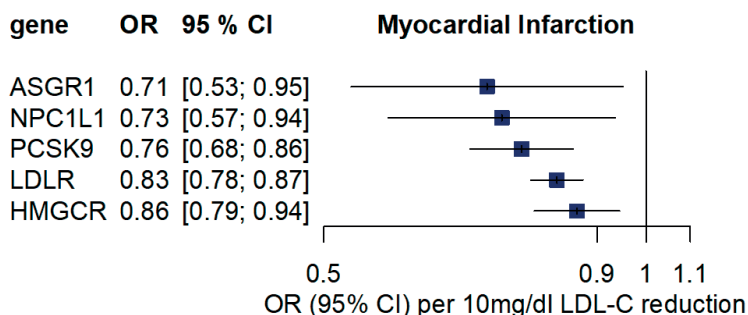


Figure 4 Risk of coronary artery disease (A) and myocardial infarction (B) per 10 mg/dl LDLc reduction as a function of *ASGR1* gene score. As a comparison gene scores in *HMGCR* [28], *NPC1L1* [38], *PCSK9*, *LDLR* [9] are provided. Boxes represent point estimates of effect and lines 95% confidence intervals. Coronary artery disease was defined as the composite of nonfatal myocardial infarction, or death from coronary heart disease and coronary revascularization. *ASGR1* = asialoglycoprotein receptor 1, *HMGCR* = 3-hydroxy-3-methylglutaryl-coenzyme A reductase; *NPC1L1* = Niemann-Pick C1-like; *PCSK9* = proprotein convertase subtilisin-kexin type 9; *LDLR* = low density lipoprotein receptor.

To further evaluate the disproportionality of the effect of *ASGR1* variants on lipids versus CAD risk, we selected three common variants located within 100 kB in and around the *ASGR1* gene that were significantly associated with LDLc. We validated the original finding that LDLc reduction by variants in *ASGR1* lowers the risk of CAD. More importantly, our results provide strong evidence that the LDLc reducing effect of genetic score in *ASGR1* on CAD overlaps with the effects of gene scores in *HMGCR*, *NPC1L1*, *PCSK9*, and *LDLR*. In Mendelian Randomization, the use of common variants in a gene score is known to provide more reliable estimates of the true effect of an exposure on clinical outcome than a single variant [34]. Therefore, we are confident that our estimates provide a more precise estimation of the effect than the *ASGR1del12* variant. Collectively, the data from our MR

study may suggest that the cardiovascular risk reducing effect of an ASGR1 therapeutic agent may be proportionally similar to the effects of other lipid-lowering agents, based on their LDLc reducing abilities.

The exact mechanisms by which ASGR1 regulates LDL homeostasis is still unresolved. ASGR1 is located on liver cells in clathrin-coated pits in in close proximity of the LDL receptor[35]. Interestingly, hypersialylation of the LDL receptor affects LDL receptor stabilization, resulting in a prolonged life cycle[17]. In contrast, the *Asgr1*^{-/-} mice have a normal lipoprotein phenotype [36, 37]. Thus, the exact mechanism underlying the lower LDLc plasma levels in carriers of *ASGR1* variants remains to be established.

This study has its limitations. First, the sample size of the cohort was small, despite including all carriers of this rare *ASGR1del12* variant from the Nijmegen Biomedical Study for *ex vivo* platelet characterization. Therefore, we cannot exclude a type II error. Additionally, it would be very interesting to evaluate these findings in homozygous carriers of the *ASGR1del12* variant. Unfortunately, no homozygous carriers were identified in the patient cohorts. Lastly, our model provides insights into the effect of lifetime exposure to a lower LDLc due to genetic variants and the results do not necessarily reflect the potential clinical benefit of inhibiting ASGR1.

In conclusion, using common variants in the *ASGR1* locus we replicate the CAD risk reducing effect found before. This effect seems to be predominantly mediated by the effect on plasma LDLc levels. In exploring potential pleiotropy, we found no evidence that the *ASGR1del12* variant affects platelet function.

References

- 1 K. J. Moore and I. Tabas. Macrophages in the pathogenesis of atherosclerosis. *Cell* 2011; 145: 341-355.
- 2 K. J. Williams and I. Tabas. Lipoprotein retention and clues for atheroma regression. *Arterioscler Thromb Vasc Biol* 2005; 25: 1536-1540.
- 3 E. P. Navarese, M. Kolodziejczak, V. Schulze, P. A. Gurbel, U. Tantry, et al. Effects of Proprotein Convertase Subtilisin/Kexin Type 9 Antibodies in Adults With Hypercholesterolemia: A Systematic Review and Meta-analysis. *Ann Intern Med* 2015; 163: 40-51.
- 4 J. G. Robinson, M. Farnier, M. Krempf, J. Bergeron, G. Luc, et al. Efficacy and safety of alirocumab in reducing lipids and cardiovascular events. *N Engl J Med* 2015; 372: 1489-1499.
- 5 M. S. Sabatine, R. P. Giugliano, S. D. Wiviott, F. J. Raal, D. J. Blom, et al. Efficacy and safety of evolocumab in reducing lipids and cardiovascular events. *N Engl J Med* 2015; 372: 1500-1509.
- 6 F. E. Dewey, V. Gusarova, R. L. Dunbar, C. O'Dushlaine, C. Schurmann, et al. Genetic and Pharmacologic Inactivation of ANGPTL3 and Cardiovascular Disease. *N Engl J Med* 2017; 377: 211-222.
- 7 M. J. Graham, R. G. Lee, T. A. Brandt, L. J. Tai, W. Fu, et al. Cardiovascular and Metabolic Effects of ANGPTL3 Antisense Oligonucleotides. *N Engl J Med* 2017; 377: 222-232.
- 8 M. G. Silverman, B. A. Ference, K. Im, S. D. Wiviott, R. P. Giugliano, et al. Association Between Lowering LDL-C and Cardiovascular Risk Reduction Among Different Therapeutic Interventions: A Systematic Review and Meta-analysis. *JAMA* 2016; 316: 1289-1297.
- 9 B. A. Ference, D. L. Bhatt, A. L. Catapano, C. J. Packard, I. Graham, et al. Association of Genetic Variants Related to Combined Exposure to Lower Low-Density Lipoproteins and Lower Systolic Blood Pressure With Lifetime Risk of Cardiovascular Disease. *JAMA* 2019: 1381-1391.
- 10 J. Brandts and K. K. Ray. LDL-Cholesterol Lowering Strategies and Population Health - Time to Move to a Cumulative Exposure Model. *Circulation* 2020.
- 11 B. A. Ference, J. G. Robinson, R. D. Brook, A. L. Catapano, M. J. Chapman, et al. Variation in PCSK9 and HMGCR and Risk of Cardiovascular Disease and Diabetes. *N Engl J Med* 2016; 375: 2144-2153.
- 12 P. Nioi, A. Sigurdsson, G. Thorleifsson, H. Helgason, A. B. Agustsdottir, et al. Variant ASGR1 Associated with a Reduced Risk of Coronary Artery Disease. *N Engl J Med* 2016; 374: 2131-2141.
- 13 M. Spiess and H. F. Lodish. Sequence of a second human asialoglycoprotein receptor: conservation of two receptor genes during evolution. *Proc Natl Acad Sci U S A* 1985; 82: 6465-6469.
- 14 K. B. Chiacchia and K. Drickamer. Direct evidence for the transmembrane orientation of the hepatic glycoprotein receptors. *J Biol Chem* 1984; 259: 15440-15446.
- 15 P. H. Weigel. Galactosyl and N-acetylgalactosaminyl homeostasis: a function for mammalian asialoglycoprotein receptors. *Bioessays* 1994; 16: 519-524.
- 16 A.V. Pshzhetsky, C. Richard, L. Michaud, S. Igdoura, S. Wang, et al. Cloning, expression and chromosomal mapping of human lysosomal sialidase and characterization of mutations in sialidosis. *Nat Genet* 1997; 15: 316-320.
- 17 A. Yang, G. Gyulay, M. Mitchell, E. White, B. L. Trigatti, et al. Hypomorphic sialidase expression decreases serum cholesterol by downregulation of VLDL production in mice. *J Lipid Res* 2012; 53: 2573-2585.
- 18 M. Ahmadian, M. J. Abbott, T. Tang, C. S. Hudak, Y. Kim, et al. Desnutrin/ATGL is regulated by AMPK and is required for a brown adipose phenotype. *Cell Metab* 2011; 13: 739-748.
- 19 B. van 't Veer and T. van der Poll. Keeping blood clots at bay in sepsis. *Nat Med* 2008; 14: 606-608.
- 20 R. Li, K. M. Hoffmeister and H. Falet. Glycans and the platelet life cycle. *Platelets* 2016; 27: 505-514.
- 21 R. Grozovsky, A. J. Begonja, K. Liu, G. Visner, J. H. Hartwig, et al. The Ashwell-Morell receptor

- regulates hepatic thrombopoietin production via JAK2-STAT3 signaling. *Nat Med* 2015; 21: 47-54.
- 22 T. E. Galesloot, S. H. Vermeulen, D. W. Swinkels, F. de Vegt, B. Franke, et al. Cohort Profile: The Nijmegen Biomedical Study (NBS). *Int J Epidemiol* 2017; 46: 1099-1100j.
- 23 W. T. Friedewald, R. I. Levy and D. S. Fredrickson. Estimation of the concentration of low-density lipoprotein cholesterol in plasma, without use of the preparative ultracentrifuge. *Clin Chem* 1972; 18: 499-502.
- 24 M. Rijkers, P. F. van der Meer, I. J. Bontekoe, B. B. Daal, D. de Korte, et al. Evaluation of the role of the GPIb-IX-V receptor complex in development of the platelet storage lesion. *Vox Sang* 2016; 111: 247-256.
- 25 M. Rijkers, A. Saris, S. Heidt, A. Mulder, L. Porcelijn, et al. A subset of anti-HLA antibodies induces FcγRIIIa-dependent platelet activation. *Haematologica* 2018; 103: 1741-1752.
- 26 M. Nikpay, A. Goel, H. H. Won, L. M. Hall, C. Willenborg, et al. A comprehensive 1,000 Genomes-based genome-wide association meta-analysis of coronary artery disease. *Nat Genet* 2015; 47: 1121-1130.
- 27 A. Genomes Project, A. Auton, L. D. Brooks, R. M. Durbin, E. P. Garrison, et al. A global reference for human genetic variation. *Nature* 2015; 526: 68-74.
- 28 B. A. Ference, K. K. Ray, A. L. Catapano, T. B. Ference, S. Burgess, et al. Mendelian Randomization Study of ACLY and Cardiovascular Disease. *N Engl J Med* 2019; 380: 1033-1042.
- 29 B. A. Ference, J. J. P. Kastelein, H. N. Ginsberg, M. J. Chapman, S. J. Nicholls, et al. Association of Genetic Variants Related to CETP Inhibitors and Statins With Lipoprotein Levels and Cardiovascular Risk. *JAMA* 2017; 318: 947-956.
- 30 S. Burgess and S. G. Thompson. Interpreting findings from Mendelian randomization using the MR-Egger method. *Eur J Epidemiol* 2017; 32: 377-389.
- 31 P. K. Grewal, S. Uchiyama, D. Ditto, N. Varki, D. T. Le, et al. The Ashwell receptor mitigates the lethal coagulopathy of sepsis. *Nat Med* 2008; 14: 648-655.
- 32 L. L. Paris, J. L. Estrada, P. Li, R. L. Blankenship, R. A. Sidner, et al. Reduced human platelet uptake by pig livers deficient in the asialoglycoprotein receptor 1 protein. *Xenotransplantation* 2015; 22: 203-210.
- 33 S. A. Igdoura. Asialoglycoprotein receptors as important mediators of plasma lipids and atherosclerosis. *Curr Opin Lipidol* 2017; 28: 209-212.
- 34 S. Burgess, F. Dudbridge and S. G. Thompson. Combining information on multiple instrumental variables in Mendelian randomization: comparison of allele score and summarized data methods. *Stat Med* 2016; 35: 1880-1906.
- 35 P. H. Weigel and J. H. Yik. Glycans as endocytosis signals: the cases of the asialoglycoprotein and hyaluronan/chondroitin sulfate receptors. *Biochim Biophys Acta* 2002; 1572: 341-363.
- 36 R. Tozawa, S. Ishibashi, J. Osuga, K. Yamamoto, H. Yagyu, et al. Asialoglycoprotein receptor deficiency in mice lacking the major receptor subunit. Its obligate requirement for the stable expression of oligomeric receptor. *J Biol Chem* 2001; 276: 12624-12628.
- 37 J. R. Braun, T. E. Willnow, S. Ishibashi, G. Ashwell and J. Herz. The major subunit of the asialoglycoprotein receptor is expressed on the hepatocellular surface in mice lacking the minor receptor subunit. *J Biol Chem* 1996; 271: 21160-21166.
- 38 B. A. Ference, F. Majeed and R. D. Brook. Effect of naturally random allocation to lower low-density lipoprotein cholesterol on the risk of coronary heart disease mediated by polymorphisms in NPC1L1, HMGCR, or both: a 2 x 2 factorial Mendelian randomization study. *J Am Coll Cardiol* 2015; 65: 1552-1561.

Supplementary material.

Table S1. The effect sizes of individual common variants in *ASGR1* on LDLc, CAD and MI

rs-ID	chr	position	Effect allele	Minor AF	LDLc effect mg/dl	p-val	Beta CAD	p-val	Beta MI	P val
55714927	17	7080316	T	0.192	-0.98	1.52E-22	-0.0357	0.014	-0.0502	0.0022
12449427	17	7173279	C	0.252	-0.67	1.73E-13	-0.2499	0.249	-0.00317	0.8167
148570698	17	7175379	T	0.098	-0.78	4.89E-09	-0.0284	0.028	-0.04319	0.0690

Table S2. The correlation matrix of the *ASGR1* variants

	rs55714927_T_C	rs12449427_C_G	rs148570698_T_C
rs55714927_T_C	1	0.353464	0.414695
rs12449427_C_G	0.353464	1	0.460889
rs148570698_T_C	0.414695	0.460889	1

Table S3: Effect size of individual variants in *ASGR1* on total cholesterol (TC), HDL cholesterol (HDLc), Triglycerides (TG), apoB and alkaline phosphatase (AP)

Rs-id	TC beta (mmol/L)	TC pval	HDLc beta (mmol/L)	HDLc pval	TG beta (mmol/L)	TG pval	AP beta (U/L)	AP pval	ApoB beta (g/L)	ApoB pval
55714927	-0.028683	1.36E-17	0.002109	0.057777	-0.0136	7.78E-06	2.3608	4.9E-196	-0.00819	3.07E-30
12449427	-0.017909	4.7E-09	0.002936	0.003712	-0.01134	4.17E-05	1.8951	6.4E-153	-0.00597	5.65E-20
148570698	-0.022296	6.78E-07	0.002564	0.08433	-0.01196	0.003248	2.2179	7.1E-98	-0.00718	6.63E-14

Table S4: *HMGCR* genetic score

RSID	minor allele	minor AF	effect allele	LDL-C effect in mg/dl	LDL-C pval	beta CAD	pval CAD	beta MI	pval MI
rs10066707	a	0.36724	G	-1.37275	1.5161E-62	-0.004348	0.6570427	-0.00046806	0.965224118
rs2006760	g	0.20325	C	-1.17742	2.5599E-32	-0.015077	0.1978287	-0.00935414	0.467969706
rs2303152	a	0.10011	G	-1.06725	5.6984E-16	-0.013252	0.3586129	-0.0107904	0.491974288
rs17238484	t	0.22497	G	-1.73153	5.9517E-75	-0.020572	0.0509173	-0.0196479	0.088005052
rs5909	a	0.093207	G	-1.63737	2.4937E-33	-0.030689	0.0483063	-0.0287267	0.093800715
rs12916	c	0.39977	T	-2.09116	6.076E-148	-0.035827	0.0001587	-0.0346145	0.000874565

Table S5: *NPC1L1* genetic score

RSID	minor allele	minor AF	effect allele	LDL-C effect in mg/dl	LDL-C pval	beta CAD	pval CAD	beta MI	pval MI
rs10234070	T	0.11943	c	-0.55534	5.5739E-06	-0.035147	0.0308803	-0.0200368	0.272004704
rs217386	A	0.42374	a	-0.78094	1.4353E-22	-0.021536	0.0285815	-0.0273201	0.011538379
rs7791240	C	0.091591	t	-0.84958	5.6107E-10	-0.021801	0.1652465	-0.016359	0.350427063
rs2300414	A	0.067822	g	-0.51682	0.0010527	-0.026378	0.0603374	-0.028325	0.074998495

Table S6: *PCSK9* genetic score

RSID	minor allele	minor AF	effect allele	LDL-C effect in mg/dl	ldl pval	beta CAD	pval CAD	beta MI	pval MI
rs2479394	G	0.27814	a	-0.86996	6.0561E-23	-0.027877	0.0045684	-0.0250996	0.022002853
rs11206510	C	0.18789	c	-1.61478	2.2345E-57	-0.074519	2.34E-08	-0.0737282	6.92785E-07
rs2149041	G	0.1873	c	1.445291	7.0185E-46	-0.039058	0.0012356	-0.0346546	0.010694122
rs2479409	G	0.34826	a	-1.1845	2.6554E-46	-0.028924	0.0054849	-0.0250143	0.03177441
rs10888897	T	0.39223	t	1.012497	7.4913E-36	-0.010569	0.3016688	-0.0190379	0.098280922
rs7552841	T	0.37586	c	0.800082	2.8361E-21	-0.01133	0.3168876	-0.00549379	0.660082125
rs562556	G	0.18003	g	0.852016	1.2456E-16	-0.000012	0.9992563	0.00516656	0.71506628

Table S7: *LDLR* genetic score

RSID	minor allele	minor AF	effect allele	LDL-C effect in mg/dl	LDL-C pval	beta CAD	pval CAD	beta MI	pval MI
rs1122608	T	0.25459	t	-1.84089	1.6034E-91	-0.073242	2.73E-11	-0.0635396	1.62318E-07
rs6511720	T	0.11894	t	-6.05069	0	-0.125298	1.42E-13	-0.100786	1.02939E-07
rs688	T	0.45239	c	1.106271	5.7813E-44	-0.036583	0.0001204	-0.0477692	6.06175E-06

Table S8: correlation matrix for *HMGCR* score

	rs10066707_A_G	rs2006760_G_C	rs2303152_A_G	rs17238484_T_G	rs5909_A_G	rs12916_C_T
rs10066707_A_G	1	0.47935	0.283095	0.539508	0.212708	0.499216
rs2006760_G_C	0.47935	1	0.519909	0.240068	0.447819	0.398727
rs2303152_A_G	0.283095	0.519909	1	0.640277	-0.12608	0.436171
rs17238484_T_G	0.539508	0.240068	0.640277	1	-0.226624	0.673118
rs5909_A_G	0.212708	0.447819	-0.12608	-0.226624	1	0.364091
rs12916_C_T	0.499216	0.398727	0.436171	0.673118	0.364091	1

Table S9: correlation matrix for *NPC1L1* score

	rs10234070_T_C	rs217386_A_G	rs7791240_C_T	rs2300414_A_G
rs10234070_T_C	1	-0.191911	0.140017	0.141758
rs217386_A_G	-0.191911	1	-0.245374	-0.212304
rs7791240_C_T	0.140017	-0.245374	1	0.591343
rs2300414_A_G	0.141758	-0.212304	0.591343	1

Table S10: correlation matrix for *PCSK9* score

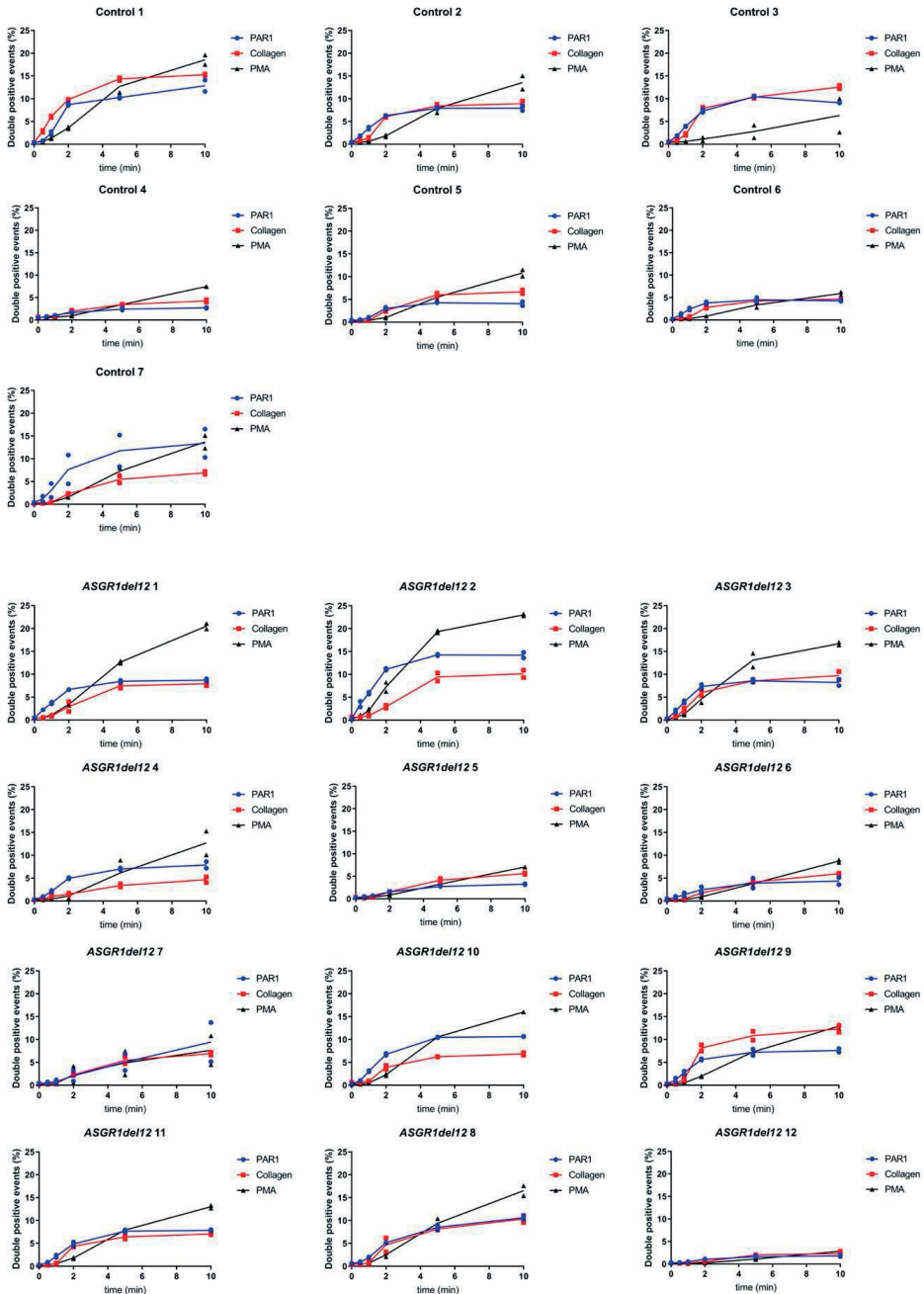
	rs2479394_G_A	rs11206510_C_T	rs2149041_G_C	rs2479409_G_A	rs10888897_T_C	rs7552841_T_C	rs562556_G_A
rs2479394_G_A	1	-0.293965	0.251963	0.207619	-0.0770863	-0.128658	-0.0232905
rs11206510_C_T	-0.293965	1	-0.163216	-0.198359	0.243534	0.118051	0.148878
rs2149041_G_C	0.251963	-0.163216	1	0.604835	-0.276993	-0.0730267	-0.177617
rs2479409_G_A	0.207619	-0.198359	0.604835	1	-0.337644	-0.0338827	-0.183905
rs10888897_T_C	-0.0770863	0.243534	-0.276993	-0.337644	1	0.0802385	0.329234
rs7552841_T_C	-0.128658	0.118051	-0.0730267	-0.0338827	0.0802385	1	-0.231842
rs562556_G_A	-0.0232905	0.148878	-0.177617	-0.183905	0.329234	-0.231842	1

Table S11: correlation matrix for *LDLR* score

	rs1122608_T_G	rs6511720_T_G	rs688_T_C
rs1122608_T_G	1	0.4682	-0.146195
rs6511720_T_G	0.4682	1	0.0930579
rs688_T_C	-0.146195	0.0930579	1

Figure S1

Aggregation curve for each individual *ASGR1del12* subject and each is given. The blue line represents PAR1 stimulation, in red are platelets stimulated with collagen and in black are the platelets stimulated with PMA.





CHAPTER 6

New insights into the role of glycosylation in lipoprotein metabolism.

Marjolein A.W. van den Boogert, Daniel J. Rader and Adriaan G. Holleboom

Current Opinion in Lipidology (2017) Review

Abstract

Purpose of review

Human genetics have provided new insights into the role of protein glycosylation in regulating lipoprotein metabolism. Here we review these new developments and discuss the biological insights they provide.

Recent findings

Case descriptions of patients with congenital defects in N-glycosylation (CDG-I) frequently describe a distinct hypocholesterolemia in these rare multi-system clinical syndromes. Two novel CDGs with disturbed Golgi homeostasis and trafficking defects result in mixed glycosylation disorders, hepatic steatosis and hypercholesterolemia. In addition, the presence of particular N-glycans is essential for physiological membrane expression of scavenger receptor B1 and for adequate lipolytic activity of endothelial lipase. GalNAc-T2, a specific O-glycosyl transferase, was found to be a direct modulator of HDL metabolism across mammals, validating its relation with HDL-c found in genome wide association studies. Furthermore, genetic variation in *ASGR1*, the major subunit of the asialoglycoprotein receptor (ASGPR), was found to be associated with a reduction in LDL-c and risk of coronary artery disease.

Summary

Protein glycosylation plays an important regulatory role in lipoprotein metabolism. Greater insight into how protein glycosylation regulates lipoprotein metabolism could provide novel approaches for the treatment of dyslipidemia.

Introduction

The beneficial effects of statins on cardiovascular risk are well established even in people with low risk of vascular disease or low levels of plasma low-density-lipoprotein (LDL-)cholesterol.[1] PCSK9 inhibitors lower LDL-c levels on top of statin therapy and have been shown to reduce cardiovascular events.[2] Yet even in persons with very low LDL-c levels, cardiovascular events still occur. New treatment strategies for preventing CV events targeting mechanisms distinct from LDL-c reduction with statins and PCSK9 inhibition are therefore needed.

A relatively novel terrain in lipoprotein metabolism is the role of protein glycosylation, one of the most prevalent posttranslational processes. Protein glycosylation involves the covalent attachment of a glycan to proteins. It is sometimes referred to as the “third language of life” after nucleic acids and proteins.[3] There are nine distinct, mammalian glycosylation pathways and they are defined by the first monosaccharide added to a protein or lipid, of which N- and O-glycosylation are the most widely studied. The effect of a specific N-glycan on function of that protein is impossible to predict and can range from irrelevant to very influential.[4] Glycans can affect the function of proteins through their physical properties (by their size and potential negative charge)[5], by being a target for glycan-binding proteins[6], or by modulating the properties of the protein to which they are attached.[4]

In recent years, the study of complex glycoproteins has been greatly enhanced by the advancements of mass spectrometry and the use of glycomics to identify specific glycan structures.[7,8] A more comprehensive insight into glycan-protein interactions has led to an interest in therapeutic exploitation in a variety of diseases. For example, malignant tumor cells upregulate sialyltransferases causing aberrant sialylation, which protects cancer cells from the host’s immunity and causes resistance to therapy.[9] Many pathogens bind carbohydrate structures on host cells and this affects adhesion and the colonization process,[10] and receptor mimicry strategies use this concept to impede infection.[11] Even specific modulation of the broadly expressed endogenous glycan metabolism by substrate reduction, product supplementation[12], enzyme replacement[13] or chaperone therapy[14] is becoming a reality.

Knowledge of the role of protein glycosylation in lipoprotein metabolism has been limited, but there is a new appreciation for the importance of this area. Human genetic studies have identified variants in genes involved in protein glycosylation that are associated with plasma lipid phenotypes and coronary artery disease[15-17], increasing interest in this field.

N-glycosylation and lipoprotein metabolism

Protein N-glycosylation has been implicated in a wide variety of processes in lipid metabolism. Many proteins involved in lipid synthesis, lipoprotein particle assembly and clearance are N-glycosylated, and disruption of these glycans affects their function. Sterol regulatory element-binding proteins (SREBPs) play a critical role in regulating intracellular and plasma cholesterol levels: they are transcription factors controlling expression of genes involved in cholesterol and fatty acid synthesis

and uptake.[18] It is well established that SREBP activation is dependent on intracellular cholesterol levels: when high, SREBP-cleavage activating protein (SCAP) undergoes a conformational change that promotes binding to insulin induced gene protein (Insig). When cellular cholesterol content decreases, the SCAP/SREBP complex dissociates from Insig and is transported to the Golgi apparatus where it is exposed to proteases which release the transcriptionally active fragment.[19,20] Recently, Cheng et al[21] showed that glucose-mediated N-glycosylation stabilized SCAP, reducing its association with Insig, allowing activation of SREBP and transcription of its target genes. In glucose-deficient conditions, sterol depletion failed to trigger SCAP/SREBP transport to the Golgi. Thus, SCAP acts as key glucose-responsive protein linking fuel availability to SREBP-dependent lipogenesis.

Sterol regulatory element-binding proteins (SREBPs) play a critical role in regulating cellular lipid metabolism and plasma lipoprotein metabolism. They are transcription factors controlling expression of genes involved in cholesterol and fatty acid synthesis and uptake. [18] It is well established that SREBP activation is dependent on intracellular cholesterol levels: when high, it is bound to SREBP-cleavage activating protein (SCAP) inducing a conformational change that promotes binding to insulin induced gene protein (Insig). When cellular cholesterol content decreases, the SCAP/SREBP complex dissociates from Insig and is transported to the Golgi apparatus where it is exposed to proteases, which release the transcriptionally active fragment. [19,20] Recently, Cheng et al[21] showed in tumor cells that glucose-mediated N-glycosylation stabilized SCAP, reducing its association with Insig, allowing activation of SREBP and transcription of its target genes. In glucose-deficient conditions, sterol depletion failed to trigger SCAP/SREBP transport to the Golgi. Thus, SCAP acts as key glucose-responsive protein linking fuel availability to SREBP-dependent lipogenesis.

Older studies established that very-low-density lipoprotein (VLDL) assembly and secretion by the liver is influenced by glycosylation of apolipoprotein B (apoB). Site-specific mutagenesis of glycosylation sites at the amino terminus of apoB decreased its secretion efficiency due to rapid degradation.[22] Inhibition of N-linked glycosylation with tunicamycin disrupted apoB conformation and accelerated degradation.[23,24] Tunicamycin treatment of fibroblasts also resulted in decreased binding and internalization of lipoproteins through a significantly reduced affinity for 125I-LDL[25], without affecting cell surface abundance of LDL receptor or its recycling.[26] More recently, studies in patients with type I congenital disorders of glycosylation (CDG) underscore the key role of N-glycosylation in apoB lipoprotein metabolism. CDG-I is caused by mutations in genes encoding one of the N-glycosylation enzymes in the endoplasmic reticulum (ER) resulting in underutilized glycosylation sites on glycoproteins. CDG-I patients have a wide spectrum of symptoms and severity, with mostly neuromuscular deficits. Interestingly, case reports of patients with CDG-I invariably mention hypocholesterolemia as an associated phenotype.[27-31] Our group has focused on the elucidation of the mechanism behind this interesting phenomenon.[32]

The inverse relationship between plasma levels of high-density lipoprotein cholesterol (HDL-c) and

cardiovascular risk has long been established,[33] but recent developments call into the question the causal nature of this relationship.[34] More insight into the complex biological processes of HDL metabolism is needed; protein glycosylation proves an interesting contributor to our understanding of HDL metabolism. *SCARB1* is the gene encoding scavenger receptor class BI (SR-BI), the major receptor for selective HDL-cholesteryl ester (CE) uptake into hepatocytes. Recently, two distinct genetic variants in *SCARB1* (T175A[35] and P376L[36]), were reported to exert their HDL-c increasing effects through altered N-glycosylation of the affected amino acid residues. In the P376L variant, this prevents transit from the ER to Golgi or further posttranslational modifications in the Golgi, which in the end causes reduced cell surface expression of SR-BI and reduced HDL-CE uptake.[36]

Endothelial lipase (EL) is an important regulator of HDL metabolism and genetic variants in the *LIPG* gene encoding the EL protein are associated with HDL-c levels.[15,16] EL has several N-glycosylation sites, and mutagenesis of one of the N-glycosylation sites or glycosylation recognition sequence enhanced enzymatic activity toward HDL without affecting cell surface association.[37] Interestingly, mutating the homologous amino acid residues in lipoprotein lipase reduced hydrolytic activity and the same mutation had no effect on hepatic lipase, demonstrating how hard it is to predict the effects of specific glycans. This is also demonstrated by the fact that the single loss of 3 of the 4 N-glycans of lecithin:cholesterol acyltransferase (LCAT) reduced its activity, but loss of the fourth increased enzymatic activity 2-fold.[38]

O-glycosylation, *GALNT2*, and lipoprotein metabolism

Human genetics studies have implicated variants in *GALNT2*, encoding the enzyme GalNAc-T2, as associated with HDL-c and triglyceride levels.[15-17] On its target proteins, the GalNAc-T2 enzyme initiates addition of mucin-type O-linked glycans through linkage of N-acetylgalactosamine (GalNAc) to specific serine or threonine residues. Both an initial animal study, consisting of a liver-specific knockdown mouse model[17], and a human study, consisting of 8 carriers of a genetic *GALNT2* variant from two Dutch families[39], implied reduced GalNAc-T2 function to be associated with increased HDL-c levels.

However, a recent extensive study of human null variants, homozygous for loss-of-function mutations in *GALNT2*, nonhuman primates treated with *GALNT2* siRNA and both murine and rat knockout models uniformly points to an opposite directionality, namely *GALNT2* loss-of-function associated with reduced HDL-c levels[40]. An unbiased quantitative O-glycoproteomics approach of human *GALNT2* null variants validated angiopoietin-like peptide 3 (ANGPTL3) and apoC-III as selective GalNAc-T2 targets. Of note, ANGPTL3 undergoes proprotein convertase processing for activation, and GalNAc-T2 may control this furin-mediated cleavage by glycosylating residues flanking the cleavage site.[41] Additional glycoproteomics in rodents identified phospholipid transfer protein (PLTP) as a target of GalNAc-T2. Indeed, both the animal models and the human null variants had reduced PLTP activity. These data suggest that *GALNT2* is required for facilitating PLTP function and maintaining HDL-c levels and established *GALNT2* as a direct modulator of HDL across mammals.

Mixed glycosylation disorders, Golgi trafficking defects, and hypercholesterolemia

An interesting and rapidly expanding subgroup of CDGs is that involving disturbed Golgi homeostasis via abnormal architecture or trafficking.[42] By sequencing human homologues of yeast V-ATPase assembly factors, we described two novel CDGs in families with formerly unsolved N- and mucin-type O-glycosylation disorders. Recently, we described hepatic steatosis and hypercholesterolemia in patients with these two novel types of glycosylation defects.[43,44]

Four individuals were identified with mutations in *TMEM199*. They presented with mild hepatic steatosis and hypercholesterolemia. Their serum glycosylation pattern was similar to that seen in other Golgi homeostasis defects[45,46], and metabolic labeling of glycans in patient fibroblasts confirmed Golgi glycosylation disorders, which were restored by complementation with wild-type *TMEM199*. [44]

In three other unrelated families with a CDG phenotype we found mutations in *CCDC115*. Affected individuals showed a storage-disease like phenotype with hepatosplenomegaly, leading to liver failure in two patients, and marked hypercholesterolemia. Serum protein mass spectrometry demonstrated abnormal N- and O-glycosylation, which was confirmed in patient fibroblasts and rescued by lentiviral transfection with wild-type *CCDC115*. [43]

In a HeLa cell model, both *TMEM199* and *CCDC115* localized to the ER-to-Golgi compartment and COPI vesicles, but their precise roles in Golgi trafficking, liver homeostasis and lipid pathways remain to be established.

It is interesting that CDG-I patients, with a global N-glycosylation problem, have a completely different cholesterol phenotype (*hypocholesterolemia*) compared to patients with *CCDC115*- or *TMEM199*-CDG, both with global mixed glycosylation disorders (*hypercholesterolemia*). This points out the need to more fully understand the relationships between specific glycoproteins and their effects on lipoprotein metabolism.

Protein sialylation and lipoprotein metabolism

The asialoglycoprotein receptor (ASGPR) is a highly conserved mainly hepatic receptor that facilitates the uptake of desialylated glycoproteins (with a terminal N-acetylgalactosamine or galactose).[47] Desialylation of glycoproteins occurs through the action of plasma or membranous sialidases and makes them prone to internalization by the ASGPR. Recently, a genetic variant in *ASGR1*, the major subunit of the (ASGPR), was reported to be associated with a significant reduction in LDL-c and risk of coronary artery disease.[*48] The del12 mutation is predicted to cause a frameshift and premature stop codon and indeed, when the mutated form was overexpressed in HeLa cells, no protein product was found. Heterozygous carriers of the *ASGR1* 12del mutation have higher levels of circulating alkaline phosphatase and vitamin B12, both glycoproteins known to be internalized through ASGPR and thus indicating that this variant is likely to be loss-of-function.[49] It was proposed that the reduction of LDL-c is due to a more stable LDL receptor (LDLR) expression

on liver cells of patients with reduced hepatic ASGPR abundance. LDLR and ASGPR are both located in clathrin-coated pits and ASGPR may promote the internalization of the LDLR after desialylation. Sialylation of LDLR plays a role in the stability of its expression.[50] Hypomorphic sialidase mice have more stable LDLR expression accompanied by more LDL uptake and ASGR1 deficient mice are viable and phenotypically normal.[51] Furthermore, there are 2 known healthy homozygous ASGR1 del12 mutation carriers. Thus, lowering ASGPR expression or inhibiting its function may be an approach to reducing LDL-c and cardiovascular risk. The links between sialylation, the ASGPR, plasma lipids and atherosclerosis have been reviewed extensively in this journal recently.[52]

Towards targeting glycosylation processes in lipid metabolism

Targeting global endogenous glycosylation machinery does not seem ideal considering the broad potential of off target effects due to the vast amount of functional glycoproteins. However as mentioned above, there are more and more ways to use glycobiology in therapeutic targeting. For example by therapeutic glycoproteins or using glycoprotein-coated particles to target therapy to carbohydrate-binding receptors.[52] These therapeutic pathways are being explored in various settings, mainly in oncology and virology.

Conclusion

There have been exciting new developments linking protein glycosylation to the regulation of lipoprotein metabolism. More insight into the complex protein glycosylation pathways and specific glycoprotein functions and how they impact on lipoprotein metabolism may lead to new therapeutic options in the treatment of dyslipidemia and atherosclerosis.

References

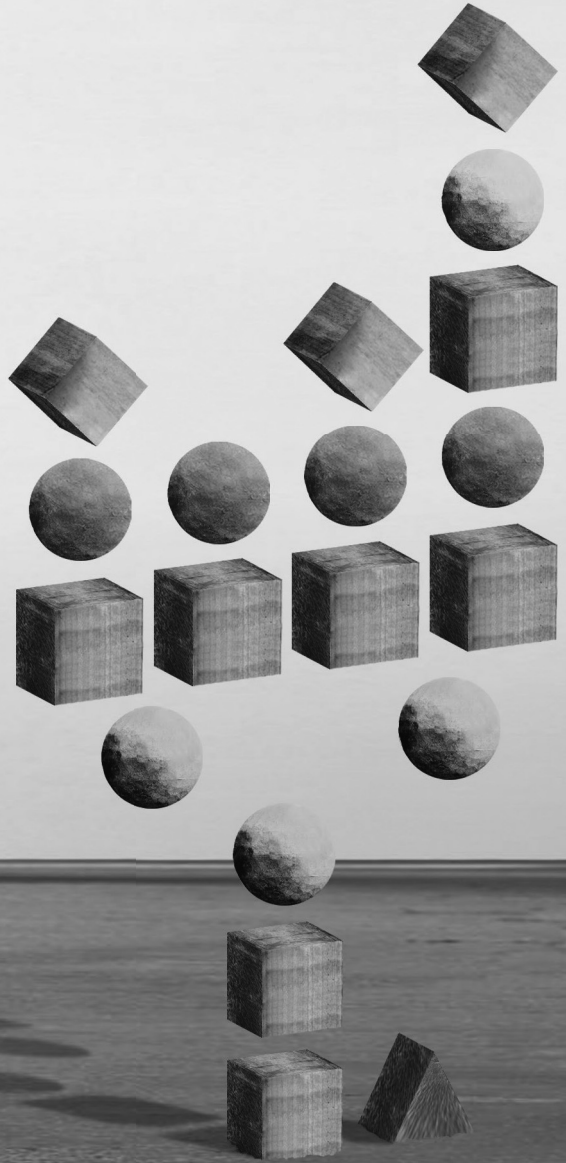
1. Cholesterol Treatment Trialists' (CTT) Collaborators, Mihaylova B, Emberson J, Blackwell L, *et al.* The effects of lowering LDL cholesterol with statin therapy in people at low risk of vascular disease: meta-analysis of individual data from 27 randomised trials. *Lancet* 2012; 380:581–590.
2. Sabatine MS, Giugliano RP, Keech AC, *et al.* Evolocumab and Clinical Outcomes in Patients with Cardiovascular Disease. *N Engl J Med* 2017; 376:1713–1722.
3. Ohtsubo K, Marth JD. Glycosylation in cellular mechanisms of health and disease. *Cell* 2006; 126:855–867.
4. Varki A, Cummings RD, Esko JD, *et al.* *Essentials of Glycobiology*. 2015, [no volume].
5. Wormald MR, Dwek RA. Glycoproteins: glycan presentation and protein-fold stability. *Structure* 1999; 7:R155–60.
6. Sperandio M, Gleissner CA, Ley K. Glycosylation in immune cell trafficking. *Immunol Rev* 2009; 230:97–113.
7. van Scherpenzeel M, Steenbergen G, Morava E, *et al.* High-resolution mass spectrometry glycoprofiling of intact transferrin for diagnosis and subtype identification in the congenital disorders of glycosylation. *Transl Res* 2015; 166:639–649.e1.
8. Reiding KR, Blank D, Kuijper DM, *et al.* High-throughput profiling of protein N-glycosylation by MALDI-TOF-MS employing linkage-specific sialic acid esterification. *Anal Chem* 2014; 86:5784–5793.
9. Büll C, Boltje TJ, Wassink M, *et al.* Targeting aberrant sialylation in cancer cells using a fluorinated sialic acid analog impairs adhesion, migration, and in vivo tumor growth. *Mol Cancer Ther* 2013; 12:1935–1946.
10. Moran AP, Gupta A, Joshi L. Sweet-talk: role of host glycosylation in bacterial pathogenesis of the gastrointestinal tract. *Gut* 2011; 60:1412–1425.
11. Dalziel M, Crispin M, Scanlan CN, *et al.* Emerging principles for the therapeutic exploitation of glycosylation. *Science* 2014; 343:1235681–1235681.
12. de Lonlay P, Seta N. The clinical spectrum of phosphomannose isomerase deficiency, with an evaluation of mannose treatment for CDG-Ib. *Biochim Biophys Acta* 2009; 1792:841–843.
13. Eng CM, Guffon N, Wilcox WR, *et al.* International Collaborative Fabry Disease Study Group. Safety and efficacy of recombinant human alpha-galactosidase A replacement therapy in Fabry's disease. *N Engl J Med* 2001; 345:9–16.
14. Yuste-Checa P, Brasil S, Gámez A, *et al.* Pharmacological Chaperoning: A Potential Treatment for PMM2-CDG. *Hum Mutat* 2017; 38:160–168.
15. Willer CJ, Sanna S, Jackson AU, *et al.* Newly identified loci that influence lipid concentrations and risk of coronary artery disease. *Nat Genet* 2008; 40:161–169.
16. Kathiresan S, Willer CJ, Peloso GM, *et al.* Common variants at 30 loci contribute to polygenic dyslipidemia. *Nat Genet* 2009; 41:56–65.
17. Teslovich TM, Musunuru K, Smith AV, *et al.* Biological, clinical and population relevance of 95 loci for blood lipids. *Nature* 2010; 466:707–713.
18. Brown MS, Goldstein JL. The SREBP pathway: regulation of cholesterol metabolism by proteolysis of a membrane-bound transcription factor. *Cell* 1997; 89:331–340.
19. Adams CM, Reitz J, De Brabander JK, *et al.* Cholesterol and 25-hydroxycholesterol inhibit activation of SREBPs by different mechanisms, both involving SCAP and Insigs. *J Biol Chem* 2004; 279:52772–52780.

20. Nohturfft A, DeBose-Boyd RA, *et al.* Sterols regulate cycling of SREBP cleavage-activating protein (SCAP) between endoplasmic reticulum and Golgi. *Proc Natl Acad Sci USA* 1999; 96:11235–11240.
21. Cheng C, Ru P, Geng F, *et al.* Glucose-Mediated N-glycosylation of SCAP Is Essential for SREBP-1 Activation and Tumor Growth. *Cancer Cell* 2015; 28:569–581.
22. Vukmirica J, Nishimaki-Mogami T, Tran K, *et al.* The N-linked oligosaccharides at the amino terminus of human apoB are important for the assembly and secretion of VLDL. *J Lipid Res* 2002; 43:1496–1507.
23. Macri J, Adeli K. Conformational changes in apolipoprotein B modulate intracellular assembly and degradation of ApoB-containing lipoprotein particles in HepG2 cells. *Arterioscler Thromb Vasc Biol* 1997; 17:2982–2994.
24. Liao W, Chan L. Tunicamycin induces ubiquitination and degradation of apolipoprotein B in HepG2 cells. *Biochem J* 2001; 353:493–501.
25. Filipovic I, Figura von K. Effect of tunicamycin on the metabolism of low-density lipoproteins by control and low-density-lipoprotein-receptor-deficient human skin fibroblasts. *Biochem J* 1980; 186:373–375.
26. Filipovic I. Effect of inhibiting N-glycosylation on the stability and binding activity of the low density lipoprotein receptor. *J Biol Chem* 1989; 264:8815–8820.
27. Jaeken J, Eggermont E, Stibler H. An apparent homozygous X-linked disorder with carbohydrate-deficient serum glycoproteins. *Lancet* 1987; 2:1398.
28. Ohno K, Yuasa I, Akaboshi S, *et al.* The carbohydrate deficient glycoprotein syndrome in three Japanese children. *Brain Dev* 1992; 14:30–35.
29. Pavone L, Fiumara A, Barone R, *et al.* Olivopontocerebellar atrophy leading to recognition of carbohydrate-deficient glycoprotein syndrome type I. *J Neurol* 1996; 243:700–705.
30. de Lonlay P, Seta N, Barrot S, *et al.* A broad spectrum of clinical presentations in congenital disorders of glycosylation I: a series of 26 cases. *J Med Genet* 2001; 38:14–19.
31. Di Rocco M, Hennet T, Grubenmann CE, *et al.* Congenital disorder of glycosylation (CDG) Ig: report on a patient and review of the literature. *J. Inherit Metab Dis* 2005; 28:1162–1164.
32. van den Boogert MAW, Kuil SD, Hovingh GK, *et al.* Genetic defects in protein glycosylation as a cause of dyslipidemia. Poster presented at: American Heart Association Scientific Sessions; Nov 16-20, 2013; Dallas, TX, USA
33. Gordon DJ, Probstfield JL, Garrison RJ, *et al.* High-density lipoprotein cholesterol and cardiovascular disease. Four prospective American studies. *Circulation* 1989; 79:8–15.
34. Rader DJ, Tall AR. The not-so-simple HDL story: Is it time to revise the HDL cholesterol hypothesis? *Nat Med* 2012; 18:1344–1346.
35. Chadwick AC, Sahoo D. Functional characterization of newly-discovered mutations in human SR-BI. *PLoS ONE* 2012; 7:e45660.
36. Zanoni P, Khetarpal SA, Larach DB, *et al.* Rare variant in scavenger receptor BI raises HDL cholesterol and increases risk of coronary heart disease. *Science* 2016; 351:1166–1171.
37. Brown RJ, Miller GC, Griffon N, *et al.* Glycosylation of endothelial lipase at asparagine-116 reduces activity and the hydrolysis of native lipoproteins in vitro and in vivo. *J Lipid Res* 2007; 48:1132–1139.
38. O K, Hill JS, Wang X, *et al.* Lecithin:cholesterol acyltransferase: role of N-linked glycosylation in enzyme function. *Biochem J* 1993; 294 (Pt 3):879–884.
39. Holleboom AG, Karlsson H, Lin R-S, *et al.* Heterozygosity for a loss-of-function mutation in

- GALNT2 improves plasma triglyceride clearance in man. *Cell Metab* 2011; 14:811–818.
40. Khetarpal SA, Schjoldager KT, Christoffersen C, *et al.* Loss of Function of GALNT2 Lowers High-Density Lipoproteins in Humans, Nonhuman Primates, and Rodents. *Cell Metab* 2016; 24:234–245.
 41. Schjoldager KT-BG, Vester-Christensen MB, Bennett EP, *et al.* O-glycosylation modulates proprotein convertase activation of angiotensin-like protein 3: possible role of polypeptide GalNAc-transferase-2 in regulation of concentrations of plasma lipids. *J Biol Chem* 2010; 285:36293–36303.
 42. Freeze HH, Chong JX, Bamshad MJ, Ng BG. Solving glycosylation disorders: fundamental approaches reveal complicated pathways. *Am J Hum Genet* 2014; 94:161–175.
 43. Jansen JC, Cirak S, van Scherpenzeel M, *et al.* CCDC115 Deficiency Causes a Disorder of Golgi Homeostasis with Abnormal Protein Glycosylation. *Am J Hum Genet* 2016, 98:310–321.
 44. Jansen JC, Timal S, van Scherpenzeel M, *et al.* TMEM199 Deficiency Is a Disorder of Golgi Homeostasis Characterized by Elevated Aminotransferases, Alkaline Phosphatase, and Cholesterol and Abnormal Glycosylation. *Am J Hum Genet* 2016; 98:322–330.
 45. Dulary E, Potelle S, Legrand D, Foulquier F. TMEM165 deficiencies in Congenital Disorders of Glycosylation type II (CDG-II): Clues and evidences for roles of the protein in Golgi functions and ion homeostasis. *Tissue Cell* 2016; doi:10.1016/j.tice.2016.06.006.
 46. Kornak U, Reynnders E, Dimopoulou A, ARCL Debré-type Study Group, *et al.* Impaired glycosylation and cutis laxa caused by mutations in the vesicular H⁺-ATPase subunit ATP6V0A2. *Nat Genet* 2008; 40:32–34.
 47. Ashwell G, Kawasaki T. A protein from mammalian liver that specifically binds galactose-terminated glycoproteins. *Meth Enzymol* 1978; 50:287–288.
 48. Nioi P, Sigurdsson A, Thorleifsson G, *et al.* Variant ASGR1 Associated with a Reduced Risk of Coronary Artery Disease. *N Engl J Med* 2016; 374:2131–2141.
 49. Blom E, Ali MM, Mortensen B, Huseby NE. Elimination of alkaline phosphatases from circulation by the galactose receptor. Different isoforms are cleared at various rates. *Clin Chim Acta* 1998; 270:125–137.
 50. Yang A, Gyulay G, Mitchell M, *et al.* Hypomorphic sialidase expression decreases serum cholesterol by downregulation of VLDL production in mice. *J Lipid Res* 2012; 53:2573–2585.
 51. Tozawa R, Ishibashi S, Osuga J, *et al.* Asialoglycoprotein receptor deficiency in mice lacking the major receptor subunit. Its obligate requirement for the stable expression of oligomeric receptor. *J Biol Chem* 2001; 276:12624–12628.
 52. Igdoura SA. Asialoglycoprotein receptors as important mediators of plasma lipids and atherosclerosis. *Curr Opin Lipidol* 2017.



SUMMARY AND GENERAL DISCUSSION



Summary of the main findings

The aim of this thesis was to gain mechanistic insights into the genetic associations between genes involved in protein glycosylation and lipid metabolism. To accomplish this, we started by studying the lipid phenotypes in patients with congenital disorders of (de)glycosylation (CD(D)Gs) in **Part I** of this thesis. In **Part II**, we studied other roles of glycosylation in lipid metabolism.

In **Chapter 1** we studied a large cohort of type I CDG patients with homozygous or compound heterozygous mutations in the ER and cytosolic enzymes ALG6 and PMM2. All patients had hypobetalipoproteinemia, with total cholesterol, LDL-c and apoB levels below the 5th percentile for their age and gender. Their clinically unaffected, heterozygous relatives also had decreased levels of plasma LDL-c, suggesting a gene-dose effect. Our *in vitro* studies provide evidence that the hypobetalipoproteinemia is at least in part due to increased abundance of LDL receptor on the surface membrane and consequently increased LDL particle uptake. Well-known potential contributing pathways were ruled out: apoB secretion was not affected in our cell models, nor did we find a role for PCSK9 in the increased LDL receptor protein expression. The effect seems to be driven by increased basal levels of processed and thus active SREBP2, the main transcription factor for LDL receptor expression. SREBP2 processing is prompted by low intracellular cholesterol levels, however in our cell models we found increased intracellular cholesterol accompanied by intact cholesterol sensing. As ER stress is another possible inducer of SREBP2 and glycosylation defects this early in the glycan tree machinery potentially cause ER stress by overloading the degradative systems, we studied ER stress markers but found no significant difference in the CDG-I cell models compared to controls. In the end we hypothesized that INSIG1, the ER protein that controls proteolytic activation of SREBP2, might be affected by the disrupted glycan assembly in the ER. Indeed, we found that overexpression of INSIG1 in our cell model abolished the increased LDL receptor expression.

The exact link between the role of INSIG1 in the increased LDL receptor expression remains to be elucidated and is an important focus for future research, as this might reveal a potential novel therapeutic target in hypercholesterolemia.

Furthermore, the fact that heterozygous carriers of the CDG-I mutations have hypocholesterolemia without the severe clinical features of the patients, makes them interesting subjects for *in vivo* tracer studies on apoB/LDL metabolism and the development of atherosclerosis.

B4GALT1-CDG is a very rare syndrome caused by homozygous mutations in *B4GALT1*, encoding an enzyme located in the Golgi apparatus responsible for the galactosylation of N-linked glycans¹⁻³. In **Chapter 2** we report distinct plasma lipid abnormalities in 3 B4GALT1-CDG patients. With fast protein liquid chromatography (FPLC) profiling for cholesterol distribution across lipoprotein fractions, we found that most of their plasma cholesterol sequestered in the HDL fraction and this was accompanied by larger HDL particles. This is a phenomenon reminiscent of the FPLC profiles found in patients with cholesteryl ester transfer protein (CETP) deficiency (reviewed in ⁴). CETP is a highly glycosylated protein that transfers cholesteryl esters from HDL particles to other lipoproteins. CETP deficiency leads to increased levels of HDL-c and decreased levels of LDL-c. We studied CETP

glycosylation in B4GALT1-CDG patients and found a marked reduction in the glycosylated CETP glyco-isoforms. Furthermore, CETP activity was reduced in these patients compared to controls, suggesting that CETP's glycosylation pattern is an important factor in its function.

In recent years, CETP inhibitors have been extensively studied, but the clinical benefit on cardiovascular risk has been underwhelming (reviewed in ⁵). Therefore, further insight into the exact mechanism to which CETP activity is affected by CETP's glycosylation is worth pursuing in the field of CETP inhibition. Especially because the deglycosylated CETP isoforms seem to give a proportionate reduction in LDL-c and apoB, in contrast with the CETP inhibitors, which, when used on top of statins, lower apoB to a smaller extent than LDL-c⁶ and apoB itself has a stronger link with atherosclerotic disease than LDL-c⁷.

A third subset of patients with genetic glycosylation disorders with mutations in *TMEM199* and *CCDC115* was studied in **Chapter 3**. *TMEM199* and *CCDC115* are both V-ATPase assembly factors and patients with deficiencies of these enzymes show mixed glycosylation disorders, marked hypercholesterolemia - comparable values to those seen in patients with familial hypercholesterolemia - and fatty liver disease^{8,9}.

The lipid phenotype showed that most cholesterol sequestered in the VLDL fraction, without elevated plasma triglycerides, and reduced cholesterol in HDL particles. As a possible explanation for the hypercholesterolemia, we found increased apoB secretion in an *in vitro* cellular model mimicking the enzyme deficiencies and this was validated in patient-derived redifferentiated induced pluripotent stem cells. The reduced lipidation of VLDL particles with triglycerides could possibly be explained by the decreased expression of microsomal triglyceride transfer protein (*MTP*) in our *in vitro* cell model. Furthermore, a murine model with a knock-in of a patient's mutation in *TMEM199*, generated using CRISPR-Cas9, also showed hepatic steatosis consistent with the patient. Although, the *TMEM199* deficient mice did not have increased plasma (V)LDL cholesterol, they did show the same reduction in cholesterol content of HDL particles seen in the patients.

Increased number and size of lipid droplets, as seen in liver biopsies of patients with *TMEM199* and *CCDC115* deficiency, was also shown in our *in vitro* cell model. This was accompanied by disturbed interaction of these lipid droplets with lysosomes, which suggests disturbed autophagy of lipid droplets, which subsequently could explain the development of hepatosteatosis.

Non-alcoholic fatty liver disease (NAFLD) is an increasingly prevalent form of hepatic steatosis due to its association with obesity and insulin resistance. Aside from lifestyle interventions¹⁰, there are currently no approved therapies specifically treating NAFLD, although several promising compounds are being tested in clinical trials¹¹⁻¹⁴. More insight into the mechanisms causing lipid accumulation, could lead to novel targets.

A relatively recently discovered inherited disease is caused by mutations in N-glycanase 1 (*NGLY1*), a deglycosylation enzyme, making it the first congenital disorder of deglycosylation^{15,16}. The lipid phenotypes in these patients were studied in **Chapter 4** and we found hypocholesterolemia. This was not explained by increased clearance of LDL-c from the plasma as we saw in patients with ALG6-

and PMM2-CDG, because LDL receptor abundance on the cell surface and LDL particle uptake were decreased in NGLY1-CDDG patient fibroblasts. A possible explanation was found in the downregulation of the rate-limiting enzyme in cholesterol synthesis, HMG-CoA-reductase (*HMGCR*), in both patient fibroblasts and the homozygous *ngly1*^{-/-} zebrafish. These *ngly1*^{-/-} zebrafish showed several of the clinical phenomena as seen in human patients, including decreased liver size and reduced area of the cerebellar granule neurons. Furthermore, the zebrafish had decreased locomotor activity.

Interestingly, in these patients the lipid phenotype seems to potentially be causal in the neurological phenotype of the patients. Early development of the central nervous system is partly dependent on high rates of cholesterol synthesis¹⁷. RNA sequencing of the *ngly1*^{-/-} zebrafish showed dysregulation of cholesterol synthesis pathways and decreased *HMGCR* expression at both the transcriptional and protein level. Both supplementing the *ngly1*^{-/-} with the metabolite of *HMGCR* activity, mevalonate, immediately following fertilization and overexpression of *HMGCR* ameliorated the reduction of cerebellar granule neurons significantly, offering a completely novel therapeutic option for patients with NGLY1 deficiency.

Obviously, these findings warrant further studies into whether mevalonate supplementation could also be beneficial in human patients.

Part II of this thesis looks at other roles for glycosylation processes in lipid metabolism and atherosclerosis. In **Chapter 5** we attempted to find possible pleiotropic effects of the del12 *ASGR1* mutation explaining the reduced cardiovascular risk described by Nioi et al¹⁸ other than by its effect on plasma LDL-c levels. The asialoglycoprotein receptor (ASGPR) has been implicated in the clearance of aged, desialylated platelets^{19,20}. We hypothesized that with less abundance of the ASGPR in *ASGR1* mutation carriers, these possibly less functional²¹, desialylated platelets would circulate longer and are less prone to aggregation. However, we could not demonstrate significant differences in platelet number or platelet aggregation in these carriers, even though their platelets were significantly less sialylated compared to the platelets of controls.

We did validate the original finding from Nioi et al¹⁸, that LDL-c reduction by variants in *ASGR1* is associated with lower CVD risk, by evaluating three common variants in and around the *ASGR1* gene. Furthermore, this effect overlapped completely with the effects of genetic scores in known, well-established players in the LDL-c pathway, like *LDLR*, *PCSK9* and *HMGCR*.

How the rare *ASGR1del12* variant affects LDL-c levels is unknown and subject of future studies.

A completely different approach to utilizing glycans in therapeutics in general is by delivering cargo, like short-interfering RNA (siRNA), to hepatocytes through the ASGPR. This is already being successfully pursued in lipid metabolism²² and other fields (e.g. hematology^{23,24}). Inclisiran is an siRNA inhibiting the translation of PCSK9 and has recently been shown to be effective in lowering plasma LDL-c in patients with familial hypercholesterolemia in a phase III trial²².

As discussed in **Chapter 5**, the ASGPR is highly expressed on the basal membrane of hepatocytes and only minimally expressed elsewhere, limiting off-target effects. Furthermore, due to its location it is readily accessible from the circulation. *N*-acetylglucosamine (GalNAc) is a derivative of the

monosaccharide glucose and has a very high affinity for the ASGPR. Conjugating siRNAs to GalNAcs has proven to be an effective way to deliver diverse cargo to hepatocytes as reviewed by Springer and Dowdy^{25,26}. RNA inhibition has great potential to treat a wide range of diseases.

Another interesting subject of further studies could be that we show that even common variants in ASGR1 are associated with lower LDL-c levels and are strongly associated with alkaline phosphatase, which was used as a readout for ASGPR function. This suggests that ASGPR function is highly variable within a population and that delivery of the GalNAc conjugated siRNA therapies could be highly variable as well.

In **Chapter 6** we reviewed known glycobiological processes that are relevant in lipid metabolism. From the lipid phenotypes observed in patients with CDG, described above, to the specific glycosylation pattern and its influence on the function of important players in lipid metabolism. The review also touches upon the possible use of this knowledge in therapeutics. It seems clear that global targeting of the endogenous glycosylation machinery would lead to wide-ranging off target effects. However, opportunities for the utilization of glycans have been pursued successfully.

General discussion

In the epigraph to this thesis I paraphrased the Extreme Value Theory by Leonard Tippett: “*Use the rare and extreme to study the common.*” and that is what we pursued in our studies. The rare and extreme clinical phenotypes of patients with CDG include their extreme lipid abnormalities and we used this to elucidate possible mechanisms that result from glycosylation disorders.

Our studies were essentially aimed to find novel targets in treating the much more common: hypercholesterolemia as a driver of atherosclerosis and CVD. But over the course of these studies, I have found nothing but genuine interest in our research from the patients and their families, and willingness to participate. They embraced the fact that our studies were not aimed to be directly beneficial to them, but understood and hoped that it could help “put these rare diseases on the map”. And even in this relatively small set of studies we have found a trove of information at the interface of lipidology, cardiovascular research and glycobiology that could hint at novel treatments. And this crosstalk led to beneficial insights even for the treatment of the CDG patients themselves. The most obvious example in this respect is that we found that some of the neurological symptoms seen in NGLY1 deficient patients might be caused, in part, by their disturbed lipid metabolism. Endogenous cholesterol synthesis is essential for the development of the central nervous system¹ and there are a variety of other neurodevelopmental disorders that are associated with cholesterol synthesis, for example Niemann-Pick syndrome^{27,28}. Our results offer a potential treatment option for patients with NGLY1-CDDG by supplementing the metabolite of the rate-limiting enzyme in cholesterol synthesis (**Chapter 3**).

There is a limit to the information we can get from rare disease patients. First and foremost because they are rare; making it impossible to get access to large numbers of patients. Secondly, many patients have intellectual and/or motor disabilities raising ethical questions as to what to study of and from these patients, when it is not directly beneficial to them. Last, it is unclear whether the extreme lipid phenotypes are of clinical relevance, as most patients are too young to develop overt atherosclerotic CVD.

Luckily, many important pathways in lipid metabolism are well characterized in a wide range of, mostly liver and fibroblast, cell models. However, to be able to study the glycosylation defects in the CDG patients, these liver cell models need to be genetically manipulated to mimic the enzymatic deficiencies. In fact, primary liver cells of patients would be ideal but are very invasive to obtain and difficult to culture. In contrast, patient fibroblasts are easy and minimally invasive to obtain, and obviously harbor the inherent glycosylation defect, making them a superior model in terms of clinical relevance. However, LDL metabolism mainly occurs in the liver. In 2006 Takahashi and Yamanaka used adult, differentiated fibroblasts and induced them with specific factors to generate induced pluripotent stem cells (iPSCs)²⁹. These pluripotent stem cells can be differentiated into specific cell lines, like liver cells, and can be used to study patient specific molecular mechanisms resulting in disease, but also to test therapeutic compounds *in vitro* (e.g. ^{30,31}). In **Chapter 1** and **Chapter 3** we used patient-derived fibroblasts to create hepatocyte-like cells with this method to study the effects of ALG6 and PMM2 deficiency and TMEM199 deficiency respectively, and found

disturbed lipid metabolism consistent to what we found in the siRNA treated HepG2 cells and consistent with the lipid phenotypes in patients. Cell models like iPSCs and the even more advanced iPSC-derived liver organoids³² are the best available models to study *in vitro* lipid metabolism in the setting of genetic glycosylation defects.

Unfortunately, a cell model can never reveal the complete picture and the lack of viable mouse models for most CDG types makes the study of *in vivo* effects of glycosylation defects on lipid metabolism considerably harder. A factor complicating this is that glycosylation is fundamental to a wide spectrum of biological processes, making mouse knockouts of glycosylation enzymes often embryonically lethal³³⁻³⁵. For example, only relatively recently viable mouse models for PMM2-CDG were developed^{33,36} and those are hypomorphic, not full knockout. In addition, one of these models needs supplementation of an intracellular substrate for the deficient enzyme, mannose, to overcome embryonic lethality³³, even though this is not effective in changing outcomes in human patients³⁷, causing its clinical relevance to be questionable. One way to get around this, would be to create liver-specific knockouts of the glycosylation enzymes, although this would still lack the effects of the glycosylation defect in for example the vascular compartment. In this thesis we describe another way to circumvent this problem by developing a viable mouse model with a knock-in of a human patient's mutation (**Chapter 3**). These mice harboring the TMEM199-Ala7Glu mutation show an N-glycan plasma profile consistent to that found in human patients and also have fatty livers. Solutions like these offer the best available *in vivo* models for studying lipid metabolism affected by genetic glycosylation defects.

A less appealing – in terms of translatability to human patients – yet easier to manage alternative is using other animals less closely related to humans. *Caenorhabditis elegans* (worm), *Drosophila melanogaster* (fruit fly) and *Danio rerio* (zebrafish)³⁸ are commonly used in this setting. In **Chapter 4** we describe the generation of an *ngly1* knockout in zebrafish resulting in a viable, stable model for *in vivo* studies of the deglycosylation defect.

As comprehension of specific glycan structures and functionality is enhanced, targeting glycosylation is being explored successfully in a variety of different fields, e.g. cancer vaccine development³⁹⁻⁴¹ and antiviral therapies^{42,43}. Enzyme replacement therapy with a recombinant analog is effective treatment in lysosomal storage disease and is promising for glycosylation disorders as well.

But when studying the rare and extreme phenotypes in these sometimes severely, clinically affected patients to find novel targets for therapies for only a certain aspect of their symptomatology, it remains to be seen whether it can be targeted specifically enough. That is, without causing the other, more severe symptoms seen in patients; or in other words “off-target effects”. Promising in this respect is, that despite the global glycosylation defects, the lipid phenotypes in these patients are very specific.

All CDG patients that we studied have a general glycosylation defect potentially affecting every glycoprotein imaginable, and yet we find distinct lipid phenotypes in the different subsets of CDG. The CDG-I patients have a defect in enzymes so early in the glycosylation machinery, that a wide

variety of proteins miss complete glycans. Nevertheless, we find hypobetalipoproteinemia in every single patient and our *in vitro* studies point to one particular lipid pathway in causing that phenotype: increased LDL receptor and consequently increased LDL uptake. A separate set of patients involves TMEM199 and CCDC115 deficiency with mixed glycosylation disorders and disrupted Golgi homeostasis - again affecting many different proteins - and in them we consistently find hypercholesterolemia and hepatic steatosis. The exact link between the glycosylation defect and the affected lipid pathways is unknown. In the ever-expanding world of the “-omics”, the relatively new glycoproteomics specifically looking at proteins involved in these pathways could point out the culprit to examine further.

But the most promising finding for the possibilities to target glycosylation pathways to affect lipid metabolism without causing harmful off-target effects in a general population, is the fact that the heterozygous carriers of at least the CDG-I mutations showed hypocholesterolemia, without any of the clinical symptoms found in the homozygous patients. This suggests a gene-dose response and that partial “tinkering” of the glycosylation patterns is something to aim for when targeting this in dyslipidemic patients.

Concluding remarks

Our studies have mined a relatively unknown source of information in cardiovascular research: at the interface of glycobiology and lipid metabolism. Further mechanistic studies into the pathways uncovered in our studies combined with glycoproteomics to identify specific glycoproteins to target, are essential for the development of future therapies. The main concerns about targeting glycosylation in general are the potential off-target effects and safety. Our studies show promising findings in this respect with distinctly affected lipid pathways even in global glycosylation defects and healthy heterozygous carriers of CDG mutations with similar lipid phenotypes as the homozygous patients. Furthermore, the recently developed techniques for drug delivery to the liver by conjugating compounds to GalNAcs can further limit off-target effects in targeting glycosylation pathways in the treatment of dyslipidemia and NAFLD in the general population.

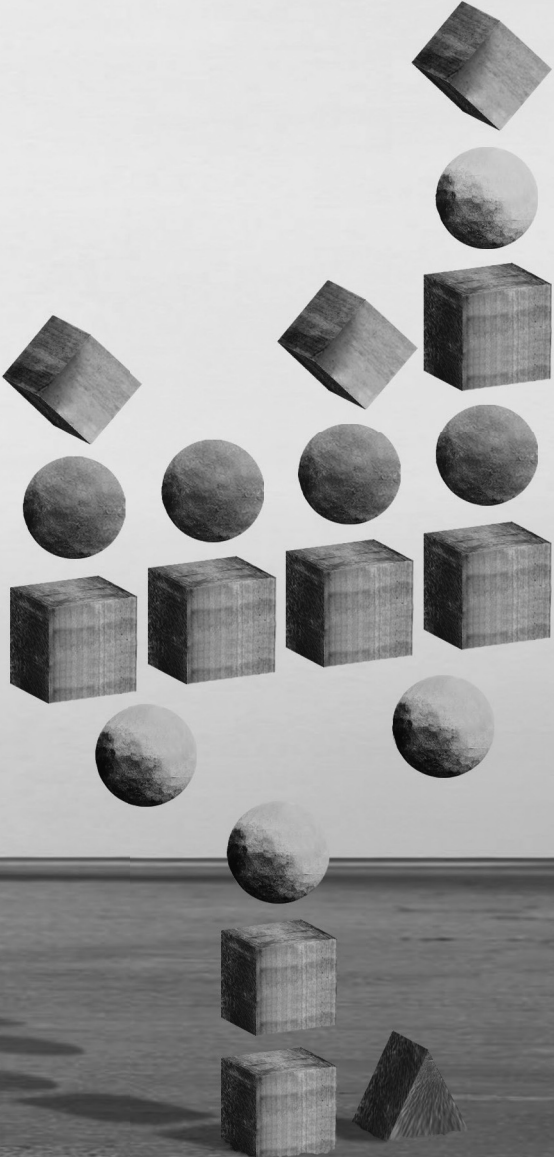
References

1. Guillard, M., *et al.* B4GALT1-congenital disorders of glycosylation presents as a non-neurologic glycosylation disorder with hepatointestinal involvement. *J Pediatr* **159**, 1041-1043 e1042 (2011).
2. Guillard, M., *et al.* Plasma N-glycan profiling by mass spectrometry for congenital disorders of glycosylation type II. *Clin Chem* **57**, 593-602 (2011).
3. Medrano, C., *et al.* Clinical and molecular diagnosis of non-phosphomannomutase 2 N-linked congenital disorders of glycosylation in Spain. *Clin Genet* **95**, 615-626 (2019).
4. Mabuchi, H., Nohara, A. & Inazu, A. Cholesteryl ester transfer protein (CETP) deficiency and CETP inhibitors. *Mol Cells* **37**, 777-784 (2014).
5. Tall, A.R. & Rader, D.J. Trials and Tribulations of CETP Inhibitors. *Circ Res* **122**, 106-112 (2018).
6. Ference, B.A., *et al.* Association of Genetic Variants Related to CETP Inhibitors and Statins With Lipoprotein Levels and Cardiovascular Risk. *JAMA* **318**, 947-956 (2017).
7. Sniderman, A.D., *et al.* Apolipoproteins versus lipids as indices of coronary risk and as targets for statin treatment. *Lancet* **361**, 777-780 (2003).
8. Jansen, J.C., *et al.* CCDC115 Deficiency Causes a Disorder of Golgi Homeostasis with Abnormal Protein Glycosylation. *Am J Hum Genet* **98**, 310-321 (2016).
9. Jansen, J.C., *et al.* TMEM199 Deficiency Is a Disorder of Golgi Homeostasis Characterized by Elevated Aminotransferases, Alkaline Phosphatase, and Cholesterol and Abnormal Glycosylation. *Am J Hum Genet* **98**, 322-330 (2016).
10. Chalasani, N., *et al.* The diagnosis and management of nonalcoholic fatty liver disease: Practice guidance from the American Association for the Study of Liver Diseases. *Hepatology* **67**, 328-357 (2018).
11. Neuschwander-Tetri, B.A., *et al.* Farnesoid X nuclear receptor ligand obeticholic acid for non-cirrhotic, non-alcoholic steatohepatitis (FLINT): a multicentre, randomised, placebo-controlled trial. *Lancet* **385**, 956-965 (2015).
12. Cariou, B., *et al.* Dual peroxisome proliferator-activated receptor alpha/delta agonist GFT505 improves hepatic and peripheral insulin sensitivity in abdominally obese subjects. *Diabetes Care* **36**, 2923-2930 (2013).
13. Armstrong, M.J., *et al.* Tiraglutide safety and efficacy in patients with non-alcoholic steatohepatitis (LEAN): a multicentre, double-blind, randomised, placebo-controlled phase 2 study. *Lancet* **387**, 679-690 (2016).
14. Kovalic, A.J., Satapathy, S.K. & Chalasani, N. Targeting incretin hormones and the ASK-1 pathway as therapeutic options in the treatment of non-alcoholic steatohepatitis. *Hepatol Int* **12**, 97-106 (2018).
15. Enns, G.M., *et al.* Mutations in NGLY1 cause an inherited disorder of the endoplasmic reticulum-associated degradation pathway. *Genet Med* **16**, 751-758 (2014).
16. Lam, C., *et al.* Prospective phenotyping of NGLY1-CDDG, the first congenital disorder of deglycosylation. *Genet Med* **19**, 160-168 (2017).
17. Zhang, T., *et al.* Evolution of the cholesterol biosynthesis pathway in animals. *Mol Biol Evol* (2019).
18. Nioi, P., *et al.* Variant ASGR1 Associated with a Reduced Risk of Coronary Artery Disease. *N Engl J Med* **374**, 2131-2141 (2016).
19. Grewal, P.K., *et al.* The Ashwell receptor mitigates the lethal coagulopathy of sepsis. *Nat Med* **14**, 648-655 (2008).
20. Grozovsky, R., *et al.* The Ashwell-Morell receptor regulates hepatic thrombopoietin production via JAK2-STAT3 signaling. *Nat Med* **21**, 47-54 (2015).
21. Jansen, A.J., *et al.* Desialylation accelerates platelet clearance after refrigeration and initiates GPIIb/IIIa metalloproteinase-mediated cleavage in mice. *Blood* **119**, 1263-1273 (2012).
22. Raal, F.J., *et al.* Inclisiran for the Treatment of Heterozygous Familial Hypercholesterolemia. *N Engl J Med*

- 382**, 1520-1530 (2020).
23. Chan, A., *et al.* Preclinical Development of a Subcutaneous ALAS1 RNAi Therapeutic for Treatment of Hepatic Porphyrrias Using Circulating RNA Quantification. *Mol Ther Nucleic Acids* **4**, e263 (2015).
 24. Yasuda, M., *et al.* RNAi-mediated silencing of hepatic Alas1 effectively prevents and treats the induced acute attacks in acute intermittent porphyria mice. *Proc Natl Acad Sci U S A* **111**, 7777-7782 (2014).
 25. Springer, A.D. & Dowdy, S.F. GalNAC-siRNA Conjugates: Leading the Way for Delivery of RNAi Therapeutics. *Nucleic Acid Ther* **28**, 109-118 (2018).
 26. Dowdy, S.F. Overcoming cellular barriers for RNA therapeutics. *Nat Biotechnol* **35**, 222-229 (2017).
 27. Carstea, E.D., *et al.* Niemann-Pick C1 disease gene: homology to mediators of cholesterol homeostasis. *Science* **277**, 228-231 (1997).
 28. Cunniff, C., Kratz, L.E., Moser, A., Natowicz, M.R. & Kelley, R.I. Clinical and biochemical spectrum of patients with RSH/Smith-Lemli-Opitz syndrome and abnormal cholesterol metabolism. *Am J Med Genet* **68**, 263-269 (1997).
 29. Takahashi, K. & Yamanaka, S. Induction of pluripotent stem cells from mouse embryonic and adult fibroblast cultures by defined factors. *Cell* **126**, 663-676 (2006).
 30. Thiesler, C.T., *et al.* Glycomic Characterization of Induced Pluripotent Stem Cells Derived from a Patient Suffering from Phosphomannomutase 2 Congenital Disorder of Glycosylation (PMM2-CDG). *Mol Cell Proteomics* **15**, 1435-1452 (2016).
 31. Cayo, M.A., *et al.* JD induced pluripotent stem cell-derived hepatocytes faithfully recapitulate the pathophysiology of familial hypercholesterolemia. *Hepatology* **56**, 2163-2171 (2012).
 32. Takebe, T., *et al.* Vascularized and functional human liver from an iPSC-derived organ bud transplant. *Nature* **499**, 481-484 (2013).
 33. Schneider, A., *et al.* Successful prenatal mannose treatment for congenital disorder of glycosylation-1a in mice. *Nat Med* **18**, 71-73 (2011).
 34. Medina-Cano, D., *et al.* High N-glycan multiplicity is critical for neuronal adhesion and sensitizes the developing cerebellum to N-glycosylation defect. *Elife* **7**(2018).
 35. Fujihira, H., *et al.* Lethality of mice bearing a knockout of the Ngly1-gene is partially rescued by the additional deletion of the Engase gene. *PLoS Genet* **13**, e1006696 (2017).
 36. Chan, B., *et al.* A mouse model of a human congenital disorder of glycosylation caused by loss of PMM2. *Hum Mol Genet* **25**, 2182-2193 (2016).
 37. Grunert, S.C., *et al.* Unsuccessful intravenous D-mannose treatment in PMM2-CDG. *Orphanet J Rare Dis* **14**, 231 (2019).
 38. Cline, A., *et al.* A zebrafish model of PMM2-CDG reveals altered neurogenesis and a substrate-accumulation mechanism for N-linked glycosylation deficiency. *Mol Biol Cell* **23**, 4175-4187 (2012).
 39. Kimura, T. & Finn, O.J. MUC1 immunotherapy is here to stay. *Expert Opin Biol Ther* **13**, 35-49 (2013).
 40. Lakshminarayanan, V., *et al.* Immune recognition of tumor-associated mucin MUC1 is achieved by a fully synthetic aberrantly glycosylated MUC1 tripartite vaccine. *Proc Natl Acad Sci U S A* **109**, 261-266 (2012).
 41. Vazquez, A.M., *et al.* Racotumomab: an anti-idiotypic vaccine related to N-glycolyl-containing gangliosides - preclinical and clinical data. *Front Oncol* **2**, 150 (2012).
 42. Lew, W., Chen, X. & Kim, C.U. Discovery and development of GS 4104 (oseltamivir): an orally active influenza neuraminidase inhibitor. *Curr Med Chem* **7**, 663-672 (2000).
 43. von Itzstein, M., *et al.* Rational design of potent sialidase-based inhibitors of influenza virus replication. *Nature* **363**, 418-423 (1993).



APPENDICES



Nederlandse Samenvatting

In de epigraaf van dit proefschrift paraphraseer ik de *extreme value theory* van Leonard Tippett (hier vrij vertaald): “Gebruik het zeldzame en extreme om het meer voorkomende te onderzoeken” en dat is wat we in de onderzoeken beschreven in dit proefschrift hebben gedaan. We hebben de extreme klinische fenotypes van de zeldzame patiënten met congenitale glycosyleringsziektes (CDG) gebruikt om meer inzicht te krijgen in het mechanisme dat hun extreme lipide afwijkingen kan verklaren. Onze onderzoeken zijn vervolgens gericht op het vinden van nieuwe therapeutische aangrijpingspunten om het veel meer voorkomende te kunnen behandelen: in dit geval hypercholesterolemie als oorzaak voor hart- en vaatziekten.

Deel I beschrijft ons onderzoek naar de lipide fenotypes in patiënten met CDG.

In **Hoofdstuk 1** hebben we een groot cohort met type I CDG patiënten met homozygote of compound heterozygote mutaties in de glycosyleringsenzymen ALG6 en PMM2 onderzocht. Alle patiënten bleken hypobetalipoproteïnemie te hebben, met totaal cholesterol, LDL-cholesterol (LDL-c) en apolipoproteïne B (apoB) concentraties onder het 5^e percentiel voor leeftijd en geslacht. De klinisch gezonde, heterozygote familieleden van de CDG-I patiënten hadden ook verlaagd LDL-cholesterol, wat een gen-dosis effect suggereert.

Onze *in vitro* cel experimenten leverden bewijs dat de hypobetalipoproteïnemie, op zijn minst deels, verklaard kan worden door verhoogde membraaneiwit expressie van de LDL receptor en verhoogde opname van LDL deeltjes. Bekende, potentieel bijdragende oorzaken aan hypobetalipoproteïnemie werden uitgesloten: apoB secretie bleek niet aangedaan en ook PCSK9 bleek geen rol te spelen. Het effect lijkt te worden gedreven door verhoogde basale activiteit van SREBP2, de belangrijkste transcriptiefactor van LDL receptor expressie. Normaal gesproken, induceert laag intracellulair cholesterol de activatie van SREBP2, echter in onze cel modellen van ALG6 en PMM2 deficiëntie vonden we verhoogd intracellulair cholesterol, terwijl cholesterol *sensing* wel intact bleek. Aangezien ER stress ook SREBP2 activatie kan geven en glycosyleringsdefecten ER stress kunnen veroorzaken door het overladen van de eiwit afbraaksystemen in de cel, onderzochten we ook ER stress markers. We vonden echter geen verschil tussen de CDG-I cellen en controles. Uiteindelijk is onze hypothese dat INSIG1, het eiwit dat proteolytische activatie van SREBP2 controleert, aangedaan is in de cellen van CDG-I patiënten. Over-expressie van INSIG1 zorgde inderdaad voor een verlaging van de LDL receptor in het CDG-I cel model.

Het exacte mechanisme tussen de rol van INSIG1 en de verhoogde LDL receptor in CDG-I is nog niet volledig opgehelderd en is een belangrijk focus voor toekomstig onderzoek, aangezien dit kan bijdragen aan het vinden van potentieel nieuwe therapeutische targets in de behandeling van hypercholesterolemie.

Verder onderzoek, zoals naar de ontwikkeling van atherosclerose en *in vivo tracer* studies van apoB/LDL metabolisme, is ook interessant om in de gezonde heterozygote familieleden te vervolgen, aangezien die ook hypocholesterolemie hebben zonder de ernstige symptomen van de patiënten.

B4GALT1-CDG is een zeer zeldzaam syndroom veroorzaakt door een homozygote mutatie in *B4GALT1*, een gen dat codeert voor een enzym dat verantwoordelijk is voor de galactosylering van N-glycanen. In **Hoofdstuk 2** beschrijven we de gevonden plasma lipide afwijkingen in 3 B4GALT1-CDG patiënten. FPLC profielen toonden dat het cholesterol van deze patiënten zich voornamelijk in de HDL fractie bevindt met ook grotere HDL deeltjes. Dit fenomeen lijkt op de FPLC profielen van patiënten met *cholesteryl ester transfer protein* (CETP) deficiëntie. CETP heeft meerdere N-glycanen en transporteert cholesteryl esters van HDL deeltjes naar andere lipoproteïnes. CETP deficiëntie leidt daarom tot verhoogd HDL-c en verlaagd LDL-c. We onderzochten de glycosylering van CETP eiwitten in B4GALT1-CDG patiënten en vonden een toename van gedeglycosyleerde isovormen van CETP. Bovendien, bleek de CETP activiteit verminderd vergeleken met controles, wat suggereert dat de glycosylering een rol speelt in de functie van het eiwit.

De afgelopen jaren is er veel onderzoek verricht naar farmacologische CETP inhibitors om HDL-c te verhogen en LDL-c te verlagen en alhoewel deze doelen gehaald worden, blijkt het klinische voordeel op het cardiovasculaire risico van deze patiënten helaas beperkt. Toekomstig onderzoek om meer inzicht te krijgen in de manier waarop de glycosylering van CETP de activiteit van het eiwit kan beïnvloeden is waardevol in dit veld.

Een derde groep van patiënten met een genetisch glycosyleringsdefect met mutaties in *TMEM199* en *CCDC115* hebben we onderzocht in **Hoofdstuk 3**. *TMEM199* en *CCDC115* zijn beiden *V-ATPase assembly factors* en patiënten met een deficiëntie van deze eiwitten hebben gemengde glycosyleringsdefecten, forse leversteatose en hypercholesterolemie, vergelijkbaar met waarden gezien in patiënten met familiale hypercholesterolemie.

Het lipide fenotype toont dat het cholesterol voornamelijk in de VLDL fractie zit, zonder verhoging van de triglyceriden. Daarnaast is verminderd cholesterol in HDL deeltjes. We vonden verhoogde apoB secretie in een *in vitro* cel model en ook in levercellen gere-differentieerd van pluripotente stamcellen van patiënten. De verhoogde apoB secretie is een mogelijke verklaring voor de hypercholesterolemie. De verminderde lipidering van de VLDL deeltjes met triglyceriden wordt mogelijk veroorzaakt door verlaagde expressie van *microsomal triglyceride transfer protein* (MTTP), aangetoond in het *in vitro* cel model.

Daarnaast hebben we door middel van CRISPR/Cas9 een muismodel gecreëerd met een *knock-in* van een mutatie van een patiënt en deze muizen hadden ook leversteatose. Het muizenmodel toonde niet verhoogd (V)LDL zoals in de patiënten, maar wel verminderde cholesterol verdeling in HDL deeltjes.

In ons *in vitro* cel model zagen we ook een verhoogd aantal, vergrote *lipid droplets*, net zoals in leverbiopten van patiënten met *TMEM199* en *CCDC115* deficiëntie. Daarnaast was er ook een verstoorde interacties tussen deze *lipid droplets* met lysosomen, wat verstoorde autofagie van *lipid droplets* suggereert wat weer de ontwikkeling van leversteatose zou kunnen verklaren.

Non-alcoholic fatty liver disease (NAFLD) komt steeds vaker voor omdat het geassocieerd is met obesitas en insuline resistentie. Naast leefstijl interventies, is er op dit moment geen behandeling specifiek gericht op NAFLD, alhoewel er wel meerdere veelbelovende medicijnen worden getest in

klinische studies. Meer inzicht in de mechanismes die lipide accumulatie veroorzaken, zoals beschreven in dit onderzoek, kunnen leiden tot nieuwe aangrijpingspunten in de behandeling.

Een relatief recent ontdekte, erfelijke ziekte wordt veroorzaakt door mutaties in *N-glycanase 1* (*NGLY1*), een deglycosyleringsenzym, wat dit de eerste congenitale deglycosyleringsziekte maakt. In **Hoofdstuk 4** hebben we de lipide fenotypes in deze patiënten onderzocht en vonden hypocholesterolemie. Het lage plasma cholesterol werd niet verklaard door verhoogde klaring van LDL-c zoals gevonden in de CDG-I patiënten, want de hoeveelheid LDL receptor en LDL deeltjes opname waren juist verminderd in de fibroblasten van *NGLY1*-CDDG patiënten. Een mogelijke verklaring werd gevonden met de *down*-regulatie van het belangrijkste enzym in de cholesterolsynthese: HMG-CoA-reductase (*HMGCR*), zowel in de fibroblasten van patiënten, als in een homozygoot *knockout* model in zebrafissen. Daarnaast toonden deze *ngly1*^{-/-} zebrafissen ook bepaalde klinische kenmerken gezien in de patiënten, namelijk kleine levers, een verminderd oppervlakte van de cerebellaire granule neuronen en verminderde locomotorische activiteit.

Wat ons onderzoek extra interessant maakt, is dat de lipide fenotypes gevonden in de patiënten, mogelijk zelfs causaal zijn in hun neurologische fenotype. De vroege ontwikkeling van het centrale zenuwstelsel is deels afhankelijk van enorm toegenomen cholesterolsynthese. *RNA sequencing* van de *ngly1*^{-/-} zebrafissen toonde dysregulatie van de cholesterolsynthese paden en verlaagde mRNA en eiwit expressie van *HMGCR*. Zowel suppletie van de metabooliet van *HMGCR* activiteit, als overexpressie van *HMGCR* zorgde voor een groter oppervlakte van cerebellaire granule neuronen. Dit biedt een therapeutische mogelijkheid die nog niet bestaat voor patiënten met *NGLY1* deficiëntie en er zal verder onderzocht moeten worden of mevalonaat suppletie ook het klinische beeld van *NGLY1*-CDDG patiënten kan verbeteren.

Deel II van dit proefschrift beschrijft andere rollen voor eiwit glycosylering in lipide metabolisme en atherosclerose. In **Hoofdstuk 5** hebben we de mogelijke pleiotrope effecten van de *del12 ASGR1* variant onderzocht. Recent is er een zeldzame variant in *ASGR1* beschreven die geassocieerd bleek met een fors gereduceerd cardiovasculair risico. Het relatief kleine effect op het plasma LDL-c in mensen met deze *ASGR1* variant, leek deze risico reductie niet genoeg te verklaren.

De asialoglycoproteïne receptor (*ASGPR*) is eerder geïmpliceerd in de klaring van verouderde, gedesialyleerde plaatjes. Onze hypothese was dat dragers van de *ASGR1* mutant mogelijk minder *ASGPR* hebben en dat hierdoor de verouderde, gedesialyleerde en mogelijk minder functionerende plaatjes langer circuleren en minder geneigd zijn tot aggregeren. Echter, dit konden we niet aantonen. Dragers van de *del12 ASGR1* variant hadden een vergelijkbare hoeveelheid plaatjes en ook de plaatjes aggregatie was niet verminderd ten opzichte van controles. Wel hebben we de originele bevinding, dat de LDL-c verlagings door varianten in *ASGR1* is geassocieerd met een verlaagd cardiovasculair risico, kunnen valideren, door drie veel voorkomende “*common*” varianten in en rond *ASGR1* te evalueren. Daarnaast bleek dit effect compleet vergelijkbaar met de effecten en gen risico scores van bekende en welomschreven andere factoren in het LDL metabolisme, zoals *LDLR*, *PCSK9* en *HMGCR*.

Hoe de zeldzame *ASGR1del12* variant de LDL-c levels verlaagt is nog onduidelijk en het onderwerp van toekomstige studies.

In **Hoofdstuk 6** hebben we overige bekende glycobioologische processen besproken die relevant zijn in lipide metabolisme. Van de lipide fenotypes gezien in CDG patiënten, zoals hierboven beschreven, tot de specifieke glycosylering patronen en de invloed daarvan op de functie van belangrijke eiwitten in het lipide metabolisme. De review bespreekt ook kort het gebruik van deze kennis voor de ontwikkeling van nieuwe therapeutische aangrijpingspunten in de behandeling van hypercholesterolemie en atherosclerose. Globaal de glycosylering machinerie aantasten lijkt niet de aangewezen methode: gezien de grote hoeveelheid endogene glycoproteïnes zou dit een breed scala aan bijwerkingen kunnen geven. Echter, in de laatste jaren kunnen glycanen steeds beter specifiek gebruikt worden in therapie en is in bepaalde velden, zoals vaccin ontwikkeling in de virologie en oncologie, zelfs al succesvol toegepast.

Authors and Affiliations

Lubna Ali

Department of Experimental Vascular Medicine, Amsterdam University Medical Centers, Location AMC, Amsterdam, The Netherlands

Patrick L.W. Chong

Department of Experimental Vascular Medicine, Amsterdam University Medical Centers, Location AMC, Amsterdam, The Netherlands

Donna Conlon

Department of Genetics and Medicine, Perelman School of Medicine at the University of Pennsylvania, Philadelphia, Pennsylvania, USA

Cleo. L. Crunelle

Vrije Universiteit Brussel, Universitair Ziekenhuis Brussel, Department of Psychiatry, Brussels, Belgium

Arjen J. Cupido

Department of Vascular Medicine, Amsterdam University Medical Centers, Location AMC, Amsterdam, The Netherlands

Geesje M. Dallinga-Thie, copromotor

Department of Experimental Vascular Medicine, Amsterdam University Medical Centers, Location AMC, Amsterdam, The Netherlands

J.P.H. Drenth

Department of Gastroenterology and Hepatology, Radboud University Medical Center, Nijmegen, The Netherlands

Maryse Guerin

ICAN - Institute of CardioMetabolism and Nutrition, Hôpital de la Pitié, Paris, France

Nicholas J. Hand

Department of Genetics and Medicine, Perelman School of Medicine at the University of Pennsylvania, Philadelphia, Pennsylvania, USA

Miao He

Department of Pathology and Laboratory Medicine, Perelman School of Medicine at the University of Pennsylvania, Philadelphia, Pennsylvania, USA.

The Children's Hospital of Philadelphia, Division of Laboratory Medicine, Philadelphia, Pennsylvania, USA.

Adriaan G. Holleboom, copromotor

Department of Vascular Medicine, Amsterdam University Medical Centers, Location AMC, Amsterdam, The Netherlands

G. Kees Hovingh

Department of Vascular Medicine, Amsterdam University Medical Centers, Location AMC, Amsterdam, The Netherlands

Jos. C. Jansen

Department of Gastroenterology and Hepatology, Radboud University Medical Center, Nijmegen, The Netherlands

J.W. Jonker

Department of Pediatrics, Section Molecular Metabolism and Nutrition, University Medical Center Groningen, University of Groningen, The Netherlands

Nicholas Katsanis

Advanced Center for Translational and Genetic Medicine (ACT-GeM), Stanley Manne Children's Research Institute, Department of Pediatrics, Ann & Robert H. Lurie Children's Hospital of Chicago, Chicago, Illinois, USA
Departments of Pediatrics and Cell and Developmental Biology, Feinberg School of Medicine, Northwestern University, Chicago, IL, USA

V. Konstantopoulou

Department of Pediatrics, Medical University of Vienna, Vienna, Austria

Jeffrey Kroon

Department of Experimental Vascular Medicine, Amsterdam University Medical Centers, Location AMC, Amsterdam, The Netherlands

Sacha D. Kuil

Department of Laboratory Medicine, Translational Metabolic Laboratory, Radboud University Medical Center, Nijmegen, The Netherlands

Jan A. Kuivenhoven

Department of Pediatrics, Section Molecular Genetics, University Medical Center Groningen, University of Groningen, The Netherlands

Lars E. Larsen

Department of Experimental Vascular Medicine, Amsterdam University Medical Centers, Location AMC, Amsterdam, The Netherlands

Dirk J. Lefeber, *promotor*

Department of Laboratory Medicine, Translational Metabolic Laboratory, Radboud University Medical Center, Nijmegen, The Netherlands

Johannes H.M. Levels

Department of Experimental Vascular Medicine, Amsterdam University Medical Centers, Location AMC, Amsterdam, The Netherlands

Anke Loregger

Department of Medical Biochemistry, Amsterdam University Medical Centers, Location AMC, Amsterdam, The Netherlands

Eva Morava

Department of Clinical genomics. Mayo Clinic, Rochester, Minnesota, USA

Jorge Peter

Department of Experimental Vascular Medicine, Amsterdam University Medical Centers, Location AMC, Amsterdam, The Netherlands

Julien Philippe

Duke Center for Neurogeneration and Neurotherapeutics, Duke University, Durham, North Carolina, USA

Tobias Raabe

Department of Medicine, Division of Translational Medicine and Human Genetics, Perelman School of Medicine at the University of Pennsylvania, Philadelphia, Pennsylvania, USA

Daniel J. Rader

Department of Genetics and Medicine, Perelman School of Medicine at the University of Pennsylvania, Philadelphia, Pennsylvania, USA

Maaïke Rijkers

Department of Cellular and Molecular Hemostasis, Sanquin Research and Landsteiner Laboratory, Amsterdam University Medical Centers, University of Amsterdam, The Netherlands

Alinda W.M. Schimmel

Department of Experimental Vascular Medicine, Amsterdam University Medical Centers, Location AMC, Amsterdam, The Netherlands

Johan G. Schnitzler

Department of Experimental Vascular Medicine, Amsterdam University Medical Centers, Location AMC, Amsterdam, The Netherlands

Gerry Steenbergen

Department of Laboratory Medicine, Translational Metabolic Laboratory, Radboud University Medical Center, Nijmegen, The Netherlands

Erik S.G. Stroes, promotor

Department of Vascular Medicine, Amsterdam University Medical Centers, Location AMC, Amsterdam, The Netherlands

I-Chun Tsai

Center for Human Disease Modeling, Duke University School of Medicine, Durham, North Carolina, USA.

Ron A. Wevers

Department of Laboratory Medicine, Translational Metabolic Laboratory, Radboud University Medical Center, Nijmegen, The Netherlands

Noam Zelcer

Department of Medical Biochemistry, Amsterdam University Medical Centers, Location AMC, Amsterdam, The Netherlands

List of publications

Lubna Ali, Arjen J. Cupido, Maaikje Rijkers, G. Kees Hovingh, Adriaan G. Holleboom, Geesje M. Dallinga-Thie, Erik S. G. Stroes, **Marjolein A.W. van den Boogert**. *Common Gene Variants in ASGR1 Gene Locus Associate with Reduced Cardiovascular Risk in Absence of Pleiotropic Effects*. *Atherosclerosis*, Jun 2020

M.A.W. van den Boogert, C. Crunelle, S. Kuil, J.H.M. Levels, V. Konstantopoulou, G.M. Dallinga-Thie, D.J. Lefeber, E.S.G. Stroes, A.G. Holleboom. *Frameshift Mutation in B4GALT1 Leads to Deglycosylated Hypoactive CETP and High HDL-cholesterol*. *Journal of Inherited Metabolic Disease*, 2019, 43(3): 611-617.

M.A.W. van den Boogert, L.E. Larsen, L. Ali, S.D. Kuil, G.M. Dallinga-Thie, J.H. Levels, J. Peters, A.W.M. Schimmel, G. Steenbergen, C. Hollack, E. Morava, R.A. Wevers, J.A. Kuivenhoven, E.S.G. Stroes, A.G. Holleboom, D.J. Lefeber. *N-glycosylation defects in man lower LDL-cholesterol through increased LDL receptor protein expression*. *Circulation*, 2019, **140**, 280-292.

M.A.W. van den Boogert, D.J. Rader, A.G. Holleboom. *New insights into the role of glycosylation in lipoprotein metabolism*. *Current Opinion in Lipidology*, 2017, **28**, 502-506, Review.

J.J. Jansen, S. Cirak, M. van Scherpenzeel, S. Timal, J. Reunert, S. Rust, B. Perez, D. Vicogne, P. Krawitz, Y. Wada, A. Ashikov, C. Perez-Cerda, C. Medrano, A. Arnoldy, A. Hoischen, K. Huijben, G. Steenbergen, D. Quelhas, L. Diogo, D. Rymen, J. Jaeken, N. Guffon, D. Cheillan, L.P. van den Heuvel, Y. Maeda, O. Kaiser, U. Schara, P. Gerner, **M.A.W. van den Boogert**, A.G. Holleboom, M.C. Nassogne, E. Sokal, J. Salomon, G. van den Bogaart, J.P.H. Drenth, M.A. Huynen, J.A. Veltman, R.A. Wevers, E. Morava, G. Matthijs, F. Foulquier, T. Marquardt, D.J. Lefeber. *CCDC115 deficiency causes a disorder of Golgi homeostasis with abnormal protein glycosylation*. *American Journal of Human Genetics*, 2016, **98**, 310-321.

J.J. Jansen, S. Timal, M. van Scherpenzeel, H. Michelakakis, D. Vicogne, A. Ashikov, M. Moraitou, A. Hoischen, K. Huijben, G. Steenbergen, **M.A.W. van den Boogert**, F. Porta, P.L. Calvo, M. Mavrikou, G. Cenacchi, G. van den Bogaart, J. Salomon, A.G. Holleboom, R.J. Rodenburg, J.P.H. Drenth, M.A. Huynen, R.A. Wevers, E. Morava, F. Foulquier, J.A. Veltman, D.J. Lefeber. *TMEM199 deficiency, a glycosylation disorder with elevated aminotransferases, alkaline phosphatase and hypercholesterolemia*. *American Journal of Human Genetics*, 2016, **98**, 322-330.

H.L. Mooij, S.J. Bernelot Moens, P.L.S.M. Gordts, K.I. Stanford, E.M. Foley, **M.A. van den Boogert**, J.J. Witjes, H.C. Hassing, M.W. Tanck, M.A. van de Sande, J.H.M. Levels, J.J.P. Kastelein, E.S.G. Stroes, G.M. Dallinga-Thie, J.D. Esko, M. Nieuwdorp. *Genetic Variation in Heparan Sulfate Proteoglycans Modestly Affects Postprandial Lipid Clearance in Humans*. *The Journal of Lipid Research*, 2015, **56**, 665-673.

R. Sah, P. Mesirca, **M. van den Boogert**, J. Rosen, J. Mably, M. Mangoni, D.E. Clapham. *The ion channel-kinase, TRPM7, is required for maintaining cardiac automaticity*. *Proceedings of the National Academy of Science*, 2013, **110**, E3037-3046

R. Sah, P. Mesirca, X. Mason, W. Gibson, C. Bates-Withers, **M. van den Boogert**, W. Pu, M.E. Mangoni, D.E. Clapham. *The Timing of Myocardial Trpm7 Deletion during Cardiogenesis Variably Disrupts Adult Ventricular Function, Conduction and Repolarization*. *Circulation*, 2013, **128**, 101-114.

Portfolio

Courses

02-2014	BROK	0.9
02-2014	Oral presentation in English	0.8
03-2014	Practical Biostatistics	1.1
04-2014	Evidence based searching	0.1
06-2013	European focus course on CDG	1.1
11-2013	Mass spectrometry, Proteomics and protein research	2.1
03-2014	DNA technology	2.1
2013-2017	Weekly department Journal Club	4
2013-2017	Weekly clinical education and grand rounds	4

Oral and poster presentations

11-2013	Poster: " <i>Genetic Defects in protein glycosylation as a cause for dyslipidemia</i> ", American Heart Association, Scientific Sessions, Dallas, TX, USA	0.5
03-2014	Oral: " <i>Hypobetalipoproteinemia in Patients with Congenital Glycosylation type 1</i> ", Cardiovasculaire Conferentie, Ermelo, The Netherlands	0.5
05-2014	Oral: " <i>Genetic Defects in protein glycosylation as a cause for dyslipidemia</i> ", European Atherosclerosis Society, Madrid, Spain	0.5
06-2014	Oral and Poster presentation: " <i>Genetic Defects in protein glycosylation as a cause for dyslipidemia</i> ", Gordon Research conference on Lipoprotein metabolism, Waterville Valley, NH, USA	1.0
09-2014	Poster presentation: " <i>Genetic Defects in protein glycosylation as a cause for dyslipidemia</i> ", Joint Glycobiology Meeting, Gent, Belgium	0.5
03-2015	Poster: " <i>N-linked glycosylation disorders cause hypobetalipoproteinemia: new insights at the interface of lipidology and glycobiology.</i> ", Gordon Research Conference on Glycobiology, Lucca, Italy	0.5
05-2015	Oral: " <i>N-linked glycosylation disorders cause hypobetalipoproteinemia</i> ", International Symposium on Atherosclerosis, Amsterdam, The Netherlands	0.5
08-2015	Invited oral: " <i>Cholesterol disturbances in patients with CDG.</i> ", Lyon, France	0.5
06-2016	Poster: " <i>Type 1 N-linked glycosylation disorders cause hypobetalipoproteinemia</i> ", Gordon Research Conference on Lipoprotein Metabolism, Waterville Valley, NH, USA	0.5

(Inter)national conferences

11-2013	American Heart Association, Scientific Sessions, Dallas, TX, USA	2.1
03-2014	Cardiovasculaire Conferentie, Ermelo, The Netherlands	0.7
05-2014	European Atherosclerosis Society, Madrid, Spain	2.1
06-2014	Gordon Research Conference, Lipoprotein Metabolism, Waterville Valley New Hampshire, USA	2.1
09-2014.A	Joint Glycobiology Meeting, Ghent, Belgium	1.4

03-2015	Gordon Research Conference, Glycobiology, Lucca, Italy	2.1
05-2015	International Symposium on Atherosclerosis, Amsterdam, The Netherlands	0.7
08-2015	World Conference on CDG, Lyon, France	1.4
06-2016	Gordon Research Conference, Lipoprotein Metabolism, Waterville Valley New Hampshire, USA	2.1

Student monitoring and teaching

2016-2017	Bachelor thesis with laboratory internship Medicine, Santino Rellum	2.0
2016-2017	Bachelor thesis with laboratory internship Life Sciences and Technology, Patrick Chong	2.0
2017	Master thesis with laboratory internship Biomedical Sciences, Amber Korn	2.0
2017	Master thesis with laboratory internship Biomedical Sciences, Sanne Lith	2.0
2017-present	Co-promotor to Lubna Ali	2.0

Parameters of esteem

11-2013	AHA/ATVB Early Career Investigator Award from the American Heart Association at the Scientific Sessions, Dallas, Texas, USA (\$ 500,-)
06-2014	AMC PhD Scholarship 2014 from AMC PhD Graduate School (€ 205.000,-)
03-2015	Best Poster Award at Glycobiology Gordon Research Conference
01-2017	Metakids grant (€ 50.000,-)

Miscellaneous activities

2015-2016	Co-chair for the Gordon Research Symposium, a forum for graduate students, post-docs, and other early career scientists, held in conjunction with the Gordon Research Conference, lipoprotein metabolism in Waterville Valley, New Hampshire, USA	2.0
-----------	--	-----

Dankwoord

De onderzoeken beschreven in dit proefschrift waren niet mogelijk geweest zonder de genereuze hulp van patiënten en hun families. Hun geweldig positieve instelling is een inspiratie. Ik heb velen van hen later nogmaals kunnen ontmoeten op de CDG World Conference wat ik als heel bijzonder heb ervaren. Ik wil hen hartelijk bedanken voor hun inzet.

Daarnaast wil ik mijn geweldige promotieteam heel erg bedanken voor de begeleiding; jullie advies en wijsheid zijn enorm gewaardeerd.

Beste Erik, jouw enthousiaste “briljant!” en “kan je het nu eens uitleggen voor de gewone stervelingen zoals wij” vanuit achter in de zaal zullen nooit vervelen – en dat terwijl ik weinig mensen ken die zo snel hun hyperintelligente theorieën en analyses kunnen neerleggen als dat jij dat kan. Je geloof in mij ervaar ik als een eer en je continue *drive* naar verbetering en innovatie zijn een inspiratie.

Beste Dirk, jouw “*voice of reason*” was regelmatig een welkom baken van rust in de soms roerige tijden die mijn promotietraject heeft gekend. Je was er altijd met wijs advies en gedetailleerde uitleg over de oneindig complexe wereld van de glycosylering. Ik heb veel bewondering voor je integere aanpak en heb ontzettend veel van je geleerd.

Beste Onno, jij bent degene die de gok heeft gewaagd om met mij dit project op te bouwen en uit te voeren. Jouw *drive* voor onderzoek en beurzen ophalen zijn ongekend en bewonderenswaardig. Daarnaast kan ik genieten van hoe wij vaak dezelfde denkpatronen hebben over onze onderzoeken. Omdat jij samen met mij bleef geloven staat ons grote stuk nu maar mooi in *Circulation*.

Beste Geesje, de lab *know-it-all*, dank voor je geduld voor mijn oneindige nieuwe ideeën voor proeven en experimenten op het lab. Niet alles was mogelijk, maar je deed altijd je best om te bedenken wat er dan wel mogelijk was. Zelfs in je pensioen ben je niet uit het lab weg te denken.

Uiteraard wil ik ook de leescommissie en opposanten, bestaande uit prof. dr. Noam Zelcer, prof. dr. Carla van Karnebeek, dr. Mirjam Langeveld, dr. Bart van der Sluis, prof. dr. Bert Groen en prof. dr. Esther Lutgens, bedanken voor de kritische beoordeling van mijn manuscript, en de bereidheid te opponeren tijdens de verdediging van mijn proefschrift.

Dit proefschrift is verder gebouwd op verschillende samenwerkingen. Ik ben veel dank verschuldigd aan mensen voor werk dat ik nooit zelf had kunnen doen.

Allereerst natuurlijk de fijne collega's op het lab van de experimentele vasculaire geneeskunde op G1. Lieve Alinda, jij bent echt van onschatbare waarde voor niet alleen mijn proefschrift, maar velen voor en na mij. Wat was het gezellig om samen onze honderden cellijnen in de celkweek te onderhouden en zelfs even een lab *bench* te delen. Jouw inzet, expertise, maar vooral gezelligheid heb ik enorm gewaardeerd! Natuurlijk zijn daar verder de immer vrolijke Miranda, van wie ik heb leren FACSen, de labmeester Hans, die zonder morren telkens weer mijn minuscule hoeveelheden patiënten plasma wilde analyseren op de Selectra, Han “*concentrations*” Levels, wiens FPLC skills in al mijn onderzoeken nodig waren, Jorge, die altijd weer een cohortje gezonde controles wist te

trekken uit de vasculaire database en Maaïke, met wie ik ook vele gezellige uren in de celkweek heb doorgebracht. Lubna, ik vond het fijn met je samenwerken en ik hoop dat ik snel bij jouw promotie kan komen kijken. Jef en Jan, het dynamische duo van het lab, wat was het gezellig, zeker op de borrels. Lieve Kobie, zonder jouw onuitputtelijke enthousiasme en inzet hebben we al die patiënten en hun families kunnen includeren in onze studies en daarvoor ben ik je erg dankbaar.

Daarnaast wil ik Gerry Steenberg en Karin Huijben van het Translationeel Metabool Laboratorium van het Radboud UMC in Nijmegen enorm bedanken voor hun hulp en geduld met mijn uitstapjes naar jullie lab. Jullie hebben ervoor gezorgd dat ik me altijd welkom voelde.

Of course, there is also my time at the Rader Lab at the University of Pennsylvania in Philadelphia. I would like to sincerely thank Dan Rader and Nick Hand for their guidance and advice during my time there and their thoughtful comments on our research.

I would also like to thank Anke Loregger and Noam Zelcer from the Biochemistry department at the AMC for always being willing to help, and their advice and efforts have greatly enhanced the studies in this thesis.

Mijn promotietijd was niet hetzelfde, maar ook vooral een stuk minder leuk geweest zonder de fijne collega's van de vasculaire geneeskunde op F4. Lieve collega's: dank jullie wel! De oneindige feestjes, borrels, de altijd gezellige lunch en het struinen over de afdeling op zoek naar afleiding en de legendarische skiweekenden zijn geweldige herinneringen. Het gaat te ver om iedereen te noemen, maar een poging is de moeite waard natuurlijk.

The coolest room met de leukste F4 Italiaan Stefano, Kristien en Loek, was een prachtig begin van mijn tijd bij de vasculaire; Ruudje Kootte met de tegenovergestelde werkwijze van mijn man en toch een onverslaanbaar duo, zeker als Hazes; de *lovely ladies* van F4 Lotte, Renate, Anne-Fleur, Nicolien en Sophie, jullie *party mood* en selfies, maar ook jullie inzet en organisatie voor alle mooie feesten en partijen van de vasculaire zijn enorm gewaardeerd; het komisch duo Joost en Julian zorgde altijd voor gezelligheid en wat een toeval dat mijn neefje naar jullie vernoemd is; Nick en Thijs, de *academic wonderboys* van de vasculaire, ik vind het altijd mooi om met jullie te brainstormen over onderzoek; Kang, ik kon me blijven verbazen over hoe jouw chaotische bureau in contrast stond met je strak georganiseerde en vooral vroeg geplande onderzoek, maar je was vooral m'n droge en super gezellige kamergenoot. Van F4 kunnen zeker Joyce en Tanja niet ontbreken: zonder jullie geduld en hulp in allerlei administratieve zaken, maar vooral ook gezelligheid, was het starten en afronden van dit promotietraject een stuk minder soepel gegaan.

Natuurlijk was deze tijd ook een stuk minder leuk geweest zonder alle leuke etentjes, borrels, weekendjes en vakanties met mijn goede vrienden.

Lieve Nanon en Laura, ik ken jullie al meer dan 20 jaar en zijn nog steeds dezelfde lieve, grappige en ambitieuze meiden die ik toen heb leren kennen en zie jullie altijd graag.

Lieve Emile, Floris, Gideon, Hanna en Tessel, aka de Harde Kern, we zijn samen begonnen als co-assistenten en konden lief en leed van die spannende tijd met elkaar delen, maar ondertussen zijn we ook uitgegroeid tot een super gezellige vriendengroep met wie ik ontzettend graag ben.

Lieve Berthe, Floor D, Floor V, Linda, Marieke en Rianne, aka de Spaanse kraag, samen de studie

ingegaan en samen aan onze carrières in de geneeskunde begonnen. Wat is het leuk om jullie te hebben zien groeien naar sommigen zelfs al volwaardig specialisten. Ik ben ontzettend blij met jullie. Esther, m'n lieve nichtje, jouw lieve steun en interesse over de afgelopen jaren zijn altijd gewaardeerd. Het is hoog tijd voor een nieuw *girls* trip.

Lieve Claire en Céline, jullie ken ik ook al heel lang en ik kijk nog steeds uit naar onze gezellige etentjes en ben altijd weer geïnspireerd door jullie ambitieuze carrières in de voor mij totaal onbekende en onbegrijpelijke financiële wereld.

Lieve Frederiek, mijn uitstapje naar de Farmacie heeft onze fijne vriendschap opgeleverd en jouw oprechte interesse is altijd voelbaar.

In dit rijtje mogen, zeker in het licht van de tripjes, borrels en etentjes van de afgelopen jaren, ook de fijne vrienden via Loek niet ontbreken: de boys (oorspronkelijk) uit Nijmegen (al moet ik nog steeds door de ballotage kameel geloof ik) en hun gezellige vriendinnen; Loeks fijne jaarclub mannen plus de Cachaladies natuurlijk; en de Waar is de borrel groep met wie we al de aardige traditie "oud en nieuw hoort in de zon" hebben weten op te bouwen.

Ik wil natuurlijk ook even stil staan bij mijn lieve paranimfen.

Lieve Emile, paranimf, als superman lid van ons quarantaine team, BABS van ons huwelijk, onofficieel benoemde peetvader van Jamie en de baby – wat ben je eigenlijk niet voor mij? Maar boven al deze titels ben je vooral een van mijn beste vrienden, op wie ik altijd kan rekenen en met wie het altijd feest is.

Lieve Adam, mijn beste vriendje al sinds we 12 zijn. En waar onze vriendschap vroeger bestond uit nog uren bellen na schooltijd, terwijl we elkaar daar al de hele dag hadden gezien, kunnen we nu nog steeds oneindig appen en kletsen, terwijl we elkaar op werk al de hele dag hebben kunnen zien. Ik geniet van onze spelletjesavonden en gezamenlijke parttime dag en vindt het geweldig dat onze kinderen nu met elkaar spelen.

Lieve Smitsen, wat ben ik blij met jullie als schoonfamilie. Lieve Paul en Liesbet, dank jullie wel voor jullie warme gezelligheid, voor jullie onvoorwaardelijke steun voor ons gezinnetje en jullie oprechte belangstelling voor alles wat we doen. Lieve Ruben en Desy, of zoals Jamie jullie noemt Desy en Desy, jullie zijn een lieve broer, zwager, schoonzus en oom en tante voor ons gezin en ik vind het super fijn om familie van jullie te zijn.

Lieve Babette en Robert, mijn grote zus en kleine grote broer, mijn beste vriendin en mijn oude huisgenoot, mijn getuigen bij ons huwelijk. Ik ben zo ontzettend blij met onze band samen. Onze humor, die soms alleen wij kunnen volgen, is altijd weer iets om naar uit te kijken. Ik vind het geweldig hoe onze reis met mama naar New York voornamelijk bestond uit gieren van het lachen tot jankens toe. Lieve Jens, ook jij bent a sinds jaar en dag als een grote, wijze maar vooral lieve broer voor mij. Wat ben ik blij dat jij m'n zwager bent. Lieve Sophie, ook al zo'n fijne schoonzus! Ik ben super blij dat Robert jou gevonden heeft.

Lieve papa, beter bekend als opa Bolo inmiddels, ik kan me nog goed herinneren dat je me een keer vroeg om mijn onderzoek in één zin op een briefje te schrijven, zodat je dat erbij kon pakken als iemand weer eens vroeg waar ik nou onderzoek naar deed. Dat briefje is er nooit gekomen, maar misschien heb je wat aan dit boekje... Dank je wel voor je steun, je humor en de altijd gezellige Bolo avonden.

Lieve mama, jouw onvoorwaardelijke liefde, steun en zorgzaamheid al mijn hele leven voor mij, maar nu ook voor mijn gezin, is niet in een paar zinnen te vangen. Jouw kracht en doorzettingsvermogen zijn echt een inspiratie, niet alleen privé, maar ook in mijn werk, en zonder jou was ik zeker niet gekomen waar ik nu ben. Ik geniet met volle teugen om jou als vrolijke oma Mickey met Jamie (en Julian, Daan en Emma natuurlijk) te zien.

Liefste Loekie, Jamie en pinguinito, jullie maken het leven *amazing* en niet zo'n klein beetje ook. Loek, jij bent zo'n ontzettend leuke man; zonder jouw liefde, jouw vrolijkheid en humor, je eeuwige geduld en zorgzaamheid, maar ook je inmiddels absurd gedetailleerde kennis van mijn onderzoeken, was dit promotietraject een stuk minder leuk en makkelijk geweest.

Ik hou ∞ van jou en onze jongens.

Curriculum Vitae



Marjolein van den Boogert is geboren in Amsterdam (15-08-1985) en groeide op met haar ouders, Arend en Anita, zus Babette en broertje Robert. Ze ging met veel plezier naar school en rondde in 2003 haar middelbare school af aan het Vossius Gymnasium. Na een uitstapje naar Utrecht voor de Bachelor in de Farmacie aan de Universiteit Utrecht, bedacht ze toch dokter te willen worden en startte ze in 2006 met veel enthousiasme aan de studie Geneeskunde aan de Universiteit van Amsterdam.

Haar passie voor onderzoek begon al vroeg tijdens haar studie geneeskunde. Na wat keuzevakken in de elektrofysiologie gedaan te hebben, heeft ze een keuze stage op het *patch clamp* lab van *the Heart Failure Research Center* van het AMC gedaan en daarna in 2010-2011 bij *the Clapham Lab* verbonden aan *Harvard Medical School* in Boston in de Verenigde Staten. Na de coschappen en het behalen van haar artsendiploma is ze begonnen aan het promotieonderzoek beschreven in dit boekje bij de Vasculaire geneeskunde in het AMC onder de bevlogen supervisie van prof. dr. Erik Stroes, prof. dr. Dirk Lefeber (Radboud UMC in Nijmegen), dr. Onno Holleboom en dr. Geesje Dallinga-Thie. Ze kreeg voor dit onderzoek de AMC *PhD Scholarship* van de AMC *Graduate School*. Een deel van haar promotieonderzoek heeft ze uitgevoerd in het lab van prof. dr. Dan Rader aan de University of Pennsylvania in Philadelphia in de Verenigde Staten.

In 2017 is ze begonnen aan de opleiding tot internist in het Amsterdam UMC, locatie AMC en zal ze zich vanaf oktober 2021 verder gaan specialiseren tot hematoloog. Ze hoopt in de toekomst haar klinische werk als hematoloog te kunnen blijven combineren met het doen van translationeel onderzoek.

Tijdens haar promotieonderzoek leerde Marjolein haar grote liefde Loek kennen. Zij trouwden in juni 2019 en wonen samen met hun zoontje Jamie in Amsterdam. In november 2020 verwachten zij hun tweede zoontje.

